

Signals in motion

Edited by

Eunice Jingmei Tan and Mark A. Elgar

Published in

Frontiers in Ecology and Evolution



FRONTIERS EBOOK COPYRIGHT STATEMENT

The copyright in the text of individual articles in this ebook is the property of their respective authors or their respective institutions or funders. The copyright in graphics and images within each article may be subject to copyright of other parties. In both cases this is subject to a license granted to Frontiers.

The compilation of articles constituting this ebook is the property of Frontiers.

Each article within this ebook, and the ebook itself, are published under the most recent version of the Creative Commons CC-BY licence. The version current at the date of publication of this ebook is CC-BY 4.0. If the CC-BY licence is updated, the licence granted by Frontiers is automatically updated to the new version.

When exercising any right under the CC-BY licence, Frontiers must be attributed as the original publisher of the article or ebook, as applicable.

Authors have the responsibility of ensuring that any graphics or other materials which are the property of others may be included in the CC-BY licence, but this should be checked before relying on the CC-BY licence to reproduce those materials. Any copyright notices relating to those materials must be complied with.

Copyright and source acknowledgement notices may not be removed and must be displayed in any copy, derivative work or partial copy which includes the elements in question.

All copyright, and all rights therein, are protected by national and international copyright laws. The above represents a summary only. For further information please read Frontiers' Conditions for Website Use and Copyright Statement, and the applicable CC-BY licence.

ISSN 1664-8714
ISBN 978-2-83251-832-8
DOI 10.3389/978-2-83251-832-8

About Frontiers

Frontiers is more than just an open access publisher of scholarly articles: it is a pioneering approach to the world of academia, radically improving the way scholarly research is managed. The grand vision of Frontiers is a world where all people have an equal opportunity to seek, share and generate knowledge. Frontiers provides immediate and permanent online open access to all its publications, but this alone is not enough to realize our grand goals.

Frontiers journal series

The Frontiers journal series is a multi-tier and interdisciplinary set of open-access, online journals, promising a paradigm shift from the current review, selection and dissemination processes in academic publishing. All Frontiers journals are driven by researchers for researchers; therefore, they constitute a service to the scholarly community. At the same time, the *Frontiers journal series* operates on a revolutionary invention, the tiered publishing system, initially addressing specific communities of scholars, and gradually climbing up to broader public understanding, thus serving the interests of the lay society, too.

Dedication to quality

Each Frontiers article is a landmark of the highest quality, thanks to genuinely collaborative interactions between authors and review editors, who include some of the world's best academicians. Research must be certified by peers before entering a stream of knowledge that may eventually reach the public - and shape society; therefore, Frontiers only applies the most rigorous and unbiased reviews. Frontiers revolutionizes research publishing by freely delivering the most outstanding research, evaluated with no bias from both the academic and social point of view. By applying the most advanced information technologies, Frontiers is catapulting scholarly publishing into a new generation.

What are Frontiers Research Topics?

Frontiers Research Topics are very popular trademarks of the *Frontiers journals series*: they are collections of at least ten articles, all centered on a particular subject. With their unique mix of varied contributions from Original Research to Review Articles, Frontiers Research Topics unify the most influential researchers, the latest key findings and historical advances in a hot research area.

Find out more on how to host your own Frontiers Research Topic or contribute to one as an author by contacting the Frontiers editorial office: frontiersin.org/about/contact

Signals in motion

Topic editors

Eunice Jingmei Tan — Yale-NUS College, Singapore

Mark A. Elgar — The University of Melbourne, Australia

Citation

Tan, E. J., Elgar, M. A., eds. (2023). *Signals in motion*. Lausanne: Frontiers Media SA.
doi: 10.3389/978-2-83251-832-8

Table of contents

- 04 **Editorial: Signals in motion**
Eunice J. Tan and Mark A. Elgar
- 07 **Territorial Displays of the *Ctenophorus decresii* Complex: A Story of Local Adaptations**
Jose A. Ramos and Richard A. Peters
- 21 **Age and Appearance Shape Behavioral Responses of Phasmids in a Dynamic Environment**
Sebastian Pohl, Haaken Z. Bungum, Kenneth E. M. Lee, Mohamad Azlin Bin Sani, Yan H. Poh, Rodzay bin Hj Abd Wahab, Y. Norma-Rashid and Eunice J. Tan
- 36 **The Adaptive Significance of Flash Behavior: A Bayesian Model**
Thomas N. Sherratt and Karl Loeffler-Henry
- 47 **Rapid Shifts in Visible Carolina Grasshopper (*Dissosteira carolina*) Coloration During Flights**
Ezekiel Martin, Henry L. Steinmetz, Seo Young Baek, Frederick R. Gilbert and Nicholas C. Brandley
- 58 **Uncovering 'Hidden' Signals: Previously Presumed Visual Signals Likely Generate Air Particle Movement**
Pallabi Kundu, Noori Choi, Aaron S. Rundus, Roger D. Santer and Eileen A. Hebets
- 73 **Shape of Evasive Prey Can Be an Important Cue That Triggers Learning in Avian Predators**
Daniel Linke, Marianne Elias, Irena Klečková, Johanna Mappes and Pável Matos-Maraví
- 86 **Movement and olfactory signals: Sexually dimorphic antennae and female flightlessness in moths**
Tamara L. Johnson, Mark A. Elgar and Matthew R. E. Symonds
- 104 **Color in motion: Generating 3-dimensional multispectral models to study dynamic visual signals in animals**
Audrey E. Miller, Benedict G. Hogan and Mary Caswell Stoddard
- 123 **Interpreting animal behaviors – A cautionary note about swaying in phasmids**
Eunice J. Tan, Mark A. Elgar, Xue Bian and Richard A. Peters



OPEN ACCESS

EDITED AND REVIEWED BY
Jordi Figuerola,
Doñana Biological Station (CSIC), Spain

*CORRESPONDENCE
Eunice J. Tan
✉ yncjte@nus.edu.sg

SPECIALTY SECTION
This article was submitted to
Behavioral and Evolutionary Ecology,
a section of the journal
Frontiers in Ecology and Evolution

RECEIVED 02 February 2023
ACCEPTED 06 February 2023
PUBLISHED 21 February 2023

CITATION
Tan EJ and Elgar MA (2023) Editorial: Signals in
motion. *Front. Ecol. Evol.* 11:1157198.
doi: 10.3389/fevo.2023.1157198

COPYRIGHT
© 2023 Tan and Elgar. This is an open-access
article distributed under the terms of the
Creative Commons Attribution License (CC BY).
The use, distribution or reproduction in other
forums is permitted, provided the original
author(s) and the copyright owner(s) are
credited and that the original publication in this
journal is cited, in accordance with accepted
academic practice. No use, distribution or
reproduction is permitted which does not
comply with these terms.

Editorial: Signals in motion

Eunice J. Tan^{1,2*} and Mark A. Elgar³

¹Division of Science, Yale-NUS College, Singapore, Singapore, ²Department of Biological Sciences, National University of Singapore, Singapore, Singapore, ³School of BioSciences, University of Melbourne, Melbourne, VIC, Australia

KEYWORDS

motion signals, flash behavior, crypsis, signaling environment, environmental noise, attack avoidance, mate location

Editorial on the Research Topic Signals in motion

Introduction

Animals use signals and cues to derive information about their environment, including the presence of food, enemies and mates, the location of nesting and provisioning sites, and the assessment of reproductive and social partners. The nature and reception of signals and cues is therefore a key focus of evolutionary and behavioral ecology, and our understanding of animal signals has expanded with the development of conceptual and technical advances. Nevertheless, our insights about the function and efficacy of animal color patterns remains largely shaped by a focus on stationary animals, typically in a static background, which rarely reflects the natural world (Cuthill et al., 2019; Tan and Elgar, 2021): most animals are mobile in their search for food and mates, and their surrounding environment is usually dynamic. There is considerable variation in animal signals within different signal modalities, including the color patterns of visual signals; the odor cocktails of chemical signals; and the amplitude and frequency of acoustic signals. These signals may act multimodally, which makes disentangling the additional contributions of animal motion and a dynamic environment even more challenging.

Our Research Topic *Signals in motion* asks how the efficacy of these signals to convey information to the intended or unintended receiver is affected by both animal movement and a potentially dynamic background. For example, there is emerging interest in how individual motion can reveal information about the signaler to the receiver but can also be a means of concealing visual cues to unintended receivers. In contrast, the impact of movement when signaling in acoustic or olfactory modalities has received little, if any, attention. The primary intention of this Research Topic is to draw attention to the importance of motion in animal signaling. Contributing authors report on diverse organisms with different behaviors, signaling modalities and background environments, and detail how motion is linked to signaling and how signalers and background movement may affect signal reception. There are few direct tests of the effects of signals in motion, but the studies in this Research Topic provide the initial steps toward understanding how motion affects signals.

Coevolution of morphology and signals

Morphology and patterns can act together to affect the signal that is perceived by predators (Linke et al.). For example, the shape of butterfly wings affects their aerodynamic performance (Ortega Ancel et al., 2017), but whether these shapes can act as cues that indicate unprofitability to potential predators has been largely overlooked. Linke et al.

examined how the shape and markings of butterfly wings can affect signaling unprofitability to predators. Their experiments revealed that blue tits *Cyanistes caeruleus* can associate white bands and hindwing tails with the difficulty of capture of dummy butterflies. This raises the intriguing possibility that butterfly tails act both to signal evasiveness as well as to divert attacks to non-essential parts of the wing.

The impact of animal movement on species that signal with volatile odors is rarely considered. [Johnson et al.](#) conducted inter-specific comparative analyses to examine how the complexity of moth antennae have evolved with the mobility of female signallers, who use sex pheromones to reveal their location to males. These analyses revealed that the loss of flight in female moths has evolved more frequently in species where males have elaborate antennae, and that elaborate antennae in males evolved more frequently in species where females are monoandrous (where remating frequency is <30%). Together, these data highlight how elaborate antennae are associated with selection favoring efficient signal detection, which in turn allows females to invest less in movement and dispersal.

Animals employ a complex suite of behaviors in motion

Technological advances, especially high-speed cameras have allowed research to investigate complex animal signals involved in flight ([Linke et al.](#); [Martin et al.](#); [Pohl et al.](#)). [Martin et al.](#) and [Pohl et al.](#) show that animal responses, in grasshoppers and phasmids respectively, can be a collection of behaviors in motion, employing a range of antipredator strategies. The Carolina grasshopper *Dissosteira carolina* has a mostly brown colouration, with contrasting black and cream hindwings that are displayed when the grasshopper takes flight. By recording high-speed videos of the grasshopper flights in the field, [Martin et al.](#) discovered that the hindwing signals change during flight, depending on the size of the hindwing in view and the markings displayed. [Martin et al.](#) suggest that the Carolina grasshopper use their contrasting hindwings to deter predators through three mechanisms: first, by startling predators through deimatic defense; secondly, by confusing the predators and disrupting their search images through protean defense; and finally, returning to crypsis. [Pohl et al.](#) examined the behavioral responses of phasmids at different ontogenetic stages to a wind stimulus (a proxy for a dynamic environment). They found that adult behaviors were mostly species-specific, while nymph behaviors varied with appearance and environmental condition. [Pohl et al.](#) suggest that the behavioral responses interact with the morphology of the insects—depending on their species and ontogeny—to help reduce detection or recognition cues by potential predators.

Animals may employ signals from several modalities. For example, male wolf spiders *Schizocosa* are thought to use static and dynamic visual signals together with vibratory signals. Nevertheless, mating in *S. retrorsa* takes place in the absence of visual and vibratory stimuli. [Kundu et al.](#) show, experimentally, that these spiders use another signal modality—air particle movement or near field sound, that is generated by rapid leg waving.

Interestingly, these signals are specific to courtship: female foraging success did not depend on near field sound ([Kundu et al.](#)).

Many signals can vary over both space and time, requiring an experimental procedure that is more nuanced than the traditional approach of investigating static models against a static background. [Miller et al.](#) provide details on how the dynamic visual signals of birds can be investigated using three dimensional multi-spectral models, which allow measures of color (including in the UV), pattern, 3D shape and motion to be considered quantitatively. This novel approach is likely to be a crucial first step at analyzing visual signals in motion.

Signals in motion may serve to benefit the animal when it resumes a stationary position. Flash signals are displayed by cryptic animals when they move: for example, the cryptic blue-winged grasshopper *Oedipoda caerulescens*, flashes highly conspicuous blue wings when in flight. While this behavior may startle the predator, the conventional view is that the putative predator incorrectly assumes the prey is always conspicuous, which compromises its subsequent searching efforts. This view has some empirical support but the underlying process leading to this benefit has not been investigated. [Sherratt and Loeffler-Henry](#) use Bayesian search theory to show that the degree of the conspicuousness of a prey item is negatively correlated with the time the predator should give up searching for it in an area where it appears to have settled. The model makes several predictions that can be readily tested experimentally.

Environmental complexity and natural context

Most experimental studies of signaling utilize a static background, yet this is rarely the experience for animals ([Cuthill et al., 2019](#); [Tan and Elgar, 2021](#)). Environmental noise is often dynamic and multi-faceted, and the individual effects on signals can be difficult to disentangle ([Pohl et al.](#); [Ramos and Peters](#)). [Ramos and Peters](#) examined the displays of six closely related agamid lizards of the *Ctenophorus decresii* complex. They compared the signal structures and contrasts in the context of the lizards' natural habitats and showed that the signaling behavior of the different lizard clades reflected local adaptations to their specific habitats. [Ramos and Peters](#) suggest common morphological and behavioral traits are likely from the ancestral state, and their study highlights the importance of taking account of the natural habitat or environment when interpreting signals and signaling behavior.

Considering the natural context is equally important for theoretical modeling. [Tan et al.](#) corrected a false assumption underpinning a model explaining swaying behavior in phasmid leaf insects. The model assumed that phasmids perched on top of the substrate and argued that the swaying behavior served a balancing function. However, [Tan et al.](#) point out that as most phasmids hang from the substrate, gravity removes any need for “balance.” [Tan et al.](#) thus caution that drawing functional explanations about animal motion, including motion signaling behavior, requires some understanding of the species' natural history.

Future directions

Several themes emerge within the *Signals in motion* Research Topic: the coevolution of morphology and signals; the complexity of behaviors in motion; and the impact of environmental complexity. A common insight across these papers is a reiteration of John Endler's seminal paper highlighting the importance of considering the natural context (Endler, 1990). It is clear, from the contributions to the *Signals in motion* Research Topic, that this includes the dynamic nature of both the signal and the background, neither of which are likely to be entirely stationary. While the papers in the *Signals in motion* Research Topic identify technical and logistic challenges in developing ways of experimentally and theoretically investigating dynamic signals and backgrounds, they also highlight a rich seam of research possibilities. We hope this stimulates increasing interest in dynamic signals in dynamic backgrounds.

Author contributions

ET and ME conceived, wrote and edited the manuscript, and approved the submitted version. All authors contributed to the article and approved the submitted version.

References

- Cuthill, I. C., Matchette, S. R., and Scott-Samuel, N. E. (2019). Camouflage in a dynamic world. *Curr. Opin. Behav. Sci.* 30, 109–115. doi: 10.1016/j.cobeha.2019.07.007
- Endler, J. A. (1990). On the measurement and classification of colour in studies of animal colour patterns. *Biol. J. Linnean Soc.* 41, 315–352. doi: 10.1111/j.1095-8312.1990.tb00839.x
- Ortega Ancel, A., Eastwood, R., Vogt, D., Ithier, C., Smith, M., Wood, R., et al. (2017). Aerodynamic evaluation of wing shape and wing orientation in four butterfly species using numerical simulations and a low-speed wind tunnel, and its implications for the design of flying micro-robots. *Interface Focus* 7:20160087. doi: 10.1098/rsfs.2016.0087
- Tan, E. J., and Elgar, M. A. (2021). Motion: enhancing signals and concealing cues. *Biol. Open* 10:bio058762. doi: 10.1242/bio.058762

Funding

This work was supported by the Ministry of Education, Singapore and Yale-NUS College Start-up Grant to ET.

Acknowledgments

We thank the authors of the nine papers in this Research Topic for their contributions.

Conflict of interest

The authors declare that the research was conducted in the absence of any commercial or financial relationships that could be construed as a potential conflict of interest.

Publisher's note

All claims expressed in this article are solely those of the authors and do not necessarily represent those of their affiliated organizations, or those of the publisher, the editors and the reviewers. Any product that may be evaluated in this article, or claim that may be made by its manufacturer, is not guaranteed or endorsed by the publisher.



Territorial Displays of the *Ctenophorus decresii* Complex: A Story of Local Adaptations

Jose A. Ramos* and Richard A. Peters

Animal Behavior Group, Department of Ecology, Environment and Evolution, La Trobe University, Melbourne, VIC, Australia

OPEN ACCESS

Edited by:

Mark A. Elgar,
The University of Melbourne, Australia

Reviewed by:

Peter Dijkstra,
Central Michigan University,
United States
Daniel Osorio,
University of Sussex, United Kingdom

*Correspondence:

Jose A. Ramos
j.ramos@latrobe.edu.au

Specialty section:

This article was submitted to
Behavioral and Evolutionary Ecology,
a section of the journal
Frontiers in Ecology and Evolution

Received: 28 June 2021

Accepted: 22 November 2021

Published: 10 December 2021

Citation:

Ramos JA and Peters RA (2021)
Territorial Displays of the *Ctenophorus*
decresii Complex: A Story of Local
Adaptations.
Front. Ecol. Evol. 9:731705.
doi: 10.3389/fevo.2021.731705

Closely related species make for interesting model systems to study the evolution of signaling behavior because they share evolutionary history but have also diverged to the point of reproductive isolation. This means that while they may have some behavioral traits in common, courtesy of a common ancestor, they are also likely to show local adaptations. The *Ctenophorus decresii* complex is such a system, and comprises six closely related agamid lizard species from Australia: *C. decresii*, *C. fionni*, *C. mirityana*, *C. modestus*, *C. tjanjalka*, and *C. vadrappa*. In this study, we analyze the motion displays of five members of the *C. decresii* complex in the context of their respective habitats by comparing signal structure, habitat characteristics and signal contrast between all species. Motor pattern use and the temporal sequence of motor patterns did not differ greatly, but the motion speed distributions generated during the displays were different for all species. There was also variation in the extent to which signals contrasted with plant motion, with *C. vadrappa* performing better than the other species at all habitats. Overall, this study provides evidence that members of the *C. decresii* complex exhibit local adaptations in signaling behavior to their respective habitat, but they also maintain some morphological and behavioral traits in common, which is likely a consequence from the ancestral state.

Keywords: agamid, signaling, environmental noise, 3D reconstruction, adaptation, display

INTRODUCTION

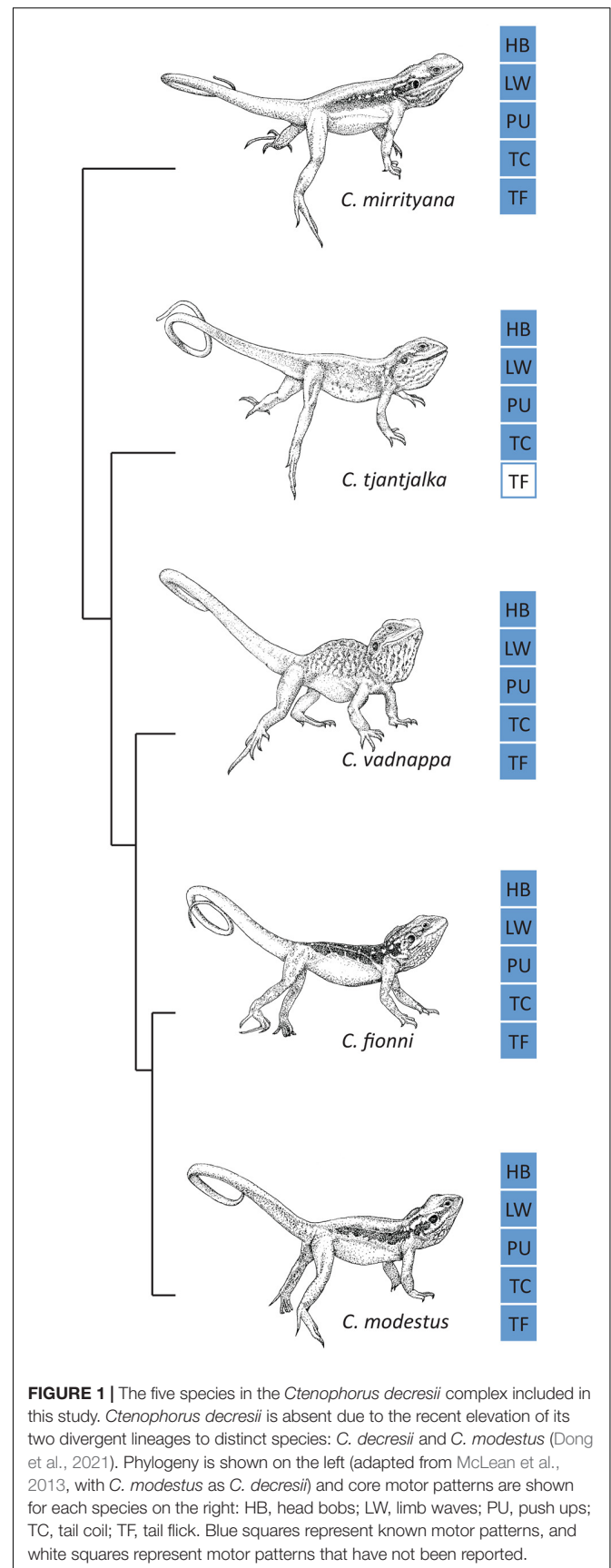
Theory suggests that animal signal structure will have phylogenetic determinants, be constrained by morphology and physiology, and influenced by the environment in which signaling takes place. The structure of present day signals can be historically contingent such that related species share characteristics that differ from more distantly related species, but also that the capacity for evolutionary divergence is constrained by the ancestral state (Ord et al., 2011; Ord, 2012). Morphological differences will dictate the kinds of signals that animals can produce. For example, body size constrains acoustic structure in mammals (Reby and McComb, 2003), amphibians (Ryan and Brenowitz, 1985) and insects (Lubanga et al., 2016), while physiological limitations of visual threat displays are related to signal performance (Brandt, 2003). The environment in which signaling takes place is also a major contributor to signal diversity. Differences in microhabitat structure lead to variation in signal structure within species (acoustic signals: Hunter and Krebs, 1979; visual signals: Ramos and Peters, 2017a), while a/biotic noise will lead to long term (Slabbekoorn and Smith, 2002) and short-term changes in signal structure in a variety of signaling

systems (Brumm, 2014), including acoustic (Slabbekoorn and Peet, 2003; Slabbekoorn, 2013) and visual (Ord et al., 2007; Peters et al., 2007) signals. What is sometimes difficult to determine is the relative contribution of environmental effects to variations in signal structure within and between species.

The influence of morphology and physiology on signal diversity can often be determined in a straightforward manner by relating specific traits to morphological measurements (Podos, 2001; Podos and Nowicki, 2004) or calculating energetic costs (Vehrencamp et al., 1989; Hoback and Wagner, 1997; Matsumasa and Murai, 2005; Stoddard and Salazar, 2011). Similarly, as closely related species are more likely to exhibit similar traits, the influence of phylogeny is now routinely examined by controlling for shared ancestry in the statistical model using phylogenetic comparative methods (PCMs; Ord and Martins, 2006; Turner et al., 2007). In contrast, environmental effects on signaling are more difficult to quantify and disentangle from morphological and phylogenetic constraints. Consequently, a useful way to consider the relative contribution of habitat characteristics and environmental effects is to select closely related species to minimize variation in phylogeny and morphology/physiology. Our understanding of environmental influence for some signaling modalities, such as sound and static visual signals, has progressed greatly with the use of playback experiments, and specialized tools like sound spectrographs and spectrophotometers (Morton, 1975; Ryan et al., 1990; Leal and Fleishman, 2004; Cocroft and Rodriguez, 2005; McLean et al., 2014). However, less information is available for motion-based visual displays as relevant environmental effects are more complex to quantify (Ramos and Peters, 2017b).

Dynamic visual signals are common in lizards and are used in a variety of contexts including male-female interactions (Peters et al., 2016), predator avoidance (Hasson, 1991), and territorial defense (Carpenter, 1978). Displays produced to defend a territory are particularly useful to lizards as they allow rivals, usually males, to assess each other from a distance and avoid physical confrontations (Peters and Ord, 2003). Color-based visual signals, which are also common among lizard families (Stuart-Fox and Ord, 2004), often require movements to expose brightly colored parts of the body, such as throat, dewlap, chest or abdomen (Mitchell, 1973; LeBas and Marshall, 2000; Stuart-Fox and Moussalli, 2008; Fleishman et al., 2009; Teasdale et al., 2013). The motor patterns involved in motion-based displays vary between species, but they often include dewlap extensions, head bobs, limb waves, tail flicks, or push ups (Carpenter, 1962; Carpenter et al., 1970; Purdue and Carpenter, 1972; Ord and Martins, 2006; Ramos and Peters, 2016).

The detection of lizard displays can be affected by the surrounding environment, as receivers need to filter out irrelevant environmental motion noise (Fleishman and Persons, 2001; Leal and Fleishman, 2002, 2004; Peters and Evans, 2003a; Peters, 2008). In the case of motion-based signaling lizards, the main source of motion noise is wind-blown plants (Fleishman, 1986; Peters and Evans, 2003a). Thus, motion-based signals are most effective when they stimulate the visual system of receivers in a way the noise environment does not (Fleishman, 1992). This means that the motion produced by the signal needs to contrast




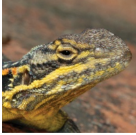
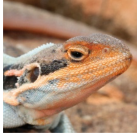


with the motion generated by the plants surrounding it (Endler, 1991; Fleishman, 1992; Peters et al., 2007; Bian et al., 2019). Additionally, the noise environment is site specific as it stems from the individual plants present and the topography of the area (Peters et al., 2008; Peters, 2013). Consequently, local adaptations to overcome noise and enhance signal efficacy should be expected in species occupying structurally distinct habitats. Within species variability of this kind has been observed (Ramos and Peters, 2017b), but data across species are limited.

We wished to examine whether environmental effects can be detected across multiple Australian agamid lizard species, controlling as much as possible for shared ancestry and differences in morphology. There are 14 genera of agamid lizards in Australia (Wilson and Swan, 2017), from which *Ctenophorus* is the most diverse ($N = 29$; McLean et al., 2013; Wilson and Swan, 2017; Dong et al., 2021) and has the highest number of known signaling species ($N = 18$; Ramos and Peters, 2016; Dong et al., 2021). Some of the most interesting species within the genus in terms of their social behavior belong to the *Ctenophorus decresii* complex, which consists of six closely related species (Figure 1; McLean et al., 2013): the tawny dragon (*C. decresii*), the peninsula dragon (*C. fionni*), the Barrier Range dragon (*C. mirrityana*), the swift rock dragon (*C. modestus*), the ochre dragon (*C. tjantjalka*), and the red-barred dragon (*C. vadrappa*). A recent study elevated the two lineages of *C. decresii* into distinct species, *C. decresii* as the southern lineage (Mount Lofty Ranges, Fleurieu Peninsula and Kangaroo Island in South

Australia; Dong et al., 2021) and *C. modestus* as the northern lineage (Flinders Ranges and Olary Ranges, in South Australia; Dong et al., 2021). These species are sexually dimorphic, and the males usually display bright and conspicuous coloration during the breeding season (Gibbons, 1979; McLean et al., 2013). They are also very similar in size, with *C. tjantjalka* possessing the smallest snout vent length (73 mm; Wilson and Swan, 2017) and *C. decresii* the largest (96 mm; Wilson and Swan, 2017). All members of the complex are dorsoventrally flattened and long-limbed; both of which are adaptations to their rocky habitats (for detailed descriptions of all species in the complex see Gibbons, 1977; Gibbons, 1979; Johnston, 1992; McLean et al., 2013; Dong et al., 2021). The six species in the *C. decresii* complex are territorial, and perform aggressive stereotyped motion displays against intruders (Gibbons, 1979; Osborne, 2005; McLean et al., 2013; Ramos, 2017). These displays can be divided in three sequential phases (Gibbons, 1979): lowering of dewlap and limb waves, hind leg push ups with tail coiling and head bobbing. While superficially similar, the displays performed by three members of the complex have been reported to differ both inter- and intra- specifically in speed, amplitude and number of repetitions of individual motor patterns (Gibbons, 1979). Additionally, it has been suggested that these differences could aid in taxonomic differentiation at the species level (Gibbons, 1979).

Our aim was to explore the signaling behavior of the *C. decresii* complex to determine whether potential environmental

TABLE 1 | General information and current study information for all species belonging to the *Ctenophorus decresii* complex included in this study.

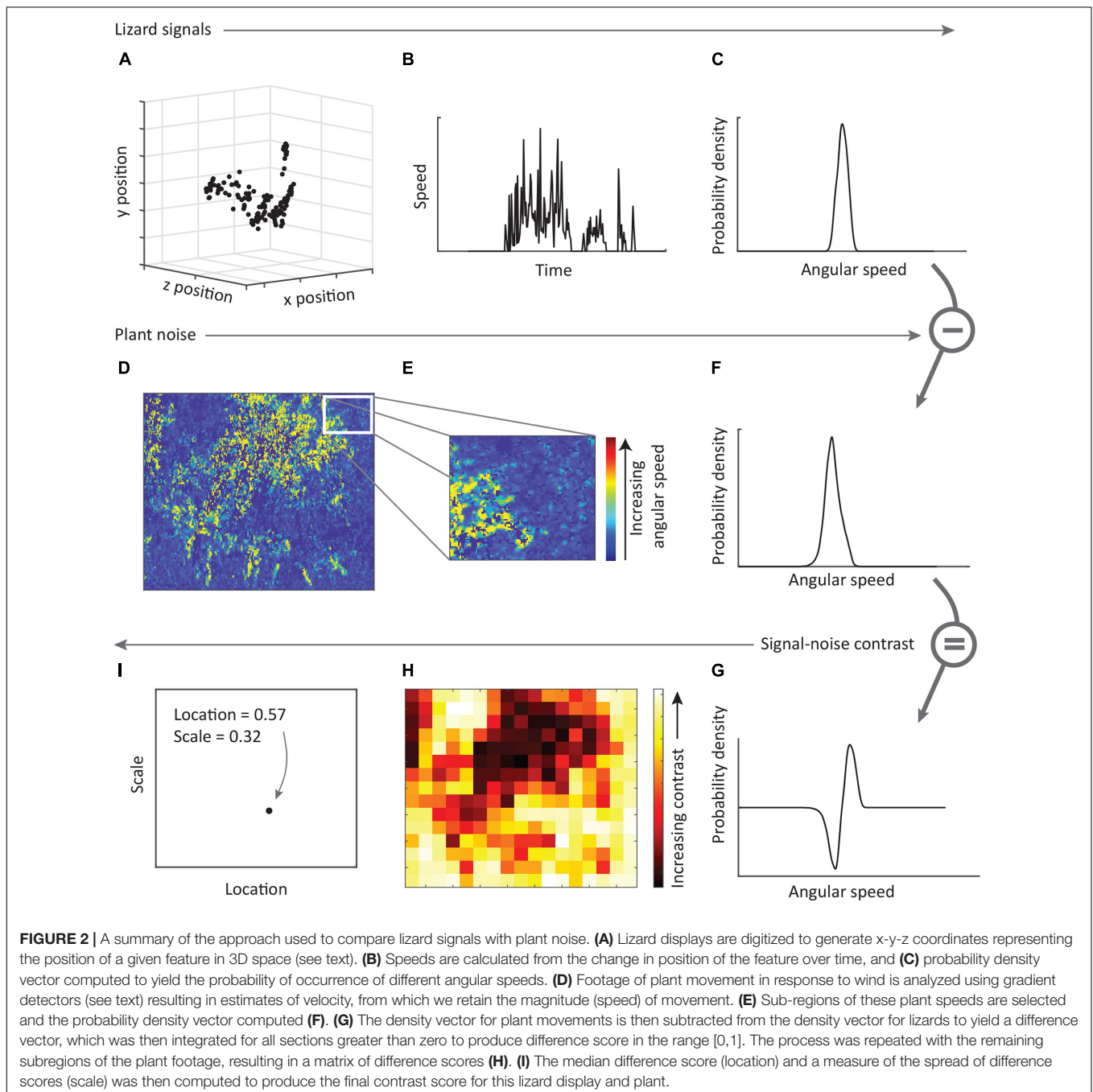
						
		Swift rock dragon <i>C. modestus</i>	Peninsula dragon <i>C. fionni</i>	Barrier Range dragon <i>C. mirrityana</i>	Ochre dragon <i>C. tjantjalka</i>	Red-barred dragon <i>C. vadrappa</i>
General information	Distribution	Rocky ranges and outcrops throughout the Flinders Ranges and Olary Ranges in South Australia	Rocky ranges and outcrops of Eyre Peninsula and adjacent areas, including islands, of South Australia	Rocky outcrops and gorges surrounding Broken Hill and hills of north-central South Australia	Rocky outcrops and stony hills of north-central South Australia	Rocky ranges and outcrops of arid central South Australia, from north Flinders Ranges to north of Lake Torrens
	Sympatry	<i>C. vadrappa</i> North of Flinders Ranges National Park	None	None	None	<i>C. modestus</i> North of Flinders Ranges National Park
Current study	Location (N)	Flinders Ranges National Park (13) S33° 32.173' E138° 36.036' Telowie Gorge Conservation Park (2) S33° 01.368' E138° 06.421'	Gawler Ranges National Park (12) S32° 35.284' E135° 26.552'	Mutawintji National Park (2) S31° 16.101' E142° 17.031'	Coober Pedy area (1) S28° 29.587' E134° 12.412'	Parachilna gorge (4) S31° 08.558' E138° 32.143'
	Habitat	Recently burnt rocky outcrop with low vegetation. Rocky gorge with small to medium vegetation.	Rocky outcrop with very little vegetation. Rocky substrate.	Rocky outcrop with small to medium vegetation. Sandy substrate with gravel.	Rocky outcrop with small to medium vegetation. Rocky substrate.	Rocky gorge with small to medium vegetation. Rocky substrate with gravel.

differences would be manifested as differences in signal structure. Our fieldwork preceded the recent reclassification of *C. decresii* and thus focuses on 5 of the 6 species (excluding *C. decresii*). This is an ideal group to examine this aim as they are closely related, morphologically similar and utilize signals that are superficially the same. However, they occupy slightly different microhabitats, and their signals have not been subjected to detailed analysis or comparison. Consequently, we address our aim by asking three underlying questions:

1. How similar are the signals of the five species?

2. How similar are the microhabitats of the five species?
3. How effective are the signals of each species in all habitats?

Our work was undertaken in the field and involved locating and filming unrestrained wild animals *in situ*, then carefully documenting the microhabitats in which signaling takes place. We have combined broad level analysis of the temporal structure and use of male territorial displays, with detailed quantification of displays following the approach described by Ramos and Peters (2017b), which involves reconstructing lizard display motion in three dimensions (3D) and comparing



it to the noise environment to calculate signal contrast. By recording the signals and the relevant features of the noise environment independently, we are able to assess the

performance of each species at the habitats of the other members of the *C. decresii* complex without physically translocating the lizards. We hypothesize that signaling displays will reflect

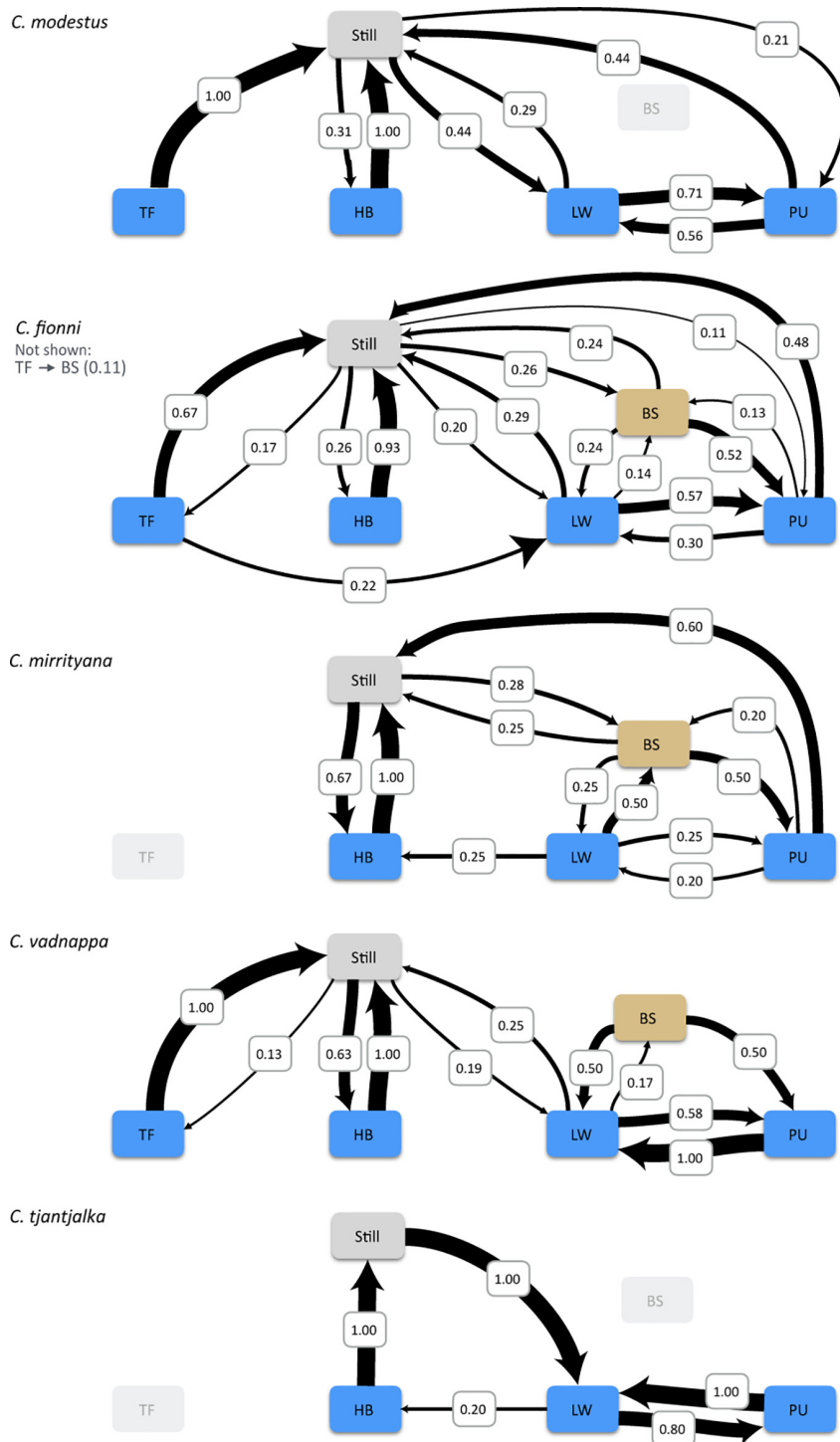


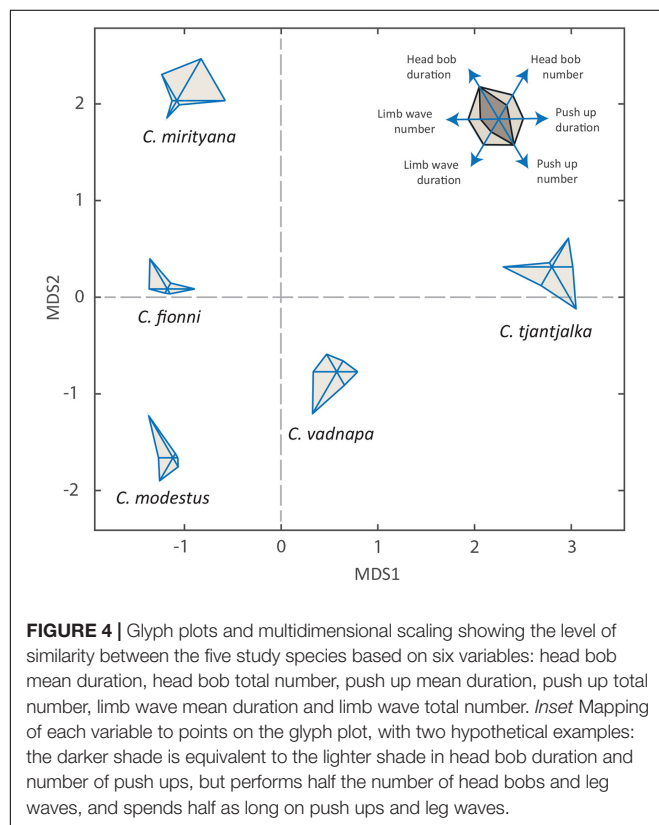
FIGURE 3 | Transition probabilities belonging to the territorial displays of the five study species. The plots illustrate the sequence in which motor patterns (HB, head bob; LW, limb wave; PU, push up; TF, tail flick) and body switch (BS; change in position) are used during the display and the probability that one motor pattern will occur after another. All sequences start from a still position. Tail flicking is known to occur in *C. mirityana* but was not observed during the analyses.

TABLE 2 | Coefficients of variation calculated within and between species for mean duration and total number of motor pattern events (HB, head bobs; PU, push ups; LW, limb waves).

	HB mean duration	HB total number	PU mean duration	PU total number	LW mean duration	LW total number
MEAN						
<i>C. modestus</i>	0.06	0.80	1.14	2.27	0.29	5.47
<i>C. fionni</i>	0.20	1.43	0.99	2.57	0.16	4.64
<i>C. mirityana</i>	0.33	15.00	0.94	1.50	0.25	4.50
<i>C. vadrappa</i>	0.16	3.33	0.83	3.00	0.42	6.33
<i>C. tjantjalka</i>	0.16	10.00	0.66	5.00	0.26	12.00
SD						
<i>C. modestus</i>	0.08	1.01	0.41	0.59	0.15	3.46
<i>C. fionni</i>	0.29	2.28	0.24	1.22	0.11	3.67
<i>C. mirityana</i>	0.06	4.24	0.05	0.71	0.35	6.36
<i>C. vadrappa</i>	0.14	3.06	0.26	1.00	0.05	2.08
<i>C. tjantjalka</i>	–	–	–	–	–	–
CV within						
<i>C. modestus</i>	1.38	1.27	0.36	0.26	0.53	0.63
<i>C. fionni</i>	1.43	1.59	0.24	0.48	0.71	0.79
<i>C. mirityana</i>	0.17	0.28	0.05	0.47	1.41	1.41
<i>C. vadrappa</i>	0.87	0.92	0.31	0.33	0.13	0.33
<i>C. tjantjalka</i>	–	–	–	–	–	–
Overall MEAN	0.14	2.12	1.04	2.41	0.25	5.12
Overall SD	0.21	3.84	0.33	0.96	0.16	3.49
CV between	1.47	1.82	0.32	0.40	0.66	0.68
CV B/W ratio	1.53	1.79	1.32	1.03	0.95	0.86

Overall values and coefficients of variation were calculated without taking *C. tjantjalka* into account due to its sample size. Overall and individual species means are included with standard deviation.

the shared ancestry of the five species to some extent, but the details will differ in a manner that is linked to local signaling conditions.



MATERIALS AND METHODS

Data Collection

We recorded territorial displays from *C. fionni*, *C. mirityana*, *C. modestus*, *C. tjantjalka*, and *C. vadrappa* at different locations in New South Wales and South Australia, Australia, between 2012 and 2017 (see **Table 1** for details). Data available for *C. tjantjalka* is limited due to the difficulty we encountered in locating this species and filming interactions. The display footage we report on herein for *C. tjantjalka* represents the only record for this species. In order to elicit these displays from free living male lizards, a tethered conspecific intruder was introduced to their territory at a distance of approximately 1 m from the resident. The displays were recorded using a dual camera approach following Hedrick (2008) and Peters et al. (2016), which allowed us to reconstruct lizard motion in 3D. The habitat of the signaling lizard was mapped and characterized in detail by identifying and filming the plants that constituted a source of motion noise under artificially created standardized windy conditions of 4 m/s (see Ramos and Peters, 2017b). As part of this process, signaler-plant distances were recorded for all relevant plants.

Display Analysis

Display sequences were analyzed using Observer XT (Noldus Inc.) by recording the start and end point of each individual motor pattern during the displays of all species. We then used these data to describe motor pattern use in terms of duration and total number of motor pattern events. Coefficients of variation within (CV_W) and between (CV_B) species were computed to determine if any of these variables differed between the members of the complex. The ratio of CV_B/CV_W provides a measure of the relative coefficient of variation between and

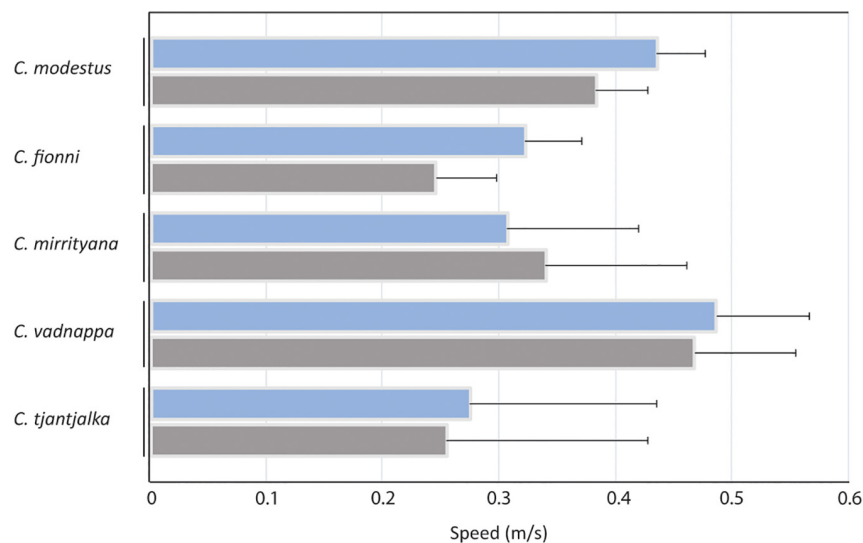


FIGURE 5 | Comparisons of the motion speeds used by all species when all motor patterns are averaged (blue), and individually for head bobs (gray). Estimated marginal means, calculated from the linear model, are presented for *C. modestus*, *C. fionni*, *C. mirityana*, *C. vadrappa* and *C. tjantjalka*. Error bars represent 95% confidence intervals.

within species, where CV_W is the average of CV_W for all species. When the ratio CV_B/CV_W is greater than 1, there is more variation between species than within species. We also explored variation in motor pattern use graphically using glyph plots in Matlab (Mathworks Inc.). We used the *glyphplot* function to define each glyph, and positioned them in space based on non-metric multidimensional scaling of the dissimilarity matrix of our set of display characteristics. Additionally, display sequence information was used to calculate transition probabilities for the motor patterns employed, as well as changes in body position and periods of being stationary during the displays.

Lizard and Plant Motion

Our approach for quantifying signal structure and environmental noise is explained in detail elsewhere (see Ramos and Peters, 2017b; **Supplementary Figure 1**). Briefly, in order to reconstruct the displays in 3D as x-y-z coordinates, several points along the body of the lizards were digitized in the footage from both cameras. These points corresponded to body parts commonly used during territorial displays, and included the eye (head bobs), both fore limbs (limb waves), and the base of the tail (four-legged push ups). The information from both cameras was then combined using direct linear transformation in Matlab. Once signal motion was reconstructed in 3D, angular speeds at a viewing distance of 1 m were computed as described by Ramos and Peters (2017b), and summarized for all motor patterns in the display individually, and for the display as a whole (all motor patterns combined). We used the *ksdensity* function in Matlab to generate a vector of relative probability at different angular speeds (kernel density estimates).

The motion generated by wind-blown plants in 5 s of footage (125 frames; 25 frames/s) was quantified using a gradient detector model (Peters et al., 2002). The output from the models comprises

direction and magnitude of movements in the image sequences. We retained the magnitude component as a measure of speed and converted from units of pixels to cm using an object of known size in the frame from the plant footage. Comparing lizard displays against the movement of the whole plant would not reflect the motion segmentation task of receivers (see Ramos and Peters, 2017b), so we divide the plant motion output into subregions, and calculated the angular speed vector (kernel density estimate) for each of these subregions, using a viewing distance of 1 m plus the signaler-plant distance for the respective plant. This was repeated for all plants in the scene.

Signal—Noise Analysis

Our goal with this analysis was to determine how well the signals of each species performs compared with other species in the complex, and also to identify the habitats that are more likely to negatively affect motion signals due to their motion noise properties. We have described fully our rationale and approach to quantifying signal contrast elsewhere (see Ramos and Peters, 2017b), and present below a summary of our method (see **Figure 2**). Angular speeds from lizard displays (**Figure 2A**) and plant motion (**Figure 2D**) were quantified separately as described above. For each subregion of a given plant, the angular speed vector (kernel density estimate) for plant motion was subtracted from that of the lizard display to produce a difference curve (**Figure 2G**). Integrating this difference curve for all values greater than zero (i.e., lizard movement greater than plant motion at that angular speed) provides a value (0–1) representing the probability that lizard movement differs from plant movement. A score close to 1 implies lizard movement is greater than plant movement, while a score of 0 indicates the reverse. This was then repeated for all subregions of the plant. The values obtained from all subregions of a given lizard-plant combination were

TABLE 3 | Outcome of statistical models for speed of movement, showing the results for all motor patterns combined, and for individual motor patterns.

	Df	Sum Sq	Mean Sq	F value	Pr (>F)
All motor patterns					
Species	4	0.144	0.036	5.874	0.002
Residuals	28	0.171	0.006		
Contrast		Value	Std. Error	t-value	p-value
<i>C. modestus</i>—<i>C. fionni</i>		−0.112	0.031	−3.614	0.001
<i>C. modestus</i>—<i>C. mirrityana</i>		−0.128	0.059	−2.165	0.039
<i>C. modestus</i> — <i>C. vадnappa</i>		0.051	0.044	1.163	0.255
<i>C. modestus</i> — <i>C. tјantјalka</i>		−0.160	0.081	−1.976	0.058
<i>C. fionni</i> — <i>C. mirrityana</i>		−0.015	0.060	−0.254	0.801
<i>C. fionni</i>—<i>C. vадnappa</i>		0.163	0.046	3.577	0.001
<i>C. fionni</i> — <i>C. tјantјalka</i>		−0.047	0.082	−0.581	0.566
<i>C. mirrityana</i>—<i>C. vадnappa</i>		0.179	0.068	2.637	0.014
<i>C. mirrityana</i> — <i>C. tјantјalka</i>		−0.032	0.096	−0.336	0.740
<i>C. vадnappa</i>—<i>C. tјantјalka</i>		−0.211	0.087	−2.411	0.023
Head bob/eye					
Species	4	0.198	0.049	7.085	0.000
Residuals	28	0.196	0.007		
Contrast		Value	Std. Error	t-value	p-value
<i>C. modestus</i>—<i>C. fionni</i>		−0.137	0.033	−4.139	0.000
<i>C. modestus</i> — <i>C. mirrityana</i>		−0.043	0.063	−0.691	0.495
<i>C. modestus</i> — <i>C. vадnappa</i>		0.085	0.047	1.799	0.083
<i>C. modestus</i> — <i>C. tјantјalka</i>		−0.128	0.086	−1.483	0.149
<i>C. fionni</i> — <i>C. mirrityana</i>		0.094	0.064	1.461	0.155
<i>C. fionni</i>—<i>C. vадnappa</i>		0.222	0.049	4.548	0.000
<i>C. fionni</i> — <i>C. tјantјalka</i>		0.009	0.087	0.107	0.915
<i>C. mirrityana</i> — <i>C. vадnappa</i>		0.128	0.072	1.770	0.088
<i>C. mirrityana</i> — <i>C. tјantјalka</i>		−0.085	0.102	−0.825	0.416
<i>C. vадnappa</i>—<i>C. tјantјalka</i>		−0.213	0.093	−2.275	0.031
Push up/tail base					
Species	4	0.104	0.026	2.641	0.059
Residuals	24	0.237	0.010		
Limb wave/foreleg					
Species	4	0.075	0.019	1.929	0.152
Residuals	17	0.165	0.010		

A linear model with "species" as the predictor variable and square-root transformed dependent variables was used. Significance is indicated in bold.

summarized by obtaining the median as a measure of central tendency (location), as well as a measure of the spread of the data. To represent this spread, we used the scale parameter rather than other measures of variance as it is more suited to non-normal distributions. A higher scale value suggests that lizard displays contrast strongly against parts of the plant, but relatively poorly against other parts because movement is not uniformly distributed across the plant. We refer to location and scale values collectively as contrast scores, and computed these for each lizard and each plant in all habitats (Figure 2I). So, we obtained contrast scores for each species at their own microhabitat, as well as all other microhabitats inhabited by their own and other species. Regardless of which lizard was considered in a given microhabitat, all lizards were positioned in the scene at the same location as the inhabitant of the given microhabitat. As such, signaler-plant distances were constant for a given microhabitat.

Statistical Analyses

As outlined above, display sequences were analyzed by comparing coefficient of variation values of motor pattern use and computing transition probabilities between motor patterns. In addition, we compared the average speed of movement across species. The speed of movement was computed from the x-y-z coordinates (see above) as the change in position between successive frames (this represents the step prior to computing angular speeds and probability density functions for signal-noise contrast analysis described above). We calculated the average speed per display across all movements, and for movement of the eye, tail base and foreleg separately. Data were analyzed using the *lm* function in the R statistical environment (R Core Team, 2016) with species as the sole predictor variable and after square-root transformation of dependent variables. The number of plants in each microhabitat was analyzed using a generalized linear model (*glm* function) in R fitting a poisson error distribution, while variation in signaler-plant distances was analyzed using a linear mixed effects model using the *lme* function from the *nlme* package in R (Pinheiro et al., 2018), with species as a fixed effect and site as a random effect to account for multiple plants at a given site. Signal contrast scores were obtained against each plant in each habitat and a convex hull was computed for each display x habitat combination. Convex hulls were compared visually.

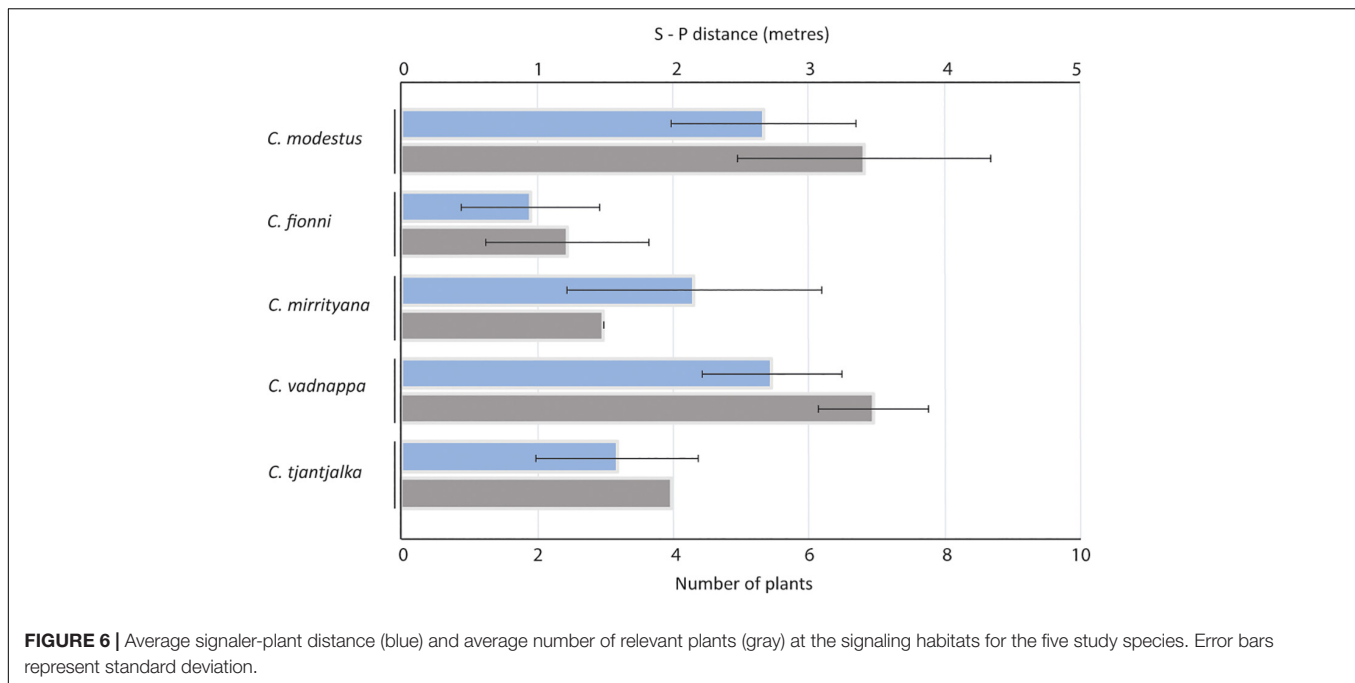
RESULTS

How Similar Are the Displays?

To the naked eye, the male territorial displays of the five study species are remarkably similar. They all include the same motor patterns, as described by Gibbons (1979) for *C. modestus* (as *C. decresii*), *C. fionni* and *C. vадnappa*: limb waves, rear limb push ups and head bobs (Figure 1). Additionally, members of the complex seem to occasionally include tail flicks at the beginning of the displays in a way reminiscent of the introductory tail flick utilized by *Amphibolurus muricatus* (Peters and Evans, 2003b; Osborne, 2005; Peters et al., 2007).

Transition probabilities between motor patterns show very little differences between species (Figure 3). In general, displays of all species can begin with tail flicking, followed by a series of limb waves, then a period of push ups, often separated by additional limb waves, and finish with a series of head bobs. Lizards might then change position and repeat the process. This sequence matches the phases described by Gibbons (1979), although it does not apply to every single display, and it is not uncommon for individual motor patterns to be absent from a given display. Tail flicking for example, is only rarely used by each species. Pauses in motion and shifts in position are also often observed in between motor patterns (Figure 3), which adds to the behavioral complexity previously described for the group. Notwithstanding small differences, the overall sequences are similar for all species.

However, variation does exist in motor pattern use at the finer scale. The frequency of use and duration of each motor pattern is summarized in Table 2. Coefficients of variation (CVs) revealed that the number of head bobs used during a display is



almost twice as variable between species as it is within species. Similarly, the ratio of between and within CVs for both head bob and push up durations suggest between species variability, albeit to a slightly lesser extent than the number of head bobs used. **Figure 4** provides a graphic representation of these data and the differences between species. Here, values for each parameter are used as vertices in glyph plots, which are then presented in multi-dimensional space to further highlight similarities/dissimilarities (**Figure 4**). *Ctenophorus modestus*, *C. fionni*, and *C. vadrappa* are considered more similar, with *C. mirrityana* and *C. tjantjalka* being differentiated from them. Interestingly, relative placements within the multi-dimensional space appear to reflect underlying phylogenetic relationships.

The average speed of movement across all motor patterns is shown in **Figure 5** and was found to differ significantly across species (**Table 3**). *Ctenophorus vadrappa* displays were significantly faster than *C. mirrityana*, *C. fionni*, and *C. tjantjalka* but equivalent to *C. modestus*. In addition, *C. modestus* was significantly faster than *C. mirrityana* and *C. fionni* but not quite reaching significance when compared with *C. tjantjalka*. **Table 3** also reports results for each motor pattern separately. An effect of species was seen for movement measured at the eye, but not quite for the tail base or forelegs.

How Similar Are the Microhabitats?

After mapping in detail the locations where the lizards performed their displays, it was clear that species occur in somewhat different plant environments. The signaling locations for *C. modestus* and *C. vadrappa* contained on average a greater number of noise producing plants than the locations for *C. fionni* and *C. mirrityana* (**Figure 6**). Furthermore, the signaler-plant distances were much larger for *C. modestus* and *C. vadrappa* than for the other species, and *C. fionni* appears to signal very

close to plants when they are present in their territory (**Figure 6**). Generalized linear models and mixed effects models, respectively, were used to compare these differences and revealed significant differences across species (**Table 4**). Pairwise contrasts suggest fewer plants present in the microhabitats of *C. fionni* compared with *C. modestus* and *C. vadrappa*, while *C. modestus* also contained significantly more plants than *C. mirrityana*. Pairwise contrasts for signaler-plant distances revealed only that *C. fionni* was signaling significantly closer to plants than *C. modestus*.

Are Signals Effective in Each Microhabitat?

Our contrast scores provide insight into the potential masking effect of plant motion in the environment and were calculated as the difference between the motion of display movements (all tracked body parts) and the movements of windblown plants. Contrast scores are binary (location, scale) and are computed separately for each plant in a given microhabitat (see Materials and Methods; Ramos and Peters, 2017b provide the rationale behind this approach). Contrast scores were obtained for all species against all plants in all habitats and are summarized as convex hulls in **Figure 7**. Species-habitat combinations with large convex hulls implies greater variability in signal-noise contrast scores, and therefore greater heterogeneity in the motion noise environment and more opportunity for signals to be masked by plant motion. Focussing on habitats (comparing columns in **Figure 6**), the area of convex hulls is greatest for *C. modestus*, *C. fionni*, and then *C. vadrappa*. These habitats also feature the most plants (*C. modestus*, *C. vadrappa*) or shortest signaler-plant distances (*C. fionni*). Focussing on species (comparing rows in **Figure 6**), *C. vadrappa* displays are predicted to be the least affected by motion noise at all habitats,

TABLE 4 | Outcome of statistical models for plant number and s-p distances, using a generalized linear model and a linear mixed model, respectively, to compare microhabitat structure for each species.

Number of plants	Model		Residual		Pr(> Chi)
	Df	Deviance	Df	Deviance	
NULL			32	45.942	
Species	4	31.804	28	14.138	< 0.001
	Contrast	Estimate	Std. Error	z-value	p-value
C. modestus—C. fionni		-1.029	0.216	-4.758	0.000
C. modestus—C. mirrityana		-0.828	0.420	-1.972	0.049
C. modestus—C. vadrappa		0.019	0.213	0.090	0.928
C. modestus—C. tjantjalka		-0.540	0.510	-1.060	0.289
C. fionni—C. mirrityana		0.201	0.451	0.445	0.657
C. fionni—C. vadrappa		1.048	0.270	3.885	0.000
C. fionni—C. tjantjalka		0.488	0.536	0.912	0.362
C. mirrityana—C. vadrappa		0.847	0.450	1.883	0.060
C. mirrityana—C. tjantjalka		0.288	0.646	0.446	0.656
C. vadrappa—C. tjantjalka		-0.560	0.535	-1.047	0.295
Signaler-plant distance	Df		F-value		p-value
	Num	Den			
Species	4	28	3.182		0.03
	Contrast	Value	Std. Error	t-value	p-value
C. modestus—C. fionni		-0.978	0.288	-3.398	0.002
C. modestus—C. mirrityana		-0.028	0.554	-0.050	0.961
C. modestus—C. vadrappa		-0.499	0.296	-1.684	0.103
C. modestus—C. tjantjalka		-0.437	0.681	-0.641	0.527
C. fionni—C. mirrityana		0.951	0.594	1.601	0.121
C. fionni—C. vadrappa		0.480	0.365	1.315	0.199
C. fionni—C. tjantjalka		0.541	0.713	0.759	0.454
C. mirrityana—C. vadrappa		-0.471	0.598	-0.788	0.437
C. mirrityana—C. tjantjalka		-0.409	0.856	-0.478	0.637
C. vadrappa—C. tjantjalka		0.062	0.717	0.086	0.932

Significance is indicated in bold.

followed by *C. modestus*, *C. tjantjalka*, *C. mirrityana*, and lastly, *C. fionni*. These results correspond with relative signaling speeds of these species.

DISCUSSION

Results of the present study confirm that the motor pattern repertoire employed during the territorial displays of species in the *Ctenophorus decresii* complex are almost indistinguishable from each other, as previously reported by Gibbons (1979) for *C. modestus* (as *C. decresii*), *C. fionni*, and *C. vadrappa*. We consider the implications of our findings below, although we acknowledge that our sample size for two species is low ($N = 1$ and 2). We made concerted efforts to locate and record the visual displays of all species, but information on the behavior of most Australian dragons is very limited (Melville and Wilson, 2019), which hampered efforts to locate and film natural behavior. Consequently, we acknowledge below when our interpretations are more speculative because of limited data.

The general design of the displays does not seem to differ. However, upon closer inspection, motor pattern use does appear to vary. The coefficients of variation indicate that head bobs, and to a lesser extend push ups, are employed differently by all species (Table 2). This variation in the use of motor patterns appears consistent with their phylogeny, particularly in terms of the number and duration of the components (Figure 4). *Ctenophorus modestus*, *C. fionni* and *C. vadrappa* are more similar to each other (Figure 4). *Ctenophorus modestus* and *C. vadrappa* also produce the highest motion speed averages (Figure 5), but in this regard, variation does not occur as neatly along phylogenetic lines. Instead, display speed is fastest in species found in the most planted habitats (Figures 5, 6). Thus, the potential masking effect of environmental noise is high in the habitats of *C. modestus* and *C. vadrappa*. This is also true for *C. fionni*, but in the case of this species, it is likely attributed to slow display speeds (Figure 5), short S-P distances (Figure 6), or both. Consequently, the *Ctenophorus decresii* complex might be an example of closely related species, retaining ancestral behavioral traits that have been modified to suit their specific habitats.

Results from the signal-noise contrast analyses revealed that displays by *C. fionni* are more susceptible to environmental noise in all habitats, while *C. vadrappa* displays are the least affected in each habitat. This was expected given that *C. vadrappa* produced the fastest motion speed averages. Gibbons (1979) determined that the push ups produced by *C. vadrappa* had greater amplitude than the equivalent motor patterns from *C. modestus* and *C. fionni*. Greater amplitudes can translate into faster speeds if the time intervals are kept equal, which indicates similarities between both studies.

Signal contrast can be used to assess the performance of motion signals and also to infer differences across habitats in the production of noise, as explained by Ramos and Peters (2017a,b). All species seem to perform much better when their signals are considered at the habitats of *C. mirrityana*, which suggests the noise environment at these sites are less likely to mask the signals produced by the lizards (Figure 7). Although we only recorded at two sites for this species, our findings can be partially explained by looking at the distribution of vegetation at these sites and the surrounding area. *Ctenophorus mirrityana* habitat not only contains a low density of relevant plants, but the signaler-plant distance average was almost as high as in *C. modestus* and *C. vadrappa* habitat (Figure 7). These two traits combined seemed to promote effective signaling in this habitat for all species. The sites utilized by *C. fionni* for signaling contain an even lower plant density, but this species also displays the shortest signaler-plant distance average of all lizards in the study. This means that *C. fionni* lizards do not often encounter plants during their territorial displays, but when they do, they signal in very close proximity, and this has consequences for motion segmentation by receivers. As such, despite superficially looking like the ideal signaling location (i.e., mostly large, flat rocks, and scarce vegetation), contrast scores are lower in *C. fionni* habitats. Overall, the potential for noise and signal masking in the habitats of *C. modestus* and *C. vadrappa* is high, but the species manage to perform relatively well according to our data. Signaling faster might be a way for these two species to offset the masking

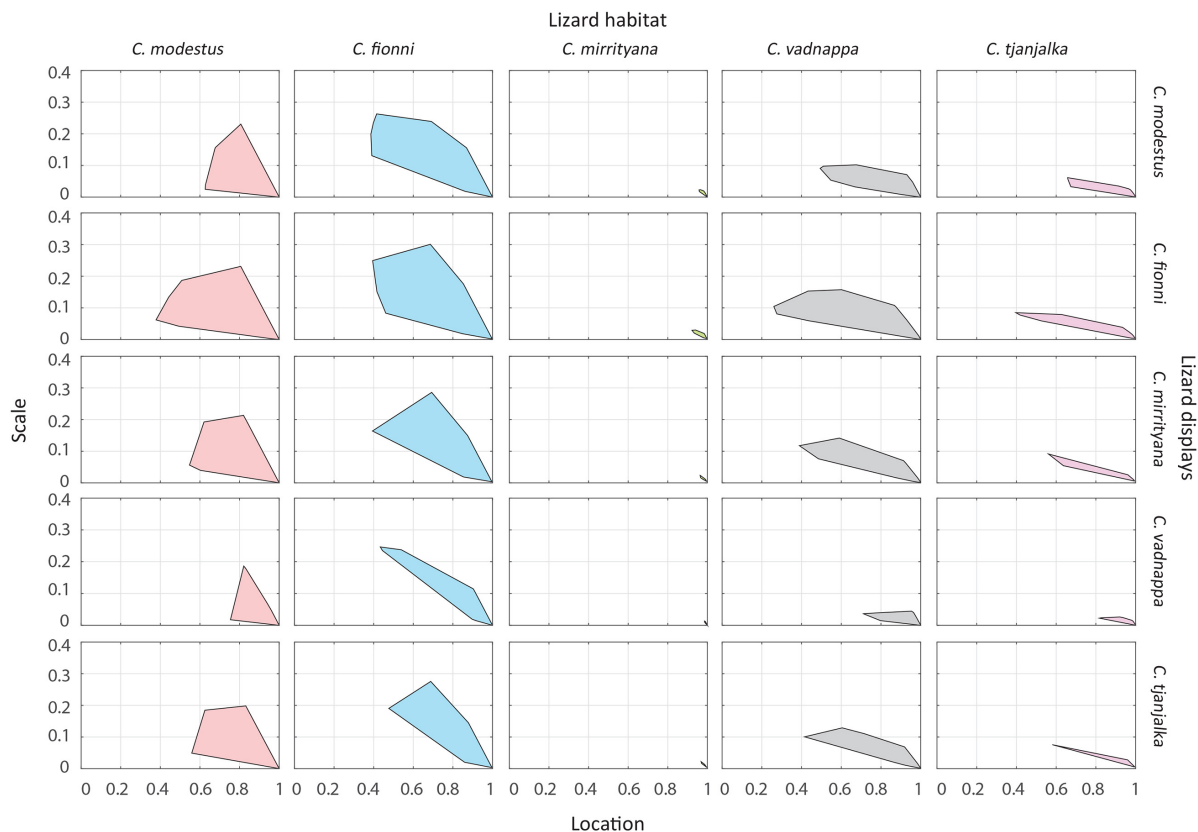


FIGURE 7 | Relative contrast of signals and noise for all species at all habitats. Each convex hull represents all the contrast values of all signals against all plants and views for a particular species at a particular habitat. The location (x axis) shows the central tendency of the contrast value, while the scale (y axis) shows the variation around the central tendency. A location value close to 1 and a scale value close to 0 indicate that display movements are much faster than plant movements. Large convex hulls indicate that there is high variability in signal contrast at the site, with some areas showing high contrast and others low contrast.

potential. As signaler-plant distances are smaller for *C. fionni*, attempts to signal faster against plant motion to improve contrast would be less effective (see Peters, 2013). Given the high speeds produced during their displays, it is not surprising that *C. vadrappa* performs best in all habitats compared to the other four species. Due to the nature of the fieldwork and the restricted and/or inaccessible distribution of some species, the sample sizes between species were inconsistent. Therefore, the results relating to comparisons of all five species should be taken with caution. This could explain the similarities between the convex hulls for *C. modestus*, *C. fionni*, and *C. vadrappa*, although our personal observations of the habitats for all species match well the sites that we sampled. It is also important to mention that despite the small sample size for *C. tjanjalka*, signaling in this species was reported in the literature for the first time in previous work (Ramos and Peters, 2016), but never recorded in free living lizards until now.

The results of this study suggest that there are signaling differences observed between species in this complex that are consistent with the notion of adaptations to the local environment. However, variation in the use of head bobs does appear relevant in a different context. Gibbons (1979) suggested that several aspects of the head bob motor pattern could have

a species recognition function and could also be employed to taxonomically differentiate the species in the complex. While the current study focused on other display characteristics and used a different approach to analyze motion signals, we also identified variation in head bob use, particularly in the average duration and number of bobs performed per display in *C. mirrityana*. This is not surprising given that the species is the most phylogenetically distant in the complex (McLean et al., 2013). *Ctenophorus mirrityana* has only recently been described and was not included in Gibbons' study, but variability in head bob use in our limited sample seems to be consistent. Nonetheless, species recognition might only be relevant for some populations of *C. modestus* and *C. vadrappa* that actually occur in sympatry. Gibbons (1979) identified the angle of the tail coil during the push up display as the most likely element for species recognition, and described it as vertical for *C. vadrappa* and horizontal for *C. modestus* (as *C. decresii*) and *C. fionni*. We did not observe the same pattern in the present study (data not presented). Instead, we compared other aspects of their signaling behavior and habitat. While we did not specifically look for differences between *C. modestus* and *C. vadrappa*, our results are mostly consistent with local adaptations and do not provide evidence that signaling behavior has a species recognition function. Historically both species

were sympatric in some of our study sites as late as the mid 1970's (Gibbons, 1979), but there currently does not seem to be an overlap in their distributions at these areas. Further studies on potential species recognition cues should target populations occurring in sympatry and therefore more likely to be influenced by the selective pressure of ensuring species recognition, and to show more obvious divergence in behavior.

Tail flicking behavior is yet another aspect worth exploring further. This motor pattern has been observed in all five species, however, according to our observations it is rarely included in the displays. In *A. muricatus*, most territorial displays are preceded by tail flicking, which tends to have a duration of several seconds (Peters and Evans, 2003b). In contrast, members of the *C. decresii* complex perform tail flicks infrequently and briefly. This might be related to the specific structure of the tail flicks, and if they are actually required to attract the attention of receivers and enhance signal efficacy, or it could be a remnant from an ancestral behavior. Regardless, it might be interesting to specifically analyze the function and structure of this motor pattern in the context of the noise environment.

Although there clearly is an effect of shared ancestry, our data provides evidence that members of the *C. decresii* complex exhibit adaptations in their signaling behavior to the local characteristics of their habitat. Some of these adaptations may also aid in species recognition, but our results are not conclusive in this matter. Many avenues of research remain untested in this group, such as the inclusion of *C. decresii* in the analyses, detailed studies of sympatric populations, and sampling of multiple populations for the wide-ranging *C. modestus* and *C. fionni*, although we are already taking the first steps (Wilson et al., 2021). Clearly, habitat structure can differentially influence the signaling behavior of closely related species with similar general signal design and morphology, which are likely a consequence of the ancestral state.

DATA AVAILABILITY STATEMENT

The raw data supporting the conclusions of this article will be made available by the authors, without undue reservation.

ETHICS STATEMENT

The animal study was reviewed and approved by the La Trobe University Animal Ethics Committee and Wildlife Ethics Committee, South Australia.

REFERENCES

- Bian, X., Chandler, T., Pinilla, A., and Peters, R. A. (2019). Now you see me, now you don't: Environmental conditions, signaler behavior, receiver response thresholds interact to determine the efficacy of a movement-based animal signal. *Front. Ecol. Evol.* 7:130. doi: 10.3389/fevo.2019.00130
- Brandt, Y. (2003). Lizard threat display handicaps endurance. *Proc. R. Soc. Lond. B* 270, 1061–1068. doi: 10.1098/rspb.2003.2343
- Brumm, H. (2014). *Animal Communication in Noise*. Berlin: Springer.
- Carpenter, C. C. (1962). A comparison of the patterns of display of *Urosaurus*, *Uta*, and *Streptosaurus*. *Herpetologica* 18, 145–152.
- Carpenter, C. C. (1978). "Ritualistic social behaviors in lizards," in *Behavior and Neurology of Lizards: An Interdisciplinary colloquium*, eds N. Greenberg and P. D. MacLean (Rockville, MD: National Institute of Mental Health), 253–267.
- Carpenter, C. C., Badham, J. A., and Kimble, B. (1970). Behavior patterns of three species of *Amphibolurus* (Agamidae). *Copeia* 1970, 497–505. doi: 10.2307/1442277
- Cocroft, R. B., and Rodriguez, R. L. (2005). The behavioral ecology of insect vibrational communication. *BioScience* 55, 323–334. doi: 10.1641/0006-3568(2005)055[0323:tbeoiv]2.0.co;2
- Dong, C. M., Johnston, G. R., Stuart-Fox, D., Moussalli, A., Rankin, K. J., and McLean, C. A. (2021). Elevation of divergent color polymorphic and

AUTHOR CONTRIBUTIONS

JR and RP designed the experiment, analyzed the data, and wrote the manuscript. JR conducted the experiment and collected the data. Both authors reviewed and approved the manuscript.

FUNDING

Funding was received from the Australian Research Council Discovery Project scheme to RP (DP170102370).

ACKNOWLEDGMENTS

We would like to thank Andrea Narvaez, Christine Giuliano, Georgia Troup, Jordan de Jong, Kate Beskeen, Matt Sleeth and Peri Bolton for their support during data collection. Data collection was performed in accordance with the ethical regulations of La Trobe University (AEC 12-37 and AEC 16-59) and South Australia (55/2012), under permits provided by DEPI in Victoria (10006812), DEWNR in South Australia (Q26078 and U26541), and NPWS in New South Wales (SL101426).

SUPPLEMENTARY MATERIAL

The Supplementary Material for this article can be found online at: <https://www.frontiersin.org/articles/10.3389/fevo.2021.731705/full#supplementary-material>

Supplementary Figure 1 | Schematic illustration of the recording of lizards and plants. *Middle Panel*: Focal (resident) male lizards were located in their natural habitat and two cameras were positioned nearby before a tethered intruder was introduced at a distance of 1 m from the focal lizard. The display response of the focal lizard was filmed with both cameras. After filming was completed and the focal lizard had departed, the scene was mapped to identify the relative position of plants to the focal lizard. This includes all plants surrounding the focal lizard (a full 360° rather than the limited set of four plants A–D shown here). *Left Panel*: Display movements were digitized separately from the footage of both cameras and subsequently combined to yield 3D positions over time, with the change in position between successive frames yielding measures of speed. *Right Panel*: The response of plants to standardized wind speed generated by a leaf blower was filmed and subsequently analyzed using motion detector algorithms. The analytical process is explained further in the text and in **Figure 2**. The rationale for, and full description of, our approach can be found in: Ramos and Peters (2017b). Quantifying Ecological Constraints on Motion Signaling. *Frontiers in Ecology and Evolution* 5:9.

- monomorphic lizard lineages (Squamata: Agamidae) to species level. *Ichthyol. Herpetol.* 109, 43–54.
- Endler, J. A. (1991). Variation in the appearance of guppy color patterns to guppies and their predators under different visual conditions. *Vision Res.* 31, 587–608. doi: 10.1016/0042-6989(91)90109-1
- Fleishman, L. J. (1986). Motion detection in the presence and absence of background motion in an *Anolis* lizard. *J. Comp. Physiol. A* 159, 711–720. doi: 10.1007/BF00612043
- Fleishman, L. J. (1992). The influence of the sensory system and the environment on motion patterns in the visual displays of Anoline lizards and other vertebrates. *Am. Nat.* 139, S36–S61.
- Fleishman, L. J., and Persons, M. (2001). The influence of stimulus and background colour on signal visibility in the lizard *Anolis cristellus*. *J. Exp. Biol.* 204, 1559–1575.
- Fleishman, L. J., Leal, M., and Persons, M. H. (2009). Habitat light and dewlap color diversity in four species of Puerto Rican anoline lizards. *J. Comp. Physiol. A* 195, 1043–1060. doi: 10.1007/s00359-009-0478-8
- Gibbons, J. R. H. (1977). *Comparative Ecology and Behaviour of Lizards of the Amphibolurus decresii Species Complex*. Adelaide, SA: The University of Adelaide.
- Gibbons, J. R. H. (1979). The hind leg pushup display of the *Amphibolurus decresii* species complex (Lacertilia: Agamidae). *Copeia* 1979, 29–40. doi: 10.2307/1443725
- Hasson, O. (1991). Pursuit-deterrent signals: communication between prey and predator. *Trends Ecol. Evol.* 6, 325–329. doi: 10.1016/0169-5347(91)90040-5
- Hedrick, T. L. (2008). Software techniques for two- and three-dimensional kinematic measurements of biological and biomimetic systems. *Bioinspir. Biomimet.* 3:034001. doi: 10.1088/1748-3182/3/3/034001
- Hoback, W. W., and Wagner, W. E. Jr. (1997). The energetic cost of calling in the variable field cricket, *Gryllus lineaticeps*. *Physiol. Entomol.* 22, 286–290.
- Hunter, M. L., and Krebs, J. R. (1979). Geographical variation in the song of the great tit (*Parus major*) in relation to ecological factors. *J. Anim. Ecol.* 48, 759–785.
- Johnston, G. R. (1992). *Ctenophorus tjantjalka*, a new dragon lizard (Lacertilia: Agamidae) from northern South Australia. *Record. S. Aust. Museum* 26, 51–59. doi: 10.3853/j.2201-4349.65.2013.1600
- Leal, M., and Fleishman, L. J. (2002). Evidence for habitat partitioning based on adaptation to environmental light in a pair of sympatric lizard species. *Proc. R. Soc. Lond. B* 269, 351–359. doi: 10.1098/rspb.2001.1904
- Leal, M., and Fleishman, L. J. (2004). Differences in visual signal design and detectability between allopatric populations of *Anolis* lizards. *Am. Nat.* 163, 26–39. doi: 10.1086/379794
- LeBas, N. R., and Marshall, N. J. (2000). The role of colour in signalling and male choice in the agamid lizard *Ctenophorus ornatus*. *Proc. R. Soc. Lond. B* 267, 445–452. doi: 10.1098/rspb.2000.1020
- Lubanga, U., Peters, R. A., and Steinbauer, M. J. (2016). Substrate-borne vibrations of male psyllids vary with body size and age but females are indifferent. *Anim. Behav.* 120, 173–182. doi: 10.1016/j.anbehav.2016.07.033
- Matsumasa, M., and Murai, M. (2005). Changes in blood glucose and lactate levels of male fiddler crabs: effects of aggression and claw waving. *Anim. Behav.* 69, 569–577. doi: 10.1016/j.anbehav.2004.06.017
- McLean, C. A., Moussalli, A., and Stuart-Fox, D. (2014). Local adaptation and divergence in colour signal conspicuousness between monomorphic and polymorphic lineages in a lizard. *J. Evol. Biol.* 27, 2654–2664. doi: 10.1111/jeb.12521
- McLean, C. A., Moussalli, A., Sass, S., and Stuart-Fox, D. (2013). Taxonomic assessment of the *Ctenophorus decresii* complex (Reptilia: Agamidae) reveals a new species of dragon lizard from Western New South Wales. *Record. Aust. Museum* 65, 51–63.
- Melville, J., and Wilson, S. (2019). *Dragon Lizards of Australia: Evolution, Ecology and a Comprehensive Fieldguide*. Melbourne, Vic: Museums Victoria.
- Mitchell, F. J. (1973). Studies on the ecology of the agamid Lizard *Amphibolurus maculosus* (Mitchell). *Trans. R. Soc. S. Aust.* 97, 47–76.
- Morton, E. S. (1975). Ecological sources of selection on avian sounds. *Am. Nat.* 109, 17–34. doi: 10.1016/j.heares.2015.05.009
- Ord, T. J. (2012). Historical contingency and behavioural divergence in territorial *Anolis* lizards. *J. Evol. Biol.* 25, 2047–2055. doi: 10.1111/j.1420-9101.2012.02582.x
- Ord, T. J., and Martins, E. P. (2006). Tracing the origins of signal diversity in anole lizards: phylogenetic approaches to inferring the evolution of complex behaviour. *Anim. Behav.* 71, 1411–1429. doi: 10.1016/j.anbehav.2005.12.003
- Ord, T. J., Charles, G. K., and Hofer, R. K. (2011). The evolution of alternative adaptive strategies for effective communication in noisy environments. *Am. Nat.* 177, 54–64. doi: 10.1086/657439
- Ord, T. J., Peters, R. A., Clucas, B., and Stamps, J. A. (2007). Lizards speed up visual displays in noisy motion habitats. *Proc. R. Soc. Lond. B* 274, 1057–1062. doi: 10.1098/rspb.2006.0263
- Osborne, L. (2005). Information content of male agonistic displays in the territorial tawny dragon (*Ctenophorus decresii*). *J. Ethol.* 23, 189–197. doi: 10.1007/s10164-005-0151-9
- Peters, R. A. (2008). Environmental motion delays the detection of movement-based signals. *Biol. Lett.* 4, 2–5. doi: 10.1098/rsbl.2007.0422
- Peters, R. A. (2013). “Noise in optic communication: motion from wind-blown plants,” in *Animal Communication in Noise*, ed. H. Brumm (Heidelberg: Springer), 311–330. doi: 10.1007/978-3-642-41494-7_11
- Peters, R. A., and Evans, C. S. (2003a). Design of the Jacky dragon visual display: signal and noise characteristics in a complex moving environment. *J. Comp. Physiol. A* 189, 447–459. doi: 10.1007/s00359-003-0423-1
- Peters, R. A., and Evans, C. S. (2003b). Introductory tail-flick of the Jacky dragon visual display: signal efficacy depends upon duration. *J. Exp. Biol.* 206, 4293–4307. doi: 10.1242/jeb.00664
- Peters, R. A., and Ord, T. J. (2003). Display response of the Jacky Dragon, *Amphibolurus muricatus* (Lacertilia: Agamidae), to intruders: a semi-Markovian process. *Austral Ecol.* 28, 499–506. doi: 10.1046/j.1442-9993.2003.01306.x
- Peters, R. A., Clifford, C. W. G., and Evans, C. S. (2002). Measuring the structure of dynamic visual signals. *Anim. Behav.* 64, 131–146. doi: 10.1006/anbe.2002.3015
- Peters, R. A., Hemmi, J. M., and Zeil, J. (2007). Signaling against the wind: modifying motion-signal structure in response to increase noise. *Curr. Biol.* 17, 1231–1234. doi: 10.1016/j.cub.2007.06.035
- Peters, R. A., Hemmi, J. M., and Zeil, J. (2008). Image motion environments: background noise for movement-based animal signals. *J. Comp. Physiol. A* 194, 441–456. doi: 10.1007/s00359-008-0317-3
- Peters, R. A., Ramos, J. A., Hernandez, J., Wu, Y., and Qi, Y. (2016). Social context affects tail displays by *Phrynocephalus vlantali* lizards from China. *Sci. Rep.* 6:31573. doi: 10.1038/srep31573
- Pinheiro, J., Bates, D., DebRoy, S., Sarkar, D., and R Core Team (2018). *nlme: Linear and Nonlinear Mixed Effects Models*. R Package Version 3.1-137. Available online at: <https://CRAN.R-project.org/package=nlme>
- Podos, J. (2001). Correlated evolution of morphology and vocal signal structure in Darwin's finches. *Nature* 409, 185–188. doi: 10.1038/35051570
- Podos, J., and Nowicki, S. (2004). Beaks, adaptations, and vocal evolution in Darwin's finches. *Biosciences* 54, 501–510. doi: 10.1641/0006-3568(2004)054[0501:baavei]2.0.co;2
- Purdue, J. R., and Carpenter, C. C. (1972). A Comparative Study of the Display Motion in the Iguanid Genera *Sceloporus*, *Uta*, and *Urosaurus*. *Herpetologica* 28, 137–141.
- R Core Team (2016). *R: A Language and Environment for Statistical Computing*. Vienna: R Foundation for Statistical Computing.
- Ramos, J. A., and Peters, R. A. (2016). Dragon wars: movement-based signalling by Australian agamid lizards in relation to species ecology. *Austral Ecol.* 41, 302–315. doi: 10.1111/aec.12312
- Ramos, J. A., and Peters, R. A. (2017a). Habitat-dependent variation in motion signal structure between allopatric populations of lizards. *Anim. Behav.* 126, 69–78. doi: 10.1016/j.anbehav.2017.01.022
- Ramos, J. A., and Peters, R. A. (2017b). Quantifying ecological constraints on motion signaling. *Front. Ecol. Evol.* 5:9. doi: 10.3389/fevo.2017.00009
- Ramos, J. R. (2017). *Dragon Wars. Relating signal structure and habitat characteristics in Australian agamid lizards*. Ph.D. thesis. Melbourne, Vic: La Trobe University.
- Reby, D., and McComb, K. (2003). Anatomical constraints generate honesty: acoustic cues to age and weight in the roars of red deer stags. *Anim. Behav.* 65, 519–530. doi: 10.1006/anbe.2003.2078

- Ryan, M. J., and Brenowitz, E. A. (1985). The role of body size, phylogeny, and ambient noise in the evolution of bird song. *Am. Nat.* 126, 87–100. doi: 10.1086/284398
- Ryan, M. J., Cocroft, R. B., and Wilczynski, W. (1990). The role of environmental selection in intraspecific divergence of mate recognition signal in the cricket frog, *Acris crepitans*. *Evolution* 44, 1869–1872. doi: 10.1111/j.1558-5646.1990.tb05256.x
- Slabbekoorn, H. (2013). Songs of the city: noise-dependent spectral plasticity in the acoustic phenotype of urban birds. *Anim. Behav.* 85, 1089–1099. doi: 10.1016/j.anbehav.2013.01.021
- Slabbekoorn, H., and Peet, M. (2003). Ecology: birds sing at a higher pitch in urban noise. *Nature* 424, 267–267. doi: 10.1038/424267a
- Slabbekoorn, H., and Smith, T. B. (2002). Habitat-dependent song divergence in the little greenbul: an analysis of environmental selection pressures on acoustic signals. *Evolution* 56, 1849–1858. doi: 10.1111/j.0014-3820.2002.tb00199.x
- Stoddard, P. K., and Salazar, V. L. (2011). Energetic cost of communication. *J. Exp. Biol.* 214, 200–205. doi: 10.1242/jeb.047910
- Stuart-Fox, D., and Moussalli, A. (2008). Selection for social signalling drives the evolution of Chameleon colour change. *PLoS Biol.* 6:e25. doi: 10.1371/journal.pbio.0060025
- Stuart-Fox, D., and Ord, T. J. (2004). Sexual selection, natural selection and the evolution of dimorphic coloration and ornamentation in agamid lizards. *Proc. R. Soc. Lond. B* 271, 2249–2255. doi: 10.1098/rspb.2004.2802
- Teasdale, L. C., Stevens, M., and Stuart-Fox, D. (2013). Discrete colour polymorphism in the tawny dragon lizard (*Ctenophorus decresii*) and differences in signal conspicuousness among morphs. *J. Evol. Biol.* 26, 1035–1046. doi: 10.1111/jeb.12115
- Turner, C. R., Derylo, M., de Santana, C. D., Alves-Gomes, J. A., and Smith, G. T. (2007). Phylogenetic comparative analysis of electric communication signals in ghost knifefishes (Gymnotiformes: Apteronotidae). *J. Exp. Biol.* 210, 4104–4122. doi: 10.1242/jeb.007930
- Vehrencamp, S. L., Bradbury, J. W., and Gibson, R. M. (1989) The energetic cost of display in male sage grouse. *Anim. Behav.* 38, 885–896.
- Wilson, B. C., Ramos, J. A., and Peters, R. A. (2021). Intraspecific variation in behaviour and ecology in a territorial agamid, *Ctenophorus fionni*. *Aust. J. Zool.* 68, 85–97. doi: 10.1071/zo20091
- Wilson, S., and Swan, G. (2017). *A Complete Guide to Reptiles of Australia*. Sydney, NSW: New Holland Publishers.

Conflict of Interest: The authors declare that the research was conducted in the absence of any commercial or financial relationships that could be construed as a potential conflict of interest.

Publisher's Note: All claims expressed in this article are solely those of the authors and do not necessarily represent those of their affiliated organizations, or those of the publisher, the editors and the reviewers. Any product that may be evaluated in this article, or claim that may be made by its manufacturer, is not guaranteed or endorsed by the publisher.

Copyright © 2021 Ramos and Peters. This is an open-access article distributed under the terms of the Creative Commons Attribution License (CC BY). The use, distribution or reproduction in other forums is permitted, provided the original author(s) and the copyright owner(s) are credited and that the original publication in this journal is cited, in accordance with accepted academic practice. No use, distribution or reproduction is permitted which does not comply with these terms.



Age and Appearance Shape Behavioral Responses of Phasmids in a Dynamic Environment

Sebastian Pohl¹, Haaken Z. Bungum¹, Kenneth E. M. Lee¹, Mohamad Azlin Bin Sani¹, Yan H. Poh¹, Rodzay bin Hj Abd Wahab², Y. Norma-Rashid³ and Eunice J. Tan^{1*}

¹ Division of Science, Yale-NUS College, Singapore, Singapore, ² Institute for Biodiversity and Environmental Research, Universiti Brunei Darussalam, Gadong, Brunei, ³ Institute of Biological Sciences, Faculty of Science, University of Malaya, Kuala Lumpur, Malaysia

OPEN ACCESS

Edited by:

Ann Valerie Hedrick,
University of California, Davis,
United States

Reviewed by:

Richard Anthony Peters,
La Trobe University, Australia
María Del Carmen Viera,
Universidad de la República, Uruguay
Yu Zeng,
Chapman University, United States

*Correspondence:

Eunice J. Tan
eunice.tan@yale-nus.edu.sg

Specialty section:

This article was submitted to
Behavioral and Evolutionary Ecology,
a section of the journal
Frontiers in Ecology and Evolution

Received: 31 August 2021

Accepted: 15 December 2021

Published: 21 January 2022

Citation:

Pohl S, Bungum HZ, Lee KEM, Sani MAB, Poh YH, Wahab RbHA, Norma-Rashid Y and Tan EJ (2022) Age and Appearance Shape Behavioral Responses of Phasmids in a Dynamic Environment. *Front. Ecol. Evol.* 9:767940. doi: 10.3389/fevo.2021.767940

Although morphological adaptations leading to crypsis or mimicry have been studied extensively, their interaction with particular behaviors to avoid detection or recognition is understudied. Yet animal behaviors interact with morphology to reduce detection risk, and the level of protection conferred likely changes according to the surrounding environment. Apart from providing a locational cue for predators, prey motion can also serve as concealing behavior in a dynamic environment to prevent detection by potential predators or prey. Phasmids are conventionally known to rely on their adaptive resemblance to plant parts for protection, and this resemblance may vary across life stages and species. However, little is known about how their behaviors interact with their appearance and their environment. We investigated two species of phasmids with varying morphology and color patterns at different ontogenetic stages and examined their behavioral responses to a wind stimulus as a proxy for a dynamic environment. While adult behaviors were mostly species-specific, behavioral responses of nymphs varied with appearance and environmental condition. Display of different behaviors classified as revealing was positively correlated, while the display of concealing behaviors, except for swaying, was mostly negatively correlated with other behaviors. Exhibition of specific behaviors varied with appearance and environmental condition, suggesting that these behavioral responses could help reduce detection or recognition cues. We discuss the differences in behavioral responses in the context of how the behaviors could reveal or conceal the phasmids from potential predators. Our results provide a novel investigation into adaptive resemblance strategies of phasmids through the interaction of behavior and morphology, and highlight the importance of considering the effects of dynamic environments on sending and receiving cues.

Keywords: adaptive resemblance, *Calvisia flavopennis*, crypsis, *Lonchodes brevipes*, motion masquerade, Phasmatodea

INTRODUCTION

Predator–prey relationships are fundamental in shaping animal morphology and animal behavior. In the constant evolutionary arms race (Dawkins and Krebs, 1979), predators need to be capable of detecting and catching prey, while potential prey need to avoid detection or escape capture through morphological or behavioral adaptations (Ruxton et al., 2018). The chances of survival

for prey can increase through minimizing cues that predators could exploit. Adaptive resemblance allows the prey to dupe a potential predator by pretending to be an inanimate object (Starrett, 1993). Concealing behaviors, such as specific postures or resting habits, can interact with morphological adaptations and decrease the risk of detection or recognition, thus improving protection from predators (Stevens and Ruxton, 2019). However, the undetectability of an inanimate object can also be broken by motion (Regan and Beverley, 1984; Ioannou and Krause, 2009; Hall et al., 2013; Cuthill, 2019). Revealing behaviors, such as locomotion, can provide information about the presence and location of an animal and function as a cue for predators (Ioannou and Krause, 2009). Although avoiding motion is clearly an effective way of reducing the risk of detection, other strategies have evolved to minimize cues that reveal the presence, location, or identity of an animal (Tan and Elgar, 2021). Motion can even decrease the probability of detection or recognition through motion camouflage or motion masquerade (Stevens and Merilaita, 2009; Hall et al., 2017; Cuthill, 2019).

Depending on the prevailing environmental conditions, animals can show different behavioral responses to improve their protection. Cryptically colored animals often modify their flight responses depending on their level of exposure (Cuadrado et al., 2001; Maritz, 2012). Behavioral modifications of resemblance strategies are especially important if the environment of the animal is not static but changes dynamically, e.g., through moving backgrounds or changes in illumination (Cuthill et al., 2019). Wind can be the underlying cause of a dynamic environment, e.g., by agitating leaves or creating water caustics (Cuthill et al., 2019). If the anti-predator behavior of an animal relies on blending in with its environment, it is necessary to take this dynamically changing background into account. For instance, several species of phasmids are known to sway in response to a wind stimulus (e.g., Rupperecht, 1971; Bian et al., 2016), which could potentially enhance the resemblance of phasmids to plants when seen against a backdrop of moving vegetation, as the swaying behavior resembles the movement patterns of the plants (Bian et al., 2016). Since wind can dynamically alter the background of an animal, its presence can be used as a proxy for a dynamic environment. If an animal can perceive changes in air currents and adjust its behavior as a response, it allows for maintaining the benefits of adaptive resemblance without the need to integrate detailed information about concrete background changes.

Animals can possess life-stage specific behaviors and color patterns to avoid detection by predators. Ontogenetic changes in color patterns can reduce detection or increase the warning signal as the animal increases in size (Grant, 2007; Tan et al., 2016), while behavioral responses can vary depending on individual size (Cuadrado et al., 2001). Ontogenetic changes in foraging behavior and habitat used are widespread across animal taxa and have profound impacts on individual survival and ecological interactions (Werner and Gilliam, 1984; Hughes et al., 1992; Lind and Welsh, 1994; Hochuli, 2001; Arthur et al., 2008; Nakazawa, 2015; Ohba and Tatsuta, 2016). However, organisms at the same life stage living in a similar habitat are expected to face similar challenges (Fairclough, 2016; Tan et al., 2017).

A textbook example of adaptive resemblance, phasmids are predominantly nocturnally foraging herbivores that are known for their remarkable resemblance to sticks or leaves. These plant-resembling phenotypes have existed for at least 47 million years (Wedmann et al., 2007), attesting to their evolutionary success. Phasmid coloration varies from cryptic green and brown colors (e.g., *Lonchodes brevipes*, **Figures 1A–C**) to more “conspicuous” red, blue, and yellow colors (e.g., *Calvisia flavopennis*, **Figures 1D,F**). As hemimetabolous insects, phasmids go through several nymphal stages before emerging as adults, which often differ to varying degrees in their appearance from the adult forms (e.g., *L. brevipes* and *C. flavopennis*, **Figure 1**). With different phenotypes and ecological requirements at different life stages, we can expect the behaviors across these life stages to differ as well. Several predator avoidance behaviors in phasmids have been described, yet their adaptive advantages have not been thoroughly studied. Upon disturbance, some phasmid species may escape by dropping from the substrates to the ground or jump off the substrate (Steiniger, 1933; Robinson, 1968a; Zeng et al., 2020), while other species of phasmids may remain immobile (Strong, 1975). In the case of detection by a predator, some phasmid species show a secondary line of defense behaviors, such as abdomen rearing, stridulation, deimatic displays, or spraying of defensive secretions (Eisner, 1965; Bedford and Chinnick, 1966; Löser and Schulten, 1981; Dräger, 2011; Hennemann et al., 2016).

To examine the interactions between behavior, life stage, and phenotype, we chose two species of phasmids that live in forest habitats in Southeast Asia. The first species, Gray’s Malayan stick insect (*L. brevipes*), is a cryptically colored phasmid with a typical stick-like morphology (Seow-Choen, 2017). The second species, *C. flavopennis*, is a brightly colored phasmid that is fully winged at adulthood and capable of flight (Seow-Choen, 2016). Both species look distinctly different at the various life stages of first-instar nymph (**Figures 1A,D**), late-instar nymph (**Figures 1B,E**), and as adult males and females (**Figures 1C,F**). We examined how the behaviors of these phasmids differ according to their appearance, as determined by species and life stage, using the presence or absence of a wind stimulus as a proxy for a dynamic environment. We predict that phasmids of different appearances exhibit corresponding differences in their behavior and selectively modify their behavioral responses in the presence of a wind stimulus. We envisage that phasmids show specific behaviors that provide them with protection from predators, according to their appearance. Specifically, we expect phasmids with cryptic coloration to adopt behaviors that enhance their adaptive resemblance to inanimate objects and thus reduce their likelihood of detection or recognition, and more conspicuously colored phasmids to adopt behaviors that lower their risk of detection or capture, such as hiding or startle displays.

MATERIALS AND METHODS

Experimental Subjects

To ensure that adaptations to domestication have not been introduced, none of the experimental subjects were from hobbyist

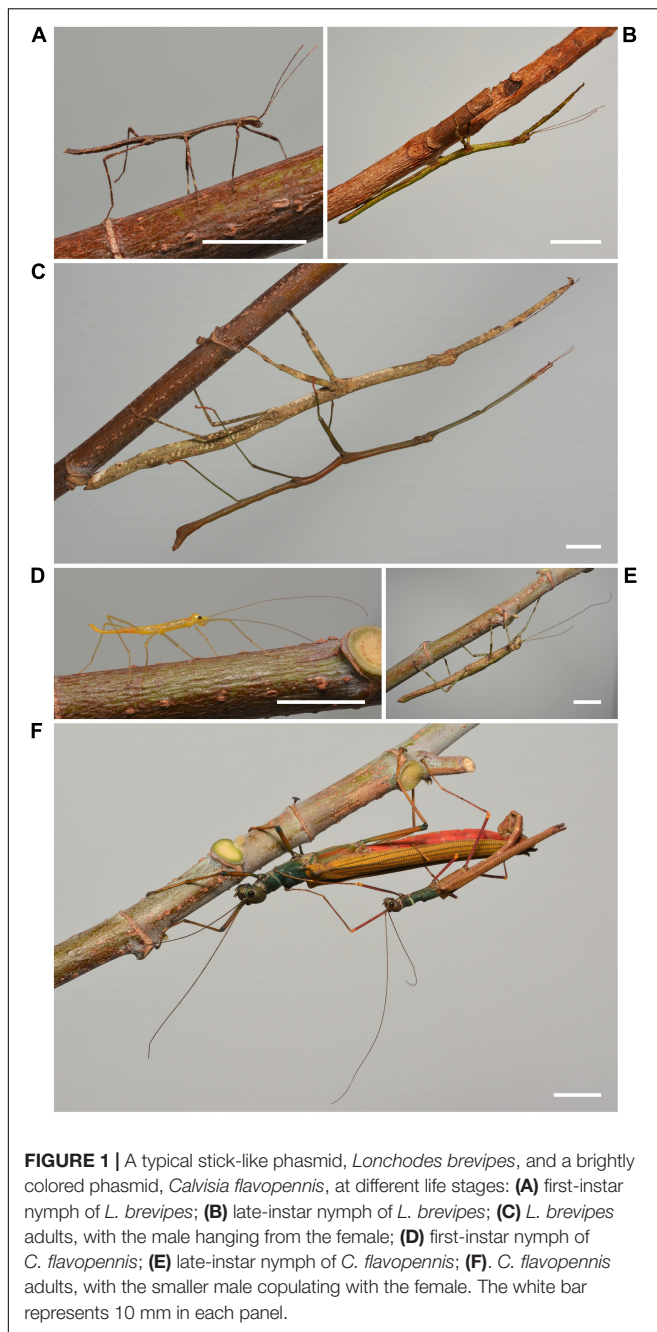


FIGURE 1 | A typical stick-like phasmid, *Lonchodes brevipes*, and a brightly colored phasmid, *Calvisia flavopennis*, at different life stages: **(A)** first-instar nymph of *L. brevipes*; **(B)** late-instar nymph of *L. brevipes*; **(C)** *L. brevipes* adults, with the male hanging from the female; **(D)** first-instar nymph of *C. flavopennis*; **(E)** late-instar nymph of *C. flavopennis*; **(F)** *C. flavopennis* adults, with the smaller male copulating with the female. The white bar represents 10 mm in each panel.

cultures. We used laboratory-reared offspring from field-caught phasmids in this study. We collected *L. brevipes* on Pulau Ubin, Singapore (1.409°N, 103.955°E), and *C. flavopennis* near the Kuala Belalong Field Studies Centre, Temburong District, Brunei Darussalam (4.547°N, 115.158°E). We carried out collections between 19:00 h and midnight while walking through the forests. Individuals of *L. brevipes* were collected from shrubs and trees between 0.5 and 2.5 m above the ground, while *C. flavopennis* was found above 3.5 m height. Phasmids were housed in a temperature-controlled laboratory at 24°C with a 12 h:12 h light:dark cycle. All individuals were provided food

plants *ad libitum* and monitored to be feeding and behaving normally before the behavioral trials. Individuals with missing or misshapen legs or wings were not used in our experiments, as these may impede their natural responses. No individual was subjected to more than one trial at each life stage. We performed 20 successful trials for each combination of species and life stage—first instar, late instar, adult male, adult female—to a total of 80 trials with *L. brevipes* and 80 trials with *C. flavopennis*. “Late instar” denotes nymphs of both species in the later stages of their development, which look dissimilar from both first instar nymphs and adults. In particular, we did not use the final instar of *C. flavopennis* as they started to develop the adult color patterns. Correspondingly, we did not use the final instar of *L. brevipes*.

Experimental Setup

Trials were performed in the same laboratory at 24°C during daylight hours under constant artificial light conditions (170–190 lx), in an enclosure (60 cm × 60 cm × 60 cm) with mesh and plastic sides to contain the phasmids during the trials. To simulate a branch for phasmids to rest on, a wooden dowel (300 mm length and 85 mm diameter) was elevated horizontally 145 mm from the bottom of the enclosure (**Supplementary Figure 1**). We used a portable fan, directed at the phasmid, to simulate a wind stimulus. The fan was moved along a fixed track parallel to the position of the phasmid on the dowel to ensure that the distance of the fan to the phasmid, and hence the wind speed, was constant during and across experiments. Before each trial, the wind velocity was measured to ensure that it was 2.0 ± 0.2 m/s from the track to the dowel. The trials were video-recorded for subsequent behavioral scoring.

Acclimatization

Before each observation, phasmids were introduced to the dowel and allowed to acclimatize for 120 s. Acclimatization was defined as successful when the phasmid adopted a stationary behavior (cf. **Table 1**) on the dowel for at least the last 30 s of the acclimatization period, and the observation commenced by exposing the phasmid to the wind or control treatment. If the phasmid moved off from the dowel, it was replaced onto the dowel and the acclimatization period would be repeated once, following the procedure above. If the phasmid did not adopt a stationary behavior within 90 s after the start of the acclimatization, the trial was aborted for the day and the phasmid was returned to its housing, until a new trial on a subsequent day.

Treatment

Each trial consisted of two separate observations, one per treatment (*control* or *wind*). Each individual was subjected to both the control and wind treatment. The order of the observations was determined by the flip of a coin, with a 180 s time-out between the two observations. During the time-out, the phasmid was placed in an interim cage with fresh leaves.

For the *wind treatment*, the fan was switched on while it was covered with a cardboard box, to allow the fan to pick up its final wind speed of 2.0 ± 0.2 m/s (see Bian et al., 2016). The box was then removed to expose the phasmid to the wind stimulus, marking the beginning of the observation. After 5 s, the cover was

TABLE 1 | List of scored behaviors and their definitions.

Behavior	Description	References
Active escape	Where the individual leaves the substrate through one of these: (i) Takes flight from the substrate (ii) Walks off from the substrate	–
Bounce	Insect body repeatedly moves toward and away from the substrate, while the insect remains in stance in contact with the substrate	–
Curl	The posterior end of the abdomen curls toward the anterior of the insect	Bedford and Chinnick, 1966
Evade	Insect orients away from the source of disturbance	–
Explore	Insect uses antennae and first pair of legs to probe gap spaces with the other four legs on the substrate	Blaesing and Cruse, 2004
<i>Extend</i>	Insect adopts a stationary position with the anterior limbs extended in line with the body axis	Robinson, 1968b
<i>Flatten</i>	Entire body is in contact with the substrate, with all legs around the substrate	–
<i>Hang</i>	Insect is hanging on the underside of the substrate	–
<i>Hug</i>	Insect brings its body closer to the stick by bending its legs, without <i>flattening</i> against the substrate	–
Raise	Abdomen raised from a position parallel to the substrate	–
<i>Stand</i>	Insect is stationary, with all legs partially or entirely straightened (compared to <i>hug</i> or <i>flatten</i>)	–
Stretch forward	Insect extends the anterior legs until they are in line with the body axis	–
Sway	Lateral rocking of the insect body, while the insect remains in stance, in contact with the substrate	Bian et al., 2016
Sway and Walk	Lateral rocking of the insect body, while the insect moves forward	–
Uncurl	Abdomen uncurls from curled position	Bedford and Chinnick, 1966
Walk	Forward movement along the substrate without any lateral movement of the body	–

All behaviors were scored as state events except for active escape, which was scored as a point event that ended the observation early. Stationary behaviors are marked in *italics*. Please refer to **Supplementary Materials** for videos and images of additionally described behaviours.

replaced to end exposure of the phasmid to the wind stimulus. For the *control treatment*, the procedure was identical, except that the fan was not switched on.

Behavioral Scoring

Video recordings of the observations were played back, and all behaviors were scored using the software BORIS (Friard and Gamba, 2016). The scored behaviors and their definitions are listed in **Table 1**. We referred to the literature for previously described behaviors, and list and describe additional behaviors (please refer to **Supplementary Materials** for videos and images of additionally described behaviours). An observation started with the beginning of the treatment and ended when the phasmid was stationary for at least 5 s after the end of the treatment. An observation could end prematurely if the insect displayed any of the active escape behaviors (e.g., flying away, **Table 1**). Behaviors were scored as *state* events, and the duration of the behavior was recorded. Two stationary behaviors (cf. **Table 1**) were mutually exclusive, while non-stationary behaviors could co-occur with stationary behaviors as well as with non-stationary behaviors. Active escape behaviors that ended an observation were scored as *point* events, i.e., they were either observed or not, and no duration was recorded.

Statistical Analyses

Statistical analyses were performed using the *R* base package (R Core Team, 2019) and PAST 4.03 (Hammer et al., 2001). To adjust for the different total duration of each observation, we calculated, separately for each observation and behavior, the behavioral response as the proportion of time (*p*) that the insect

displayed that behavior during an observation, by dividing the time an individual showed that specific behavior (*b*) by the total duration of the observation (*o*): $p = b/o$. We then performed a permutational multivariate analysis of variance (PERMANOVA) using the function *adonis2* from the *vegan* package (Oksanen et al., 2019) to test the differences in these behavioral responses, with Bray–Curtis distances and 9,999 permutations. The full model included morphological type (specified as the combination of species and life stage), treatment (wind or control), and an interaction term between morphological type and treatment, with the behavioral responses as response variables. We tested for pairwise differences between groups using the function *pairwise.adonis* from the *pairwiseAdonis* package (Martinez Arbizu, 2020), with Bray–Curtis distances, 9,999 permutations, and Benjamini–Hochberg adjusted *p*-values.

Using the *metaMDS* function from the *vegan* package (Oksanen et al., 2019), we performed non-metric multidimensional scaling (NMDS) with Bray–Curtis distances, 999 random starts, and *autotransform* set to *FALSE* to analyze the differences in behavioral responses between individuals. We used the *envfit* function from the *vegan* package with 9,999 permutations to determine the behaviors (i.e., the intrinsic variables) that shape the distribution pattern of the ordination. We visualized the results in NMDS ordination plots and added arrows to visualize the direction of behavioral responses that significantly contributed to the distribution pattern.

Integrating data from all individuals, separately for the control and the wind treatment, we created correlation matrices for the significantly contributing behaviors using the function *cor* from the *R* base package with Spearman correlation coefficients and

the packages *reshape2* (Wickham, 2007) and *ggplot2* (Wickham, 2016) to examine if any of these behaviors are correlated in the control or the wind treatment. We tested correlations for significance using the function *rcorr* from the package *Hmisc* (Harrell, 2021).

We performed Kruskal–Wallis and Dunn’s *post hoc* tests using PAST to determine differences in the proportion of total duration of these behaviors between the different groups (characterized by morphological type and treatment), as indicated by Bonferroni corrected *p*-values. We visualized the proportion of total duration of these behaviors in the different groups with radar plots using the package *fmsb* (Nakazawa, 2021).

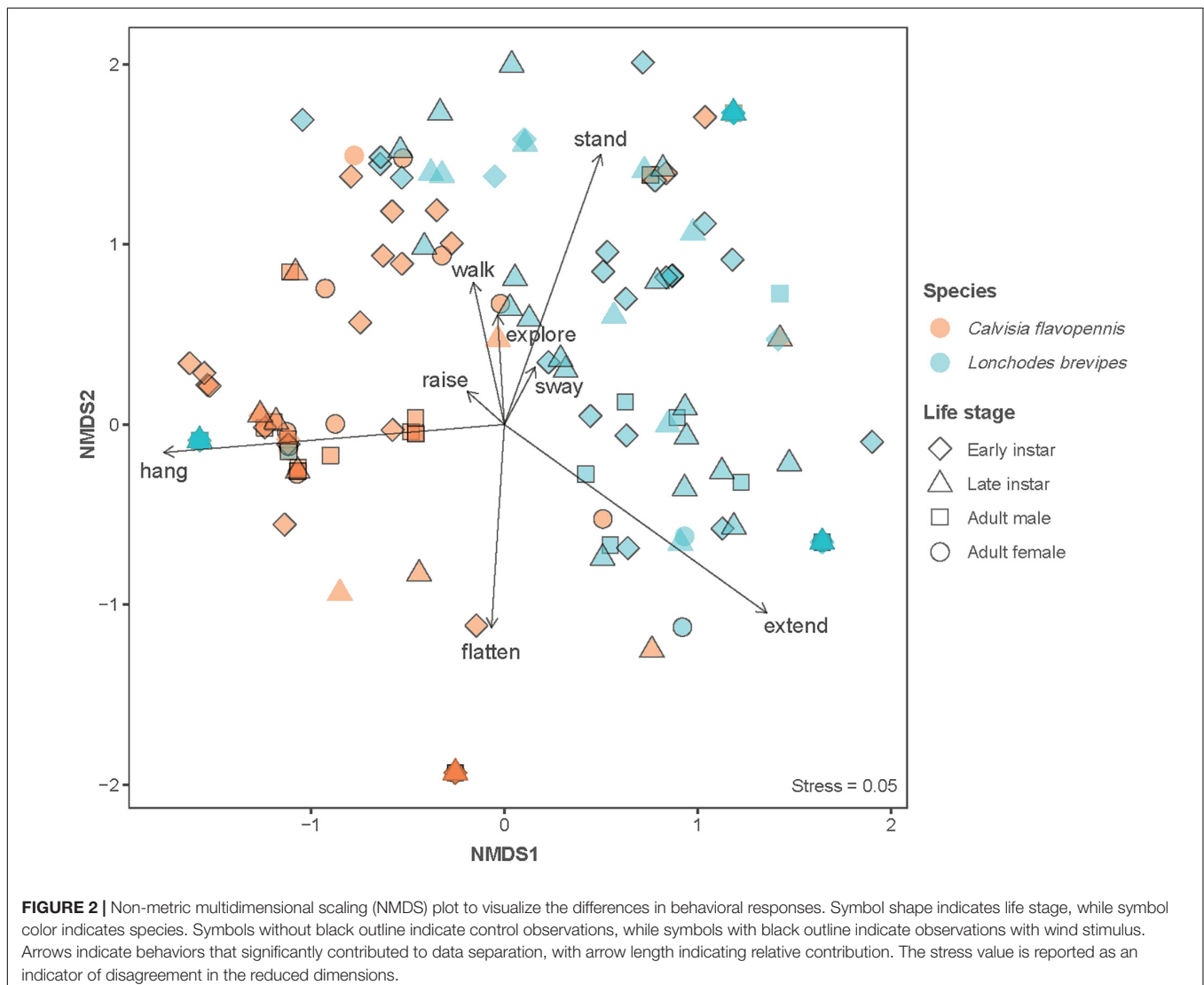
RESULTS

In our experiments, phasmids exhibited a range of different behaviors, in both the control and the wind treatment. We found differences in the behavioral responses between species as well

as across life stages of the same species. Morphological type and treatment affected the proportion of time a specific behavior was displayed. Revealing behaviors were positively correlated while concealing behaviors, except for *swaying*, were mostly negatively correlated.

Comparison of Overall Behavioral Responses Across Groups

Phasmid behavior differs with appearance and environmental condition. We found differences in the overall behavioral responses between individuals depending on morphological type (PERMANOVA, $F_{7,319} = 28.55$, $p = 0.0001$) and treatment (PERMANOVA, $F_{1,319} = 9.44$, $p = 0.0001$), as well as an interaction term between morphological type and treatment (PERMANOVA, $F_{7,312} = 1.77$, $p = 0.0134$). Differences in the overall behavioral responses between groups are visualized in an NMDS plot in **Figure 2**. Of the 15 recorded state behaviors, eight behaviors contributed significantly to the NMDS data



separation: explore, extend, flatten, hang, raise, stand, sway, and walk (all $p \leq 0.041$; **Table 2**). Pairwise comparisons revealed differences in the overall behavioral responses between specific groups (**Supplementary Table 1** and **Supplementary Figure 2**). In the control treatment, all morphological types differed in their overall behavioral responses from each other, except for two sets: (1) adult male *C. flavopennis*, adult female *C. flavopennis*, and first instars of *C. flavopennis*, and (2) adult male *L. brevipes* and adult female *L. brevipes* (**Table 3A** and **Figure 3A**). In the wind treatment, all morphological types show differences in their overall behavioral responses from each other, except for the following three sets: (1) all *C. flavopennis*, (2) adult male *L. brevipes* and adult female *L. brevipes*, and (3) first instar *L. brevipes* and late instar *L. brevipes* (**Table 3B** and **Figure 3B**). Comparing the overall behavioral responses of individuals of the same morphological type between the control and wind treatments, we found differences only for first instars of *C. flavopennis* ($F = 3.82$, $p = 0.0188$) and first instars of *L. brevipes* ($F = 6.92$, $p = 0.0002$; **Table 3C**).

Comparison of Specific Behaviors Across Groups

For each of the eight behaviors that contributed significantly to the NMDS data separation, we found differences in the proportion of total duration of the behavior between the sixteen combinations of two species, four life stages, and two treatments (Kruskal–Wallis tests, all $p < 0.001$, **Table 4** and **Figure 4**). We highlight notable patterns of differences between combinations of morphological type and treatment for these behaviors, as indicated by Dunn's *post hoc* tests (all p -values are Bonferroni corrected; for full results, please refer to **Supplementary Table 2**). We group the behaviors according to their potential to conceal or reveal the phasmids.

TABLE 2 | The contribution of individual behaviors to the non-metric multidimensional scaling (NMDS) data separation.

Behavioral response	NMDS1	NMDS2	R^2	p -value
Bounce	0.429	−0.903	0.001	0.940
Curl	0.534	0.846	0.012	0.131
Evade	0.251	0.968	0.005	0.481
Explore	−0.059	0.998	0.092	<0.001
Extend	0.792	−0.610	0.734	<0.001
Flatten	−0.059	−0.998	0.319	<0.001
Hang	−0.996	−0.088	0.781	<0.001
Hug	−0.332	−0.943	0.002	0.726
Raise	−0.724	0.690	0.018	0.041
Stand	0.316	0.949	0.624	<0.001
Stretch forward	0.801	−0.598	0.010	0.189
Sway	0.447	0.894	0.032	0.006
Sway and walk	0.502	0.865	0.001	0.889
Uncurl	−0.718	−0.696	0.004	0.812
Walk	−0.199	0.980	0.161	<0.001

Behaviors with significant p -values at the 0.05 level are marked in bold.

Concealing Behaviors

Displays of concealing behaviors varied depending on species, life stage, and treatment. Adult *L. brevipes* spent a higher proportion of time with their anterior limbs *extended* than any *C. flavopennis*, regardless of treatment (all $p < 0.001$). Within *L. brevipes*, adults in the wind treatment spent a higher proportion of time with their anterior limbs *extended* than both first and late instars in either treatment (all $p < 0.016$). Adults in the control treatment spent a higher proportion of time with their anterior limbs *extended* than first instars in either treatment (all $p < 0.002$), and adult males in the control treatment spent a higher proportion of time with their anterior limbs *extended* than late instars in the control treatment ($p = 0.024$). Late instar *C. flavopennis* in the control treatment spent a higher proportion of time *flattened* than all other morphological types in either treatment (all $p < 0.001$), except for late instar *C. flavopennis* in the wind treatment ($p = 1$). First instar *C. flavopennis*, adult male *C. flavopennis*, and adult female *C. flavopennis* in the control treatment spent a higher proportion of time *hanging* than all life stages of *L. brevipes* in either treatment (all $p < 0.008$). In the wind treatment, these three morphological types spent a higher proportion of time *hanging* than all life stages of *L. brevipes* in the wind treatment (all $p < 0.036$). First and late instar *L. brevipes* in the wind treatment spent a higher proportion of time *swaying* than all other morphological types in either treatment (all $p < 0.017$), except for adult female *C. flavopennis* in the wind treatment (all $p > 0.21$). We recorded a *raised* abdomen only occasionally ($N = 7$ observations) and only in the wind treatment. Except for one first instar *L. brevipes* individual, only first instar *C. flavopennis* showed this behavior; the latter spent a higher proportion of time raising their abdomens than all other morphological types in either treatment (all $p < 0.001$).

Revealing Behaviors

Revealing behaviors were observed across the two species and varied depending on species, life stage, and treatment. Late instar *L. brevipes* in the wind treatment spent a higher proportion of time *exploring* than all other morphological types in either treatment (all $p < 0.024$), except for first instar *L. brevipes*, first instar *C. flavopennis*, and adult female *C. flavopennis* in the wind treatment (all $p > 0.57$). First instar *L. brevipes* under wind conditions spent a higher proportion of time *exploring* than adult male *C. flavopennis* and adult female *L. brevipes* in either treatment, than late instar *C. flavopennis* in the wind treatment, as well as than first instar *C. flavopennis* and adult male *L. brevipes* in the control treatment (all $p < 0.013$). First instar *L. brevipes* in the control treatment spent a higher proportion of time *standing* than all other morphological types in either treatment (all $p < 0.004$), except for first instar *L. brevipes* in the wind treatment and late instar *L. brevipes* in either treatment (all $p > 0.37$). First instar *L. brevipes* in the wind treatment and late instar *L. brevipes* in both treatments spent a higher proportion of time *standing* than adult female *L. brevipes* in either treatment and adult male *L. brevipes* in the wind treatment (all $p < 0.032$). First instar *C. flavopennis* in the wind treatment spent a higher proportion of time *walking* than adult female *L. brevipes* in either treatment,

TABLE 3 | Pairwise comparisons of the overall behavioral responses between **(A)** all morphological types in the control treatment and **(B)** all morphological types in the wind treatment, and **(C)** comparisons of the overall behavioral responses between the wind and control treatments for individuals of the same morphological type.

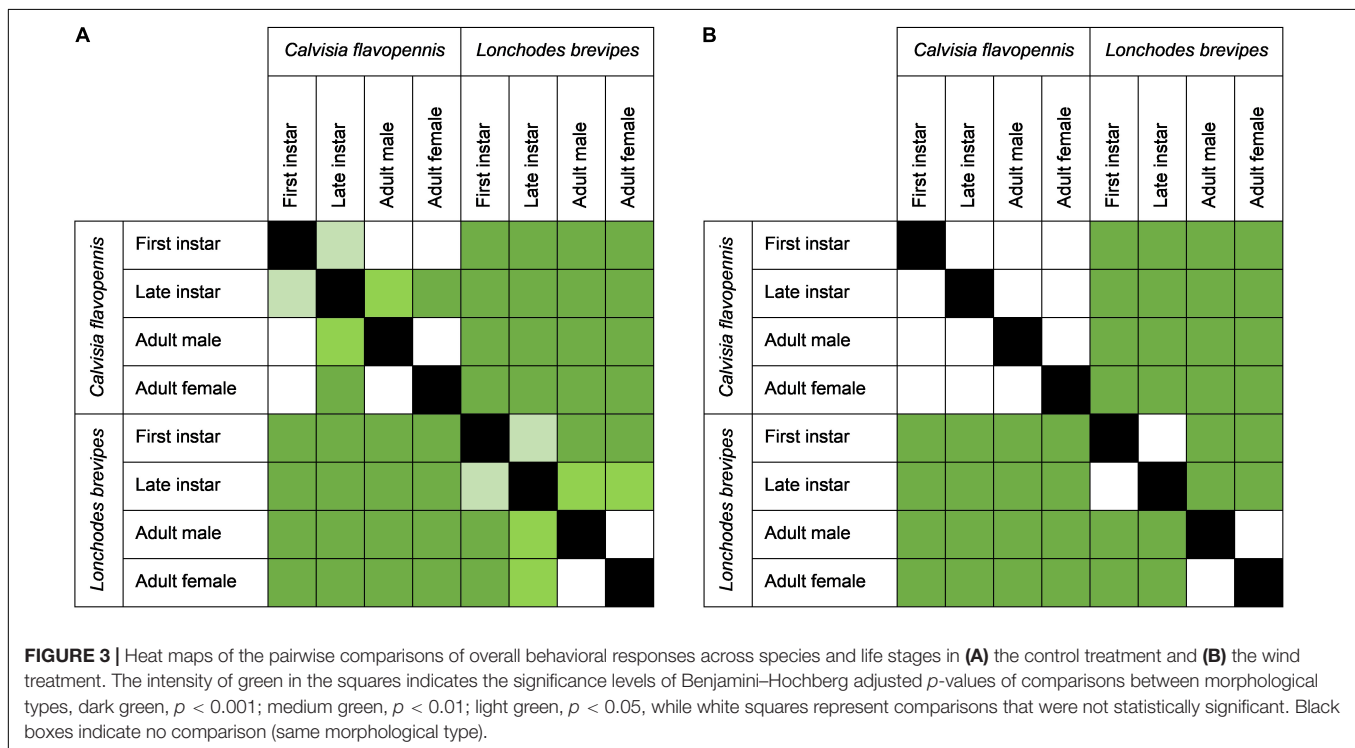
Group 1	Group 2	df	Sums of squares	F model	R ²	Adjusted p-value	Sig.
(A)							
<i>C. flavopennis</i> first instar	<i>C. flavopennis</i> late instar	1	1.20	4.91	0.114	0.024	*
<i>C. flavopennis</i> first instar	<i>C. flavopennis</i> adult male	1	0.18	1.29	0.033	0.296	n.s.
<i>C. flavopennis</i> first instar	<i>C. flavopennis</i> adult female	1	0.17	1.28	0.033	0.323	n.s.
<i>C. flavopennis</i> first instar	<i>L. brevipes</i> first instar	1	5.07	25.63	0.403	0.000	***
<i>C. flavopennis</i> first instar	<i>L. brevipes</i> late instar	1	3.43	12.60	0.249	0.000	***
<i>C. flavopennis</i> first instar	<i>L. brevipes</i> adult male	1	5.95	35.26	0.481	0.000	***
<i>C. flavopennis</i> first instar	<i>L. brevipes</i> adult female	1	5.11	29.57	0.438	0.000	***
<i>C. flavopennis</i> late instar	<i>C. flavopennis</i> adult male	1	2.18	10.73	0.220	0.001	**
<i>C. flavopennis</i> late instar	<i>C. flavopennis</i> adult female	1	2.19	10.70	0.220	0.000	***
<i>C. flavopennis</i> late instar	<i>L. brevipes</i> first instar	1	3.66	13.79	0.266	0.000	***
<i>C. flavopennis</i> late instar	<i>L. brevipes</i> late instar	1	2.42	7.13	0.158	0.000	***
<i>C. flavopennis</i> late instar	<i>L. brevipes</i> adult male	1	4.98	21.09	0.357	0.000	***
<i>C. flavopennis</i> late instar	<i>L. brevipes</i> adult female	1	4.58	19.04	0.334	0.000	***
<i>C. flavopennis</i> adult male	<i>C. flavopennis</i> adult female	1	0.03	0.26	0.007	1.000	n.s.
<i>C. flavopennis</i> adult male	<i>L. brevipes</i> first instar	1	5.38	34.25	0.474	0.000	***
<i>C. flavopennis</i> adult male	<i>L. brevipes</i> late instar	1	3.88	16.76	0.306	0.000	***
<i>C. flavopennis</i> adult male	<i>L. brevipes</i> adult male	1	6.58	51.45	0.575	0.000	***
<i>C. flavopennis</i> adult male	<i>L. brevipes</i> adult female	1	5.69	43.10	0.531	0.000	***
<i>C. flavopennis</i> adult female	<i>L. brevipes</i> first instar	1	5.68	35.84	0.485	0.000	***
<i>C. flavopennis</i> adult female	<i>L. brevipes</i> late instar	1	3.97	17.02	0.309	0.000	***
<i>C. flavopennis</i> adult female	<i>L. brevipes</i> adult male	1	6.60	51.05	0.573	0.000	***
<i>C. flavopennis</i> adult female	<i>L. brevipes</i> adult female	1	5.66	42.44	0.528	0.000	***
<i>L. brevipes</i> first instar	<i>L. brevipes</i> late instar	1	0.98	3.35	0.081	0.033	*
<i>L. brevipes</i> first instar	<i>L. brevipes</i> adult male	1	4.46	23.47	0.382	0.000	***
<i>L. brevipes</i> first instar	<i>L. brevipes</i> adult female	1	5.01	25.76	0.404	0.000	***
<i>L. brevipes</i> late instar	<i>L. brevipes</i> adult male	1	1.76	6.64	0.149	0.002	**
<i>L. brevipes</i> late instar	<i>L. brevipes</i> adult female	1	1.95	7.25	0.160	0.002	**
<i>L. brevipes</i> adult male	<i>L. brevipes</i> adult female	1	0.10	0.59	0.015	0.547	n.s.
(B)							
<i>C. flavopennis</i> first instar	<i>C. flavopennis</i> late instar	1	0.58	1.82	0.046	0.143	n.s.
<i>C. flavopennis</i> first instar	<i>C. flavopennis</i> adult male	1	0.60	2.31	0.057	0.075	n.s.
<i>C. flavopennis</i> first instar	<i>C. flavopennis</i> adult female	1	0.32	1.17	0.030	0.325	n.s.
<i>C. flavopennis</i> first instar	<i>L. brevipes</i> first instar	1	2.46	7.87	0.172	0.000	***
<i>C. flavopennis</i> first instar	<i>L. brevipes</i> late instar	1	2.52	7.96	0.173	0.000	***
<i>C. flavopennis</i> first instar	<i>L. brevipes</i> adult male	1	5.44	25.58	0.402	0.000	***
<i>C. flavopennis</i> first instar	<i>L. brevipes</i> adult female	1	6.22	33.90	0.471	0.000	***
<i>C. flavopennis</i> late instar	<i>C. flavopennis</i> adult male	1	0.60	2.16	0.054	0.114	n.s.
<i>C. flavopennis</i> late instar	<i>C. flavopennis</i> adult female	1	0.53	1.82	0.046	0.144	n.s.
<i>C. flavopennis</i> late instar	<i>L. brevipes</i> first instar	1	2.95	9.01	0.192	0.000	***
<i>C. flavopennis</i> late instar	<i>L. brevipes</i> late instar	1	2.82	8.52	0.183	0.000	***
<i>C. flavopennis</i> late instar	<i>L. brevipes</i> adult male	1	4.27	18.79	0.331	0.000	***
<i>C. flavopennis</i> late instar	<i>L. brevipes</i> adult female	1	4.77	24.08	0.388	0.000	***
<i>C. flavopennis</i> adult male	<i>C. flavopennis</i> adult female	1	0.18	0.77	0.020	0.534	n.s.
<i>C. flavopennis</i> adult male	<i>L. brevipes</i> first instar	1	3.66	13.65	0.264	0.000	***
<i>C. flavopennis</i> adult male	<i>L. brevipes</i> late instar	1	3.79	13.95	0.269	0.000	***
<i>C. flavopennis</i> adult male	<i>L. brevipes</i> adult male	1	6.25	37.30	0.495	0.000	***
<i>C. flavopennis</i> adult male	<i>L. brevipes</i> adult female	1	6.97	50.39	0.570	0.000	***
<i>C. flavopennis</i> adult female	<i>L. brevipes</i> first instar	1	3.78	13.38	0.260	0.000	***
<i>C. flavopennis</i> adult female	<i>L. brevipes</i> late instar	1	3.54	12.39	0.246	0.000	***

(Continued)

TABLE 3 | (Continued)

Group 1	Group 2	df	Sums of squares	F model	R ²	Adjusted <i>p</i> -value	Sig.
(B)							
<i>C. flavopennis</i> adult female	<i>L. brevipes</i> adult male	1	5.57	30.61	0.446	0.000	***
<i>C. flavopennis</i> adult female	<i>L. brevipes</i> adult female	1	6.24	40.81	0.518	0.000	***
<i>L. brevipes</i> first instar	<i>L. brevipes</i> late instar	1	0.30	0.93	0.024	0.466	n.s.
<i>L. brevipes</i> first instar	<i>L. brevipes</i> adult male	1	3.78	17.24	0.312	0.000	***
<i>L. brevipes</i> first instar	<i>L. brevipes</i> adult female	1	4.76	25.03	0.397	0.000	***
<i>L. brevipes</i> late instar	<i>L. brevipes</i> adult male	1	2.26	10.15	0.211	0.000	***
<i>L. brevipes</i> late instar	<i>L. brevipes</i> adult female	1	3.06	15.82	0.294	0.000	***
<i>L. brevipes</i> adult male	<i>L. brevipes</i> adult female	1	0.07	0.77	0.020	0.558	n.s.
(C)							
<i>C. flavopennis</i> first instar	<i>C. flavopennis</i> first instar	1	0.92	3.82	0.091	0.019	*
<i>C. flavopennis</i> late instar	<i>C. flavopennis</i> late instar	1	0.29	0.90	0.023	0.433	n.s.
<i>C. flavopennis</i> adult male	<i>C. flavopennis</i> adult male	1	0.36	2.30	0.057	0.110	n.s.
<i>C. flavopennis</i> adult female	<i>C. flavopennis</i> adult female	1	0.36	2.12	0.053	0.118	n.s.
<i>L. brevipes</i> first instar	<i>L. brevipes</i> first instar	1	1.87	6.92	0.154	0.000	***
<i>L. brevipes</i> late instar	<i>L. brevipes</i> late instar	1	0.68	1.96	0.049	0.118	n.s.
<i>L. brevipes</i> adult male	<i>L. brevipes</i> adult male	1	0.11	0.79	0.020	0.474	n.s.
<i>L. brevipes</i> adult female	<i>L. brevipes</i> adult female	1	0.22	1.88	0.047	0.294	n.s.

Sig., significance level of Benjamini–Hochberg adjusted *p*-value. ****p* < 0.001; ***p* < 0.01; **p* < 0.05; n.s., not significant.



as well as than adult male *L. brevipes* and first instar and adult male *C. flavopennis* in the control treatment (all *p* < 0.021).

Correlation of Behaviors in Control and Wind Treatments

We found correlations between several behaviors in both the control treatment (Table 5A and Figure 5A) and the wind treatment (Table 5B and Figure 5B), integrating data from all

individuals in a treatment. Except for *swaying*, we found positive correlations only between revealing behaviors, while we found negative correlations between concealing behaviors and both other concealing behaviors and revealing behaviors alike. In the control treatment, *hang* was negatively correlated with *explore*, *extend*, *flatten*, *stand*, and *walk* (all *p* < 0.043). *Extend* was negatively correlated with *flatten* and *stand* (all *p* < 0.024). *Walk* was positively correlated with *explore* and *stand* (all *p* < 0.002),

TABLE 4 | Differences in individual behaviors between experimental groups, for behaviors that significantly contributed to the distribution pattern during NMDS.

Behavioral response	<i>H</i> (<i>chi</i> ²)	<i>H</i> _c (tie corrected)	<i>p</i> -value
Extend	134.9	205	<0.001
Explore	18.20	69.08	<0.001
Flatten	17.02	70.95	<0.001
Hang	119.3	153.6	<0.001
Raise	5.084	79.19	<0.001
Stand	55.04	105.4	<0.001
Sway	31.22	103.7	<0.001
Walk	12.29	45.34	<0.001

Behaviors with significant *p*-values at the 0.05 level are marked in bold.

and *explore* was positively correlated with *stand* ($p = 0.019$). In the wind treatment, *hang* was negatively correlated with *explore*, *extend*, *flatten*, *stand*, and *sway* (all $p < 0.024$). *Extend* was negatively correlated with *explore*, *stand*, *walk*, and *sway* (all $p < 0.024$). *Flatten* was negatively correlated with *stand* and *sway* (all $p < 0.041$). *Explore* was positively correlated with *stand*, *sway*, and *walk* (all $p < 0.001$). *Stand* was positively correlated with *sway* and *walk* (all $p < 0.011$), and *raise* was positively correlated with *hang* ($p = 0.019$).

DISCUSSION

Our study provides a first insight into the variability of behavioral responses of different phasmid species and life stages in response to a variable environmental factor. The results for both the control and the wind treatment indicate that the behaviors of phasmids varied through ontogeny and between species. The proportion of time spent on specific behaviors differed between groups of different morphological types and treatments. Within the same morphological type, only first instars showed significant changes in their overall behavior as a response to different environmental conditions. Through the interaction of behavior and morphology, phasmids may be able to adjust their adaptive resemblance strategies to specific situations. We discuss the differences in behavioral responses in the context of how the behaviors could reveal the phasmids or conceal them from potential predators. Investigating the behavioral components of predator avoidance strategies is a further step toward a more complete understanding of the complex interactions between morphology, behavior, sensory ecology, and environmental factors. Ultimately, this work will allow us to understand the selective pressures and evolutionary dynamics that shape evolutionary strategies of phasmids.

Overall Behavioral Differences

Adaptive strategies to evade predation can be shaped by extrinsic factors, such as the predator community, and intrinsic factors, such as current life history requirements (Mappes et al., 2014; Valkonen et al., 2014). Individuals at the same life stage leading a similar lifestyle in a similar habitat might be expected to face similar challenges and thus exhibit similar behaviors and color patterns, even across species (Tan et al., 2017). Life stage

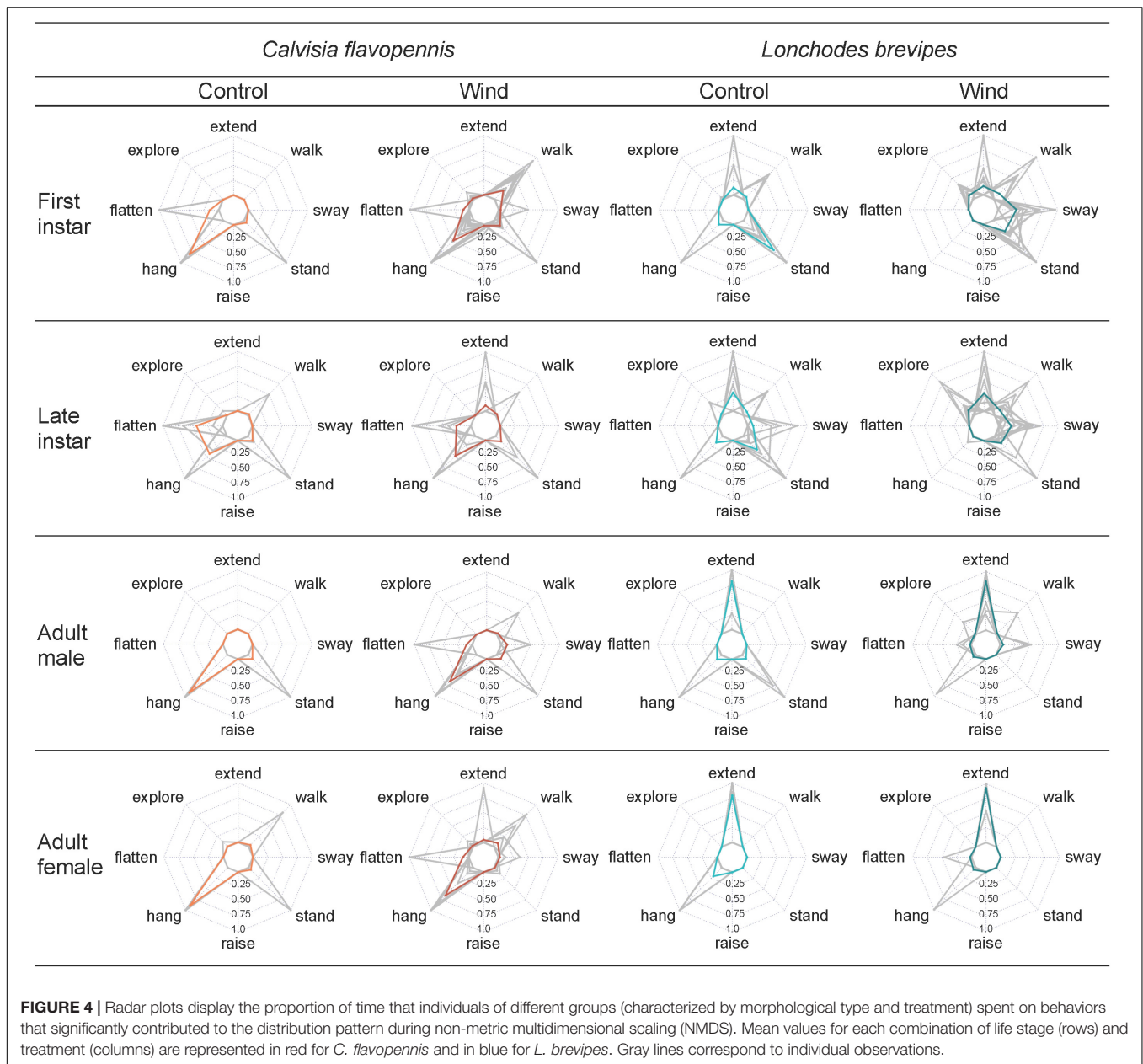
influences phasmid behavior, particularly in the absence of wind, yet species is a better predictor of phasmid behavior across environmental conditions. The two species in this study differ in their overall behavior, regardless of life stage and treatment. Additionally, ontogenetic changes could be accompanied by changes in behavior. For example, the shield bug *Graphosoma lineatum* changes from a cryptic appearance pre-hibernation to an aposematic appearance post-hibernation, with aposematic forms showing higher mobility than cryptic forms (Johansen et al., 2011). The overall behavioral responses of *C. flavopennis* to wind do not differ across life stages, whereas *L. brevipes* in the wind treatment show differences in the overall behavior between adults and nymphs, but not between adult sexes or nymphs of different ages. Intraspecific behavioral differences depending on the life stage are also observed in other phasmid species, with smaller and younger individuals of *Timema cristinae* stick insects more likely to exhibit thanatosis (Farkas, 2016). While our study directly compares the behavior of different life stages of two phasmid species, identification of broad evolutionary trends would require comparative analyses to adjust for phylogenetic relationships (Harvey and Pagel, 1991).

Group-Specific Behaviors

By disguising their shape, prey can become unrecognizable to predators (Merilaita et al., 2017). Behaviors such as extend and flatten have the potential to conceal the presence of an individual and hence reduce the likelihood of detection or recognition by potential predators. The extension of anterior limbs aligned with the antennae masks the typical morphology of an insect, as phasmids lose the distinctive shape of six legs and antennae (Robinson, 1968b). Unlike *C. flavopennis*, *L. brevipes* individuals have legs that fit closely to the head when extended with the antennae, and all life stages of the cryptically colored species *L. brevipes* resemble twigs and branches of plants. Extension of anterior limbs was more common in the adults of *L. brevipes*. Possibly due to their larger size, and thus detectability, it might be more important for larger insects to adopt this behavior, which alters their appearance.

Plant resemblance could also play a role during the flattening behavior. By flattening themselves against the substrate, phasmids could lose the distinct morphology of an insect, and thus reduce detection. Flattening can additionally enhance protection by eliminating shadow casting, as seen in frogs (Ferreira et al., 2019). Combined with cryptic coloration, a phasmid flattened against its substrate would be concealed from predators. In fact, late instar *C. flavopennis*, which have a mottled brown, bark-like appearance (Figure 1E), behaved distinctly different from the other life stages: in the control treatment, they spent a higher proportion of time flattened than all other morphological types. As the wooden dowel used in the experimental setup resembles a plant branch, flattening against a branch could be a behavior that reduces the detection of the insect. The combination of flattened resting positions with a dorsoventrally flattened morphology has been demonstrated to reduce detection by predators in the spider mite *Aponychus corpuzae* (Chittenden and Saito, 2006).

Prey can reduce their exposure to predators by selecting specific microhabitats. For instance, prey location and foliage



structure influence prey capture rates, with lower leaf surfaces experiencing less predation overall (Whelan, 2001; Johnson et al., 2007). By *hanging* under the substrate, the phasmid could be concealed from predators above. Contrary to our expectations, hanging was more often observed in brightly colored individuals of *C. flavopennis* than in *L. brevipes*. First instar *C. flavopennis*, adult male *C. flavopennis*, and adult female *C. flavopennis* spent a higher proportion of time hanging than all life stages of *L. brevipes* in the same treatment. Instead of performing evasive behaviors, hanging under a substrate could be an adaptation by the brightly colored life stages of *C. flavopennis* to reduce the risk of predation. Although the main predators of *C. flavopennis* are currently unknown, a field study of insectivorous bird species in a similar tropical forest in Malaysia found that

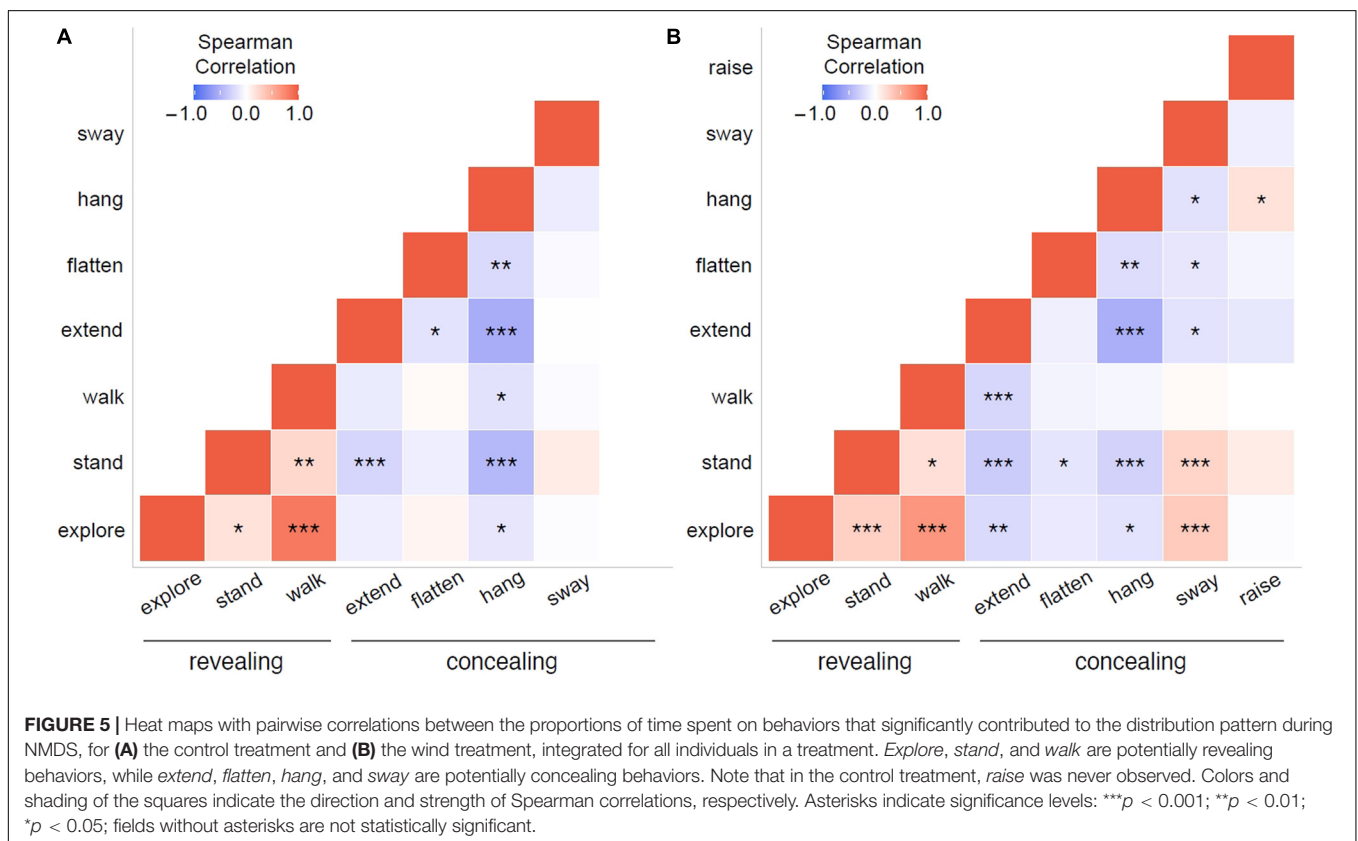
these insectivores rarely foraged from the underside of branches (Mansor and Mohd Sah, 2012).

While movement may alert a predator to the presence of prey, it does not necessarily compromise camouflage, as there are several ways in which prey may specifically incorporate motion into their arsenal of defense strategies to compromise the cues used by their natural enemies (reviewed by Stevens and Ruxton, 2019; Caro and Koneru, 2021). In some cases, specific motion can enhance the effectiveness of camouflage (Fleishman, 1985; Huffard et al., 2005; Cuthill et al., 2019). Under dynamic background conditions, such as those caused by wind, *swaying* could improve concealment by reducing the signal-to-noise ratio (Cuthill et al., 2019). Swaying has previously been reported as a behavior that enhances camouflage

TABLE 5 | Pairwise correlations between the proportions of time spent on behaviors that significantly contributed to the distribution pattern during NMDS, for **(A)** the control treatment and **(B)** the wind treatment, integrated for all individuals in a treatment.

(A)								
Control	Explore	Stand	Walk	Extend	Flatten	Hang	Sway	
Sway	0.755	0.141	0.711	0.942	0.606	0.119		
Hang	0.042	3.32E-10	0.015	1.64E-13	0.002		−0.12	
Flatten	0.402	0.148	0.640	0.023		−0.24	−0.04	
Extend	0.173	4.99E-04	0.104		−0.18	−0.54	−0.01	
Walk	0.000	0.002		−0.13	0.04	−0.19	−0.03	
Stand	0.019		0.25	−0.27	−0.11	−0.47	0.12	
Explore		0.18	0.83	−0.11	0.07	−0.16	−0.02	
(B)								
Wind	Explore	Stand	Walk	Extend	Flatten	Hang	Sway	Raise
Raise	0.774	0.146	0.962	0.053	0.388	0.019	0.174	
Sway	1.55E-05	6.76E-04	0.637	0.023	0.040	0.014		−0.11
Hang	0.024	2.28E-04	0.474	5.97E-13	0.006		−0.19	0.18
Flatten	0.076	0.033	0.295	0.200		−0.22	−0.16	−0.07
Extend	0.002	2.19E-05	9.14E-04		−0.10	−0.53	−0.18	−0.15
Walk	0.000	0.010		−0.26	−0.08	−0.06	0.04	0.00
Stand	1.20E-04		0.20	−0.33	−0.17	−0.29	0.27	0.12
Explore		0.30	0.66	−0.24	−0.14	−0.18	0.33	−0.02

Explore, stand, and walk are potentially revealing behaviors, while extend, flatten, hang, and sway are potentially concealing behaviors. Note that in the control treatment, raise was never observed. The upper-left triangle shows p-values, while the lower-right triangle shows Spearman correlations. Correlations with significant p-values at the 0.05 level and associated Spearman correlations are marked in bold.



in other cryptically colored animals, such as snakes, mantids, and spiders (e.g., Fleishman, 1985; Jackson, 1985; Watanabe and Yano, 2009, 2012, 2013). In the presence of wind, *L. brevipes* first and late instars generally spent more time swaying than the other morphological types. Swaying could enhance the resemblance of phasmids to an uninteresting object through motion masquerade (Hall et al., 2017; Cuthill, 2019). As prey animals will risk predation to continue with other profitable activities if the risk is low (Ydenberg and Dill, 1986), swaying could reduce the detection risk of phasmids during activities such as foraging, which is crucial for developing nymphs. Swaying in the phasmid *Extatosoma tiaratum* was quantitatively similar to that of moving plants, consistent with motion masquerade where animals may use motion as a concealing behavior against a moving background (Bian et al., 2016).

Unlike concealing behaviors, behaviors such as standing, exploring, and walking could reveal the identity and/or location of an individual. When insects are *standing* with their body elevated from the substrate, they exhibit a distinct form, with their body, six legs, and antennae visible. The cryptically colored first instar *L. brevipes*, particularly in the control treatment, spent more time standing than *C. flavopennis* and adult *L. brevipes*. It is possible that the combination of cryptic coloration and smaller size makes them less detectable and, hence, standing disrupts their cryptic appearance less. *Explore*, where the insect probes a gap with its antennae and first pair of legs (Blaesing and Cruse, 2004), reveals the presence of the insect and is similarly risky. In the field, one of the authors (ET) observed a phasmid being preyed on during exploration. Wind is a cue to inform jumping spiders whether it is appropriate to jump (Aguilar-Arguello et al., 2021) and might similarly serve as a cue for exploration in phasmids. *Walking*, which is the forward movement along the substrate, is risky as it can break the crypsis of the insect. In the presence of predators, the caridean shrimp *Tozeuma carolinense* decreases the time spent walking on their seagrass blade substrate and shows an increase in clinging behavior that resembles flattening in phasmids (Main, 1987). In the wind treatment, exploration behavior was increased in both *L. brevipes* instars, while first instar *C. flavopennis* spent a higher proportion of time walking than other groups. The risk of detection during these behaviors could be lower for nymphs due to their smaller size.

Interaction of Concealing and Revealing Behaviors

Once phasmids adopt a concealing behavior, a change of behavior could break their concealment. However, if phasmids already adopted a revealing behavior, there could be fewer costs to switching to a different revealing behavior. In fact, they could then benefit from a combination of different behaviors – for example, a combination of exploring and walking could lead them to a better-suited spot for resting or feeding. The phasmid *Haplopus scabricollis* was observed to intersperse walking with exploration behaviors often during locomotion (Stockard, 1908). We found that *sway* was the only concealing behavior that correlated positively with any revealing behaviors (*stand* and *explore*, in the wind treatment). Swaying at

intervals could thus provide phasmids some form of concealment between revealing behaviors through motion masquerade in a dynamic environment.

CONCLUSION

Future studies to test the predictions about the role of particular behaviors as antipredator strategies will need to determine how likely predators are to detect phasmids. Using prey models that systematically vary in size, coloration, posture, and location (e.g., Cuthill and Székely, 2009; Webster et al., 2009; Tan et al., 2016, 2020), it will be possible to elucidate the importance of these characteristics for concealment and predator avoidance in phasmids. Field observations can provide information about the range of natural predators of phasmids and indicate the preferred foraging microhabitats of the predators. Anecdotal reports describe spiders, mantids, and birds (Paine, 1968; Robinson and Robinson, 1973; Bragg, 1992; Suetsugu et al., 2018) as natural predators of phasmids in the wild. In captivity, phasmids are readily accepted by lizards and amphibians (Bragg, 1992), suggesting that these animals could be potential predators of phasmids in the natural environment. Specific knowledge about phasmid predators will also provide further insight into the role of coloration, as color vision differs between different predator groups (Jacobs, 1993; Briscoe and Chittka, 2001; Hart, 2001; Théry and Gomez, 2010; Fabricant and Herberstein, 2015). Species-specific attributes, such as the presence or absence of wings, and the resulting different niches could provide additional explanations for differences in the behaviors between species. Behavioral experiments would be required to investigate the effect and function of active behaviors. For example, to investigate whether swaying behavior in the species tested in this study is a form of motion masquerade as suggested for *E. tiaratum* (Bian et al., 2016), it is necessary to examine the effect of swaying on potential predators and to quantify the swaying behavior in response to wind. Future studies, such as a comparative analysis of morphology and behaviors across phasmid species that considers the phylogenetic relationships, would allow us to elucidate the evolution of predator avoidance strategies. By using an integrated approach that combines behavioral experiments with biophysical measurements and field observations, it will be possible to gain further insights into processes of adaptive resemblance.

DATA AVAILABILITY STATEMENT

The original contributions presented in the study are included in the article/**Supplementary Material**, further inquiries can be directed to the corresponding author.

ETHICS STATEMENT

The research reported in this article, which involved insects only, was exempt from ethics approval procedures by the National University of Singapore. We collected *L. brevipes* in Singapore

(permit number NP/RP18-062) and *C. flavopennis* in Brunei Darussalam (export permit number BioRIC/HoB/TAD/51-131).

and the Ministry of Education, Singapore, and Yale-NUS College Start-up Grant to ET.

AUTHOR CONTRIBUTIONS

ET and SP conceptualized the project. ET, SP, and YN-R acquired funding. RW coordinated the access to Bruneian phasmids. ET, SP, MS, and KL collected the specimens. KL, HB, MS, and YP performed data collection. ET and SP performed data analyses and wrote the first draft of the manuscript. All authors contributed to manuscript revision, read, and approved the final manuscript.

FUNDING

This project was funded in part by the grant of a National Geographic Explorer (NGS-KOR-301R-18) to ET, SP, and YN-R; a Yale-NUS College Summer Research Programme grant to HB;

ACKNOWLEDGMENTS

The authors thank Francis Seow-Choen for his help in identifying the species, Mishak Shunari and John Lee for their help with fieldwork, as well as Salleh Abdullah and the staff at Kuala Belalong Field Studies Center for the field support. The authors are grateful to Bruno Kneubühler for his advice with phasmid husbandry, to Andreia Ko and Anuji Diyana for their help with recording videos of phasmids, and to Mark Elgar for valuable comments on an earlier draft of this manuscript.

SUPPLEMENTARY MATERIAL

The Supplementary Material for this article can be found online at: <https://www.frontiersin.org/articles/10.3389/fevo.2021.767940/full#supplementary-material>

REFERENCES

- Aguilar-Arguello, S., Taylor, A. H., and Nelson, X. J. (2021). Jumping spiders attend to information from multiple modalities when preparing to jump. *Anim. Behav.* 171, 99–109. doi: 10.1016/j.anbehav.2020.11.013
- Arthur, K. E., Boyle, M. C., and Limpus, C. J. (2008). Ontogenetic changes in diet and habitat use in green sea turtle (*Chelonia mydas*) life history. *Mar. Ecol. Prog. Ser.* 362, 303–311. doi: 10.3354/meps07440
- Bedford, G. O., and Chinnick, L. J. (1966). Conspicuous displays in two species of Australian stick insects. *Anim. Behav.* 14, 518–521. doi: 10.1016/S0003-3472(66)80053-2
- Bian, X., Elgar, M. A., and Peters, R. A. (2016). The swaying behavior of *Extatosoma tiaratum*: motion camouflage in a stick insect? *Behav. Ecol.* 27, 83–92. doi: 10.1093/beheco/arv125
- Blaesing, B., and Cruse, H. (2004). Stick insect locomotion in a complex environment: climbing over large gaps. *J. Exp. Biol.* 207, 1273–1286. doi: 10.1242/jeb.00888
- Bragg, P. E. (1992). Phasmids and cockroaches as prey of spiders and mantids. *Bull. Amat. Entomol. Soc.* 51, 19–20.
- Briscoe, A. D., and Chittka, L. (2001). The Evolution of color vision in insects. *Annu. Rev. Entomol.* 46, 471–510. doi: 10.1146/annurev.ento.46.1.471
- Caro, T., and Koneru, M. (2021). Towards an ecology of protective coloration. *Biol. Rev.* 96, 611–614. doi: 10.1111/brv.12670
- Chittenden, A. R., and Saito, Y. (2006). Tactile crypsis against non-visual predators in the spider mite, *Aponychus corpuzae* Rimando (*Acari: Tetranychidae*). *J. Insect. Behav.* 19, 419–428. doi: 10.1007/s10905-006-9019-2
- Cuadrado, M., Martín, J., and López, P. (2001). Camouflage and escape decisions in the common chameleon *Chamaeleo chamaeleon*. *Biol. J. Linn. Soc.* 72, 547–554. doi: 10.1111/j.1095-8312.2001.tb01337.x
- Cuthill, I. C. (2019). Camouflage. *J. Zool.* 308, 75–92. doi: 10.1111/jzo.12682
- Cuthill, I. C., and Székely, A. (2009). Coincident disruptive coloration. *Philos. Trans. R. Soc. B Biol. Sci.* 364, 489–496. doi: 10.1098/rstb.2008.0266
- Cuthill, I. C., Matchette, S. R., and Scott-Samuel, N. E. (2019). Camouflage in a dynamic world. *Curr. Opin. Behav. Sci.* 30, 109–115. doi: 10.1016/j.cobeha.2019.07.007
- Dawkins, R., and Krebs, J. R. (1979). Arms races between and within species. *Proc. R. Soc. London. Ser. B. Biol. Sci.* 205, 489–511. doi: 10.1098/rspb.1979.0081
- Dräger, H. (2011). Die gespenstschrecken der familie heteropterygidae KIRBY, 1896 (Phasmatoidea) - ein Überblick über bisher gehaltene Arten. Teil 1: die Unterfamilie Heteropteryginae KIRBY, 1896. *ZAG Phoenix* 2, 38–61.
- Eisner, T. (1965). Defensive spray of a phasmid insect. *Science* 148, 966–968. doi: 10.1126/science.148.3672.966
- Fabricant, S. A., and Herberstein, M. E. (2015). Hidden in plain orange: aposematic coloration is cryptic to a colorblind insect predator. *Behav. Ecol.* 26, 38–44. doi: 10.1093/beheco/aru157
- Fairclough, D. V. (2016). Similar cryptic behaviour during the early juvenile phase of two unrelated reef fishes: *Epinephelides armatus* and *Bodianus frenchii*. *Mar. Freshw. Behav. Physiol.* 49, 109–117. doi: 10.1080/10236244.2015.1125122
- Farkas, T. E. (2016). Body size, not maladaptive gene flow, explains death-feigning behaviour in *Timema cristinae* stick insects. *Evol. Ecol.* 30, 623–634. doi: 10.1007/s10682-016-9832-9
- Ferreira, R. B., Lourenço-de-Moraes, R., Zocca, C., Duca, C., Beard, K. H., and Brodie, E. D. (2019). Antipredator mechanisms of post-metamorphic anurans: a global database and classification system. *Behav. Ecol. Sociobiol.* 73:69. doi: 10.1007/s00265-019-2680-1
- Fleishman, L. J. (1985). Cryptic movement in the vine snake oxybelis aeneus. *Copeia* 1985, 242–245. doi: 10.2307/1444822
- Friard, O., and Gamba, M. (2016). BORIS: a free, versatile open-source event-logging software for video/audio coding and live observations. *Methods Ecol. Evol.* 7, 1325–1330. doi: 10.1111/2041-210X.12584
- Grant, J. B. (2007). Ontogenetic colour change and the evolution of aposematism: a case study in panic moth caterpillars. *J. Anim. Ecol.* 76, 439–447. doi: 10.2307/4539147
- Hall, J. R., Baddeley, R., Scott-Samuel, N. E., Shohet, A. J., and Cuthill, I. C. (2017). Camouflaging moving objects: crypsis and masquerade. *Behav. Ecol.* 28, 1248–1255. doi: 10.1093/beheco/arx085
- Hall, J. R., Cuthill, I. C., Baddeley, R., Shohet, A. J., and Scott-Samuel, N. E. (2013). Camouflage, detection and identification of moving targets. *Proc. R. Soc. B Biol. Sci.* 280:20130064. doi: 10.1098/rspb.2013.0064
- Hammer, Ø, Harper, D. A. T., and Ryan, P. D. (2001). PAST: paleontological Statistics software package for education and data analysis. *Palaeontol. Electron.* 4:9.
- Harrell, F. E. (2021). *Hmisc: Harrell Miscellaneous*. Available online at: <https://cran.r-project.org/package=Hmisc> (accessed May 27, 2021).
- Hart, N. S. (2001). The visual ecology of avian photoreceptors. *Prog. Retin. Eye Res.* 20, 675–703. doi: 10.1016/S1350-9462(01)00009-X
- Harvey, P. H., and Pagel, M. (1991). *The Comparative Method In Evolutionary Biology*. Oxford: Oxford University Press.
- Hennemann, F. H., Conle, O. V., Brock, P. D., and Seow-Choen, F. (2016). Revision of the Oriental subfamily Heteropteryginae Kirby, 1896, with a re-arrangement of the family Heteropterygidae and the descriptions of five new species of

- Haaniella Kirby, 1904. (*Phasmatodea: Areolatae: Heteropterygidae*). *Zootaxa* 4159, 1–219. doi: 10.11646/zootaxa.4159.1.1
- Hochuli, D. F. (2001). Insect herbivory and ontogeny: how do growth and development influence feeding behaviour, morphology and host use? *Austral. Ecol.* 26, 563–570. doi: 10.1046/j.1442-9993.2001.01135.x
- Huffard, C. L., Boneka, F., and Full, R. J. (2005). Underwater bipedal locomotion by octopuses in disguise. *Science* 307:1927. doi: 10.1126/science.1109616
- Hughes, R. N., Burrows, M. T., and Rogers, S. E. B. (1992). Ontogenetic changes in foraging behaviour of the dogwhelk *Nucella lapillus* (L.). *J. Exp. Mar. Bio. Ecol.* 155, 199–212. doi: 10.1016/0022-0981(92)90063-G
- Ioannou, C. C., and Krause, J. (2009). Interactions between background matching and motion during visual detection can explain why cryptic animals keep still. *Biol. Lett.* 5, 191–193. doi: 10.1098/rsbl.2008.0758
- Jackson, R. R. (1985). A web-building jumping spider. *Sci. Am.* 253, 102–115. doi: 10.1038/SCIENTIFICAMERICAN985-102
- Jacobs, G. H. (1993). The distribution and nature of colour vision among the mammals. *Biol. Rev.* 68, 413–471. doi: 10.1111/j.1469-185X.1993.tb00738.x
- Johansen, A. I., Tullberg, B. S., and Gambrale-Stille, G. (2011). Motion level in *Graphosoma lineatum* coincides with ontogenetic change in defensive colouration. *Entomol. Exp. Appl.* 141, 163–167. doi: 10.1111/j.1570-7458.2011.01182.x
- Johnson, M.-L., Armitage, S., Scholz, B. C. G., Merritt, D. J., Cribb, B. W., and Zalucki, M. P. (2007). Predator presence moves *Helicoverpa armigera* larvae to distraction. *J. Insect Behav.* 20, 1–18. doi: 10.1007/s10905-006-9048-x
- Lind, A. J., and Welsh, H. H. (1994). Ontogenetic changes in foraging behaviour and habitat use by the Oregon garter snake, *Thamnophis atratus hydrophilus*. *Anim. Behav.* 48, 1261–1273. doi: 10.1006/anbe.1994.1362
- Löser, S., and Schulten, D. (1981). Fortpflanzung und Verhalten der malayischen riesengespenstschrecke *Heteropteryx dilatata* Park (*Phasmatodea: Phylliidae*). *Löbbecke Museum Aquarium Düsseldorf* 24, 23–27.
- Main, K. L. (1987). Predator avoidance in seagrass meadows: prey behavior. Microhabitat selection, and cryptic coloration. *Ecology* 68, 170–180. doi: 10.2307/1938817
- Mansor, M. S., and Mohd Sah, S. A. (2012). Foraging patterns reveal niche separation in tropical insectivorous birds. *Acta Ornithol.* 47, 27–36. doi: 10.3161/000164512X653890
- Mappes, J., Kokko, H., Ojala, K., and Lindström, L. (2014). Seasonal changes in predator community switch the direction of selection for prey defences. *Nat. Commun.* 5:5016. doi: 10.1038/ncomms6016
- Maritz, B. (2012). To run or hide?: escape behaviour in a cryptic African snake. *Afr. Zool.* 47, 270–274. doi: 10.1080/15627020.2012.11407555
- Martinez Arbizu, P. (2020). *PairwiseAdonis: Pairwise Multilevel Comparison Using Adonis*. R package version 0.4. Available online at: <https://github.com/pmartinezarbizu/pairwiseAdonis> (accessed December 14, 2020).
- Merilaita, S., Scott-Samuel, N. E., and Cuthill, I. C. (2017). How camouflage works. *Philos. Trans. R. Soc. B Biol. Sci.* 372:20160341. doi: 10.1098/rstb.2016.0341
- Nakazawa, M. (2021). *Fmsb: Functions For Medical Statistics Book With Some Demographic Data*. Available online at: <https://cran.r-project.org/package=fmsb> (accessed May 27, 2021).
- Nakazawa, T. (2015). Ontogenetic niche shifts matter in community ecology: a review and future perspectives. *Popul. Ecol.* 57, 347–354. doi: 10.1007/s10144-014-0448-z
- Ohba, S.-Y., and Tatsuta, H. (2016). Young giant water bug nymphs prefer larger prey: changes in foraging behaviour with nymphal growth in *Kirkaldyia deyrolli*. *Biol. J. Linn. Soc.* 117, 601–606. doi: 10.1111/bij.12693
- Oksanen, J., Blanchet, F. G., Friendly, M., Kindt, R., Legendre, P., McGlinn, D., et al. (2019). *Vegan: Community Ecology Package*. Available online at: <https://cran.r-project.org/package=vegan> (accessed July 15, 2020).
- Paine, R. W. (1968). Investigations for the biological control in Fiji of the coconut stick-insect *Graeffea crouanii* (Le Guillou). *Bull. Entomol. Res.* 57, 567–604. doi: 10.1017/S0007485300052937
- R Core Team (2019). *R: A Language And Environment For Statistical Computing*. R Foundation for Statistical Computing, Vienna, Austria. Available online at: [URL https://www.R-project.org/](https://www.R-project.org/) (accessed July 15, 2020).
- Regan, D., and Beverley, K. I. (1984). Figure-ground segregation by motion contrast and by luminance contrast. *J. Opt. Soc. Am. A* 1, 433–442. doi: 10.1364/JOSAA.1.000433
- Robinson, M. H. (1968a). The defensive behaviour of the Javanese stick insect, *Orxines mackloti* De Haan, with a note on the startle display of *Metriotes diocles* Westw. (*Phasmatodea, Phasmidae*). *Entomol. Mon. Mag.* 104, 46–54.
- Robinson, M. H. (1968b). The defensive behaviour of *Pterinoxylus spinulosus* Redtenbacher, a winged stick insect from Panama (*Phasmatodea*). *Psyche* 75, 195–207. doi: 10.1155/1968/19150
- Robinson, M. H., and Robinson, B. C. (1973). Ecology and behavior of the giant wood spider *Nephila maculata* (Fabricius) in New Guinea. *Smithson. Contrib. Zool.* 149, 1–76. doi: 10.5479/SL00810282.149
- Rupprecht, R. (1971). Bewegungsmimikry bei *Carausius morosus* Br. (*Phasmida*). *Experientia* 27, 1437–1438. doi: 10.1007/BF02154275
- Ruxton, G. D., Allen, W. L., Sherratt, T. N., and Speed, M. P. (2018). *Avoiding Attack: The Evolutionary Ecology Of Crypsis, Warning Signals And Mimicry*, 2nd Edn. Oxford: Oxford University Press.
- Seow-Choen, F. (2016). *A Taxonomic Guide To The Stick Insects Of Borneo*. Kota Kinabalu: Natural History Publications (Borneo).
- Seow-Choen, F. (2017). *A Taxonomic Guide To The Stick Insects Of Singapore*. Kota Kinabalu: Natural History Publications (Borneo).
- Starrett, A. (1993). Adaptive resemblance: a unifying concept for mimicry and crypsis. *Biol. J. Linn. Soc.* 48, 299–317. doi: 10.1111/j.1095-8312.1993.tb02093.x
- Steiniger, F. (1933). Die erscheinungen der katalepsie bei stabheuschrecken und wasserläufer. *Z. Morph. Ökol. Tiere* 26, 591–708.
- Stevens, M., and Merilaita, S. (2009). Animal camouflage: current issues and new perspectives. *Philos. Trans. R. Soc. B Biol. Sci.* 364, 423–427. doi: 10.1098/rstb.2008.0217
- Stevens, M., and Ruxton, G. D. (2019). The key role of behaviour in animal camouflage. *Biol. Rev.* 94, 116–134. doi: 10.1111/brv.12438
- Stockard, C. R. (1908). Habits, reactions and mating instincts of the “Walking Stick,” *Aplopus mayeri*. *Pap. Tortugas Lab.* 2, 43–59.
- Strong, L. (1975). Defence glands in the giant spiny phasmid *Extatosoma tiaratum*. *J. Entomol. Ser. A Gen. Entomol.* 50, 65–72. doi: 10.1111/j.1365-3032.1975.tb00093.x
- Suetsugu, K., Funaki, S., Takahashi, A., Ito, K., and Yokoyama, T. (2018). Potential role of bird predation in the dispersal of otherwise flightless stick insects. *Ecology* 99, 1504–1506. doi: 10.1002/ecy.2230
- Tan, E. J., and Elgar, M. A. (2021). Motion: enhancing signals and concealing cues. *Biol. Open* 10:bio058762. doi: 10.1242/bio.058762
- Tan, E. J., Reid, C. A. M., and Elgar, M. A. (2016). Colour pattern variation affects predation in chrysomeline larvae. *Anim. Behav.* 118, 3–10. doi: 10.1016/j.anbehav.2016.05.019
- Tan, E. J., Reid, C. A. M., and Elgar, M. A. (2017). Predators, parasites and heterospecific aggregations in chrysomeline larvae. *Ethology* 123, 293–306. doi: 10.1111/eth.12598
- Tan, E. J., Wilts, B. D., Tan, B. T. K., and Monteiro, A. (2020). What's in a band? The function of the color and banding pattern of the Banded Swallowtail. *Ecol. Evol.* 10, 2021–2029. doi: 10.1002/eece3.6034
- Théry, M., and Gomez, D. (2010). “Insect colours and visual appearance in the eyes of their predators,” in *Advances in Insect Physiology: Insect Integument and Colour*, eds J. Casas and S. J. Simpson (Cambridge, MA: Academic Press), 267–353. doi: 10.1016/S0065-2806(10)38001-5
- Valkonen, J. K., Nokelainen, O., Jokimäki, M., Kuusinen, E., Paloranta, M., Peura, M., et al. (2014). From deception to frankness: benefits of ontogenetic shift in the anti-predator strategy of alder moth *Acronicta alni* larvae. *Curr. Zool.* 60, 114–122. doi: 10.1093/czoolo/60.1.114
- Watanabe, H., and Yano, E. (2009). Behavioral response of mantid *Hierodula patellifera* to wind as an antipredator strategy. *Ann. Entomol. Soc. Am.* 102, 517–522. doi: 10.1603/008.102.0323
- Watanabe, H., and Yano, E. (2012). Behavioral response of male mantid *Tenodera aridifolia* (Mantodea: Mantidae) to windy conditions as a female approach strategy. *Entomol. Sci.* 15, 384–391. doi: 10.1111/j.1479-8298.2012.00535.x
- Watanabe, H., and Yano, E. (2013). Behavioral response of mantid *Tenodera aridifolia* (Mantodea: Mantidae) to windy conditions as a cryptic approach strategy for approaching prey. *Entomol. Sci.* 16, 40–46. doi: 10.1111/j.1479-8298.2012.00536.x
- Webster, R. J., Callahan, A., Godin, J.-G. J., and Sherratt, T. N. (2009). Behaviourally mediated crypsis in two nocturnal moths with contrasting appearance. *Philos. Trans. R. Soc. B Biol. Sci.* 364, 503–510. doi: 10.1098/rstb.2008.0215

- Wedmann, S., Bradler, S., and Rust, J. (2007). The first fossil leaf insect: 47 million years of specialized cryptic morphology and behavior. *Proc. Natl. Acad. Sci.* 104, 565–569. doi: 10.1073/pnas.0606937104
- Werner, E. E., and Gilliam, J. F. (1984). The ontogenetic niche and species interactions in size-structured populations. *Annu. Rev. Ecol. Syst.* 15, 393–425. doi: 10.1146/annurev.es.15.110184.002141
- Whelan, C. J. (2001). Foliage structure influences foraging of insectivorous forest birds: an experimental study. *Ecology* 82, 219–231. doi: 10.1890/0012-9658(2001)082[0219:FSIFOI]2.0.CO;2
- Wickham, H. (2007). Reshaping data with the reshape package. *J. Stat. Softw.* 21, 1–20. doi: 10.18637/jss.v021.i12
- Wickham, H. (2016). *ggplot2: Elegant Graphics for Data Analysis*. New York, NY: Springer-Verlag.
- Ydenberg, R. C., and Dill, L. M. (1986). “The economics of fleeing from predators,” in *Advances in the Study of Behavior*, eds J. S. Rosenblatt, C. Beer, M.-C. Busnel, and P. J. B. Slater (Cambridge, MA: Academic Press), 229–249. doi: 10.1016/S0065-3454(08)60192-8
- Zeng, Y., Chang, S. W., Williams, J. Y., Nguyen, L. Y.-N., Tang, J., Naing, G., et al. (2020). Canopy parkour: movement ecology of post-hatch dispersal in a gliding nymphal stick insect, *Extatosoma tiaratum*. *J. Exp. Biol.* 223:jeb226266. doi: 10.1242/jeb.226266
- Conflict of Interest:** The authors declare that the research was conducted in the absence of any commercial or financial relationships that could be construed as a potential conflict of interest.
- Publisher’s Note:** All claims expressed in this article are solely those of the authors and do not necessarily represent those of their affiliated organizations, or those of the publisher, the editors and the reviewers. Any product that may be evaluated in this article, or claim that may be made by its manufacturer, is not guaranteed or endorsed by the publisher.

Copyright © 2022 Pohl, Bungum, Lee, Sani, Poh, Wahab, Norma-Rashid and Tan. This is an open-access article distributed under the terms of the Creative Commons Attribution License (CC BY). The use, distribution or reproduction in other forums is permitted, provided the original author(s) and the copyright owner(s) are credited and that the original publication in this journal is cited, in accordance with accepted academic practice. No use, distribution or reproduction is permitted which does not comply with these terms.



The Adaptive Significance of Flash Behavior: A Bayesian Model

Thomas N. Sherratt* and Karl Loeffler-Henry

Department of Biology, Carleton University, Ottawa, ON, Canada

OPEN ACCESS

Edited by:

Eunice Jingmei Tan,
Yale-NUS College, Singapore

Reviewed by:

Richard Anthony Peters,
La Trobe University, Australia
Olivier Penacchio,
University of St Andrews,
United Kingdom

*Correspondence:

Thomas N. Sherratt
Tom.Sherratt@Carleton.ca

Specialty section:

This article was submitted to
Behavioral and Evolutionary Ecology,
a section of the journal
Frontiers in Ecology and Evolution

Received: 24 March 2022

Accepted: 25 April 2022

Published: 11 May 2022

Citation:

Sherratt TN and Loeffler-Henry K
(2022) The Adaptive Significance
of Flash Behavior: A Bayesian Model.
Front. Ecol. Evol. 10:903769.
doi: 10.3389/fevo.2022.903769

Some cryptic animals have conspicuous color patches that are displayed when they move. This “flash behavior” may serve several functions, but perhaps the most widely invoked explanation is that the display makes it harder for the signaler to be found by predators once it has settled. There is now some experimental evidence that flash behavior while fleeing can enhance the survivorship of prey in the manner proposed. However, to date there has been no explicit mathematical model to help understand the way in which flash displays might interfere with the search process of predators. Here we apply Bayesian search theory to show that the higher the conspicuousness of a prey item, the sooner a predator should give up searching for it in an area where it appears to have settled, although the relationship is not always monotonically decreasing. Thus, fleeing prey that give the impression of being conspicuous will tend to survive at a higher rate than prey seen to flee in their cryptic state, since predators search for flashing prey for an inappropriately short period of time. The model is readily parameterized and makes several intuitive predictions including: (1) the more confident a predator is that a prey item has settled in a given area, the longer it will search there, (2) the more conspicuous the flash display, the greater its effect in reducing predation, (3) flash behavior will especially benefit those prey with an intermediate level of crypsis when at rest, and (4) the success of flash displays depends on the predator being uncertain of the prey’s resting appearance. We evaluate the empirical evidence for these predictions and discuss how the model might be further developed, including the incorporation of mimicry which would maintain the deception indefinitely.

Keywords: flash behavior, anti-predator signal, Bayesian search theory, marginal value theorem, optimal foraging

INTRODUCTION

Some animals are cryptic at rest yet display conspicuous colors and/or sounds when they move, before resuming their cryptic state as they settle (Cott, 1940; Anonymous, 1945). Putative examples of this “flash behavior” include the conspicuous hindwing displays of many insect species [including Orthoptera (see **Figure 1**) and Lepidoptera], the prominent tail flagging of some Artiodactyla and Leporidae, and the exposure of the gaudy tail feathers of many otherwise cryptic bird species (Edmunds, 1974, 2008). In each of these cases, the conspicuous traits remain hidden while the organism is at rest and yet they are suddenly revealed while fleeing. Since the hidden conspicuous traits of flashing species tend to be found in both males and females (Loeffler-Henry et al., 2019, 2021) and the flash display is invariably elicited by disturbance, the behavior likely serves as an anti-predator defense rather than as a sexual signal.

Precisely how do conspicuous traits “*which flash out during movement and vanish again, like a conjurer’s rabbit*” (Cott, 1940, p. 376) serve as an anti-predator defense? It is possible that flash behavior may startle any would-be predator (Umbers et al., 2015) and/or make the signaler harder to catch while fleeing (Murali, 2018). However, the most widely discussed benefit is that would-be predators are misled into believing the prey item is always conspicuous in appearance, which hinders the predator’s subsequent search for it (Cott, 1940; Anonymous, 1945). Edmunds (1974, p. 146) made this case most explicitly, noting that a predator “*may follow this color and be deceived by its sudden disappearance into assuming the prey has vanished whereas in reality the prey has come to rest in its normal cryptic posture with the colored structures hidden.*” An implication of the hypothesis is that any predator coming to search for a conspicuous prey item would give up looking sooner if it did not see the prey item, since if the prey is not immediately found, it will likely be elsewhere (Figure 2).

Despite their widespread taxonomic distribution, flash displays have only recently begun to be investigated. In a series of computer-based experiments using humans as visual predators, Loeffler-Henry et al. (2018) and Bae et al. (2019) found that participants were indeed more likely to give up looking for prey that had displayed conspicuous colors in motion but resumed crypsis when settled, compared to those prey that were cryptic in motion and at rest. Loeffler-Henry et al. (2021) ran similar experiments and found that flashing prey had a higher survival rate than non-flashing prey but only if predators were unaware of the true resting appearance of the prey, indicating that the benefit of the display was contingent on deception.

While we have an experimental “proof of concept” using computer-generated prey, to date no formal model has been proposed to help explain precisely how and when flash behavior would enhance survivorship. The development of such a model would be an advance for several reasons. First, it would help make the mechanism through which flash behavior hinders predator search more transparent. Second, it will help reveal implicit assumptions and render explicit predictions. Third, it would provide an extra level of rigor in establishing the plausibility of verbal arguments on a quantitative level. Fourth, a parameterizable model could provide a basis for experimental investigation. Here we present and explore just such a model, built on basic biological assumptions. As the model is based on a flashing species giving a misleading impression of its conspicuousness when settled, we first describe how predators should search for prey items of known conspicuousness. Most methods of efficient search use the logic of conditional probabilities and are therefore Bayesian in nature. We then describe how a fleeing prey can enhance its survivorship by giving the impression that it is more conspicuous at rest than it is.

METHODS AND RESULTS

Imagine you have lost your wallet. You decide, quite rationally, to first look for your wallet in the place it is most likely to be, namely your bedroom. However, the longer you search your bedroom

without finding it, the less likely it is to be there. After a while, there will reach a time at which it makes sense to check another room for your wallet, such as the kitchen. So, you move to the kitchen to look for it there, although this doesn’t preclude you coming back to continue to search your bedroom. As further time passes, with no sign of your wallet in all its plausible locations, you start to entertain the possibility the wallet has been stolen. Of course, you may never know for sure whether this is the case, but the prospect of finding your wallet in the house are becoming increasingly slim. After extensive fruitless search you simply give up because life is too short to waste more time looking.

The above scenario may sound all too familiar and the logic underlying the search intuitive. As we will see, with a formal model of the search process for a lost object, we can quantitatively identify the length of time one should spend searching in a given area before moving on. This model starts with a prior belief, expressed as a probability, that the object is in a certain location. As time passes and the object is not found there then this information can be combined with the prior belief to generate a posterior belief that the object is in the area being searched. The process of turning a prior belief into a posterior belief based on new data uses the algebra of conditional probabilities, namely Bayes’ rule (Courville et al., 2006; McNamara et al., 2006; McElreath, 2020). Bayesian search theory is a well-developed research field and involves the application of Bayesian inference to improve the efficiency of search for lost objects (Koopman, 1957, 1980; Stone, 1975). The approach has previously been used in a range of contexts from finding sunken treasure, to recovering flight recorders (McGrayne, 2012). Here we apply it in the context of a simple foraging problem in which a predator searches for prey. We then show how prey can exploit this optimal search strategy, and thereby improve their survivorship.

Optimal Search for a Hidden Object

We start by introducing the foraging problem. A predator (such as a bird) has disturbed a prey item (such as a grasshopper) and observed it flee. The predator believes that the prey item has settled in a certain area (a patch), but it is not entirely sure. The predator then attempts to pursue this prey item. Let us assume that a prey item has a fixed instantaneous rate λ (>0) of being detected by a predator if the predator is searching for the prey in the patch it has settled. Under these conditions, the probability density of the time taken of the predator to discover the prey will follow an exponential distribution, so the cumulative probability a predator will not have found the prey item by time t (i.e., the probability the prey remains undetected) will be:

$$u(t) = e^{-\lambda t} \quad (1)$$

We use λ parameter (otherwise known as the instantaneous hazard rate) as a measure of the prey item’s conspicuousness. Indeed, given the exponential distribution, the mean time taken to discover the prey item if it is present in the patch being searched is $(1/\lambda)$ with variance $(1/\lambda^2)$, so a higher conspicuousness translates to shorter and less variable time to detection.



FIGURE 1 | Examples of flash behavior in Orthoptera (grasshoppers and crickets). Many grasshoppers are cryptic at rest and have transparent wings when they fly. However, the blue-winged grasshopper *Oedipoda caerulescens* (Linnaeus) exposes bright blue wings when flying, before settling into a cryptic resting state (row 1). The Carolina locust *Dissosteira carolina* (Linnaeus) exposes dark brown wings in flight yet resumes crypsis when it settles (row 2). Similarly, the short-horned grasshopper *Arphia conspersa* (Scudd) flashes conspicuous yellow wings in flight (row 3). The images (except those provided by KL-H) were derived from Wikimedia Commons and are reproduced under the Creative Commons Licence. Photo credits (by row, left and right): (1) Charles Sharp, Didier Descouens; (2) anonymous, Karl Loeffler-Henry; (3) Even Dankowicz, Karl Loeffler-Henry.

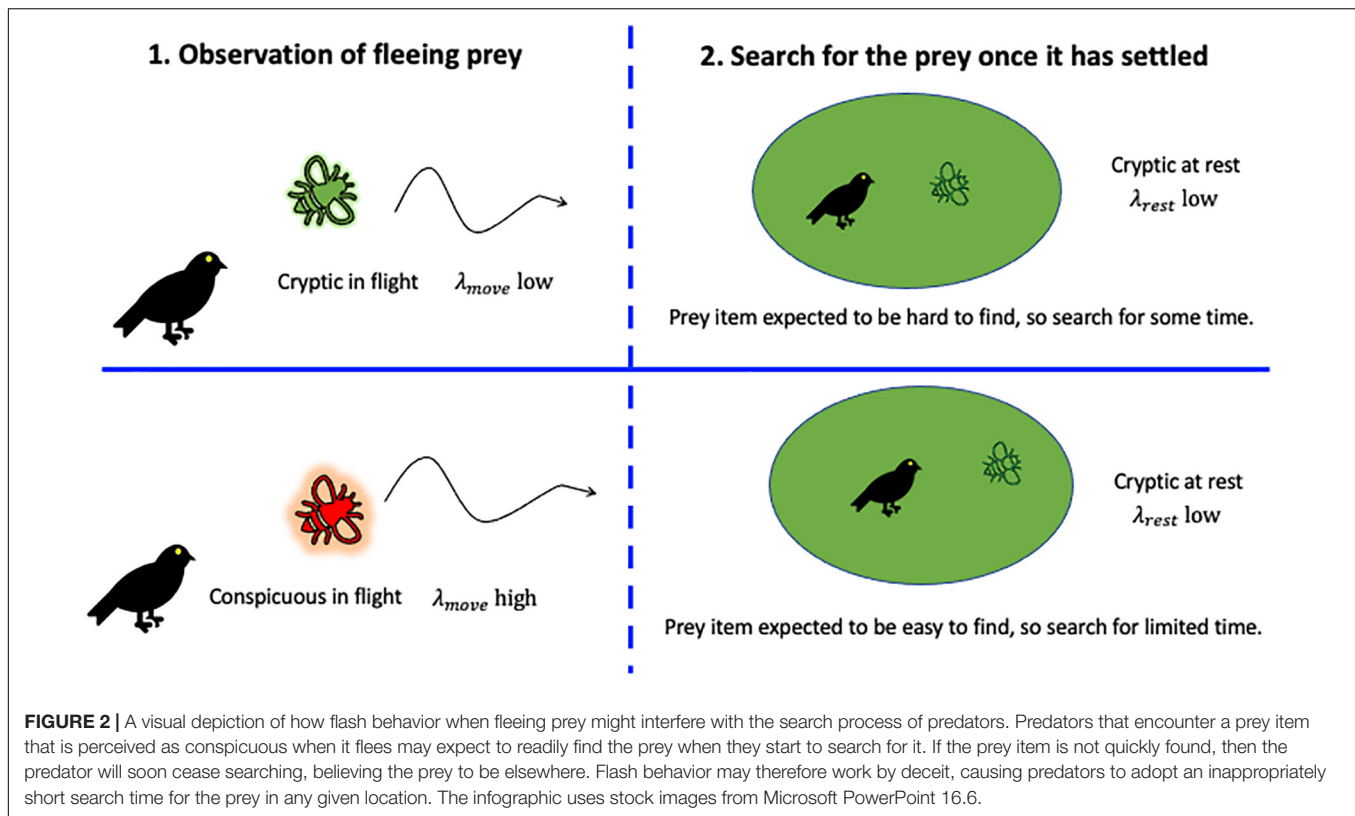
Of course, even if a predator observes a prey item with conspicuousness λ while fleeing, it may not be entirely confident where it has settled and so may consider several possibilities. We therefore assume that the predator has prior probabilities p_1, p_2, \dots, p_n that the fleeing prey item has settled in each of n (> 1) alternative patches (so that $0 < p_i < 1$ and $\sum_1^n p_i = 1$). With no loss of generality we allow the subscripts to refer to the order of magnitude of prior probabilities such that $p_1 > p_2 > \dots > p_n$. Naturally, all else being equal, the predator should start its search in patch 1, where the prey item is most likely to be. However, the longer the predator searches in patch 1 without discovering the prey item, the less likely the prey item is in the patch. This lack of success provides information with which it can continually revise its beliefs that the prey item is in the patch (McNamara and Houston, 1985; Killeen et al., 1996).

Let A_i represent the event that the prey has settled in patch i and $u(t)$ be the event that the prey has not been found in patch 1 after the predator spends time t searching there. For reasons that will become evident, we focus solely on decisions made on the

first patch, so do not use a patch-specific subscript for either u or t . Expressed in mathematical terms we seek $\Pr(A_1 | u(t))$, i.e., the posterior probability that patch 1 contains the prey item, given that the predator has been searching in that patch for the prey item for time t and it remains undetected. Invoking Bayes' rule for conditional probabilities we know that:

$$\Pr(A_1 | u(t)) = \frac{\Pr(u(t) | A_1) \Pr(A_1)}{u(t)} \quad (2)$$

Here $\Pr(A_1)$ represents the prior probability that the prey item has settled in patch 1 ($= p_1$), while $\Pr(u(t) | A_1)$ refers to probability that the prey item remains undiscovered by time t given that it has indeed settled in patch 1. The normalizing denominator $u(t)$ refers to the overall likelihood of the prey item being undetected when the predator searches in patch 1, whether it has settled in patch 1 or not. There are two ways the prey item can remain undetected when the predator searches patch 1. It could be present in patch 1 but remain undiscovered which will arise with combined probability $p_1 e^{-\lambda t}$ or it could be in one of the other patches, in which case it will certainly remain



undetected. This outcome will arise with expected probability $1 - p_1$. Substituting for the expressions in Eq. 2, we have:

$$\Pr(A_1 | u(t)) = \frac{e^{-\lambda t} p_1}{p_1 e^{-\lambda t} + (1 - p_1)} \quad (3)$$

Which simplifies to:

$$\Pr(A_1 | u(t)) = \frac{p_1}{p_1 + (1 - p_1) e^{\lambda t}} \quad (4)$$

Note that $\Pr(A_1 | u(0)) = p_1$ (with no information, a predator only uses its prior to estimate the probability that the prey item is in patch 1) and $\Pr(A_1 | u(\infty)) = 0$ (the prey item is increasingly unlikely to be in patch 1 the longer the predator searches this patch without discovering it). If the candidate patches are close by one another, so that the travel time between them is negligible, then the predator should switch from patch 1 to patch 2 (the next likely area) when the estimated (posterior) probability of finding it in patch 1 falls to match the probability of finding it in the second patch. Naturally, however, the posteriors for the second patch are not unchanged – if the prey item is not found in the first patch in time t then this increases the probability that it is found in the other patches. Bayes' theorem comes to the rescue again:

$$\Pr(A_2 | u(t)) = \frac{\Pr(u(t) | A_2) \Pr(A_2)}{u(t)} \quad (5)$$

Here $\Pr(u(t) | A_2) = 1$ since it is certain that the prey item will not be found after searching time t in patch 1, given that the prey item is in patch 2.

Substituting, for $\Pr(A_2) (= p_2)$ and $u(t)$ we have:

$$\Pr(A_2 | u(t)) = \frac{p_2}{p_1 e^{-\lambda t} + (1 - p_1)} \quad (6)$$

Note that $\Pr(A_2 | u(0)) = p_2$ (with no time spent so far on patch 1, the predator will use its prior to estimate the probability that the prey item is present in patch 2) and $\Pr(A_2 | u(\infty)) = \frac{p_2}{(1 - p_1)}$ (since the prey item is highly unlikely to be in patch 1 after extensive search, the probability of the prey item being in patch 2 and all other patches commensurately increases).

We can identify the critical time (t_1^*) time a predator would spend searching fruitlessly for the prey item in patch 1 before the (posterior) probability of it occurring in patch 1 declines to equal the (increasing) posterior probability of the prey item being in patch 2. This is the critical time t_1^* that satisfies:

$$\Pr(A_1 | u(t_1^*)) = \Pr(A_2 | u(t_1^*)) \quad (7)$$

Substituting Eqs 4, 6 in Eq. 7 and solving indicates:

$$t_1^* = \frac{\text{Log} \left[\frac{p_1}{p_2} \right]}{\lambda} \quad (8)$$

Note at the outset that this critical time is not the expected time a predator will spend searching in patch 1 but the predicted maximum time it should spend searching, because a proportion of times the prey item will have been present in the patch and it will have been found before the threshold is reached (McNamara and Houston, 1985). A direct consequence of Eq. 8 is that the

more conspicuous a prey item is (i.e., the higher λ) the shorter the length of time a predator should look for it in patch 1 before moving on to the next most likely patch. Moreover, as might be expected, the more initially convinced a predator is that the prey item has settled in patch 1 (i.e., the higher p_1) the longer it will look there before moving on.

Abandoning Search: The Marginal Value Theorem

The above mathematics provides the optimal Bayesian search sequence of n patches, but all else being equal, if the predator moves to patch 2 and no prey item is immediately found then the predator should return to patch 1, moving back and forth until either it finds the prey item or the posterior (conditional) probabilities of being in either patch both become so low that patch 3 now becomes a plausible location where the prey item could be and is included in the search set (Killeen et al., 1996). Naturally, if the prey item is present in one of the n possible patches, and the predator has no incentive to stop, then the prey item will eventually be found. Even if the prey item is not present in any of the n patches (so that the prey item has settled in a patch outside the candidate set, despite the predator's prior belief that this would arise with probability zero) then without a stopping rule the predator will continue to search the n patches forever.

There are many reasons why a searching predator might eventually give up searching the network of patches. One important reason is that time is valuable to the predator. Thus, rather than continuing to search without success, a time will come when it will be more profitable for the predator to stop searching for the lost prey and continue on its way. One could introduce a simple stopping rule in which a predator gives up searching a patch if the posterior probability of the prey item being present there falls below a certain threshold. However, this approach does not explicitly identify the search strategy that maximizes an appropriate fitness-related currency, such as the long-term rate of capture of prey. Charnov's marginal value theorem (MVT) (Charnov, 1976) is an appropriate rule to invoke for this purpose and states a predator will maximize its long-term rate of reward if it leaves a given patch when its instantaneous rate of gain falls below that which could be gained from moving on and seeking an alternative patch. Here we apply this intuitive rule and explore its implications. For mathematical convenience, we focus on instances in which the predator starts out searching the most likely candidate patch, and if evidence accumulates that it is not present in the patch it abandons its search altogether rather than looking at the second most plausible patch. This strategy will be appropriate if there was only one area that could be profitably searched – for example, any prey item that had settled outside the patch being searched is able to conceal itself, or make its escape, while the predator is looking elsewhere. Note that this is not an overly restrictive assumption since the MVT would apply if the predator could search several patches before moving on, but it would complicate the model unnecessarily.

The original formulation of Charnov (1976) assumed a smooth deterministic gain function, and yet here any patch that is searched contains one prey item at most, which

is found by chance. Models with stochastic encounters do not necessarily share the same optimal solutions as their deterministic counterparts (Oaten, 1977; Green, 1980; McNair, 1982). For example, if patch quality varies and the quality of the patch can be inferred from the predator's accumulating experience, then a predator that uses patch-specific information will generally receive a higher payoff than a predator that uses some kind of average experience (Oaten, 1977). In our case, we have already allowed predators to use information on time spent searching to infer patch quality (i.e., the likelihood it contains a prey item). However, rather than use the actual rate of gain of an individual predator on a patch (which will be zero until it finds the prey item), we instead use the expected rate of gain of the predator in the immediate future as a measure of the predator's short-term anticipated rate of success (McNamara, 1982; McNamara and Houston, 1985). We refer to the predator's expected instantaneous rate of reward as $r(t)$, noting that it will fall the longer the predator has been searching in a patch.

If the prey item is known to be present in the patch being searched, then the initial expected instantaneous rate at which the predator will detect the prey item [i.e., $r(0)$] will be λ . If the prey item is known to be absent from the patch being searched, then the instantaneous rate of detection of the prey item in this patch will always be 0. However, the searching predator will in general not know the prey item's true location with certainty until it has found it. In this case, the instantaneous expected instantaneous rate of gain of the predator will be λ multiplied by the posterior probability of that the prey item is present in the patch given that it has not yet been found, namely:

$$r(t) = \lambda \Pr(A_1 | u(t)) \quad (9)$$

Substituting Eq. 4 in Eq. 9 we have:

$$r(t) = \frac{\lambda p_1}{p_1 + (1 - p_1) e^{\lambda t}} \quad (10)$$

Note that the expected instantaneous rate of gain of the predator starts at λp_1 at time 0 and moves toward zero as the time without finding the prey item increases, reflecting the fact that the prey item is increasingly less likely to be on the patch (see **Supplementary Figure 1**). We should now compare the expected instantaneous rate of gain of a searching predator with the rate of gain the predator could achieve by abandoning its current search and moving elsewhere. If all flush and search events of prey had the same characteristics, then we could calculate the expected long-term rate of gain of the predator by treating the current patch as a typical patch and incorporating a travel time between new prey items (τ) into the appropriate rate calculations (e.g., see McNamara and Houston, 1985). However, if there are a range of prey types that vary in energy content, conspicuousness, and ease at which they can be followed when fleeing, then the long-term rate of gain cannot be calculated from the characteristics of any single example of an encounter with prey. We therefore give the long-term rate of gain a fixed value of g .

The MVT dictates that a predator will abandon its search when the instantaneous expected rate of gain (which diminishes as search time continues) from searching for the prey item (see

Eq. 10) falls below the long-term rate of gain from moving on, namely if:

$$\frac{\lambda p_1}{p_1 + (1 - p_1) e^{\lambda t}} < g \quad (11)$$

Solving for the time at which the instantaneous gain matches the long-term gain from abandoning search, we have:

$$t_s^* = \frac{\text{Log} \left[\frac{p_1(\lambda - g)}{g(1 - p_1)} \right]}{\lambda} \quad (12)$$

which is greater than zero so long as $\lambda p_1 > g$, i.e., the expected initial instantaneous rate of gain from searching exceeds the long-term rate of gain of the predator from moving on, otherwise the predator would not initiate searching.

Figure 3 shows the predicted relationship between the optimal time spent searching on patch 1 and the conspicuousness of the settled prey item. The optimal search time before moving on is typically shorter for prey items that are more conspicuous (indeed, $t_s^* \rightarrow 0$ as $\lambda \rightarrow \infty$). However, since $t_s^* \rightarrow 0$ for $\lambda p_1 \rightarrow g$ from above and $t_s^* > 0$ when $\lambda p_1 > g$ then the optimal maximum search time initially increases for low permissible λ and thereafter decreases. This maximum in optimal search time is readily explained by the fact that while the expected instantaneous rate of gain of a predator declines more rapidly for higher λ , the initial expected instantaneous rate of gain (i.e., the intercept λp_1) is lower for patches with more cryptic prey. So, if the threshold g happens to be close to λp_1 for cryptic prey, the optimal time spent searching for them may be less than that of a more conspicuous prey item (see **Supplementary Figure 1**). Put another way, for small λ then $r(t) \approx \lambda p_1$ (because a lack of success in finding cryptic prey does not have a strong effect on the posterior), so the contribution of λ to $r(t)$ is positive. However, for large λ , the posterior probability is approximately proportional to $e^{-\lambda t}$ and since it dominates $r(t)$ the contribution of λ to $r(t)$ is negative.

Since the derivative of t_s^* (Eq. 12) with respect to p_1 is $\{\lambda p_1 (1 - p_1)\}^{-1}$, which is always positive the more initially convinced the predator is that the prey item is present in the patch the longer it will search the patch before giving up. Likewise, the derivative of t_s^* with respect to g is $\{g (g - \lambda)\}^{-1}$ which is always negative for $\lambda p_1 > g$, so the higher g , the less time a predator will spend searching on a patch before moving on.

The Survival Implications of Optimal Search for Prey

We now quantify the implications of the predator optimal search behavior for prey survivorship. Let us assume that the prey item does indeed land in patch 1 with probability p_1 , as the predator initially believes. The probability of the prey item going undetected if the predator forages in the above optimal way is therefore given by:

$$u(t_s^*) = p_1 e^{-\lambda t_s^*} + (1 - p_1) \quad (13)$$

Substituting for t_s^* from Eq. 12 in Eq. 13 we obtain a simple expression for prey survivorship following optimal search namely:

$$u(t_s^*) = \frac{\lambda (1 - p_1)}{(\lambda - g)} \quad (14)$$

Since the derivative of this function with respect to λ is negative for $\lambda > g$, then the survivorship of prey declines with their increasing conspicuousness, reaching an asymptote at $(1 - p_1)$: the only way an extremely conspicuous prey item can survive undetected by a predator is if it has settled in a patch that is not first explored.

Enhancing Prey Survival by Giving a False Idea of Conspicuousness

We can now formally quantify the survival benefits of a flash display. So far, we have assumed that a predator can infer the conspicuousness of a prey item at rest (λ_{rest}) from observing it in motion (λ_{move}). Naturally a predator's estimation of the conspicuousness of a prey item will not be perfect, but probably sufficient for the predator to know whether it will be subsequently searching for something that is easy to find, or hard to find. Here we consider the implications of a fleeing prey giving a predator the false impression that it will be easy to find once it settles (i.e., conspicuous) when in fact it is hard to find (i.e., cryptic).

Let us assume that with non-flashing prey $\lambda_{move} = \lambda_{rest}$. In contrast, we assume that due to their colorful display flashing prey give a false impression of a higher conspicuousness at rest, such that $\lambda_{move} > \lambda_{rest}$. The probability of a prey item surviving undetected by a predator that is searching for it will therefore be dependent on its ease of detection when at rest (a function of λ_{rest}) and the maximum time the predator is prepared to search for it in the patch (a function of λ_{move}). Re-writing Eq. 13 and substituting for t_s^* from Eq. 12 we have:

$$u(t_s^*) = p_1 e^{-\lambda_{rest} \left(\frac{\text{Log} \left[\frac{p_1(\lambda_{move} - g)}{g(1 - p_1)} \right]}{\lambda_{move}} \right)} + (1 - p_1) \quad (15)$$

Which simplifies to:

$$u(t_s^*) = (1 - p_1) + p_1 \left\{ \frac{g(1 - p_1)}{p_1(\lambda_{move} - g)} \right\}^{\frac{\lambda_{rest}}{\lambda_{move}}} \quad (16)$$

When $\lambda_{move} = \lambda_{rest}$ then Eq. 16 reduces to Eq. 14. Moreover, if $\lambda_{move} p_1 > g$ (so that the prey item is sufficiently conspicuous, and sufficiently likely to be in a given patch, to be pursued) then $0 < \frac{g(1 - p_1)}{p_1(\lambda_{move} - g)} < 1$. So, for a fixed λ_{move} the lower λ_{rest} the higher the overall survival. In other words, making a prey more cryptic when it settles will always enhance the prey item's survivorship. However, since λ_{move} is also part of the denominator of Eq. 16, the reverse is not always true: a conspicuous flash does not unconditionally generate a higher survival rate in prey with a given fixed crypsis when settled, although this is often the case (**Figure 4**). As before, the counter intuitive results arise when g is slightly less than $\lambda_{move} p_1$ in which case predators will search for less time for a prey item they believe

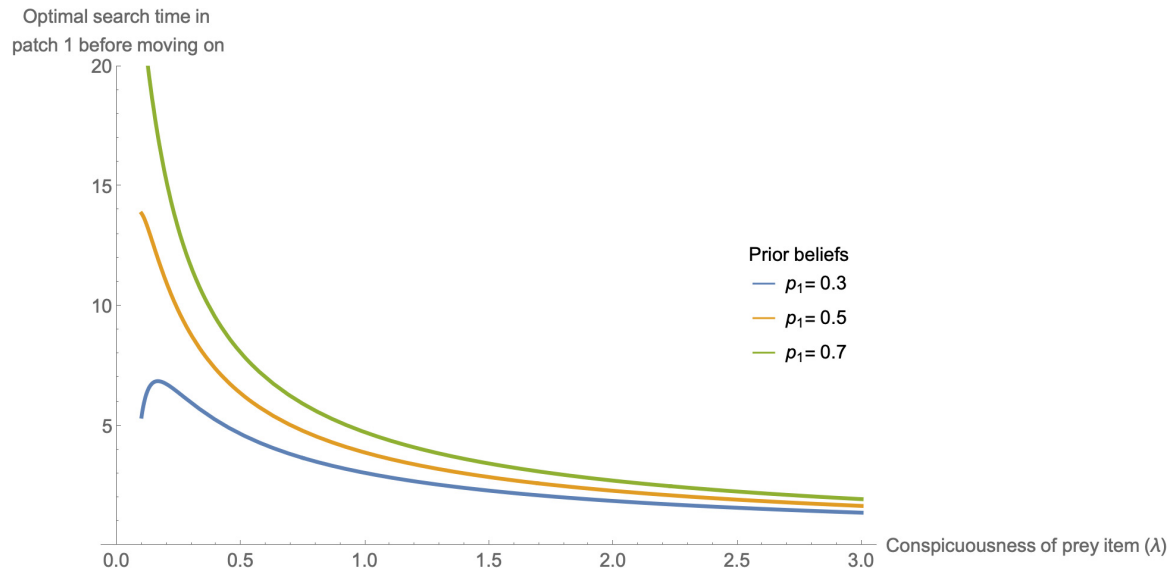


FIGURE 3 | The optimal maximum search time of a predator looking for a prey item in patch 1 (the patch it believes the prey is most likely hiding) before abandoning its search and looking for prey elsewhere. Here we set the average long-term rate of gain from abandoning search (g) to be 0.02 and vary the conspicuousness of the fleeing prey item (λ) from 0.1 to 3 (so that it is always profitable to pursue the prey item so long as $p_1 > 0.2$). The predator's prior probability that the most plausible patch 1 contains the prey item (p_1) is considered at three different levels (0.3, 0.5, and 0.7). In general, the higher the conspicuousness of the prey item, the shorter the maximal search time before abandonment (although it may pay a predator to search for cryptic prey items of borderline profitability for a relatively short period of time, hence a peak). The more confident the predator is that the prey have landed in the patch, the longer it should search.

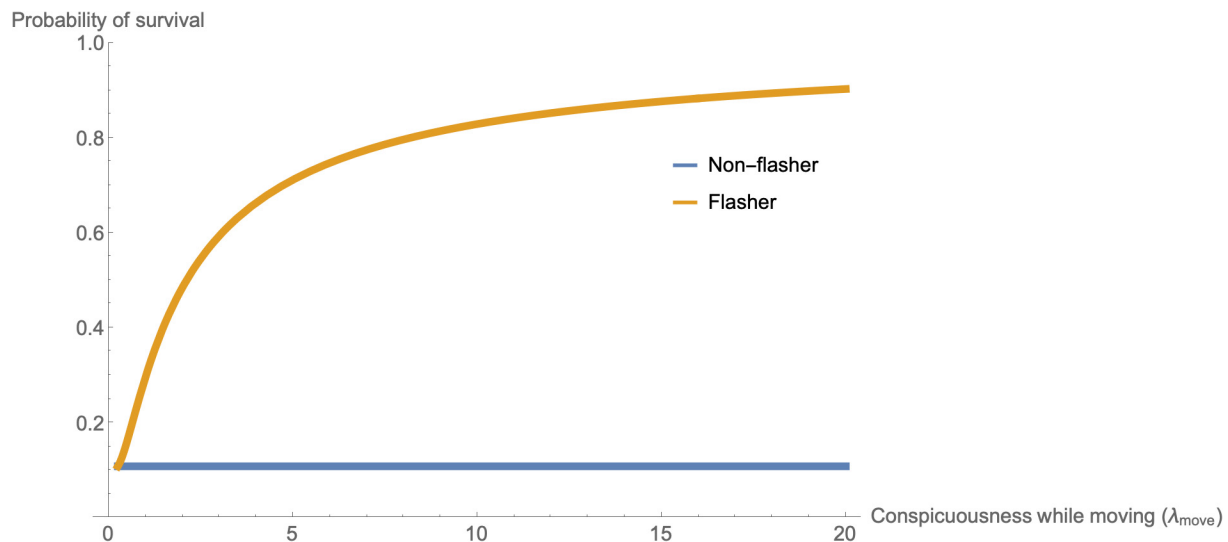


FIGURE 4 | The survival rate of a non-flashing cryptic species (blue) that has the same appearance when moving as it does at rest ($\lambda_{move} = \lambda_{rest}$) compared with the survival rate of a flashing species that gives the false impression of being more conspicuous when it is seen moving than it is once settled ($\lambda_{move} > \lambda_{rest}$). Here the apparent conspicuousness of the fleeing prey (λ_{move}) influences the time the predator spends searching for prey. In general, the higher the conspicuousness of the flashing prey while fleeing (x-axis) the greater its survivorship advantage over non-flashing prey because the lower the maximum amount of time predators are prepared to look for it. Here $\lambda_{rest} = 0.25$, $p_1 = 0.9$, $g = 0.02$, and λ_{move} is varied from 0.25 to 20. See **Supplementary Figure 2** for a comparable plot when prey items are of borderline profitability to pursue, i.e., $g = 0.2$, so that $\lambda_{move} p_1 \approx g$ for low λ_{move} .

is cryptic than one they believe is slightly more conspicuous (see **Supplementary Figure 2**). Since $r(t)$ declines more rapidly with increasing conspicuousness, then the slope will effectively overpower the intercept so that any solutions involving long t_s^*

(i.e., low g) will inevitably involve conspicuous prey items being searched for less time without success than cryptic prey items, and a corresponding increase in the survivorship of flashing prey. Indeed, as $\lambda_{move} \rightarrow \infty$ then $u(t_s^*) \rightarrow 1$, so a prey item that is

extremely conspicuous when in flight for a given λ_{rest} will always enhance the survival of the item.

Some Predictions of the Model

To help draw the modeling threads together, here we take the opportunity to identify some basic predictions of our model. We consider the available evidence for and against these predictions in our Discussion.

Prediction 1: The More Confident a Predator Is That a Prey Is Present, the Longer the Search Time Before Giving up

The positive derivative of optimal prey search time (Eq. 12) with respect to p_1 suggests that the more initially convinced a predator is that the prey item is hiding in a patch, the longer it will spend searching there before giving up.

Prediction 2: The More Conspicuous the Flash Display, the Greater Its Effect in Reducing Predation

Figure 4 and **Supplementary Figure 2** and the associated analysis (Eq. 16) indicate that, in general, the higher the conspicuousness of a flashing prey while moving, the shorter the subsequent optimal search time for the prey and the greater the flasher's chances of surviving the search. This arises simply because if a prey item is believed to be conspicuous then it should be found quickly; so, if the prey fleeing item is not found quickly, it is unlikely to be present. Intriguingly, the relationship between optimal search time and perceived prey conspicuousness is not always monotonically increasing. However, a peak in search time only occurs when fleeing prey appear so hard to find and/or their location of settlement is so uncertain that they are of marginal profitability to pursue.

Prediction 3: Flash Behavior Will Especially Benefit Prey With an Intermediate Level of Crypsis

One might expect that prey items that are highly cryptic at rest would not benefit significantly from flash displays because the behavior would add little to their already high survivorship. Conversely, prey that are highly conspicuous at rest may be so easy to find that a flash display would also do little to protect them. The mathematical model supports this intuition. **Figure 5** for example shows the relative survival benefits of a flash display (a species where $\lambda_{move} > \lambda_{rest}$) compared to a prey that lacks the flash (a species where $\lambda_{move} = \lambda_{rest}$) using Eq. 16 to determine the survivorship of the flasher and the survivorship of the non-flasher as we vary λ_{rest} . The ratio of survival of a flasher to a non-flasher is generally above 1, indicating a fitness benefit of a flash display. The higher the conspicuousness of the flash display used while in motion, the higher the relative benefit of the flash display (see also section "Prediction 2: The More Conspicuous the Flash Display, the Greater Its Effect in Reducing Predation"). However, prey that are extremely cryptic or extremely conspicuous at rest have little to gain from flash displays – indeed a flash display may harm a highly cryptic prey (survival ratio < 1) if the flash causes a predator to pursue the prey item it would not otherwise seek. For highly conspicuous prey the survival ratio approaches 1

as prey conspicuousness increases, indicating no benefit. The result is a nuanced relationship, in which the greatest relative benefit of a given flash display is for prey of intermediate conspicuousness (**Figure 5**).

Prediction 4: Species With Flash Displays Will Benefit More If the Predator Is Unaware of the Prey's Resting Appearance

We have shown that when $\lambda_{move} > \lambda_{rest}$ then the predator will frequently give up its search sooner because it expects to find a conspicuous prey item. However, if the predator learns that a prey type will be cryptic in appearance when settled, it should no longer apply an inappropriate search strategy and the benefits of the flash display will be removed entirely.

DISCUSSION

If a predator is sufficiently confident of a prey item's location, then it will search the patch where it believes the prey has landed so long as its immediate expected gain exceeds that of ignoring it and moving on to flush out another prey item. Assuming the predator decides to search the patch for the prey item that has fled, there will come a time when the predator gives up a fruitless search since it is increasingly likely that the prey is not present. We first show how Bayes' rule can be used to update the predator's belief that the fleeing prey item has settled in a patch that is being searched, given that it has not been found there yet. We then show that the optimal time spent looking in any given patch before moving on will in general be shorter for conspicuous items than cryptic prey items (which, by definition, tend to take time to find). Next, we show how the MVT of Charnov (1976) can be used to identify the time at which a predator should abandon a search that has so far been unsuccessful. Finally, we take the prey's perspective and show how a cryptic prey item that gives the impression of being conspicuous while fleeing can exploit the predator's optimal search strategy by causing the predator to move on sooner than it would otherwise do so. Since this simple form of deception will tend to enhance the survivorship of the prey, it readily explains how flash behavior evolves and is maintained.

Our model is relatively intuitive and can be readily parameterized. For example, λ can be estimated by fitting an exponential model to the distribution of discovery times for prey, whether the predator finds them or not (right censored). Likewise, g can be thought of as the reciprocal of the mean time taken between successful captures of prey (assuming the prey are of similar quality).

Evaluation of Model Predictions

While the primary purpose of our model was to show in a transparent way how flash displays can interfere with the search process and enhance prey survivorship, the model makes several testable predictions (see section "Some Predictions of the Model") which evaluate below.

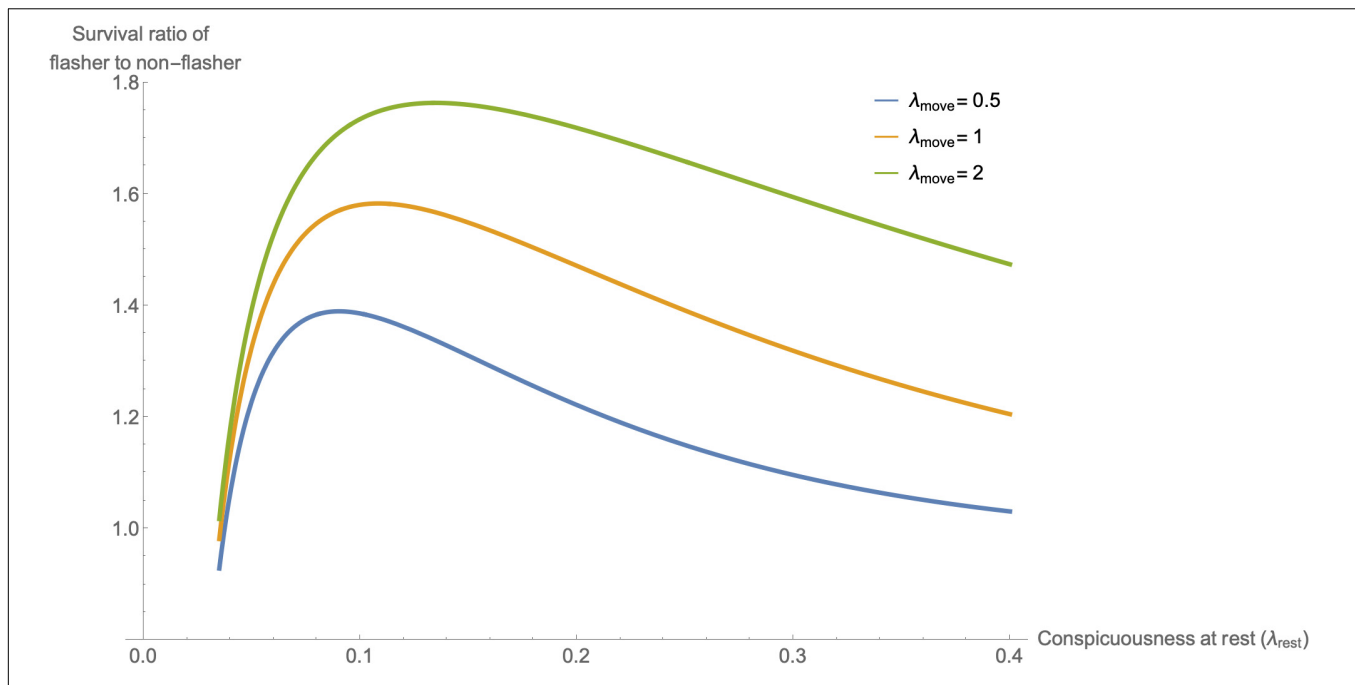


FIGURE 5 | The ratio of survival for flashers compared to non-flashers as the level of prey conspicuousness when at rest (λ_{rest}) is varied (from 0.035 to 0.4). Here flashers exhibit fixed levels of the conspicuousness while moving, with $\lambda_{move} = 0.5, 1$ or 2 and we assume $g = 0.02$ and $p_1 = 0.6$. Prey that are highly cryptic at rest have little to gain from flashing (indeed they may be harmed by having a display). Prey that are highly conspicuous at rest will be readily seen whatever the nature of their flash display, so also have little to gain from flashing. For any flash display there is an intermediate level of resting crypsis (λ_{rest}) that maximizes the relative survival benefits of flashing.

Prediction 1: The More Confident a Predator Is That a Prey Is Present, the Longer the Search Time Before Giving up

There is some evidence to support the intuitive prediction, although it is understandably indirect. In their experimental “proof of concept” paper, Loeffler-Henry et al. (2018) first trained human volunteers to follow moving prey of a given conspicuousness and search for them where they settled. They then introduced flashers and non-flashers and recorded whether each prey type was found, as well as the time taken to its discovery or abandonment of search. For the first 6 prey presented in the training phase, the authors introduced a 25% probability that the prey would not be present in the search phase. They incorporated these “duds” as a way of familiarizing volunteers with the possibility that there can sometimes be no prey present, so that they give up sooner. Indeed, if the human volunteers felt for certain there would always be a prey present, then with unlimited time to complete the experiment they might be motivated to persist a lot longer.

Clearly then, the number of duds experienced in the training phase will likely influence the perceived prior probability p_1 of the prey being present in the test phase, but precisely how? One way to quantify the relationship between the number of duds (d) experienced and p_1 is to assume that the volunteers begin with a Beta prior for the probability of the prey item being present in the search area. The Beta distribution provides a convenient prior not only because it is bounded by 0 and 1, but also because it is the conjugate for the binomial; that is,

following new information the posteriors will also follow a Beta distribution, albeit with different parameters (DeGroot, 1970). The expectation of a Beta (α, β) is $\alpha/(\alpha + \beta)$ with Beta (1, 1) representing a uniform distribution. Due to the conjugacy, if a volunteer starts with a Beta (α, β) prior and finds that no prey is present on d occasions from n trials, then the posterior probability distribution of the prey item being present in the search screen will follow Beta ($\alpha + n - d, \beta + d$) with expectation $(\alpha + n - d)/(\alpha + \beta + n)$. So, with $n = 6$ conspicuous training prey, and assuming that volunteers start with uniform priors, the maximum estimate of p_1 following training would be (7/8) when $d = 0$, and the minimum estimate of p_1 would be (1/8) when $d = 6$. Loeffler-Henry et al. (2018) reported that the number of duds significantly reduced the time taken before a search for prey was abandoned (Eq. 12), and consequently the probability that a prey was detected (Eq. 16), which are entirely consistent with the predictions of our model.

Prediction 2: The More Conspicuous the Flash Display, the Greater Its Effect in Reducing Predation

The model predicts that prey with conspicuous flash displays will tend to survive at a higher rate than prey with less conspicuous flash displays, since in the former case predators will give up their search sooner. Bae et al. (2019) presented a follow-up experiment to Loeffler-Henry et al. (2018) in which they manipulated the conspicuousness of the flash display to human volunteers. Intriguingly, they found that a flash display that was conspicuous (CONS) in motion had a greater effect in

reducing predation than a flash display that simply involved a distinct cryptic color (CRY). Moreover, the mean giving-up time of the volunteer predators was significantly longer for the CRY prey than the CONS prey. As our model shows, if predators are searching for something that they believe to be cryptic (no matter how distinct it is) they should be prepared to spend longer looking for it. The results of Bae et al. (2019) therefore match what one would expect if the flash behavior enhanced survival by interfering with a search strategy of predators based on conspicuousness rather than novelty or distinctiveness.

Prediction 3: Flash Behavior Will Especially Benefit Prey With an Intermediate Level of Crypsis

In addition to varying conspicuousness, Bae et al. (2019) conducted a related experiment and found that flash coloration was more effective in reducing predation in large prey compared to small prey. They explained this finding on the basis that small prey items are intrinsically hard to find, so that flash displays would add little to already high survivorship. Naturally, however, as section “Prediction 3: Flash Behavior Will Especially Benefit Prey With an Intermediate Level of Crypsis” argues, there must be a sweet spot – prey that are highly conspicuous at rest (such as very large prey) may be so easy to detect that a flash display would do little to protect them. As such, Bae et al. (2019) provide some support for the model, although the possibility of an upper limit of resting conspicuousness beyond which there is no benefit has yet to be empirically established.

Prediction 4: Species With Flash Displays Will Benefit More If the Predator Is Unaware of the Prey's Resting Appearance

Our model assumes that the benefits of the flash display are contingent on deception. So, if the true nature of the prey is revealed, then the predicted survival benefit should be diminished. This prediction was supported by a recent study by Loeffler-Henry et al. (2021) who showed that flash displays conferred a survivorship advantage but only in computer-generated prey that moved before the volunteer predator was able to observe their resting appearance.

Flash Display Mimicry?

The potential to recognize the nature of the trick being played (see section “Prediction 4: Species With Flash Displays Will Benefit More If the Predator Is Unaware of the Prey's Resting Appearance”) is an obvious Achilles' heel of the flashing strategy, just as startle (deimatic) displays can eventually be habituated to, see Ingalls (1993). If the flashing species is commonly encountered, then all else being equal, it is likely predators would learn to associate the conspicuous flash display with a prey item that is cryptic at rest. There is one important way, however, in which the effectiveness of the flash display may be maintained despite the ability of predators to catch on to the trick being played. Specifically, if the flash display were to resemble another organism or object familiar to the predator, which is conspicuous both when fleeing and when

settled, then one might expect it would reduce the rate at which predators make the association. Indeed, the uncertainty generated by this form of mimicry could allow the flash behavior to persist indefinitely, just as Batesian mimics can co-exist with models (Ruxton et al., 2018). One prey species that is cryptic at rest but displays conspicuous color patterns in flight is the Carolina locust *Dissosteira carolina* (Linnaeus), seen in **Figure 1** (middle row). Intriguingly, this species has long been speculated to resemble the sympatric mourning cloak butterfly *Nymphalis antiopa* (Linnaeus) both in appearance and flight behavior (Acorn, 2018); see **Supplementary Figure 3** (top). Similarly, the otherwise cryptic speckle-winged rangeland grasshopper *Arphia conspersa* (Scudd.), seen in **Figure 1** (bottom row), flashes conspicuous yellow wings in flight that resemble the alfalfa butterfly *Colias eurytheme* (Boisd.) (Balgooyen, 1997); see **Supplementary Figure 3** (bottom). So, the conspicuous displays made by certain species when fleeing may not be arbitrary but instead selected to resemble other species or objects familiar to the predator that retain their conspicuous state throughout. We have not introduced the possibility of mimicry into the current model, although its effects could be thought of as the converse of “duds” (section “Prediction 1: The More Confident a Predator Is That a Prey Is Present, the Longer the Search Time Before Giving up”). If the conspicuous model was unprofitable to attack due to their unpalatability or evasiveness (which would account for their consistent conspicuousness), then the predator will be faced with an extra level of uncertainty that will influence whether the fleeing prey is pursued. If the prey item is pursued (because the models are profitable to capture and consume, or because the predator is sufficiently convinced it is a mimic) then the time a predator spends searching on a patch will not only affect the posterior probability that there is a prey present, but also whether it is one type of prey or another (since flashing species will be cryptic at rest, but the model will retain its conspicuousness).

CONCLUSION

The theory of optimal search is inherently Bayesian since it uses information gathered during the search (notably the lack of success) to revise beliefs as to where the hidden object might be (Stone, 1975; Koopman, 1980; Assaf and Zamir, 1985). At its core, it requires a consideration of all things that might have happened to a missing object, in terms of a prior probability distribution of it being in certain locations. It also requires an understanding of the probability of discovering the object within an area as a function of search time or effort applied there (since the ease and cost of detecting a lost object can potentially vary among locations). The theory has been applied in multiple real-life situations such as the search for missing aircraft and naval vessels (Richardson and Stone, 1971) and is even integrated into the United States coast-guard computer assisted search and rescue (Richardson and Discenza, 1980). Here we apply it in a somewhat unusual way to understand why some organisms are selected to give the illusion of being conspicuous, when they are cryptic at rest.

DATA AVAILABILITY STATEMENT

Additional results and model explorations are included in the article/**Supplementary Material**, further inquiries can be directed to the corresponding author.

AUTHOR CONTRIBUTIONS

TS and KL-H contributed to planning of approach and second drafting of the manuscript. TS contributed to development of and exploration of model and first drafting of the manuscript. Both authors contributed to the article and approved the submitted version.

REFERENCES

- Acorn, J. (2018). *Cool Insects: The Mourning Cloak Butterfly* [Online]. Available online at: <https://esc-sec.ca/2018/05/29/cool-insectsthe-mourning-cloak-butterfly/>. (Accessed date March 22 2022).
- Anonymous (1945). Animal concealment and flash coloration. *Nature* 155, 232–233.
- Assaf, D., and Zamir, S. (1985). Optimal sequential search: a Bayesian approach. *Ann. Stat.* 12:1219.
- Bae, S., Kim, D., Sherratt, T. N., Caro, T., and Kang, C. (2019). How size and conspicuousness affect the efficacy of flash coloration. *Behav. Ecol.* 30, 697–702. doi: 10.1093/beheco/arz006
- Balگوoyen, T. G. (1997). Evasive mimicry involving a butterfly model and grasshopper mimic. *Am. Midl. Natural.* 137, 183–187. doi: 10.2307/2426768
- Charnov, E. L. (1976). Optimal foraging: the marginal value theorem. *Theoret. Populat. Biol.* 9, 129–136.
- Cott, H. B. (1940). *Adaptive Coloration in Animals*. London: Methuen & Co.
- Courville, A. C., Daw, N. D., and Touretzky, D. S. (2006). Bayesian theories of conditioning in a changing world. *Trends Cogn. Sci.* 10, 294–300. doi: 10.1016/j.tics.2006.05.004
- DeGroot, M. H. (1970). *Optimal Statistical Decisions*. New Jersey, NJ: John Wiley & Sons.
- Edmunds, M. (1974). *Defence in Animals: a Survey of Anti-predator Defences*. Essex: Longman.
- Edmunds, M. (2008). “Flash colors,” in *Encyclopedia of Entomology*, ed. J. L. Capinera (Dordrecht (NL): Springer).
- Green, R. F. (1980). Bayesian birds: a simple example of Oaten’s stochastic model of optimal foraging. *Theoret. Popul. Biol.* 18, 244–256. doi: 10.1016/0040-5809(80)90051-9
- Ingalls, V. (1993). Startle and habituation responses of blue jays (*Cyanocitta cristata*) in a laboratory simulation of antipredator defenses of *Catocala* moths (Lepidoptera, Noctuidae). *Behaviour* 126, 77–96. doi: 10.1163/156853993x00353
- Killeen, P. R., Palombo, G.-M., Gottlob, L. R., and Beam, J. (1996). Bayesian analysis of foraging by pigeons (*Columba livia*). *J. Exp. Psychol. Anim. Behav. Proc.* 22, 480–496. doi: 10.1037//0097-7403.22.4.480
- Koopman, B. O. (1957). The theory of search: III. The optimum distribution of searching effort. *Operat. Res.* 5, 613–626.
- Koopman, B. O. (1980). *Search and Screening*. New York, NY: Pergamon Press.
- Loeffler-Henry, K., Kang, C., and Sherratt, T. N. (2019). Consistent associations between body size and hidden contrasting color signals across a range of insect taxa. *Am. Natural.* 194, 28–37. doi: 10.1086/703535
- Loeffler-Henry, K., Kang, C., and Sherratt, T. N. (2021). The anti-predation benefit of flash displays is related to the distance at which the prey initiates its escape. *Proc. R. Soc. B* 288:0210866. doi: 10.1098/rspb.2021.0866
- Loeffler-Henry, K., Kang, C., Yip, Y., Caro, T., and Sherratt, T. N. (2018). Flash behavior increases prey survival. *Behav. Ecol.* 29, 528–533.
- McElreath, R. (2020). *Statistical Rethinking. A Bayesian Course with Examples in R and Stan*. Boca Raton: CRC Press.

FUNDING

TS and KL-H were funded by an NSERC Discovery Grant to TS.

ACKNOWLEDGMENTS

We thank Ian Dewan and our reviewers for insightful comments.

SUPPLEMENTARY MATERIAL

The Supplementary Material for this article can be found online at: <https://www.frontiersin.org/articles/10.3389/fevo.2022.903769/full#supplementary-material>

- McGrayne, S. B. (2012). *The Theory That Would Not Die: How Bayes’ Rule Cracked the Enigma Code, Hunted Down Russian Submarines, and Emerged Triumphant from Two Centuries of Controversy*. Yale: Yale University Press.
- McNair, J. N. (1982). Optimal giving-up times and the marginal value theorem. *Am. Natural.* 119, 511–529. doi: 10.1086/283929
- McNamara, J., and Houston, A. (1985). A simple model of information use in the exploitation of patchily distributed food. *Anim. Behav.* 33, 553–560. doi: 10.1016/s0003-3472(85)80078-6
- McNamara, J. M. (1982). Optimal patch use in a stochastic environment. *Theoret. Populat. Biol.* 21, 269–288. doi: 10.1016/0040-5809(82)90018-1
- McNamara, J. M., Green, R. F., and Olsson, O. (2006). Bayes’ theorem and its applications in animal behaviour. *Oikos* 112, 243–251. doi: 10.1111/j.0030-1299.2006.14228.x
- Murali, G. (2018). Now you see me, now you don’t: dynamic flash coloration as an antipredator strategy in motion. *Anim. Behav.* 142, 207–220. doi: 10.1016/j.anbehav.2018.06.017
- Oaten, A. (1977). Optimal foraging in patches: a case tbr stochasticity. *Theoret. Populat. Biol.* 12, 263–285. doi: 10.1016/0040-5809(77)90046-6
- Richardson, H. R., and Discenza, J. H. (1980). The United States Coast Guard computer-assisted search planning system (CASP). *Nav. Res. Logist. Q.* 27, 659–680. doi: 10.1002/nav.3800270413
- Richardson, H. R., and Stone, L. D. (1971). Operations analysis during the underwater search for Scorpion. *Naval Res. Logist. Q.* 18, 141–157.
- Ruxton, G. D., Allen, W. L., Sherratt, T. N., and Speed, M. P. (2018). *Avoiding Attack: The Evolutionary Ecology of Crypsis, Aposematism and Mimicry*. Oxford: Oxford University Press.
- Stone, L. D. (1975). *Theory of Optimal Search*. New York, NY: Academic Press.
- Umbers, K. D. L., Lehtonen, J., and Mappes, J. (2015). Deimatic displays. *Curr. Biol.* 25, R58–R59. doi: 10.1016/j.cub.2014.11.011

Conflict of Interest: The authors declare that the research was conducted in the absence of any commercial or financial relationships that could be construed as a potential conflict of interest.

The reviewer OP declared a past co-authorship with one of the authors TS to the handling editor.

Publisher’s Note: All claims expressed in this article are solely those of the authors and do not necessarily represent those of their affiliated organizations, or those of the publisher, the editors and the reviewers. Any product that may be evaluated in this article, or claim that may be made by its manufacturer, is not guaranteed or endorsed by the publisher.

Copyright © 2022 Sherratt and Loeffler-Henry. This is an open-access article distributed under the terms of the Creative Commons Attribution License (CC BY). The use, distribution or reproduction in other forums is permitted, provided the original author(s) and the copyright owner(s) are credited and that the original publication in this journal is cited, in accordance with accepted academic practice. No use, distribution or reproduction is permitted which does not comply with these terms.



Rapid Shifts in Visible Carolina Grasshopper (*Dissosteira carolina*) Coloration During Flights

Ezekiel Martin, Henry L. Steinmetz, Seo Young Baek, Frederick R. Gilbert and Nicholas C. Brandley*

Department of Biology, The College of Wooster, Wooster, OH, United States

OPEN ACCESS

Edited by:

Eunice Jingmei Tan,
Yale-NUS College, Singapore

Reviewed by:

Katja Rönkä,
University of Helsinki, Finland
Amanda Franklin,
The University of Melbourne, Australia

*Correspondence:

Nicholas C. Brandley
nbrandley@wooster.edu

Specialty section:

This article was submitted to
Behavioral and Evolutionary Ecology,
a section of the journal
Frontiers in Ecology and Evolution

Received: 20 March 2022

Accepted: 23 May 2022

Published: 24 June 2022

Citation:

Martin E, Steinmetz HL, Baek SY,
Gilbert FR and Brandley NC (2022)
Rapid Shifts in Visible Carolina
Grasshopper (*Dissosteira carolina*)
Coloration During Flights.
Front. Ecol. Evol. 10:900544.
doi: 10.3389/fevo.2022.900544

Some brightly colored structures are only visible when organisms are moving, such as parts of wings that are only visible in flight. For example, the primarily brown Carolina grasshopper (*Dissosteira carolina*) has contrasting black-and-cream hindwings that appear suddenly when it takes off, then oscillate unpredictably throughout the main flight before disappearing rapidly upon landing. However, the temporal dynamics of hindwing coloration in motion have not previously been investigated, particularly for animals that differ from humans in their temporal vision. To examine how quickly this coloration appears to a variety of non-human observers, we took high-speed videos of *D. carolina* flights in the field. For each of the best-quality takeoffs and landings, we performed a frame-by-frame analysis on how the relative sizes of the different-colored body parts changed over time. We found that in the first 7.6 ± 1.5 ms of takeoff, the hindwings unfurled to encompass 50% of the visible grasshopper, causing it to roughly double in size. During the main flight, the hindwings transitioned 6.4 ± 0.4 times per second between pauses and periods of active wing-beating (31.4 ± 0.5 Hz), creating an unstable, confusing image. Finally, during landings, the hindwings disappeared in 11.3 ± 3.0 ms, shrinking the grasshopper to $69 \pm 9\%$ of its main flight size. Notably, these takeoffs and landings occurred faster than most recorded species are able to sample images, which suggests that they would be near-instantaneous to a variety of different viewers. We therefore suggest that *D. carolina* uses its hindwings to initially startle predators (deimatic defense) and then confuse them and disrupt their search images (protean defense) before rapidly returning to crypsis.

Keywords: orthoptera, Oedipodinae, deimatic defense, protean defense, crypsis, critical flicker fusion, temporal vision

INTRODUCTION

Most animals' surroundings are full of motion, and therefore the ability to perceive moving stimuli may play a large role in their evolutionary success (Tan and Elgar, 2021). For example, movement can enhance visual signals (Peters et al., 2007; Ord and Stamps, 2008), reveal prey to predators (Ioannou and Krause, 2009; Hall et al., 2013), or be used to confuse predators once prey are detected (Maldonado, 1970; How and Zanker, 2014; Umbers et al., 2015; Ruxton et al., 2018; Murali et al., 2019). Yet in many cases, studies of animal appearances focus on static scenes, limiting our knowledge of how they may function in a moving world.

The motion of patterns is further complicated when they change over time. In these cases, it is not solely movement that matters, but the temporal changes in the stimulus. For example,

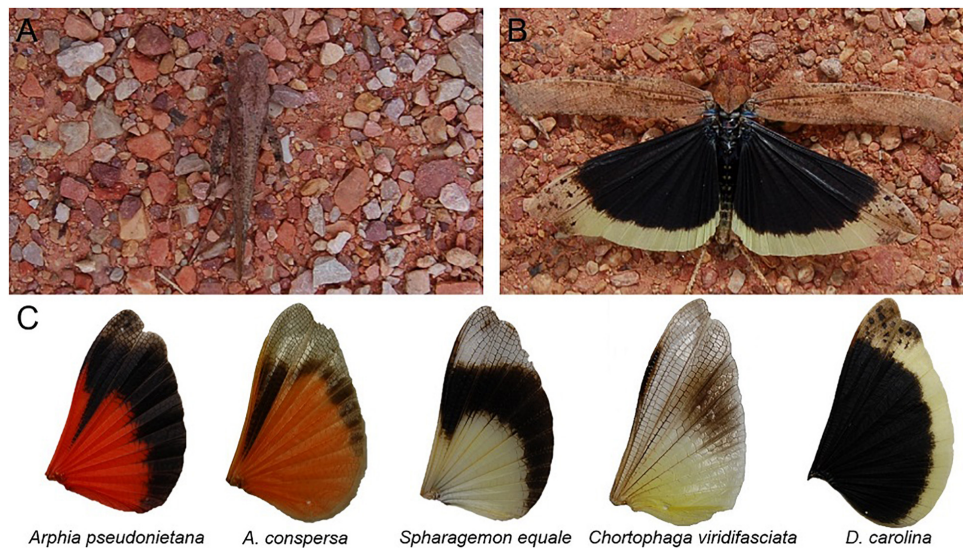


FIGURE 1 | The of band-winged grasshoppers are revealed in flight. **(A)** When at rest the Carolina grasshopper's (*Dissosteira carolina*) main body coloration often matches the environment, rendering it cryptic. **(B)** A posed grasshopper shows the conspicuous and high-contrast hindwings that are unveiled during flight. **(C)** Hindwing patterning is variable across species including in color, location and size of the black band, and transparency. Proper understanding of this patterning requires accounting for its motion and temporal dynamics.

some cephalopods actively produce a “passing cloud” appearance (Mather and Mather, 2004; Laan et al., 2014), male peacock spiders unfurl their colorful opisthosomal flaps before signaling (Girard et al., 2011), and some butterflies transition between camouflage and conspicuous eye spots by showing different sides of their wings (Vallin et al., 2005; Olofsson et al., 2013). In each case, these behaviors may depend both on movement and on the changes between appearances.

Band-winged grasshoppers (subfamily Oedipodinae) present an interesting case study on movement and changing appearances because of the variety of patterns found on their hindwings (Figure 1; Otte, 1985; Cooper, 2006). In most species, these hindwings include regions of black which to a human observer contrast sharply against neighboring yellow, orange, or red regions. Notably, the hindwings are hidden when the grasshopper is on the ground but are suddenly unfurled in flight (Figure 1). To a human observer, the hindwings appear to visually facilitate escape through three separate mechanisms. First, the initial change from camouflage to bright and contrasting coloration may startle a potential predator in a process known as a deimatic defense (Maldonado, 1970). Second, during flight, the grasshopper's appearance changes depending on whether it is gliding or actively flapping its wings (and thus causing its colors to fuse together *via* the flicker-fusion effect; Jackson et al., 1976; Umeton et al., 2017). Thus, movement of the wings in flight may disrupt a predator's search image *via* protean defense or dynamic flash coloration (Humphries and Driver, 1970; Murali, 2018). Third, when landing, the grasshopper transitions back to camouflage so quickly that researchers have “often incorrectly guessed the landing locations of ... grasshoppers due to their sudden disappearance” (Cooper, 2006). Taken all together, transitions

in grasshopper appearance could allow them to initially startle predators, then make tracking difficult, and ultimately disappear back into camouflage.

However, modern sensory biology revolves around *umwelt*—the idea that each species, perhaps even each organism, perceives its surroundings differently—and therefore one cannot understand the defensive function of grasshopper coloration in flight without considering the views of relevant predators. Ideally, one should account for both behavioral differences (e.g., distance and angle of view) and physiological differences (e.g., color vision and visual acuity). Notably, when discussing grasshopper coloration in motion, we need to account for their predators' temporal vision—how quickly their visual systems form images. Temporal vision is often measured using critical flicker fusion (CFF), which is the frequency necessary for flickers in light to be perceived (or, in the case of non-human animals, reacted to) as identical to a constant light with a light level midway between the on and off states of the actual, flickering light (Donner, 2021). Many species of North American band-winged grasshoppers are preyed on primarily by passerine birds (Belovsky and Slade, 1993). Passerines specialized in catching aerial insects may have temporal vision that is twice as fast as humans' (e.g., ~120 Hz vs. ~60 Hz; Brundrett, 1974; Boström et al., 2016), which would halve their integration times (the time required for their visual systems to form images). Therefore, to account for differences in predatory temporal *umwelts*, we must measure the speeds at which band-winged grasshopper coloration changes.

Here, to begin to understand the temporal mechanics of band-winged grasshopper appearance, we used high-speed video to examine the escape flights of one species of band-winged grasshopper, the Carolina grasshopper (*Dissosteira carolina*). First, we visually modeled how avian predators would view the

color and spatial aspects of a stationary grasshopper hindwing. We then filmed grasshopper flights in the field, before analyzing the highest quality footage of (1) takeoff, (2) main flight, and (3) landing. In each case, we analyzed videos frame-by-frame to understand how *D. carolina*'s coloration changes, and ultimately account for differences in predator temporal vision.

MATERIALS AND METHODS

Stationary Coloration and Pattern Modeling

Dissosteira carolina ($n = 51$) were collected on private property between July and September of 2019. Collection occurred in one suburban site with both grassy and gravelly areas in Wayne County, OH, and one rural site consisting of a network of secluded, grassy fields and paths in Holmes County, OH. Prior to reflectance measurements, grasshoppers were euthanized *via* freezing for around 1 h. Reflectance of various grasshopper body parts (body, cream band of the hindwing, black region of the hindwing) was measured in OceanView with a spectrometer (model: FLAME-S-UV-VIS) combined with a 600- μ m fiber optic probe, a PX-2 UV-visible light source, and a WS-1 diffuse reflectance standard (all Ocean Optics, Inc., Dunedin, FL, United States). The light source was directed from above, and the probe was held in place by clamps ~ 1 cm from the surface at an angle of 45° .

To model how potential avian predators would view these colors, unweighted Euclidean color distances and achromatic contrasts were modeled using the pavo package (Maia et al., 2019) in R. Spectrums (300–700 nm) were first processed *via* the procspec function with a loess smoothing coefficient of 0.1 and negative values set to zero. Relative quantum catches for each photoreceptor class of a blue tit's visual system (including the achromatic double cone; Vorobyev et al., 1998; Hart, 2001) were calculated using the default vismodel function settings (ideal lighting setting, quantum catch is for each photoreceptor and not transformed, no von Kries correction). Values were then transformed into tetrahedral avian color space *via* the colspec function (Stoddard and Prum, 2008), before unweighted Euclidean color distances and achromatic contrasts were calculated *via* the coldist function (noise = neural).

To understand the maximum distance at which avian predators could fully resolve the spatial aspects of hindwing patterning, images of stationary and fully extended *D. carolina* hindwings ($n = 38$; courtesy of Brae Salazar) were measured in ImageJ (Schneider et al., 2012). We first identified the midpoint of the black region of the hindwing, before measuring the width of the cream band at the vein nearest to this midpoint. We then calculated the maximum distance at which the cream band could be fully resolved by an avian predator with a visual acuity of 10 cycles per degree (minimum resolvable angle = 0.05°) *via* the equation:

$$\text{maximum distance} = \frac{\text{width of cream band}}{\tan(0.05^\circ)}$$

Video Study Organisms and Site

Adult *D. carolina* were located in the same two sites as those used for the stationary color measurements. Filming took place on most days between July 19th and September 4th, 2021, and was limited to primarily sunny days without strong winds.

Video Gathering and Categorization

Videos were usually taken in a 1–2-h session each day between the hours of 11 AM and 2 PM. Videos ($n = 386$) were taken at 480 frames per second (fps; with an average shot length of 3.67 s) using a Sony RX100 VI HFR camera (Sony Group Corporation, Minato City, Tokyo, Japan). For each video, while filming, we briskly approached a targeted grasshopper, and then followed it if necessary. To maximize video clarity, a variety of techniques were implemented based on the circumstances of individual shots. For example, when conditions allowed, the filmer would crouch and hold the camera just below the knees to get closer to the grasshopper. To obtain landing shots in cases where subjects were unusually reactive to an approach, the filmer would sometimes use the zoom function and a longer focus to simulate a shorter distance to the subject. In other cases, subjects would be unusually latent to react and refrain from flying away during approach; in these cases, the filmer would approach more slowly (from behind, when possible), and quicken their pace once distance to target was within a yard or so. Regardless of technique, grasshoppers were typically located *via* an initial flight, so the recorded flights usually represented the second or third flight in a sequence.

D. carolina may cover tens of meters in a single flight, so analysis required prioritizing segments of flights to ensure quality footage. Of the 386 initial videos, the highest-quality takeoffs ($n = 8$; average max grasshopper size = 381 pixels), in-flight videos ($n = 14$), and landings ($n = 8$; average max grasshopper size = 478 pixels) were selected for frame-by-frame analysis (see below). These videos were chosen based on focus, lack of obstruction, and distance to the grasshopper.

Takeoff Frame-by-Frame Analysis

For each takeoff video ($n = 8$), we scored how the visible body parts—and thus coloration—of the grasshopper changed over the course of takeoff. To obtain these measurements, 120 frames (0.25 s) from each video were downloaded in R one image at a time using the packages ggplot2 (Wickham, 2016) and imager (Barthelmé and Tschumperlé, 2019) and then analyzed in ImageJ (Schneider et al., 2012). Three coloration categories were used:

- (1) “brown,” encompassing all visible pixels of the forewings and brown regions of the body of the grasshopper (primarily the head and hindmost section of the abdomen; see **Figure 1**) but excluding the legs, which were too thin and indistinct to be accurately measured,
- (2) “black,” encompassing all visible pixels of the black portion of the grasshopper's hindwings and the small black region between the hindwings, and
- (3) “cream,” encompassing all visible pixels of the cream fringe of the grasshopper's hindwings.

For each frame, we measured the size (in pixels) of the three different color regions using the freehand selection tool in ImageJ. In cases where a frame contained multiple separate shapes of the same color, these shapes were measured separately, then added together. Each color category was measured twice for each frame, and all measurements were only observed after a frame was fully processed. We then averaged the pairs of measurements into single values and converted them to percentages based on the combined values of all three regions. To ensure accurate measurements, four different accuracy checks were implemented throughout this process (**Supplemental Information**).

For each video, we measured the speed of transition between camouflage and conspicuousness in two different ways: (1) the time elapsed between the last fully brown frame and the first frame where brown and hindwings were equally visible or (2) the time elapsed between the last fully brown frame and the first frame where black and cream decreased in size (indicating the beginning of main flight oscillation).

Main Flight Wingbeat Frequencies

Because of the length and distance of flights, extended main flight footage was not suitable for the same frame-by-frame analysis used for take-offs. Instead, to understand how wing movement affects visible coloration during the main flight, we scored each wingbeat at the point where the wings were lowest in their flight cycle. Video quality allowed us to do this for most of the flight, though the landings were excluded. Two scorers independently viewed each video ($n = 14$ videos) and recorded the frames in which wingbeats occurred. We then reconciled this data by either (1) averaging the results if they were within five frames (10 ms) of each other or (2) for larger differences, reviewing the videos together, and revising the scores. In the rare cases where one viewer scored a wingbeat that the other did not, videos were reviewed together to make a final determination.

Because *D. carolina* flight alternates between periods of active wing-beating and pauses, wingbeat frequency was calculated only within a cluster of active wingbeats, but the alternating periods of activity and pauses were also recorded. We classified pauses between wingbeats based on their duration. Values ≥ 0.05 s but < 0.1 s were classified as skips as they typically corresponded to one to two skipped wingbeats. Additionally, values ≥ 0.1 s but < 0.25 s were classified as short glides, while values ≥ 0.25 s were classified as long glides.

Landing Frame-by-Frame Analysis

Procedures for landings ($n = 8$ videos) resembled those for takeoffs, with the last 120 frames (0.25 s) of flight being used instead. The speed of return to camouflage during landing was recorded as either (1) the time elapsed between the first frame of over 50% brown and the first fully brown frame or (2) the time elapsed between the end of the main flight oscillation (as measured for takeoffs) and the first fully brown frame.

Comparative Temporal Visual Models of Takeoff and Landing

For each takeoff or landing video, we modeled how the percent colorations of the wings would change to viewers with differing critical flicker fusions (CFF). These values included 240 Hz (used as an effective upper limit, above all known values), 120 Hz (approximate for specialized passerine predators; Boström et al., 2016), and 60 Hz (approximate for humans and non-specialist birds; Brundrett, 1974; Healy et al., 2013). In these models, the color percentages were averaged over an increasingly large number of frames, mimicking how visual stimuli occurring at a higher frequency than the viewer's CFF fuse together into a single blur. Because our videos were shot at 480 fps, for the 240 Hz CFF model, the average included the central frame and a half-weight of the frames on either side. Similarly, the averages for the 120 Hz model included the central frame, the frames on either side of it, and a half-weight of the frames on either side of those; and those for the 60 Hz model included the central frame, the three frames on either side of it, and a half-weight of the frames on either side of those.

Finally, we obtained the 90th and 10th percentiles for each color using the = PERCENTILE.INC function in Excel. Because most colors varied within this range for each video, these percentiles helped us better understand how colors oscillated in each CFF model. Values examined started from the first hindwing maximum and ended at the last frame able to be accurately measured in 60 Hz vision (frame 117).

RESULTS

Stationary Color and Pattern Modeling

Avian visual modeling shows that the black and cream regions of the hindwing contrast both chromatically and achromatically with each other (**Figure 2**, mean unweighted Euclidean color distance = 0.23 ± 0.004 SEM, mean Weber contrast = 11.62 ± 0.93). Both regions also contrast with the brown of the body, although to a lesser degree (body vs. black of hindwing Euclidean color distance = 0.19 ± 0.009 , Weber contrast = 5.34 ± 0.59 ; body vs. cream band Euclidean color distance = 0.11 ± 0.004 , Weber contrast = 1.17 ± 0.08).

In a stationary, fully extended hindwing, the cream band had an average width of 3.9 ± 0.1 mm, meaning that its spatial characteristics should be fully resolvable by a bird with a visual acuity of 10 cycles per degree at a distance of ~ 4.5 m.

Takeoff

Each takeoff consisted of a rapid transition to a contrasting appearance (time to 50% of the viewable grasshopper being the hindwings = $7.6 \text{ ms} \pm 1.5$, **Figures 3A,B** and **Table 1**) with a corresponding sudden doubling in grasshopper size (relative size at 50% of the viewable grasshopper being the hindwings = 2.0 ± 0.3 ; **Figures 3C,D** and **Table 1**). This initial burst was followed by erratic periods of visible color change during the first ~ 0.25 s of flight (**Figures 3A,B**), with all three color regions varying temporally in their relative contributions (**Table 1**).

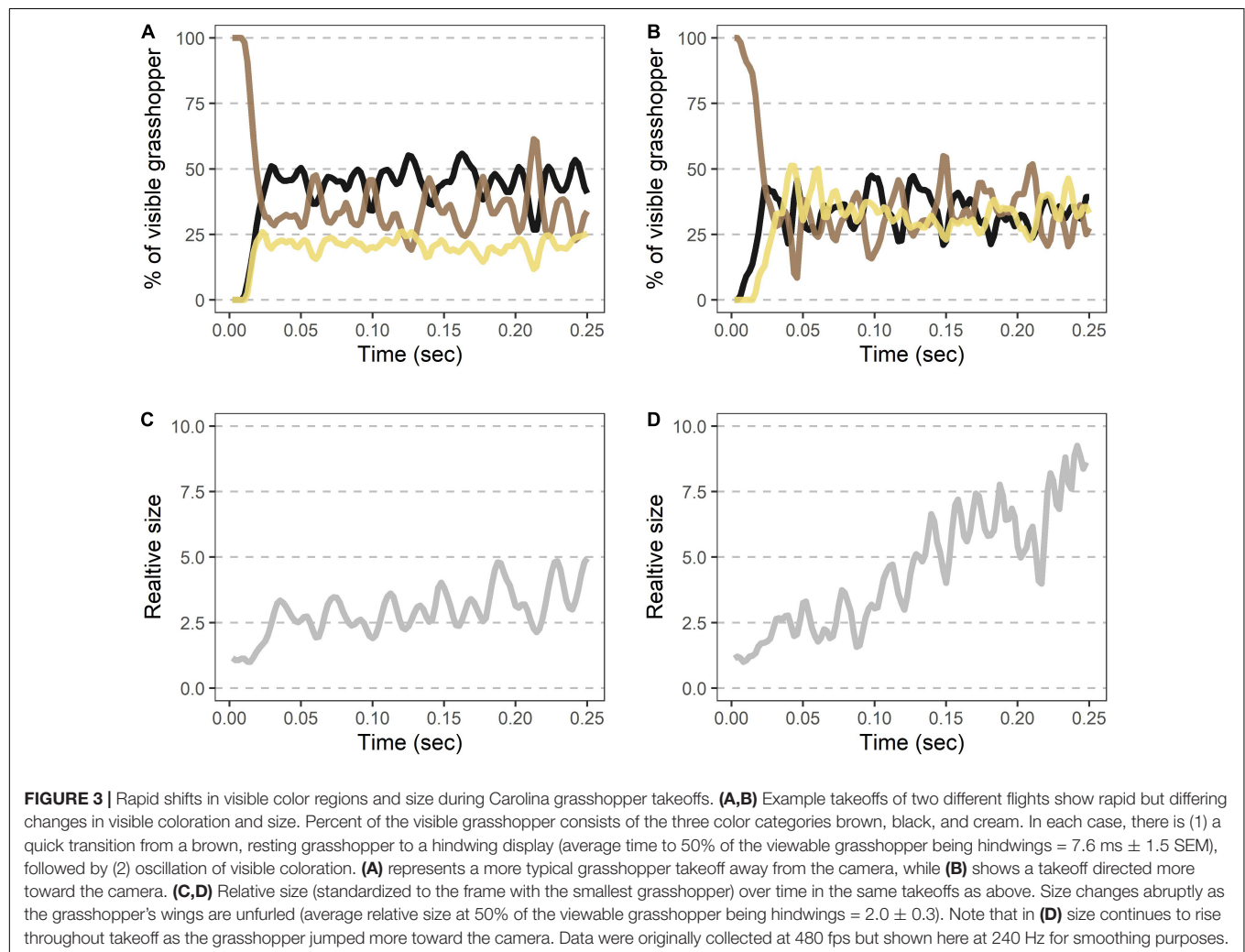
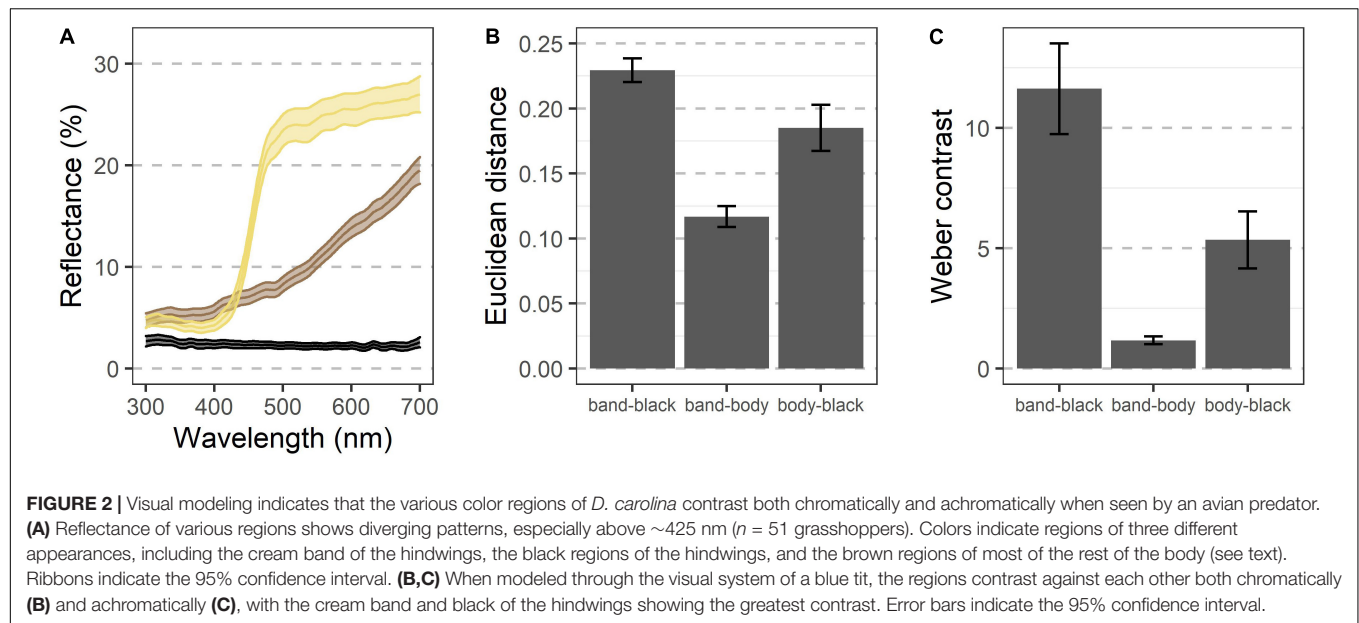


TABLE 1 | Spatiotemporal characteristics of *D. carolina* escape flights.

Parameter	Takeoff	
	Average	Sample size
Time to 50% of the viewable grasshopper being hindwings (ms)	7.6 ± 1.5 ^a	<i>n</i> = 8
Relative size when 50% of the visible grasshopper = hindwings	2.0 ± 0.3	<i>n</i> = 8
Time to first hindwing visibility maximum (ms)	13.5 ± 2.1	<i>n</i> = 8
Relative size at first hindwing visibility maximum	2.5 ± 0.2	<i>n</i> = 8
Brown region 10th percentile during oscillation (%)	23.2 ± 2.0	<i>n</i> = 8
Brown region 90th percentile during oscillation (%)	49.7 ± 2.3	<i>n</i> = 8
Black region 10th percentile during oscillation (%)	24.9 ± 2.3	<i>n</i> = 8
Black region 90th percentile during oscillation (%)	43.6 ± 2.1	<i>n</i> = 8
Cream region 10th percentile during oscillation (%)	22.3 ± 1.4	<i>n</i> = 8
Cream region 90th percentile during oscillation (%)	37.1 ± 2.2	<i>n</i> = 8
Parameter	Main flight	
	Average	Sample size
Wingbeat frequency (active; Hz)	31.4 ± 0.5	<i>n</i> = 14
Active wingbeat time (%)	42 ± 2	<i>n</i> = 14
Periods of active wingbeats per flight	6.1 ± 0.7	<i>n</i> = 14
Transitions between active wingbeats and pauses (transitions/sec)	6.4 ± 0.4	<i>n</i> = 14
Parameter	Landing	
	Average	Sample size
Time from 50% brown to fully brown (ms)	11.3 ± 3.0	<i>n</i> = 7 ^b
Relative size from 50% brown to fully brown	0.69 ± 0.09	<i>n</i> = 7 ^b
Time from last hindwing maximum to fully brown (ms)	22.7 ± 3.2	<i>n</i> = 8
Relative size from last hindwing maximum to fully brown	0.54 ± 0.09	<i>n</i> = 8
Brown 10th percentile during oscillation (%)	29.0 ± 3.1	<i>n</i> = 8
Brown 90th percentile during oscillation (%)	54.1 ± 3.2	<i>n</i> = 8
Black 10th percentile during oscillation (%)	23.7 ± 2.3	<i>n</i> = 8
Black 90th percentile during oscillation (%)	42.7 ± 2.4	<i>n</i> = 8
Cream 10th percentile during oscillation (%)	18.4 ± 2.0	<i>n</i> = 8
Cream 90th percentile during oscillation (%)	32.2 ± 2.7	<i>n</i> = 8

^a SEM, ^b one landing excluded from analysis as brown regions were never less than 50% of visible grasshopper near landing.

Main Flight

During the main flight, grasshopper appearances changed as they alternated between periods of active wingbeats and pauses (Figure 4 and Table 1). When actively beating their wings, grasshoppers showed a wingbeat frequency of 31.4 ± 0.5 Hz. Grasshoppers were actively beating their wings during $42 \pm 2\%$ of

the recorded flight time (excluding final landings, see methods). Flights consisted of 6.1 ± 0.7 different periods of active wingbeats and averaged 6.4 ± 0.4 transitions between active wingbeats and pauses per second. Pauses varied in their duration and included skipping 1–2 wingbeats, shorter glides, and longer glides (Figures 4C,D).

Landings

Landings showed the same characteristics as takeoffs, albeit in a reverse order and at a slower speed (Figure 5 and Table 1). Oscillations in the last ~ 0.25 s of each flight were similar in magnitude to those seen after takeoffs (Table 1). The grasshopper's speed of return to all-brown (measured from 50% brown) was highly variable (min = 2.1 ms, max = 27 ms) with an average of 11.3 ± 3 ms. This was accompanied by a reduction in size to 0.69 ± 0.09 relative to when the hindwings took up 50% of the visible grasshopper.

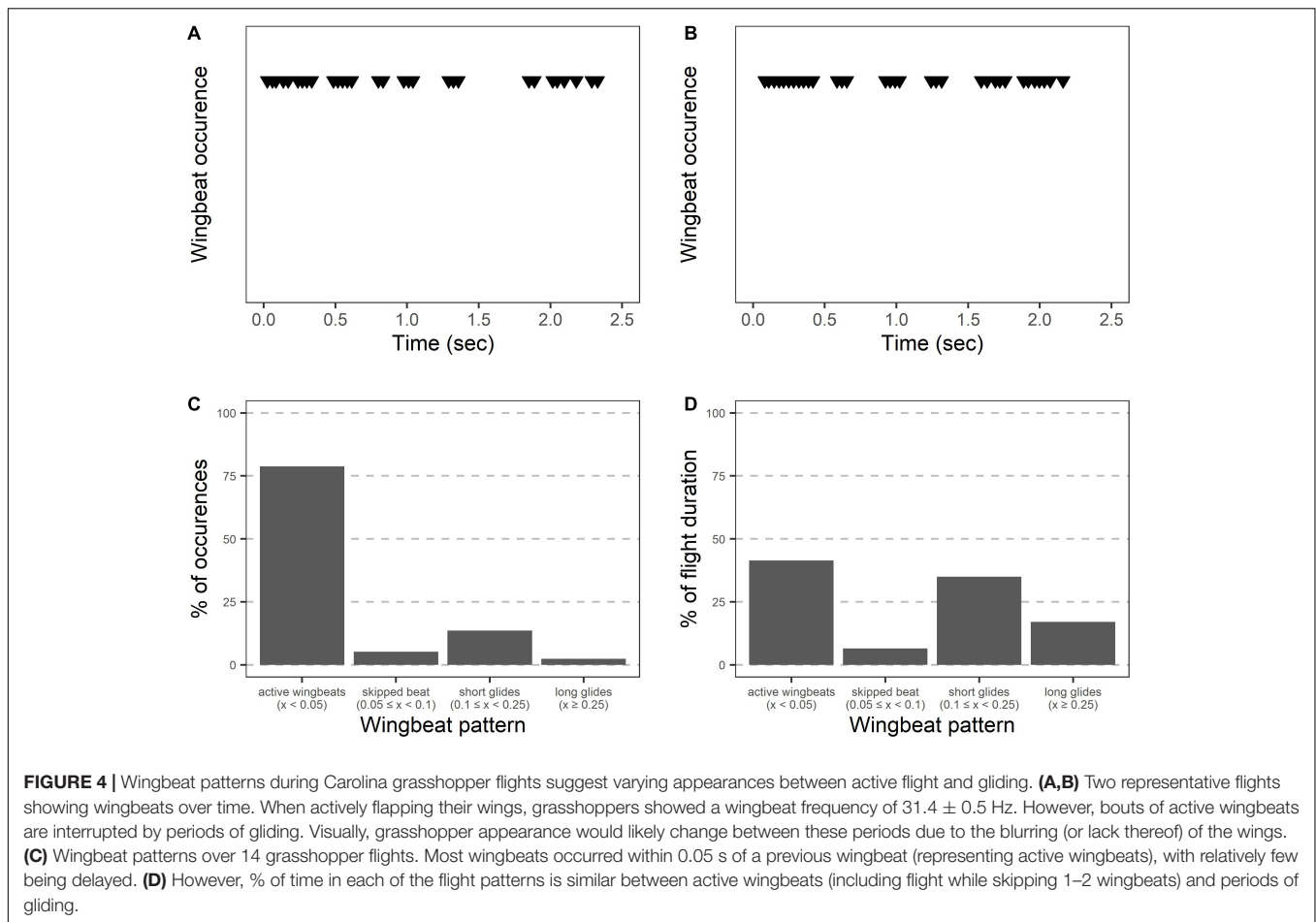
Comparative Temporal Visual Models of Takeoff and Landing

Models examining the oscillation of colors during takeoff showed that increasingly fast visual speeds lead to greater magnitudes of oscillations in color during these time periods (Figure 6). Modeled values for 240 Hz vision showed significantly greater oscillations than 120 Hz vision for all three color regions (all $p < 0.01$, Student's *t*-test), and 120 Hz vision showed differences in oscillations from 60 Hz that were significantly greater than 0 (all $p < 0.01$, one-sample *t*-test).

DISCUSSION

The hindwings of *D. carolina* contrast both chromatically and achromatically when modeled through an avian visual system (Figure 2). Notably, the smallest region of the Carolina grasshopper's patterning—and thus likely a limiting factor in its spatial information—is the cream band with a width of 3.9 ± 0.1 mm (Figure 1). However, when stationary this region should be fully resolvable to a bird with modest spatial vision (10 cycles per degree; Kiltie, 2000) at distances of up to ~ 4.5 m. All of these previous models ignore that the hindwings are typically only visible when in motion, and by quantifying how the visible coloration of the Carolina grasshopper changes during escape flights, we can better understand how it may be viewed by relevant predators.

During takeoff, the quick transition to this contrasting pattern may function as a deimatic defense by startling a predator. It took 7.6 ± 1.5 ms to unfurl the hindwings to 50% of the visible grasshopper, and 13.5 ± 2.1 ms for them to reach their first peak in size (Table 1 and Figures 3A,B). Notably, these values would be near instantaneous to a variety of relevant observers when considering their temporal vision (human observers and non-specialist predators = CFF ~ 60 Hz or 16.7 ms, Brundrett, 1974; specialist predators = CFF ~ 120 Hz or 8.3 ms, Boström et al., 2016; Figure 6). Many studies on deimatic defenses have qualitatively noted their quick speed (Table 2), suggesting that speed could aid the effectiveness of startling a predator



(Holmes et al., 2018; Murali et al., 2019). Our quantified values are consistent with this hypothesis, as the transition takes at most two integration times even to specialized predators.

Although some deimatic displays are followed by movement (Table 2; Maldonado, 1970; Vallin et al., 2005; King and Adamo, 2006; Olofsson et al., 2012; Kang et al., 2017; Badiane et al., 2018), the Carolina grasshopper's is extreme as the initial transition is followed by rapid oscillations in visible colorations (Figures 3A,B). These oscillations represent a variety of factors (e.g., hindwing and forewing beats, changes in visual angle, forewings visibly overlapping hindwings) and typically follow no consistent pattern. These sorts of rapid, confusing changes in appearance, which have gone by a variety of names [e.g., protean defense (Humphries and Driver, 1970), dazzle camouflage (Behrens, 2012), flash display (Davis, 1948)], may work *via* disrupting the predator's search image (Humphries and Driver, 1970). Future studies could better elucidate whether these oscillations continue to aid the grasshopper *via* a deimatic defense (i.e., by startling the predator) and/or *via* disrupting the search image. Notably, the magnitudes of these oscillations increase with faster vision (Figure 6), making it a potential counter-adaptation for predators with quicker integration times. This would be because they would therefore perceive more of the confusing detail and potentially find it harder to follow their prey.

During the main flight, band-winged grasshoppers continued to change as a visual target. Grasshoppers alternated between periods of actively flapping their hindwings (at a frequency of 31.4 ± 0.5 Hz) and periods of gliding without wingbeats (Figure 4 and Table 2). From a search image perspective, grasshoppers transition between these periods frequently (6.4 ± 0.4 transitions per second) and do not spend most of their time in just one period (active wingbeat time = $42 \pm 2\%$ of the total flight time). During the periods of active wingbeats, the grasshopper's hindwings would likely blur and/or flash to relevant observers, as an entire wing cycle would take around two integration times for viewers at 60 Hz, and four for specialized predators at 120 Hz. Conversely, glides lasted 0.19 ± 1.5 s, and therefore provided a steadier image that would contrast between active wingbeats. Dynamic changes in patterning can decrease predator accuracy in tracking and the success of capture (Humphries and Driver, 1970; Murali, 2018; Murali et al., 2019), suggesting that the wingbeat patterns of the Carolina grasshopper's main flight may serve a visual anti-predator purpose.

How quickly the hindwings disappear during landing represents a less studied—yet likely biologically important—phenomenon. Visible color regions oscillated before landing (Figures 5A,B and Table 1), at which point they returned to an all-brown appearance (time from 50% brown to fully

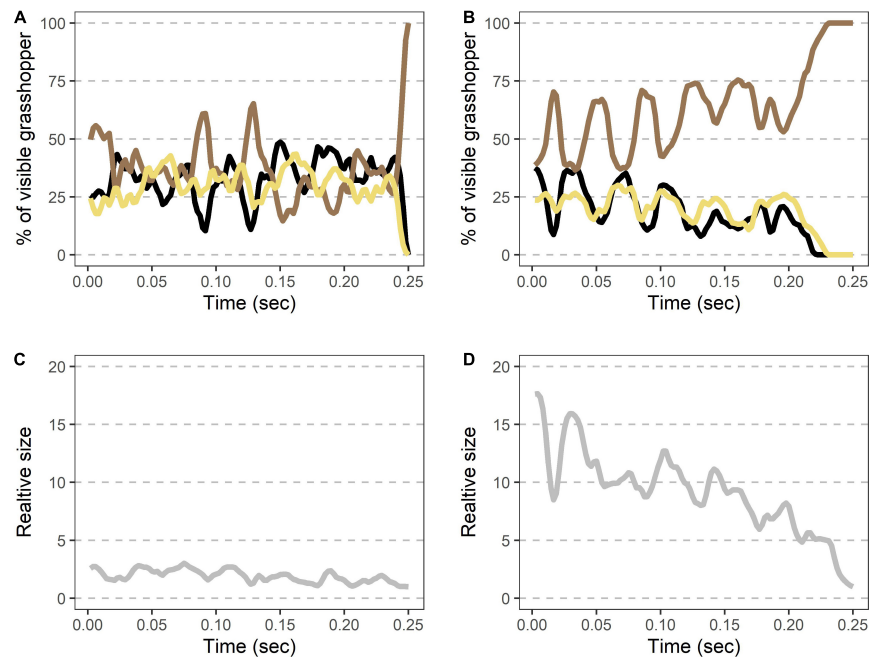


FIGURE 5 | Rapid shifts in visible color regions and size during Carolina grasshopper landings. **(A,B)** Example landings from two different flights show rapid but variable changes in visible coloration and size. **(A,B)** Percent of the visible grasshopper consisting of the three color categories brown, black, and cream. In each case, there is (1) a period of color oscillation followed by (2) a rapid return to the brown camouflaged coloration (time from 50% brown to fully brown = $11.3 \text{ ms} \pm 3.0$). In general, the return to camouflage was slower and more variable in speed than during takeoffs. **(A)** Represents a quicker change to camouflage, while **(B)** is a more gradual landing. **(C,D)** Relative size (standardized to the frame with the smallest grasshopper) over time in the same landings as above. On average, visible grasshoppers at landing were just $54 \pm 9\%$ as large as during their last hindwing maximum. Data were originally collected at 480 fps but are shown here at 240 Hz for smoothing purposes.

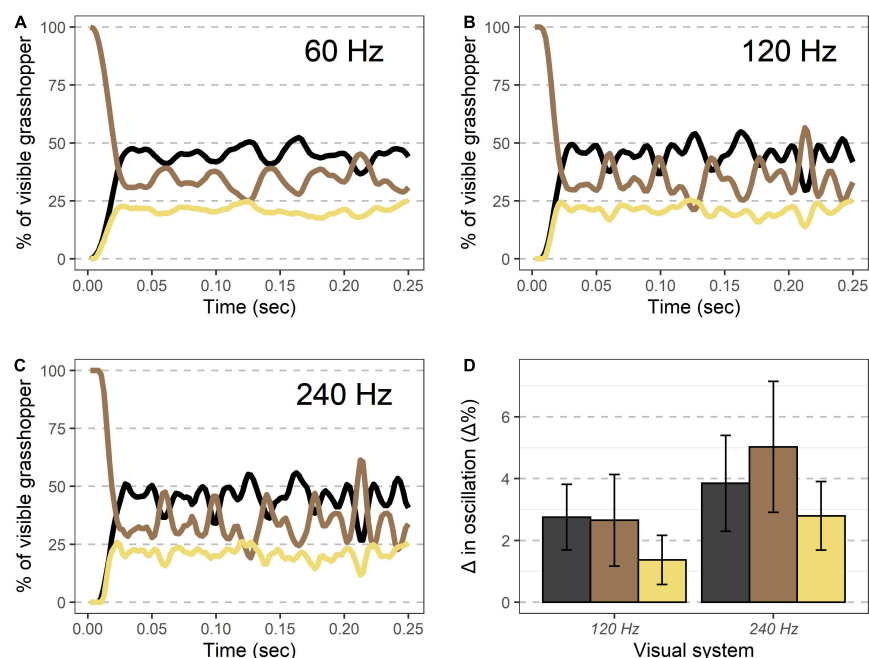


FIGURE 6 | Visible coloration shifts during takeoff modeled under different temporal visions. **(A–C)** An example takeoff of a Carolina grasshopper as seen by different visual systems. Percent of the visible grasshopper consisting of the three color categories brown, black, and cream are plotted. Compared to human vision ($\sim 60 \text{ Hz}$, **A**), oscillations in coloration are more pronounced for specialist bird predators ($\sim 120 \text{ Hz}$, **B**), and even more at the theoretical limit of visual speed ($\sim 240 \text{ Hz}$, **C**). **(D)** Oscillation magnitude for each color (90th percentile–10th percentile for values after initial takeoff) are more pronounced in non-human visual systems for each color examined. See text for complete methods and statistics.

TABLE 2 | Temporal aspects of deimatic displays in various species.

Species	Qualitative transition speed	Quantitative transition speed	Frequency of display	Display duration	Movement after?	n
Northern Bluetongue skink (<i>Tiliqua scincoides intermedia</i>) ^a	"Rapid; sudden"	-	0.1–0.2/sec	-	Yes	13
Spotted lanternfly (<i>Lycorma delicatula</i>) ^b	"Sudden"	-	-	15.16 ± 1.71 secs	Yes	91
<i>Stagmatoptera biocellata</i> ^c	"Violent; dramatic"	-	-	Typically 2–45 min	Yes	20
Large brown mantis (<i>Archimantis latistyla</i>) ^d	"Sudden"	-	-	-	-	35
Giant rainforest mantis (<i>Hierodula majuscula</i>) ^d	"Sudden"	-	-	-	-	20
False garden mantis (<i>Pseudomantis albofimbriata</i>) ^d	"Sudden"	-	-	-	-	25
European swallowtail butterfly (<i>Papilio machaon</i>) ^e	"Sudden"	-	Up to 0.3/min	-	Yes	27
Mountain katydid (<i>Acripeza reticulata</i>) ^f	"Sudden"	-	-	≤ 300 s	-	32
Peacock butterfly (<i>Inachis io</i>) ^g	"Sudden"	-	< 2/min	-	Yes	54
Common cuttlefish (<i>Sepia officinalis</i>) ^h	"Rapid; sudden"	-	-	3–12 s	Yes	6
Ringneck snake (<i>Diadophis punctatus</i>) ⁱ	"Sudden"	-	-	-	No	25

^aBadiane et al. (2018), ^bKang et al. (2017), ^cMaldonado (1970), ^dO'Hanlon et al. (2018), ^eOlofsson et al. (2012), ^fUmbers and Mappes (2015), ^gVallin et al. (2005), ^hKing and Adamo (2006), ⁱCox et al. (2021).

brown = 11.3 ± 3.0 ms) while simultaneously reducing their overall size (Figures 5C,D). The speed of this return was slower than the transition during takeoff and varied considerably between individuals (compare Figure 5A vs. Figure 5B). This could be due to some grasshoppers requiring more control when landing on certain surfaces. However, specialized predators would still only be able to form, at most, around four images of the transition before their prey returned to an all-brown appearance, which as Cooper (2006) suggested, may cause "predators [to] misjudge the landing site." Therefore, this quick disappearance of a highly contrasting region may constitute a third interwoven phase in the escape strategy of the Carolina grasshopper, alongside deimatic and protean defenses. If so, this bears a resemblance to the blanch-ink-jet behavior of longfin squid, in which the squid turns clear to hide itself, and then uses an ink cloud to confuse and/or startle predators as it flees, thereby similarly combining a transition with deimatic/protean defenses (Staudinger et al., 2011). Notably in the Carolina grasshopper, landing occurs last within this sequence, so its effectiveness may depend on the distances created by prior defenses.

Our simplistic measurements of color in this system likely represent an underestimate of its true temporal variability. We categorized color into three categories because Carolina grasshopper coloration is fairly distinct between body regions and consistent within them (e.g., Figures 1, 2). However, a predator's perception of the grasshopper is also dependent on other factors, including both environmental and physiological properties. Environmentally, the variability of color and patterning in flight would be increased by changes in illumination (Endler, 1993) or angular dependence of reflection (Stuart-Fox et al., 2021). Physiologically, our measurements do not account for the spatiotemporal variation of where these different colorations are located, and thus their interactions with predator vision (Hughes, 1977; Smolka and Hemmi, 2009). As technology improves, future studies could account for all these factors simultaneously. However, we feel that our simplified color measurements provide

a biologically relevant and feasible step in characterizing variation at these temporal resolutions.

Furthermore, the appearance of Carolina grasshoppers to their avian predators will not be identical to our experience watching these videos because of differences in visual Umwelt, distance, and angle of view. Avian color vision is both tetrachromatic and refined via the presence of oil droplets (Bowmaker et al., 1997; Hart and Vorobyev, 2005). As a result, their perception of hindwing color differs from ours, although it is still highly contrasting because of the dark and bright hindwing regions (Figure 2). Additionally, excluding birds of prey, many birds have coarser spatial vision than our own, which may blur some of the patterning (Caves et al., 2018). This combined with uncertainty in the distance from the bird to the grasshopper during pursuit could lead to different outcomes of colors blending or being seen as distinct. Lastly, an avian predator may approach from an angle that differs from our camera, and pursuit may change this angle. Differences in angle can lead to varying visual scenes (e.g., Cummings et al., 2008; Brandley et al., 2016), and future work should thoroughly investigate this phenomenon in a more natural context.

At the evolutionary level, the hindwings of band-winged grasshoppers present an interesting case study of how a single structure may be under multiple different selective pressures. In addition to their anti-predator purposes and inherent biomechanical function, hindwings may also serve in visual conspecific signaling (Otte, 1970, 1985; although behavioral data is lacking). Hindwing patterning often varies between species of band-winged grasshoppers, including in areas of transparency, placement of the band, hue, and likely in achromatic properties. Notably, transparent regions, which some other band-winged species possess (Figure 1C), could allow for differences between the biomechanical and visual properties of the wings, and the coarse visual acuity of band-winged grasshoppers (Horridge, 1978; Krapp and Gabbiani, 2005; Duncan et al., 2021) may make fine-scale patterning less important for conspecific signaling than for anti-predator purposes. Differences in color vision may also

play a role, with some species lacking a long-wavelength receptor (Vishnevskaya and Shura-Bura, 1990; Schmeling et al., 2014). However, in order to study why hindwing patterning varies between species, researchers will need to understand how these structures move in nature, and how this motion may be viewed by relevant receivers.

By quantifying the speed of visible pattern change in our study, we have begun to infer how these escape flights may appear to observers with differing temporal visual systems. Work in other visual parameters such as color vision (Endler, 1980; Cummings et al., 2003; Brandley et al., 2013) and visual acuity (Melin et al., 2016; Caves et al., 2018) has demonstrated the necessity of viewing natural phenomena through the eyes of relevant receivers. Therefore, when considering the differences in temporal vision across species (Healy et al., 2013), future studies must quantify natural motion patterns rather than relying on the human experience.

DATA AVAILABILITY STATEMENT

The original contributions presented in this study are included in the article/Supplementary Material, further inquiries can be directed to the corresponding author.

AUTHOR CONTRIBUTIONS

EM and NB conceptualized the project, performed the data analysis, and wrote the first draft of the manuscript.

REFERENCES

- Badiane, A., Carazo, P., Price-Rees, S. J., Ferrando-Bernal, M., and Whiting, M. J. (2018). Why blue tongue? A potential UV-based deimatic display in a lizard. *Behav. Ecol. Sociobiol.* 72:104. doi: 10.1007/s00265-018-2512-8
- Barthelmé, S., and Tschumperlé, D. (2019). Imager: an R package for image processing based on CImg. *J. Open Source Softw.* 4:1012. doi: 10.21105/joss.01012
- Behrens, R. R. (2012). *Ship Shape, a Dazzle Camouflage Sourcebook*. Dysart, IA: Bobolink Books.
- Belovsky, G. E., and Slade, J. B. (1993). The role of vertebrate and invertebrate predators in a grasshopper community. *Oikos* 68, 193–201. doi: 10.2307/3544830
- Boström, J. E., Dimitrova, M., Canton, C., Håstad, O., Qvarnström, A., and Ödeen, A. (2016). Ultra-rapid vision in birds. *PLoS One* 11:e0151099. doi: 10.1371/journal.pone.0151099
- Bowmaker, J. K., Health, L. A., Wilkie, S. E., and Hunt, D. M. (1997). Visual pigments and oil droplets from six classes of photoreceptor in the retinas of birds. *Vision Res.* 37, 2183–2194. doi: 10.1016/S0042-6989(97)00026-6
- Brandley, N., Johnson, M., and Johnsen, S. (2016). Aposematic signals in North American black widows are more conspicuous to predators than to prey. *Behav. Ecol.* 27, 1104–1112. doi: 10.1093/beheco/arw014
- Brandley, N. C., Speiser, D. I., and Johnsen, S. (2013). Eavesdropping on visual secrets. *Evol. Ecol.* 27, 1045–1068. doi: 10.1007/s10682-013-9656-9
- Brundrett, G. W. (1974). Human sensitivity to flicker. *Light. Res. Technol.* 6, 127–143. doi: 10.1177/096032717400600302
- Caves, E. M., Brandley, N. C., and Johnsen, S. (2018). Visual acuity and the evolution of signals. *Trends Ecol. Evol.* 33, 358–372. doi: 10.1016/j.tree.2018.03.001
- Cooper, W. E. (2006). Risk factors and escape strategy in the grasshopper *Dissosteira carolina*. *Behaviour* 143, 1201–1218.

NB acquired funding. EM collected all videos from the field and scored all takeoffs and landings. SB and HS scored all main flight videos. FG performed all spectrometry including collection of grasshoppers. All authors contributed to the article and approved the submitted version.

FUNDING

HS was supported by the College of Wooster's Sophomore Research Program. Funds for equipment came from the College of Wooster's Start-up Grant to NB.

ACKNOWLEDGMENTS

We thank Teddi Farson, Cameron Papp, and Christa Zianni for support in the field, Brae Salazar for photos of band-winged grasshopper hindwings, and Michael Rosario for consultation regarding high-speed video options.

SUPPLEMENTARY MATERIAL

The Supplementary Material for this article can be found online at: <https://www.frontiersin.org/articles/10.3389/fevo.2022.900544/full#supplementary-material>

- Cox, C. L., Chung, A. K., Blackwell, C., Davis, M. M., Gulsby, M., Islam, H., et al. (2021). Tactile stimuli induce deimatic antipredator displays in ringneck snakes. *Ethology* 127, 465–474. doi: 10.1111/eth.13152
- Cummings, M. E., Jordão, J. M., Cronin, T. W., and Oliveira, R. F. (2008). Visual ecology of the fiddler crab, *Uca tangeri*: effects of sex, viewer and background on conspicuousness. *Anim. Behav.* 75, 175–188. doi: 10.1016/j.anbehav.2007.04.016
- Cummings, M. E., Rosenthal, G. G., and Ryan, M. J. (2003). A private ultraviolet channel in visual communication. *Proc. Biol. Sci.* 270, 897–904. doi: 10.1098/rspb.2003.2334
- Davis, D. D. (1948). Flash display of aposematic colors in *Farancia* and other snakes. *Copeia* 1948, 208–211. doi: 10.2307/1438456
- Donner, K. (2021). Temporal vision: measures, mechanisms and meaning. *J. Exp. Biol.* 224:jeb222679. doi: 10.1242/jeb.222679
- Duncan, A. B., Salazar, B. A., Garcia, S. R., and Brandley, N. C. (2021). A sexual dimorphism in the spatial vision of North American band-winged grasshoppers. *Integr. Comp. Biol.* 3:obab008. doi: 10.1093/iob/obab008
- Endler, J. A. (1980). Natural selection on color patterns in *Poecilia reticulata*. *Evolution* 34, 76–91. doi: 10.2307/2408316
- Endler, J. A. (1993). The color of light in forests and its implications. *Ecol. Monogr.* 63, 1–27. doi: 10.2307/2937121
- Girard, M. B., Kasumovic, M. M., Elias, D. O., and Dyer, A. G. (2011). Multi-modal courtship in the peacock spider, *Maratus volans* (O.P.-Cambridge, 1874). *PLoS One* 6:e25390. doi: 10.1371/journal.pone.0025390
- Hall, J. R., Cuthill, I. C., Baddeley, R., Shohet, A. J., and Scott-Samuel, N. E. (2013). Camouflage, detection and identification of moving targets. *Proc. Biol. Sci.* 280:20130064. doi: 10.1098/rspb.2013.0064
- Hart, N. S. (2001). The visual ecology of avian photoreceptors. *Prog. Retin. Eye Res.* 20, 675–703. doi: 10.1016/S1350-9462(01)00009-X
- Hart, N. S., and Vorobyev, M. (2005). Modelling oil droplet absorption spectra and spectral sensitivities of bird cone photoreceptors. *J. Comp. Physiol.* 191, 381–392. doi: 10.1007/s00359-004-0595-3

- Healy, K., McNally, L., Ruxton, G. D., Cooper, N., and Jackson, A. L. (2013). Metabolic rate and body size are linked with perception of temporal information. *Anim. Behav.* 86, 685–696. doi: 10.1016/j.anbehav.2013.06.018
- Holmes, G. G., Delferrière, E., Rowe, C., Troscianko, J., and Skelhorn, J. (2018). Testing the feasibility of the startle-first route to deimatism. *Sci. Rep.* 8:10737. doi: 10.1038/s41598-018-28565-w
- Horridge, G. A. (1978). The separation of visual axes in apposition compound eyes. *Philos. Trans. R. Soc. Lond. B Biol. Sci.* 285, 1–59. doi: 10.1098/rstb.1978.0093
- How, M. J., and Zanker, J. M. (2014). Motion camouflage induced by zebra stripes. *Zoology* 117, 163–170. doi: 10.1016/j.zool.2013.10.004
- Hughes, A. (1977). “The Topography of Vision in Mammals of Contrasting Life Style: Comparative Optics and Retinal Organisation,” in *The Visual System in Vertebrates*, eds F. Crescitelli, C. A. Dvorak, D. J. Eder, A. M. Granda, D. Hamasaki, K. Holmberg, et al. (Berlin: Springer), 613–756.
- Humphries, D. A., and Driver, P. M. (1970). Protean defence by prey animals. *Oecologia* 5, 285–302. doi: 10.1007/BF00815496
- Ioannou, C. C., and Krause, J. (2009). Interactions between background matching and motion during visual detection can explain why cryptic animals keep still. *Biol. Lett.* 5, 191–193. doi: 10.1098/rsbl.2008.0758
- Jackson, J. F., Ingram, W., and Campbell, H. W. (1976). The dorsal pigmentation pattern of snakes as an antipredator strategy: a multivariate approach. *Am. Nat.* 110, 1029–1053. doi: 10.1086/283125
- Kang, C., Moon, H., Sherratt, T. N., Lee, S., and Jablonski, P. G. (2017). Multiple lines of anti-predator defence in the spotted lanternfly, *Lycorma delicatula* (Hemiptera: Fulgoridae). *Biol. J. Linn. Soc.* 120, 115–124. doi: 10.1111/bij.12847
- Kiltie, R. A. (2000). Scaling of visual acuity with body size in mammals and birds. *Funct. Ecol.* 14, 226–234. doi: 10.1046/j.1365-2435.2000.00404.x
- King, A. J., and Adamo, S. A. (2006). The ventilatory, cardiac and behavioural responses of resting cuttlefish (*Sepia officinalis* L.) to sudden visual stimuli. *J. Exp. Biol.* 209, 1101–1111. doi: 10.1242/jeb.02116
- Krapp, H. G., and Gabbiani, F. (2005). Spatial distribution of inputs and local receptive field properties of a wide-field, looming sensitive neuron. *J. Neurophysiol.* 93, 2240–2253. doi: 10.1152/jn.00965.2004
- Laan, A., Gutnick, T., Kuba, M. J., and Laurent, G. (2014). Behavioral analysis of cuttlefish traveling waves and its implications for neural control. *Curr. Biol.* 24, 1737–1742. doi: 10.1016/j.cub.2014.06.027
- Maia, R., Gruson, H., Endler, J. A., and White, T. E. (2019). pavo 2: new tools for the spectral and spatial analysis of colour in R. *Methods Ecol. Evol.* 10, 1097–1107. doi: 10.1111/2041-210X.13174
- Maldonado, H. (1970). The deimatic reaction in the praying mantis *Stagmatoptera biocellata*. *Z. Vergl. Physiol.* 68, 60–71. doi: 10.1007/BF00297812
- Mather, J. A., and Mather, D. L. (2004). Apparent movement in a visual display: the ‘passing cloud’ of *Octopus cyanea* (Mollusca: Cephalopoda). *J. Zool.* 263, 89–94. doi: 10.1017/S0952836904004911
- Melin, A. D., Kline, D. W., Hiramatsu, C., Caro, T., and Osorio, D. (2016). Zebra stripes through the eyes of their predators, zebras, and humans. *PLoS One* 11:e0145679. doi: 10.1371/journal.pone.0145679
- Murali, G. (2018). Now you see me, now you don’t: dynamic flash coloration as an antipredator strategy in motion. *Anim. Behav.* 142, 207–220. doi: 10.1016/j.anbehav.2018.06.017
- Murali, G., Kumari, K., and Kodandaramaiah, U. (2019). Dynamic colour change and the confusion effect against predation. *Sci. Rep.* 9:274. doi: 10.1038/s41598-018-36541-7
- O’Hanlon, J. C., Rathnayake, D. N., Barry, K. L., and Umbers, K. D. L. (2018). Post-attack defensive displays in three praying mantis species. *Behav. Ecol. Sociobiol.* 72:176. doi: 10.1007/s00265-018-2591-6
- Olofsson, M., Eriksson, S., Jakobsson, S., Wiklund, C., and Osorio, D. (2012). Deimatic display in the European swallowtail butterfly as a secondary defence against attacks from great tits. *PLoS One* 7:e47092. doi: 10.1371/journal.pone.0047092
- Olofsson, M., Løvlie, H., Tibblin, J., Jakobsson, S., and Wiklund, C. (2013). Eyespot display in the peacock butterfly triggers antipredator behaviors in naïve adult fowl. *Behav. Ecol.* 24, 305–310. doi: 10.1093/beheco/ars167
- Ord, T. J., and Stamps, J. A. (2008). Alert signals enhance animal communication in “noisy” environments. *Proc. Natl. Acad. Sci. U.S.A.* 105, 18830–18835. doi: 10.1073/pnas.0807657105
- Otte, D. (1970). A comparative study of communicative behavior in grasshoppers. *Misc. Pub. Mus. Zool. Univ. Mich.* 141, 1–169.
- Otte, D. (1985). *The North American Grasshoppers*, Vol. 2. Cambridge, MA: Harvard UP.
- Peters, R. A., Hemmi, J. M., and Zeil, J. (2007). Signaling against the wind: modifying motion-signal structure in response to increased noise. *Curr. Biol.* 17, 1231–1234. doi: 10.1016/j.cub.2007.06.035
- Ruxton, G. D., Allen, W. L., Sherratt, T. N., and Speed, M. P. (2018). *Avoiding Attack: The Evolutionary Ecology of Crypsis, Aposematism, and Mimicry*. Oxford: Oxford University Press.
- Schmeling, F., Wakakuwa, M., Tegtmeier, J., Kinoshita, M., Bockhorst, T., Arikawa, K., et al. (2014). Opsin expression, physiological characterization and identification of photoreceptor cells in the dorsal rim area and main retina of the desert locust, *Schistocerca gregaria*. *J. Exp. Biol.* 217, 3557–3568. doi: 10.1242/jeb.108514
- Schneider, C. A., Rasband, W. S., and Eliceiri, K. W. (2012). NIH Image to ImageJ: 25 years of image analysis. *Nat. Methods* 9, 671–675. doi: 10.1038/nmeth.2089
- Smolka, J., and Hemmi, J. M. (2009). Topography of vision and behaviour. *J. Exp. Biol.* 212, 3522–3532. doi: 10.1242/jeb.032359
- Staudinger, M. D., Hanlon, R. T., and Juanes, F. (2011). Primary and secondary defences of squid to cruising and ambush fish predators: variable tactics and their survival value. *Anim. Behav.* 81, 585–594. doi: 10.1016/j.anbehav.2010.12.002
- Stoddard, M. C., and Prum, R. O. (2008). Evolution of avian plumage coloration in a tetrahedral color space: a phylogenetic analysis of new world buntings. *Am. Nat.* 171, 755–776. doi: 10.1086/587526
- Stuart-Fox, D., Ospina-Rozo, L., Ng, L., and Franklin, A. M. (2021). The paradox of iridescent signals. *Trends Ecol. Evol.* 36, 187–195. doi: 10.1016/j.tree.2020.10.009
- Tan, E. J., and Elgar, M. A. (2021). Motion: enhancing signals and concealing cues. *Biol. Open* 10: bio058762. doi: 10.1242/bio.058762
- Umbers, K. D. L., Lehtonen, J., and Mappes, J. (2015). Deimatic displays. *Curr. Biol.* 25, R58–R59. doi: 10.1016/j.cub.2014.11.011
- Umbers, K. D. L., and Mappes, J. (2015). Postattack deimatic display in the mountain katydid, *Acripeza reticulata*. *Anim. Behav.* 100, 68–73. doi: 10.1016/j.anbehav.2014.11.009
- Umeton, D., Read, J. C. A., and Rowe, C. (2017). Unravelling the illusion of flicker fusion. *Biol. Lett.* 13:20160831. doi: 10.1098/rsbl.2016.0831
- Vallin, A., Jakobsson, S., Lind, J., and Wiklund, C. (2005). Prey survival by predator intimidation: an experimental study of peacock butterfly defence against blue tits. *Proc. Biol. Sci.* 272, 1203–1207. doi: 10.1098/rspb.2004.3034
- Vishnevskaya, T. M., and Shura-Bura, T. M. (1990). “Spectral Sensitivity of Photoreceptors and Spectral Inputs to the Neurons of the First Optic Ganglion in the Locust (*Locusta migratoria*)”, in *Sensory Systems and Communication in Arthropods*, eds F. G. Gribakin, K. Wiese, and A. V. Popov (Basel: Birkhäuser), 106–111.
- Vorobyev, M., Osorio, D., Bennett, A., Marshall, N., and Cuthill, I. (1998). Tetrachromacy, oil droplets and bird plumage colours. *J. Comp. Physiol. A Neuroethol. Sens. Neural. Behav. Physiol.* 183, 621–633. doi: 10.1007/s003590050286
- Wickham, H. (2016). *ggplot2: Elegant Graphics for Data Analysis*. New York, NY: Springer-Verlag.

Conflict of Interest: The authors declare that the research was conducted in the absence of any commercial or financial relationships that could be construed as a potential conflict of interest.

Publisher’s Note: All claims expressed in this article are solely those of the authors and do not necessarily represent those of their affiliated organizations, or those of the publisher, the editors and the reviewers. Any product that may be evaluated in this article, or claim that may be made by its manufacturer, is not guaranteed or endorsed by the publisher.

Copyright © 2022 Martin, Steinmetz, Baek, Gilbert and Brandley. This is an open-access article distributed under the terms of the Creative Commons Attribution License (CC BY). The use, distribution or reproduction in other forums is permitted, provided the original author(s) and the copyright owner(s) are credited and that the original publication in this journal is cited, in accordance with accepted academic practice. No use, distribution or reproduction is permitted which does not comply with these terms.



Uncovering ‘Hidden’ Signals: Previously Presumed Visual Signals Likely Generate Air Particle Movement

Pallabi Kundu¹, Noori Choi¹, Aaron S. Rundus², Roger D. Santer³ and Eileen A. Hebets^{1*}

¹ School of Biological Sciences, University of Nebraska-Lincoln, Lincoln, NE, United States, ² Department of Psychology, West Chester University, West Chester, PA, United States, ³ Institute of Biological, Environmental and Rural Sciences, Aberystwyth University, Aberystwyth, United Kingdom

OPEN ACCESS

Edited by:

Eunice Jingmei Tan,
Yale-NUS College, Singapore

Reviewed by:

Brent Stoffer,
University of Cincinnati, United States
Caroline Fabre,
University of Cambridge,
United Kingdom

*Correspondence:

Eileen A. Hebets
ehbets2@unl.edu

Specialty section:

This article was submitted to
Behavioral and Evolutionary Ecology,
a section of the journal
Frontiers in Ecology and Evolution

Received: 08 May 2022

Accepted: 16 June 2022

Published: 05 July 2022

Citation:

Kundu P, Choi N, Rundus AS,
Santer RD and Hebets EA (2022)
Uncovering ‘Hidden’ Signals:
Previously Presumed Visual Signals
Likely Generate Air Particle
Movement.
Front. Ecol. Evol. 10:939133.
doi: 10.3389/fevo.2022.939133

Wolf spiders within the genus *Schizocosa* have become a model system for exploring the form and function of multimodal communication. In terms of male signaling, much past research has focused on the role and importance of dynamic and static visual and substrate-borne vibratory communication. Studies on *S. retrorsa*, however, have found that female-male pairs were able to successfully mate in the absence of both visual and vibratory stimuli, suggesting a reduced or non-existent role of these signaling modalities in this species. Given these prior findings, it has been suggested that *S. retrorsa* males may utilize an additional signaling modality during courtship—air particle movement, often referred to as near-field sound—which they likely produce with rapid leg waving and receive using thin filiform sensory hairs called trichobothria. In this study, we tested the role of air-particle movement in mating success by conducting two independent sets of mating trials with randomly paired *S. retrorsa* females and males in the dark and on granite (i.e., without visual or vibratory signals) in two different signaling environments—(i) without (“No Noise”) and (ii) with (“Noise”) introduced air-particle movement intended to disrupt signaling in that modality. We also ran foraging trials in No Noise/Noise environments to explore the impact of our treatments on overall behavior. Across both mating experiments, our treatments significantly impacted mating success, with more mating in the No Noise signaling environments compared to the Noise environments. The rate of leg waving—a previously assumed visual dynamic movement that has also been shown to be able to produce air particle displacement—was higher in the No Noise than Noise environments. Across both treatments, males with higher rates of leg waving had higher mating success. In contrast to mating trials results, foraging success was not influenced by Noise. Our results indicate that artificially induced air particle movement disrupts successful mating and alters male courtship signaling but does not interfere with a female’s ability to receive and assess the rate of male leg waving.

Keywords: wolf spider, *Schizocosa retrorsa*, mating success, near-field sound, multimodal signaling, signaling environment, behavioral plasticity, environmental noise

INTRODUCTION

Animals communicate with each other for a multitude of reasons with displays that can often be received and processed by different sensory systems (Hebets, 2011; Higham and Hebets, 2013). Wild spotted hyenas (*Crocuta crocuta*), for example, receive visual signals from relaxed open mouths and head-bobbing behavior of conspecifics that leads to the initiation of play fights with playmates (Nolfo et al., 2021); Oriental magpie robins (*Copsychus saularis*) receive information from conspecifics about threats, submission, or distress through different acoustic signals (Manshor and Augustine Gawin, 2020); red-eyed treefrog males (*Agalychnis callidryas*) assess their opponents' size and status through their vibratory signals, or tremulations (Caldwell et al., 2010); and ovulating female sea lamprey (*Petromyzon marinus*) are attracted to males by their pheromones, or olfactory signals (Teeter, 1980; Siefkes et al., 2005). Animal communication research has focused on many animal systems such as these where the signal is presumed to operate through a single sensory modality. There is also widespread recognition, however, that many animal displays incorporate signals in multiple sensory modalities, i.e., many animals engage in multimodal signaling (Rowe and Guilford, 1996; Partan and Marler, 1999; Hebets and Papaj, 2005; Hebets and McGinley, 2019). Multimodal communication displays that incorporate signals of various form can also be received and processed through multiple independent sensory systems (Hebets, 2011; Higham and Hebets, 2013; Halfwerk et al., 2019).

A first step in understanding the evolution and function of multimodal signaling is to identify potential sensory systems that might be involved (Halfwerk et al., 2019). To date, much research in this area has focused on presumed bimodal signaling systems, or on the reaction of receivers to signals received by two sensory systems. Male fowl (*Gallus gallus*), for example, have been studied for their use of movements (visual) and calls (acoustic—air borne sound) to attract a female's attention (Smith et al., 2011). Estrildid finches (Family Estrildidae) are known to use singing (acoustic), dancing (visual), and color patterns (visual) as part of their multimodal courtship displays (Gomes et al., 2017); and many frog species incorporate combinations of visual, acoustic, substrate-borne vibratory (hereafter “vibratory”), and chemical components during signaling (reviewed in Starnberger et al., 2014). Similarly, within the multimodal courtship signaling of male wolf spiders, studies to date on the genus *Schizocosa* have focused predominantly on the female's reactions to static and dynamic visual and vibratory signaling, and their potential interactions (Hebets, 2005; Hebets et al., 2011, 2021; Uetz et al., 2016; Hebets and McGinley, 2019; Choi and Hebets, 2021; Starrett et al., 2022).

The classification of signaler displays as unimodal vs. bimodal represents our current best attempts to understand signal form and function given our human sensory biases, our limitations in understanding the sensory physiology of focal taxa, and sometimes limitations to experimental designs. In all the previous examples of bimodal signaling, for example, signal detection might be informed by more than two different sensory systems. Dynamic movements that we presume to be visual signals, for

example, may generate air particle movement that is detectable by receivers. Indeed, past discoveries of the involvement of previously unknown or underappreciated sensory systems have been arguably among the most exciting advances in animal communication research. We now know, for example, that big brown bats (*Eptesicus fuscus*) use ultrasonic calls not only to find food but that their calls also have unique properties to recognize individuals and thus function in communication (Masters et al., 1995). California ground squirrels (*Spermophilus beecheyi*) can add a thermal component to their tail flagging to defend themselves against infrared-sensitive rattlesnakes (Rundus et al., 2007). Several species of moths, including the Asian corn borer (*Ostrinia furnacalis*), produce ultrasonic frequencies of sound at a low level as a part of their courtship ritual so that their mates can hear them, but predators remain unaware (Nakano et al., 2009). More recent findings show that bottlenose dolphins (*Tursiops truncatus*) can respond to electric fields using the vibrissal crypts on their snouts (Hüttner et al., 2022) and orb-weaving spiders (*Larinioides sclopetarius*) can detect airborne sounds using their webs (Zhou et al., 2022). In many of these examples, the focal animals have sensory systems that differ markedly to those of humans, and it is only through an appreciation of these sensory abilities that signaling traits and interactions can be understood (Eakin, 1972; Budelmann, 1992).

There is huge variation in sensory systems across animal taxa and many of these systems are poorly understood. Within the arthropods, for example, we observe multiple spectral classes of photoreceptors in mantis shrimp (Order Stomatopoda) (Marshall, 1988; Marshall et al., 2007), the Johnston's organ in insects (Order Diptera) (Johnston, 1855; Boekhoff-Falk, 2005; Gibson and Russell, 2006), pectines of scorpions (Order Scorpiones) (Brownell, 1988; Wolf, 2017), malleoli of solifugae (Order Solifugae) (Brownell and Farley, 1974), elongate sensory legs of amblypygids (Order Amblypygi) (Igelmund, 1987; Santer and Hebets, 2011) and enlarged anterior median eyes of jumping spiders (Order Araneae, Family Salticidae) (Land, 1969; Harland and Jackson, 2002), among others. For many of these sensory organs, we have a very superficial understanding of their function. Several orders of arachnids also possess a type of particularly fine filiform hair sensilla called trichobothria (Görner and Andrews, 1969; Barth et al., 1993; Barth, 2000). Trichobothria and similar hair sensilla in crustaceans and insects are extremely sensitive to very small medium particle displacements (Görner and Andrews, 1969; Breithaupt, 2002; Shimozaawa et al., 2003). Spiders can possess multiple trichobothria on their legs and the currently known hair functions include prey capture and predator avoidance (Barth et al., 1995; Suter, 2003), with no existing examples (in spiders) of their use in receiving air particle movement signals as part of courtship assessment.

The potential incorporation of air particle movement in the production and reception of communication displays has not received much research attention beyond a few focal taxonomic groups. The well-known waggle dance of honeybees, for example, generates air particle movement (265–350 Hz) that enables hive mates to find the dancer even in the dark (Tsujiuchi et al., 2007). Directional air particle movement produced by the wings of male *Drosophila* is an important aspect of their courtship display

(Tauber and Eberl, 2003). In courtship displays of African cave crickets (*Phaeophilacris spectrum*), males perform a series of wing flicks at a low frequency of 8–12 Hz which the females respond to by calming down into a receptive state for copulation (Heidelbach et al., 1991; Heidelbach and Dambach, 1997). Finally, during agonistic contests in the amblypygid *Phrynus marginemaculatus*, individuals rapidly vibrate their antenniform legs close to their opponent at a frequency of around 29 Hz (Santer and Hebets, 2008). The duration of these antenniform leg vibrations is predictive of contest winners (Fowler-Finn and Hebets, 2006; Santer and Hebets, 2008) and trichobothria were shown to be responsive to the displayed frequencies of air particle movement (Santer and Hebets, 2008). In a follow-up study, when these trichobothria were ablated, contests increased in duration (Santer and Hebets, 2011), consistent with the idea that the production and reception of air particle movement is a critical part of agonistic signaling in this species.

While a communication function has only been explored in a handful of arthropod taxa, the production and reception of air particle movements is important in many other contexts. The trichobothria of wandering spiders (*Cupiennius salei*), for example, can respond to the wingbeats of a fly more than 25 cm away (Barth et al., 1995). In the fishing spider, *Dolomedes triton*, air particle movements detected by trichobothria enable spiders to respond faster to attacks by predators (Suter, 2003). Caterpillars *Baratha brassicae* L. (Lepidoptera, Noctuidae) exhibit defensive displays in response to low frequency stimuli which they receive with filiform hairs on their dorsal surface (Markl and Tautz, 1975), and mosquitoes (*Toxorhynchites brevipalpis*) use the Johnston's organ at the base of the antennae to sense the air particle movement generated by the wingbeats of other mosquitoes (Gibson and Russell, 2006). Given the prevalence and importance of air particle movement in other contexts, we propose that air particle movement is a likely “hidden” modality in the communication displays of many arthropods.

Like in other taxonomic groups, studies of male courtship signaling in spiders have thus far focused predominantly on bimodal (in this case static and dynamic visual and vibratory) signaling and sensory reception. Jumping spiders in the genus *Habronattus*, for example, are impressive in their coordination of sexually dimorphic ornamentation and associated dynamic visual displays with their complex vibratory songs that can consist of up to 20 elements (Elias et al., 2003, 2012). Similarly, decades of research on wolf spiders in the genus *Schizocosa* have explored the form and function of visual (ornamentation and dynamic movements) and vibratory signaling (reviewed in Uetz and Roberts, 2002; Stratton, 2005; Hebets et al., 2013; Uetz et al., 2016; Hebets and McGinley, 2019; Starrett et al., 2022). Despite major advances in our understanding of bimodal signal interactions in select species [e.g., *S. ocreata* (Scheffer et al., 1996; Uetz et al., 2016); *S. uetzi* (Hebets, 2005); *S. stridulans*, (Hebets et al., 2011); *S. floridana* (Rosenthal and Hebets, 2012)], there remains one *Schizocosa* species where the visual and vibratory signaling appear non-functional from the female's perspective—*Schizocosa retrorsa* (Banks, 1911).

Schizocosa retrorsa males engage in a multimodal courtship display that conspicuously (to humans) includes visual and

vibratory signaling (Rundus et al., 2010; Hebets et al., 2013; Hebets and McGinley, 2019). With their blackened femurs contrasting against the adjacent lightened foreleg segments (Stratton, 2005; Starrett et al., 2022), males extend their legs and rapidly wave them up and down in an “extended leg tap” (hereafter “leg wave”) followed by a “push-up” display (Hebets et al., 1996). There are distinct vibratory signals that accompany the production of both dynamic visual movements (**Supplementary Video 1**). Nonetheless, multiple studies have now confirmed that *S. retrorsa* males can successfully mate when females are unable to detect signals in either, or both, of these signaling modalities (Hebets et al., 2008; Rundus et al., 2010; Choi et al., 2019). In mating trials run in complete darkness [without the potential for females to detect visual signaling (DeVoe et al., 1969; DeVoe, 1972)] and on granite (removing the potential for females to detect vibratory signals Elias et al., 2004), pairs were still able to mate as successfully as in trials where they could detect both visual and vibratory stimuli (Rundus et al., 2010). Furthermore, across all signaling environments, even in the absence of visual and vibratory stimuli, the rate of male leg waving was predictive of mating success. Males who engaged in more bouts of leg waving had higher copulation success regardless of the presence or absence of visual or vibratory signals (Rundus et al., 2010), suggesting that females are attending to and assessing the leg waving rate itself. The authors of this latter study calculated the leg waving frequency to be 13.55 Hz and argued that the male's dynamic leg waving could generate air particle movement that was detectable by a female *S. retrorsa* (Rundus et al., 2010). Multiple studies have now suggested the potential presence of air particle movement signals in the courtship display of *S. retrorsa* (Rundus et al., 2010; Choi et al., 2019), but the actual involvement of this signaling modality has not been tested until now.

This study tests the hypothesis that air particle displacement generated by the dynamic leg waving display of *S. retrorsa* males is crucial for a male's mating success. Support for this hypothesis would indicate that females rely on a previously overlooked sensory system to detect and assess courtship signaling. The (substrate-borne) vibrations that are common and important in many *Schizocosa* species' courtship displays, for example (Hebets et al., 2013), are assumed to be detected by lyriform slit sense organs on the walking legs. These sensory organs are the vibration receptors of spiders and detect physical deformation or cuticular strain in response to vibrations on the surface in contact with the legs (Walcott, 1969; Barth and Bohnenberger, 1978; Barth, 2002). The specific type of vibrations (leg taps or pedipalp drumming by males) that these organs respond to can vary by the placement of the organs on the legs (Knowlton and Gaffin, 2019). Air particle movement, in contrast, is assumed to be detected by filiform sensory hairs (trichobothria) which are deflected by the force of air particles (Barth and Holler, 1999; Barth, 2002). Depending on the frequency of air particle movements, the trichobothria are deflected at certain angles to elicit responses (Barth et al., 1993, 1995) and this can also provide the spider with directional information (Friedel and Barth, 1997). In this study, in the absence of visual or vibratory signals, we aim

to test the hypothesis that female *S. retrorsa* can detect and assess males through the air particle movement generated during courtship leg waving.

To test our hypothesis, we conducted mating trials in the absence (No Noise) and presence (Noise) of artificially introduced air particle movement, or “noise,” intended to reduce the air particle movement signal-to-noise ratio. We also ran foraging trials in No Noise and Noise treatments to ensure that our experimental manipulations did not have overarching effects on behavior. In our mating trials, if air particle movement is a critical signaling channel for *S. retrorsa* males, we would expect higher mating success in the No Noise treatment group compared to the Noise treatment group. We would also expect that the rate of leg waving would still predict a male’s mating success, even in the absence of visual or vibratory stimuli. Finally, if air particle movement noise reduces or removes a female’s capacity to assess the leg waving display, then we would expect that leg waving rate would only predict mating success in the No Noise signaling environments.

MATERIALS AND METHODS

We conducted two similar, yet independent, experiments to explore the impact of artificially induced air particle movement (i.e., Noise that would presumably impede the detection of air particle movement signals) on the mating success of *Schizocosa retrorsa*. Experiment 1 ($n = 14$ per treatment) was conducted in 2008 at a laboratory on the University of Nebraska-Lincoln’s (UNL) city campus and used white noise as a stimulus for artificially induced air particle movement. Experiment 2 ($n = 26$ per treatment) was conducted in 2021 at UNL’s field station in western Nebraska (Cedar Point Biological Station) and used a 100 Hz frequency stimulus. The experiment was repeated (Exp 2) with a larger sample size in order to increase our confidence in the results. Given the slightly different experimental design, we analyzed the two experiments separately.

Study Animals

We collected juvenile *Schizocosa retrorsa* from Marshall, Co., Mississippi, United States near Wall Doxey State Park (34°40’N, 89°28’W) on 19th May 2008 (Exp 1) and from Panola Co., Mississippi, United States near Sardis Dam T8S R6W Sect. 13 (34°23’N 89°47’30’’W) on 5th May 2021 (Exp 2). We transported spiders to the laboratory where we housed them individually in plastic cages (5.8 × 5.8 × 7.9 cm, AMAC Plastic Products, United States) covered with masking tape to visually isolate individuals. The top of the cage had a hole fitted with a cork for feeding and the bottom had a hole with a wick that sucked in water. The inside of the cages had screening on 2 sides so the spiders could climb. We placed all cages on top of chicken wire mesh inside a plastic tub (65 × 37 × 14.5 cm) filled with 2–3 cm of water and in a controlled light environment (12 h light, 12 h dark) and constant temperature of 25°C. We fed the spiders twice a week with two 1/16th inch crickets (*Gryllodes sigillatus* from Ghann’s Cricket Farm). We checked spiders every 1–2 days for molts (shed exoskeleton indicating growth and often

sexual maturation) and used only mature females and males in our experiments. We identified mature females by observing the opening of their epigynum on the ventral surface of their abdomen and mature males by their bulbous pedipalps (Foelix, 1996) and black pigmentation on the femur of the first pair of legs (Hebets et al., 1996).

Environmental Treatments (Exp 1 and 2)

To test the influence of artificially introduced air particle movement on the mating success of *S. retrorsa*, we assessed mating success and associated courtship behavior of males under two experimental signaling environments: (i) No Noise (**Figure 1A**) and (ii) artificially induced air particle movement or Noise (**Figure 1B**). We created our No Noise environment by removing the speaker cone from the first speaker (DD Audio, Model: DB65A, **Figure 1C**, left image) to prevent the introduction of air particle movement. We created a Noise environment by using an identical speaker (DD Audio, Model: DB65A), with the speaker cone intact (**Figure 1C**, right image) to introduce artificially induced air particle movement into the mating arena.

We positioned the speakers directly above the mating arenas (the outer rim of the speakers was 7.5 cm from the arena floor) using two mechanical arms with magnets (Brand: StrongHand, Model: Snake Magnet, Supplier: StrongHand Tools, United States) attached to the countertop. We connected the speakers to an amplifier (Brand: Rolls, Model: PA71plus MicroMix Power Amplifier) which connected to the laptop.

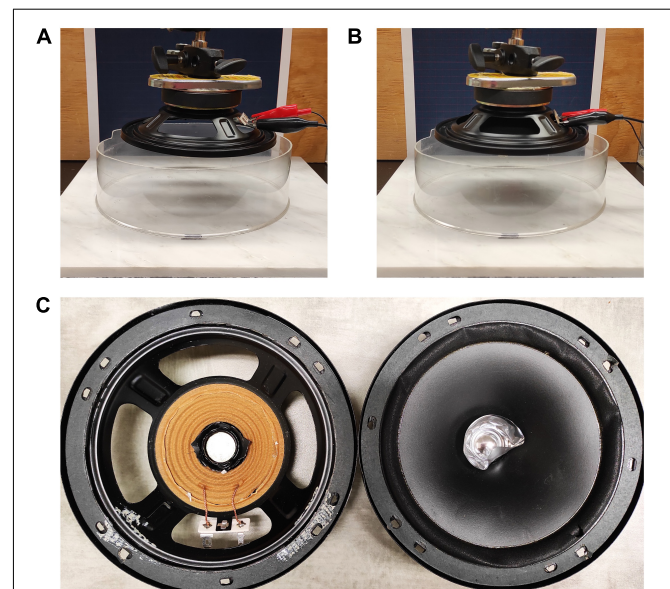


FIGURE 1 | Environmental Treatments—No Noise and Noise Signaling Environments. The mating arenas were set on a granite platform with the speakers held on top of the arena with mechanical arms (**A,B**). One of the speakers had the speaker cone removed (**A,C** left) and thus did not introduce air particle movement. The other speaker had the speaker cone intact (**B,C** right) and introduced air particle movement. All trials were run in the dark.

The laptop screen remained completely dark for the entire duration of each trial.

We employed 22–250 Hz white noise oscillations (Exp 1) or constant 100 Hz oscillations of the speaker cone (Exp 2) in order to stimulate trichobothria of a range of lengths on the walking legs of *S. retrorsa*. The walking legs of spiders are equipped with large numbers of trichobothria of varying lengths, and the frequency tuning of each trichobothrium depends upon its length (Barth, 2002). In the relatively larger wandering spider *Cupiennius salei*, the best frequencies of trichobothria range from 40 to 600 Hz, but each hair can respond to a relatively broad range of frequencies, and both short and long trichobothria could reliably follow medium oscillations between 10 and 950 Hz (Barth, 2002). We verified that trichobothria were stimulated in both our experiments by observing their movement under a dissecting microscope in response to the stimulus using the speaker with speaker cone intact (Noise, **Supplementary Video 2**). We also verified that there was no movement of the trichobothria when we used the speaker without speaker cone (No Noise). We adjusted the speaker with the speaker cone intact to a sound level of ~88 dB (Exp 1) and ~74 dB (Exp 2) using a digital sound level meter (Brand: RadioShack, Model: Digital Sound Level Meter 33-2055). The speaker with its cone removed was driven with matched amplifier level settings.

To ensure that pairs were not able to detect each other visually or through vibrations, we ran all mating trials in a dark room with no light source and on a surface of granite. Previous studies have demonstrated that granite effectively ablates the transmission of spider courtship signals (Elias et al., 2004). Finally, to record all trials for later analysis, we placed an infrared camera (Brand: Sony, Model: FDR-AX53) in front of the experimental setup at an angle of 10 degrees downwards from the horizontal and an infrared light source (Brand: IR Illuminator, Model: CM-IR110) close to the experimental setup.

Mating Trials (Exp 1 and 2)

Underneath the speakers, our mating arenas consisted of a transparent plastic circular enclosure (diameter 20 cm and height 7.6 cm Exp 1 and 6.3 cm Exp 2) resting on top of a granite slab. We coated the top inner circumference of the arena wall with petroleum jelly to prevent spiders from climbing out. Before each mating trial, we cleaned the arena and granite slab with deionized water (Wilder et al., 2005). We cleaned everything with 70% ethanol at the end of each day. We always ran one No Noise and one Noise treatment simultaneously in Experiment 1 and back-to-back trials (due to limited space) in Experiment 2. In Experiment 1, the arenas were separated by ~5.4 cm. Given that the speakers were directly above each mating arena, it was unlikely that air particle movement was being introduced into our No Noise arena from the adjacent Noise speaker. We randomly paired females and males, and each individual spider was only used once.

On the day of the experiment, we weighed focal females and placed them in the mating arena in the dark on granite for 30 min for acclimatization. During that time, we weighed the paired males. After 30 min of acclimatization, we introduced the male into the arena, but restrained him underneath a

small removable barrier (a plastic cylinder, open on the ends, diameter 3 cm). We turned on the speakers and the infrared camera, released the male and allowed the pair to interact for 30 min.

After 30 min, we recorded whether the pairs were mating or not. *Schizocosa retrorsa* mate for an extended duration (150–160 min, Hebets et al., 1996), making it unlikely for us to have missed a mating. We also scored all the trials using our infrared recordings. Following all trials, we euthanized females and males by freezing, and we preserved them in 70% ethanol. The spiders were at the end of their natural life (life span: 1 year) and the preserved specimens are retained in our collection (Hebets laboratory) at the University of Nebraska-Lincoln.

Behavioral Scoring (Exp 1 and 2)

We used BORIS-2021-09-20: v.7.12.2 to quantify the videos of the mating trials. We calculated the “latency to courtship” as the time (in seconds) from when the males were released into the arena until the males started courting. We calculated “latency to mate” as the time (in seconds) from when the males started courting until they mated, or till the end of trial (Exp 1) or the last time they courted right before the trial ended (Exp 2). For Experiment 1 and 2, we calculated the “rate of leg waving bouts” (#/second) as the number of recorded leg waving bouts divided by “latency to mate.” We defined a “bout” as a period of leg waving separated by walking, grooming, inactivity, or push-up displays. This variable has been scored and used previously for *S. retrorsa* behavioral analyses (Hebets et al., 1996), and similar measures have been used in other *Schizocosa* species to calculate courtship rate (e.g., Rosenthal and Hebets, 2012). For Experiment 2, we additionally calculated the “rate of individual leg waves” (#/second) as the number of individual leg waves divided by “latency to mate.” Because we are interested in the potential for each leg wave to generate air particle movement, we felt this was a better measure of leg waving rate than considering only each leg waving bout. Unfortunately, the same data (i.e., # individual leg waves) were not available for Experiment 1. Nonetheless, an analysis of the relationship between rate of leg waving bouts and rate of individual leg waves in Experiment 2 shows that they are highly correlated (**Supplementary Figure 1**). Finally, push-up displays are generally associated with leg waving bouts and for Experiment 2, we also calculated the “rate of push-up” (#/second) as the number of recorded push-up divided by “latency to mate” (data unavailable for Exp 1).

Foraging Trials (Exp 2)

In Experiment 2, we aimed to further explore the impact that our experimental treatments had on general female and male behavior and so we examined foraging behavior. We ran foraging trials 12–20 h before the mating trials. In the foraging trials, we used the same environment—No Noise or Noise—that each individual would be exposed to for their mating trial. We released spiders into the “mating” arena (diameter: 20 cm, height: 6.3 cm; in the dark; on granite) where we allowed them to roam freely for 3–4 min with the speakers playing the treatment stimulus. We then introduced a single 0.32 cm (1/8th inch) cricket (*Grylloides sigillatus*) into the arena opposite to the position of the spider.

We left the spider and cricket to interact for 3 min, after which time we noted whether the spider ate the cricket or not.

Statistical Analyses

We analyzed each mating experiment (Experiment 1 and 2) separately. For each, to ensure that there were no differences between our treatments (No Noise/Noise) with respect to female/male age or weight, we compared the ages and weights of females and males. Also, we compared age and weight differences of the females and males between the No Noise and Noise trials. We ran unpaired *t*-tests to make sure there were no significant differences in these categories.

To determine if the experimental signaling environments (No Noise/Noise) influenced mating success (yes/no), we used a Chi-square test to compare mating frequency across each signal environment. We performed a Kaplan Meier survival analysis to determine if there were differences in “latency to mate” between the signaling environments.

To determine if the experimental treatments (No Noise/Noise) influenced male courtship behavior, we compared the rate of leg waving bouts between the No Noise/Noise treatments for each experiment separately using independent two-sample *t*-tests. For Experiment 2, we also compared the rate of individual leg waves, and the rate of push-ups between the signaling environments using independent two-sample *t*-tests. We only did this for Experiment 2 because we did not have these data for Experiment 1. We also explored the relationship between rate of leg waving bouts and rate of push-up (Exp 2) using Pearson's correlation analysis (**Supplementary Figure 2**).

Finally, given that we found differences in male signaling rates between the signaling environments for both Experiment 1 and 2 (see “Results” section), we built binomial logistic regression models for each experiment with predictor variables including female age, male age, female weight, male weight, signaling environment (Noise/No Noise), and rate of leg waving bouts and an interaction between signaling environment and rate of leg waving bouts. Our response variable was mating (yes/no). We did not include rate of push-up in these analyses since we were explicitly interested in the impact of air particle movement, which are suggested to be generated by the dynamic motion associated with leg waving, not push-up (Rundus et al., 2010). We dropped all the terms except the signaling environments and the rate of leg waving bouts by backward selection for significant terms. We ran a second model for Experiment 2 using the rate of individual leg waves in place of leg waving bouts. The results of the models were summarized using Anova Type II and Wald Test. Given that our results suggested an influence of leg waving (analyzed as both bouts and individual waves) on mating success in both experiments, we also compared the rate of leg waving bouts between males that mated compared to the ones that did not mate for each experiment using independent two sample *t*-tests.

To determine if the experimental treatments (No Noise or Noise) had an influence on foraging behavior (Exp 2 only), we built a binomial logistic regression model with foraging success (yes/no) as the response variable and signaling environments, sex, and signaling environments by sex as the predictor variables.

The data were analyzed using the R 4.1.3 binary [for macOS 10.13 (High Sierra) and higher] through RStudio Desktop. The packages used in R are tidyverse, ggplot2, survival (function Surv), car (function Anova), ggpubr (function *t_test*), and stats.

RESULTS

Environmental Treatments (Exp 1 and 2)

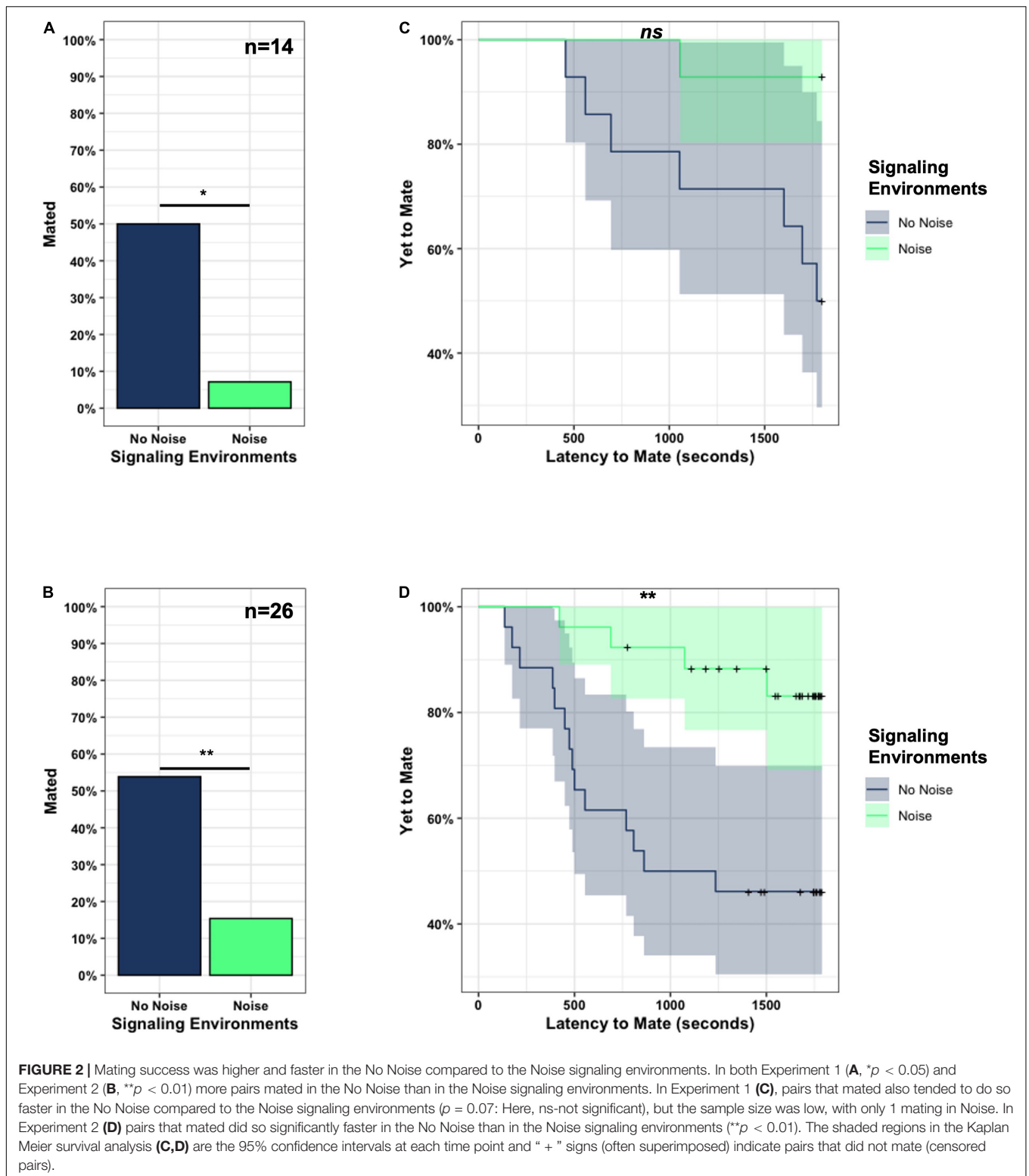
For Experiment 1, females were on average 22.429 ± 3.91 days post-maturation, while males were 31.821 ± 2.816 days post-maturation. Females weighed 79 ± 14 mg while the males weighed 53 ± 7 mg. For Experiment 2, females were on average 13.88 ± 0.92 days post-maturation, while males were 24 ± 1.83 days post-maturation. Females weighed 56.5 ± 5 mg while the males weighed 41.88 ± 3.9 mg. There was no significant difference in the ages or weights of the females and males between the treatment groups in either Experiment 1 (**Supplementary Table 1**) or Experiment 2 (**Supplementary Table 2**) or in the pairwise difference between female/male age or weight within pairs across the treatment groups (**Supplementary Tables 1, 2**).

Mating Trials (Exp 1 and 2)

Mating success was influenced by the signaling environment across both experiments. In Experiment 1, significantly more pairs mated in the No Noise (7/14; 50%) than in the Noise (1/14; 7.14%) signaling environments ($\chi^2 = 6.3$, $df = 1$, $p = 0.012^*$) (**Figure 2A**). We found comparable results in Experiment 2 where mating success was significantly higher in the No Noise (14/26; 53.85%) than in the Noise (4/26; 15.38%) signaling environments ($\chi^2 = 8.497$, $df = 1$, $p = 0.004^{**}$) (**Figure 2B**).

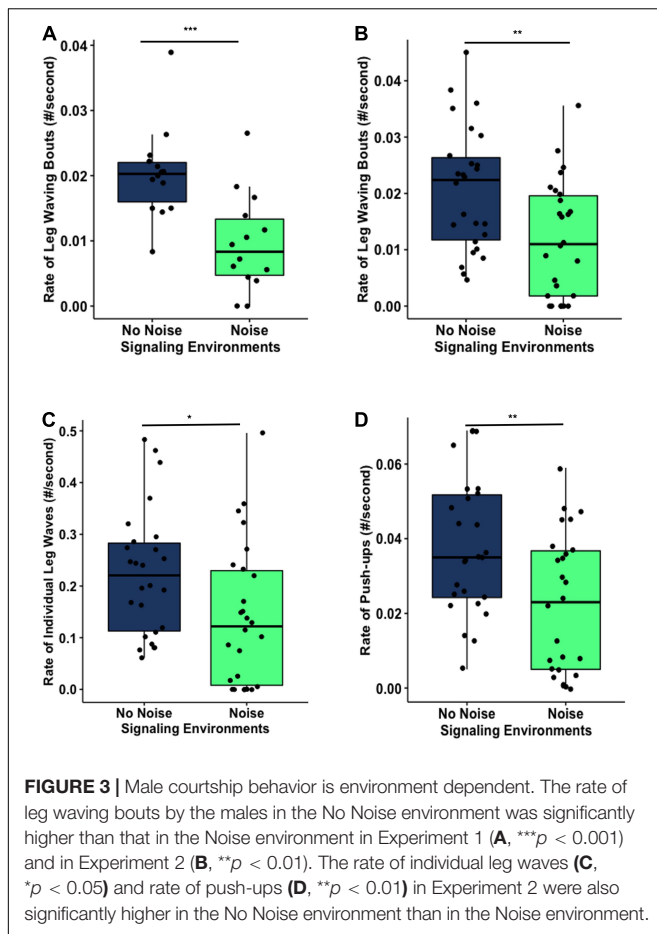
The signaling environments also influenced the time to mate once courtship started (i.e., “latency to mate”). Pairs tended to mate more quickly in the No Noise environments. This trend was marginally non-significant in Experiment 1 (**Figure 2C**, latency to mate—No Noise: 1459.643 ± 522.776 s, Noise: 1746.857 ± 198.842 s, Test-statistic = -1.921 , $df = 16.684$, $p = 0.072$), and significant in Experiment 2 (**Figure 2D**, latency to mate—No Noise: 1062.142 ± 629.598 s, Noise: 1472.138 ± 382.298 s, Test-statistic = -2.838 , $df = 41.229$, $p = 0.007^{**}$).

The signaling environments significantly influenced the rate of leg waving bouts in both experiments. In Experiment 1, males had a significantly higher rate of leg waving bouts in No Noise than in Noise signaling environments (No Noise: 0.02 ± 0.007 #leg waving bouts/s; Noise: 0.01 ± 0.007 #leg waving bouts/s, test-statistic = 3.938 , $df = 25.905$, $p < 0.001^{***}$; **Figure 3A**). In Experiment 2, males also showed a significantly higher rate of leg waving bouts in No Noise (0.021 ± 0.011 #leg waving bouts/s) compared to Noise (0.012 ± 0.01 #leg waving bouts/second) signaling environments (test-statistic = 3.009 , $df = 49.81$, $p = 0.004^{**}$; **Figure 3B**). In Experiment 2, we also examined the rate of individual leg waves and rate of push-ups. We found that rate of individual leg waves was significantly higher in No Noise (0.224 ± 0.122 #individual leg waves/s) compared to Noise (0.14 ± 0.137 #individual leg waves/s) signaling environments



(test-statistic = 2.324, $df = 49.363$, $p = 0.024^*$; **Figure 3C**). The rate of push-ups was also significantly higher for No Noise (0.038 ± 0.018 #push-ups/s) than for Noise (0.022 ± 0.019 #push-ups/s) signaling environments (test-statistic = 3.074, $df = 49.983$,

$p = 0.003^{**}$, **Figure 3D**). As described in previous studies (Hebets et al., 1996; Rundus et al., 2010), rate of leg waving bouts and rate of push-ups are correlated in the courtship of *S. retrorsa* (**Supplementary Figure 2**).



To evaluate the relative importance of the signaling environment (Figure 2) and rate of leg waving bouts (Figure 3) on mating success, we used a binomial logistic regression model. With the smaller sample size of Experiment 1, our overall model was marginally non-significant (Wald $\chi^2 = 4.7$, $df = 2$, $p = 0.094$). For Experiment 2, when we used the rate of leg waving bouts for the model, our overall model was significant (Wald $\chi^2 = 12.2$, $df = 2$, $p = 0.002^{**}$) with rate of leg waving bouts being highly significant (LR $\chi^2 = 13.857$, $df = 1$, $p < 0.001^{***}$) and the signaling environment marginally non-significant (LR $\chi^2 = 3.243$, $df = 1$, $p = 0.072$). When we used the rate of individual leg waves for the Experiment 2 model, the overall model is again significant (Wald $\chi^2 = 10.6$, $df = 2$, $p = 0.005^{**}$), and both the rate of individual leg waves (LR $\chi^2 = 7.4515$, $df = 1$, $p = 0.006^{**}$) and the signaling environment (LR $\chi^2 = 5.409$, $df = 1$, $p = 0.02^{*}$) showed a significant influence on mating success.

In Experiment 1, males that mated had significantly higher rates of leg waving bouts (Mated: 0.034 ± 0.013 leg wave/s; non-Mated: 0.015 ± 0.008 leg wave/s; test-statistic = 4.238, $df = 12.40168$, $p = 0.001^{**}$; Figure 4A). We found the same result in Experiment 2 (Mated: 0.025 ± 0.01 leg wave/s; non-Mated: 0.012 ± 0.009 leg wave/s; test-statistic = 3.399, $df = 31.177$, $p < 0.001^{***}$; Figure 4B).

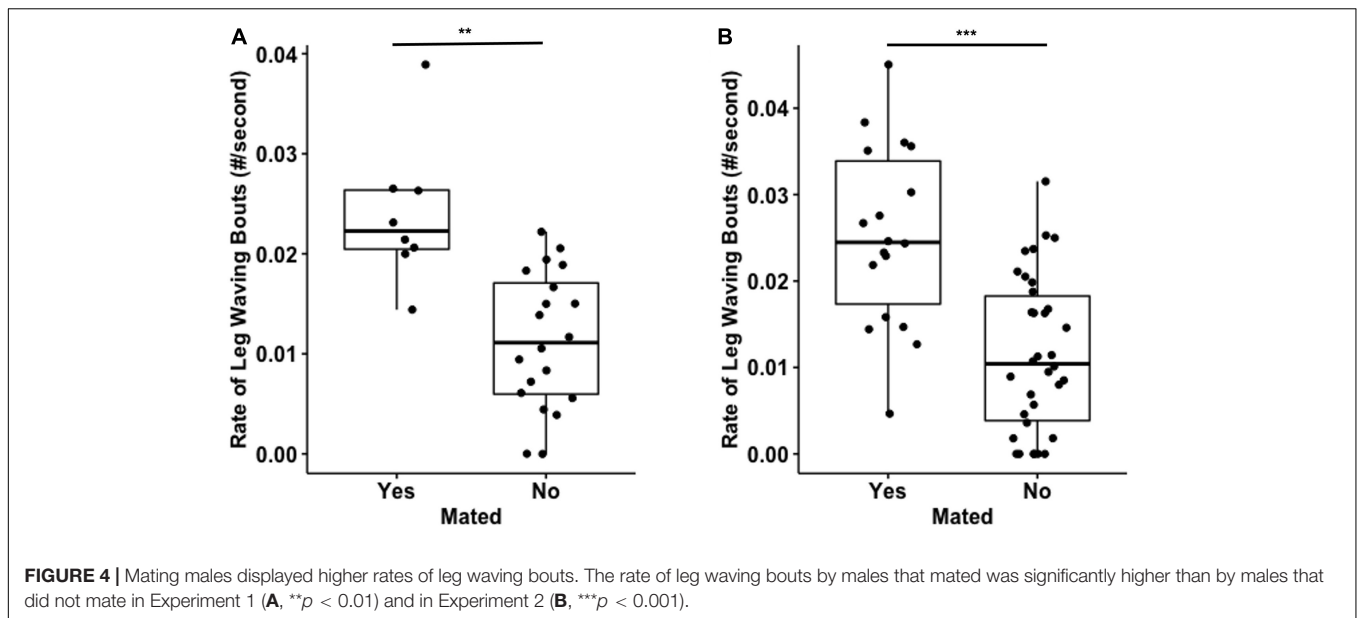
Foraging Trials (Exp 2)

In the No Noise signaling environment, 14/26 females successfully captured prey (54%) while 13/26 females (50%) did so in the Noise environment. For males, 11/26 successfully captured prey (42%) in the No Noise environment while 9/26 males (35%) did so in the Noise environment. Our model exploring the influence of sex and environment on the likelihood to forage was not significant (Overall Model: Wald $\chi^2 = 2.3$, $df = 3$, $p = 0.52$), indicating that there was no influence of the signaling environment, nor was there an interaction between signaling environment and sex, on the likelihood of successfully catching a cricket.

DISCUSSION

Our results demonstrate that the addition of air particle movement into the environment disrupts the mating success of *S. retrorsa* and alters male courtship behavior but does not impact foraging success. These results confirm that *S. retrorsa* can detect air particle movement and suggest that this previously under-explored sensory modality is critical in their courtship communication. The dynamic motion display of *S. retrorsa* leg waving, formerly presumed to be important in visual signal production/detection, had been proposed to (i) generate stimuli detectable by the thin filiform sensory hairs (trichobothria) located on *S. retrorsa* walking legs and (ii) be important in female mating decisions (Rundus et al., 2010). Our results support these hypotheses. Across two similar yet independent experiments, we observed higher mating success in environments without (No Noise) compared to with (Noise) artificially induced air particle movement, or “noise.” Mating also happened faster in the No Noise as compared to the Noise signaling environments. Notably, in addition to influencing mating success, our manipulated signaling environments also affected male behavior, with overall rates of leg waving bouts, individual leg waves and push-ups being higher in the No Noise compared to Noise environments. Regardless of this plasticity in male courtship effort, however, females appeared to use leg waving rate as a means of assessing males independent of the signaling environment. Across all treatments in both experiments, male leg waving rate was a good predictor of mating success, with no observed interaction with the signaling environment. Given that all mating trials were run in environments that presumably prevented the female’s detection of visual and vibratory signals/cues, we propose that leg waving rate was detected with the female’s trichobothria, which are sensitive to air particle movement. Although previous research alluded to a role of air particle movement in the courtship display of *Schizocosa retrorsa* (Rundus et al., 2010; Choi et al., 2019), this study provides more direct support for its importance.

Mating success was higher and the latency to mate was shorter in the No Noise than the Noise signaling environments in both Experiment 1 and 2. Presumably, this is because females are more easily able to assess male leg waving in the absence of artificially induced air particle movement and are thus able to make mate choice decisions based on leg waving rate more quickly. The



quality of decision making across animals is proposed to depend on speed-accuracy tradeoffs (Chittka et al., 2009). In our Noise environment, since the accuracy of the information that males were communicating (i.e., leg waving rate) was disrupted by the addition of air particle movement, or at least the signal-to-noise ratio was reduced, assessment challenges were likely imposed on females. The outcome was that fewer females accepted males, and those that did accept males took longer to make that decision. Speed-accuracy tradeoffs with respect to mating decisions have been observed in other taxa as well. Fiddler crabs (*Uca annulipes*) must accurately time their larval release to coincide with the next nocturnal spring tide. At the beginning of sampling period, the female crabs are choosy and sample the bigger males of the population. However, toward end of the sampling period, females are less selective due to the time constraints (Backwell and Passmore, 1996). When female sand gobies (*Pomatoschistus minutus*) were exposed to a high female to male ratio, the mate choice decisions were sped up and these females end up choosing males with low fecundity. However, in the opposite situation where female to male ratio was lower, female sand gobies took longer to make spawning decisions and chose males with high fecundity and good parenting skills (Diaz Pauli and Lindström, 2021).

An alternative explanation to air particle noise disrupting a female's ability to assess male courtship is that it disrupted the behavior of females and/or males, leading to lower mating rates. To attempt to address this concern, as part of Experiment 2 we conducted foraging trials under both signaling environments (No Noise/Noise) and found no impact of the signaling environment on prey capture. A lack of difference in foraging success across our treatments suggests that overall behavior of females and males (e.g., movement rate, motivation to forage, and/or prey detection) were likely not impacted by our environmental manipulations. These foraging trials were also run in the dark and on granite, presumably removing visual and vibratory cues

for prey detection and thus leaving air particle movement, chemical, and tactile (e.g., running into the prey) cues as means of detecting prey. The lack of a treatment effect on foraging success suggests the spiders in our experiment did not use air particle movement to detect prey, leaving open the possibility of chemical and/or tactile prey detection. Although it remains possible that spiders might also be good at filtering out air particle noise when detecting environmental stimuli. Regardless, our foraging trials provide no evidence of general behavioral impacts of our experimental treatments on *S. retrorsa* females or males.

In contrast to the results of our foraging trials, we found that our environmental treatments in the mating trials did influence male courtship effort. Male leg waving rates and push-up displays were significantly higher in the No Noise than in the Noise conditions across both experiments. These results suggest that the detection of artificial air particle movement by males influenced their courtship behavior specifically (i.e., not foraging behavior), causing them to court less intensely or less vigorously. Previous studies have similarly shown *S. retrorsa* male courtship behavior to be dependent upon environmental conditions. In a study that examined the influence of age on courtship, younger *S. retrorsa* engaged in more courtship toward virgin females (and associated chemical signals) while older males courted virgin and mated females indiscriminately (Rundus et al., 2015). More recently, it was shown that vibratory cues associated with male density can influence a *S. retrorsa* male's courtship effort (Choi and Hebets, 2021). Our findings of behavioral plasticity in courtship corroborate these earlier findings and highlight the importance of the signaling environment on male signaling in *S. retrorsa*.

The continually observed relationship between courtship rate (i.e., leg waving rate) and mating success in *S. retrorsa* (Rundus et al., 2010; present study) suggests that females choose males based on motor performance, or vigor (see Byers et al., 2010). If such behavior is energetically costly, and if males perceive that the signaling environment may not be conducive to signal

transmission (for example, due to noise in the environment), they may reduce their effort, resulting in a lower leg waving rate. This is but one potential explanation for our observed reduction in courtship rate in the presence of noise. A few other possibilities are that males are simply distracted by the addition of noise, or that there are sensory constraints on processing, for example. To explore the possibility that our noise treatment distracted males or led to a decrease in overall movement of males, including courtship behavior, we used data from Experiment 2 to examine the relationship between the number of female-male contacts (a potential proxy of “activity” or “movement”) and male leg waving rate. We did not find a significant relationship between rate of contacts and rate of leg waving bouts ($R = 0.037$, $p = 0.8$) or between rate of contacts and rate of individual leg waves ($R = -0.033$, $p = 0.82$). While certainly not definitive, these results indicate that our mating differences are more likely driven by female detection of male-generated air particle movement than by overall male behavior itself.

Environmental noise is known to have broad-ranging effects on wildlife (reviewed in Shannon et al., 2016) and the more we look, the more examples we find of animals that adjust their signaling to overcome environmental noise. The alteration or adjustment of signaling in response to environmental noise has been documented in numerous diverse taxa. For example, common cuttlefish (*Sepia officinalis*) change their color (visual display) more frequently in presence of anthropogenic noise, even though these fish do not rely on acoustic signaling (Kunc et al., 2014), and Bornean rock frogs (*Staurois parvus*) use multiple visual signals and modified air-borne acoustic signals to communicate with conspecifics when presented with a noisy environment (Grafe et al., 2012). Similarly, in response to environmental noise, tokay geckos (*Gekko gecko*) lengthen certain high amplitude call syllables (Brumm and Zollinger, 2017); male great tits (*Parus major*) sing at a higher average frequency (Slabbekoorn and Peet, 2003); budgerigars (*Melopsittacus undulatus*) and cotton top tamarins (*Saguinus oedipus*) increase the amplitude of their signal in the presence of background noise (Manabe et al., 1998; Roian Egnor and Hauser, 2006); and greater mouse-eared bat (*Myotis myotis*) actively avoid areas with noise while foraging (Schaub et al., 2008), to name a few. Thus, while it is not particularly surprising that male *S. retrorsa* alter their signaling rate in the presence of air particle noise, it does highlight that behavioral plasticity and responses to the environment are common across all taxonomic groups.

Noise or disturbance in the signaling environment can also alter the receiver's behavior. In Painted Goby (*Pomatoschistus pictus*), females depended more on visual signals as opposed to acoustic signals from the male for mate choice decisions when additional noise was introduced in the system (de Jong et al., 2018). Female three-spined stickleback (*Gasterosteus aculeatus*) paid more attention to visual cues than olfactory cues in clear water but in turbid water, olfactory cues were more important (Heuschele et al., 2009). Recent work on female tungara frog, *Physalaemus pustulosus*, demonstrated that air-borne noise influences the expression of female mating preferences (Taylor et al., 2021). In our study, noise impacted signaler behavior

but its effect on mate choice of the receivers still needs to be investigated further.

In Experiment 1, our higher mating success in the No Noise signaling environment appears to be driven by male behavior. Males courted less vigorously in the No Noise treatment, and since courtship rate predicts mating success, our results could be explained solely by changes in male behavior across the environments. Because our sample size in Experiment 1 was low, and the influence of male courtship rate on mating success was so high, we were unable to detect or disentangle an influence of the signaling environment itself on mate choice. Thus, we repeated the experiment. In Experiment 2, with a larger sample size, we were able to detect the influence of both male behavior (i.e., rate of leg waving bouts as well as individual leg waves) and the overall signaling environment on mating success. Results of Experiment 2 suggest that lower mating success in the Noise condition was driven by both (a) changes in male behavior and (b) an overall effect of the signaling environment on female mate choice. Indeed, when we use individual leg waves in our model for Experiment 2, we find an effect of both rate of individual leg waves and signaling environment on mating success.

Overall, our results support the possibility that female *S. retrorsa* use detected air particle movement from male leg waving displays to make mate choice decisions. Regardless of whether noise was absent or present, females mated more frequently with males that displayed higher rates of leg waving across both experiments. If our artificially induced air particle movement completely disrupted a female's ability to detect the air particle movement generated by male leg waving displays, we would have expected to find a significant interaction between leg waving rate and signaling environment on mating success. In particular, we would have expected leg waving rate to predict mating success in the No Noise, but not the Noise environments. The absence of this result suggests that the female's ability to assess the “rate” of male leg waving, presumably by the detection of air particle movement, was not impacted by our noise treatment; though overall detection and speed of detection was likely compromised (see previous discussion). We note, however, that even in the case of a significant interaction, the signal might still work, just less effectively.

An alternative explanation to female's detecting air particle movement is that leg waving rate is correlated with a signal in another modality, such as chemical signaling, that females are still able to detect. If, for example, males release a pheromone and use leg waving as a means of dispersing it, then we might expect the same results as those observed across our experiments. This possibility remains to be tested. There are currently no known airborne chemical signals in *Schizocosa* communication, but there are many examples of silk-borne cues/signals (Roberts and Uetz, 2005; Baruffaldi and Costa, 2010; Vaccaro et al., 2010). Confirmation of the importance of air particle detection per se will require some combination of trichobothria removal experiments and electrophysiology.

The absence of an interaction between signaling environment and leg waving rate in either experiment may be due, in part, to our choice of “noise” stimuli. In Experiment 1, our artificial stimulus was a white noise band with frequencies of

22–250 Hz while in Experiment 2, it was a 100 Hz. Previous calculations of *S. retrorsa* leg waving rate were 13.55 Hz, which is lower than either of our artificial stimuli. This non-overlap in frequency range between our introduced noise and male leg waving rate is the simplest explanation for why female mate choice did not appear disrupted by air particle “noise.” We would expect that if a noise stimulus that directly overlaps with male signaling rates were introduced, female mate assessment would be compromised. Future studies could test this prediction.

We are confident that our artificial air particle movement stimuli were sufficient to elicit responses from *S. retrorsa* trichobothria. First, air particle movement receptors are incredibly sensitive (Shimozawa and Kanou, 1984; Humphrey and Barth, 2007) and are often tuned to low frequencies (<500 Hz) (Rinberg and Davidowitz, 2000; Shamble et al., 2016; Raboin and Elias, 2019). Second, we confirmed the deflection of trichobothria from our stimuli by viewing their movement under a dissecting scope prior to the start of our trials. Third, we observed a change in male behavior in the presence of introduced air particle movement, i.e., reduced leg waving and push-up rate. Our choice of stimuli for introducing air particle movement was based upon working knowledge of general sensitivities of trichobothria (Barth, 2002). This working knowledge all comes from one model spider system, *Cupiennius salei*, but it is assumed to be generalizable across spiders.

Previous dogma has understood that the reception, and thus importance, of air particle movement in communication would be limited because it only occurs at short distances from the source—approximately 0.5–1 wavelength (Kinsler, 1999; Jacobsen, 2007; Raboin and Elias, 2019). Recent studies, however (e.g., Shamble et al., 2016; Menda et al., 2019; Stafstrom et al., 2020) suggest that the detection of air particle movement may take place at much longer distances than previously thought (reviewed in Raboin and Elias, 2019), making it a viable mode of communication. Nonetheless, air particle movement (also referred to as near-field sound) has been overlooked and underappreciated as a signaling modality, and the impact of noise on this understudied signaling modality is even more unknown (Raboin and Elias, 2019).

Air particle movement in the natural environment is produced by numerous sources including abiotic (e.g., wind) as well as biotic (e.g., anthropogenic, animal movements) sources. Many sources of anthropogenic noise, for example, occur in the same low frequencies often associated with air particle movement, e.g., noise from roads (Hayek, 1990) and railways (Talotte et al., 2003), among others (reviewed in Raboin and Elias, 2019). In terms of biological sources, bees, flies, and related insects have wing beat frequencies ranging from 48 to 250 Hz (Corben, 1983). Thus, it seems likely that spiders, and other arthropods, are exposed to air particle noise. The extent to which this disrupts communication in nature requires additional exploration (Raboin and Elias, 2019).

In our study, results suggest that *S. retrorsa* males produce air particle movement using dynamic leg waving displays during courtship and that this movement is likely detected and assessed by females. The detection of such air particle

movement is likely coincident with the detection of visual movement and vibratory courtship songs (Hebets et al., 1996). If and how females integrate these components, received by different sensory organs (vision—eyes; vibration—slit sensilla; air particle movement—trichobothria), during their assessment of male courtship remains an open question. Multimodal integration, or the combining of information received from multiple sensory modalities to influence decision-making (see Munoz and Blumstein, 2012) is not well understood in most animal systems. Within arthropods, the best studied systems include insects such as female mosquitos, *Aedes aegypti*, that integrate carbon dioxide, visual, and thermal cues (McMeniman et al., 2014); female bush crickets, *Requena verticalis*, that integrate visual and acoustic cues (Bailey et al., 2003); and the fly model *Drosophila melanogaster* that integrates visual, auditory, chemosensory, and mechanosensory signals during courtship (Spieth, 1974; Hall, 1994; Lasbleiz et al., 2006); among others (reviewed in Thiagarajan and Sachse, 2022). Within arachnids, recent evidence suggests that the amblypygid *Phrynos marginemaculatus* integrates visual and tactile cues during navigation (Flanigan et al., 2021). In wolf spider genus *Schizocosa*, numerous studies have demonstrated an interactive effect of multimodal signals on receiver behavior (Hebets, 2011; Higham and Hebets, 2013; Halfwerk et al., 2019). In our experimental design, we prevented the integration of modalities, as we purposefully created environments where females could not detect visual or vibratory stimuli. It will be worthwhile to explore these possibilities in *S. retrorsa* with respect to the female's perception and potential integration of multisensory signal components.

CONCLUSION

In summary, our mating trials were run in environments where females were unable to detect visual and substrate-borne vibratory signals, and we found that (i) the presence of air particle noise reduced mating frequency and (ii) increased the latency to mating. Additionally, across all signaling environments (iii) mating was predicted by leg waving rate, despite (iv) leg waving rate being influenced by the signaling environment. These results suggest that male courtship is plastic and results are consistent with the hypothesis that the dynamic motion of leg waving generates air particle movement that is detected and assessed by females during mate choice.

The understanding of multimodal communication in organisms that are more distantly related to humans, like arachnids, is often limited because of our own sensory biases and experimental constraints. It is also often challenging to determine which sensory systems receivers rely upon while assessing complex communication displays. Finally, the potential integration of sensory stimuli and how that influences decision making is still not understood in most animal signaling systems. Our study demonstrates the potential importance of a previously underappreciated signaling modality and we suspect that many similar instances exist across disparate animal groups.

DATA AVAILABILITY STATEMENT

The raw data supporting the conclusions of this article will be made available by the authors, without undue reservation.

AUTHOR CONTRIBUTIONS

AR, RS, and EH conceptualized and designed the experiment. AR conducted experiment 1. PK conducted experiment 2. NC helped with experiment 2 set-up. All authors contributed to data analysis, interpretation, writing and editing.

ACKNOWLEDGMENTS

We acknowledge Madison Hays, Drs. Rowan McGinley, Guilherme Oyarzabal da Silva, Gail Stratton, and Pat Miller for their help with collecting the spiders. We thank Dr. Gail Stratton and Pat Miller for food and lodging during collecting trips. We thank members of the Hebets, Basolo, Wagner, and Shizuka laboratories for their feedback on the experiments. We thank Dr. Rowan McGinley for **Supplementary Video 1**. We thank our funding sources NSF (IOS—1556153, IOS—1037901, IOS—1456817), the Searle Scholars Program and UNL QLSI Summer Graduate Student Fund. We thank Cedar Point Biological Station for food, lodging and a place to run Experiment 2. Finally, we also thank the editors of this special issue for the invitation to contribute and we are especially grateful to two reviewers that provided incredibly thoughtful and helpful comments that strengthened this manuscript greatly.

REFERENCES

- Backwell, P. R. Y., and Passmore, N. I. (1996). Time constraints and multiple choice criteria in the sampling behaviour and mate choice of the fiddler crab, *Uca annulipes*. *Behav. Ecol. Sociobiol.* 38, 407–416. doi: 10.1007/s002650050258
- Bailey, W. J., Ager, E. I., O'Brien, E. K., and Watson, D. L. (2003). Searching by visual and acoustic cues among bushcrickets (Orthoptera: Tettigoniidae): will females remain faithful to a male who stops calling? *Physiol. Entomol.* 28, 209–214. doi: 10.1046/j.1365-3032.2003.00334.x
- Banks, N. (1911). Some Arachnida from North Carolina. *Proc. Acad. Nat. Sci. Phila.* 63, 440–456.
- Barth, F. G. (2000). How to catch the wind: spider hairs specialized for sensing the movement of air. *Naturwissenschaften* 87, 51–58. doi: 10.1007/s001140050010
- Barth, F. G. (2002). *A Spider's World: Senses and Behavior*. Berlin: Springer.
- Barth, F. G., and Bohnenberger, J. (1978). Lyriform slit sense organ: thresholds and stimulus amplitude ranges in a multi-unit mechanoreceptor. *J. Comp. Physiol.* 125, 37–43. doi: 10.1007/BF00656829
- Barth, F. G., and Holler, A. (1999). Dynamics of arthropod filiform hairs. V. The response of spider trichobothria to natural stimuli. *Philos. Trans. Biol. Sci.* 354, 183–192.
- Barth, F. G., Humphrey, J. A. C., Wastl, U., Halbritter, J., and Brittinger, W. (1995). Dynamics of arthropod filiform hairs. III. Flow patterns related to air movement detection in a spider (*Cupiennius salei* KEYS.). *Philos. Trans. R. Soc. Lond. B Biol. Sci.* 347, 397–412. doi: 10.1098/rstb.1995.0032
- Barth, F. G., Wastl, U., Humphrey, J. A. C., and Devarakonda, R. (1993). Dynamics of arthropod filiform hairs. II. Mechanical properties of spider trichobothria (*Cupiennius salei* Keys.). *Philos. Trans. R. Soc. Lond. B Biol. Sci.* 340, 445–461. doi: 10.1098/rstb.1993.0084
- Baruffaldi, L., and Costa, F. G. (2010). Changes in male sexual responses from silk cues of females at different reproductive states in the wolf spider *Schizocosa malitiosa*. *J. Ethol.* 28, 75–85. doi: 10.1007/s10164-009-0158-8
- Boekhoff-Falk, G. (2005). Hearing in *Drosophila*: development of Johnston's organ and emerging parallels to vertebrate ear development. *Dev. Dyn.* 232, 550–558. doi: 10.1002/dvdy.20207
- Breithaupt, T. (2002). "Sound perception in aquatic crustaceans," in *The Crustacean Nervous System*, ed. K. Wiese (Berlin: Springer), 548–558. doi: 10.1007/978-3-662-04843-6_41
- Brownell, P. H. (1988). Properties and functions of the pectin chemosensory system of scorpions. *Chem. Senses* 13:677.
- Brownell, P. H., and Farley, R. D. (1974). The organization of the malleolar sensory system in the solpugid, *Chanbria* sp. *Tissue Cell* 6, 471–485.
- Brumm, H., and Zollinger, S. A. (2017). Vocal plasticity in a reptile. *Proc. R. Soc. B Biol. Sci.* 284:20170451. doi: 10.1098/rspb.2017.0451
- Budelmann, B. U. (1992). "Hearing in nonarthropod invertebrates," in *The Evolutionary Biology of Hearing*, eds D. B. Webster, A. N. Popper, and R. R. Fay (New York, NY: Springer), 141–155. doi: 10.1007/978-1-4612-2784-7_10
- Byers, J., Hebets, E., and Podos, J. (2010). Female mate choice based upon male motor performance. *Anim. Behav.* 79, 771–778. doi: 10.1016/j.anbehav.2010.01.009
- Caldwell, M. S., Johnston, G. R., McDaniel, J. G., and Warkentin, K. M. (2010). Vibrational signaling in the agonistic interactions of red-eyed treefrogs. *Curr. Biol.* 20, 1012–1017. doi: 10.1016/j.cub.2010.03.069

SUPPLEMENTARY MATERIAL

The Supplementary Material for this article can be found online at: <https://www.frontiersin.org/articles/10.3389/fevo.2022.939133/full#supplementary-material>

Supplementary Figure 1 | Rate of leg waving bouts and rate of individual leg waves are correlated. There is a strong correlation between the rate of leg waving bouts and rate of individual leg waves ($R = 0.9$, $p < 2.2e-16$).

Supplementary Figure 2 | Rate of leg waving bouts and rate of push-ups are correlated. There is a strong relationship between the rate of leg waving bouts and the rate of push-ups ($R = 0.74$, $p = 5.2e-10$).

Supplementary Table 1 | Comparison of age and weight of the spiders based on sex and signaling environments for Experiment 1. When the age and weight of females and males were compared for the two signaling environments, there was no significant difference between the groups (weights of two females from each No Noise and Noise groups were missing). There was no significant difference between the age difference and weight difference of the females and males in each of the groups either.

Supplementary Table 2 | Comparison of age and weight of the spiders based on sex and signaling environments for Experiment 2. When the age and weight of females and males were compared for the two signaling environments, there was no significant difference between the groups. There was no significant difference between the age difference and weight difference of the females and males in each of the groups either.

Supplementary Video 1 | Male *Schizocosa retrorsa* courtship behavior. Male *Schizocosa retrorsa* displaying courtship behavior including push-up and leg waves.

Supplementary Video 2 | Observed movement of the trichobothria on female *Schizocosa retrorsa*. To provide a more focused noise stimulus in Experiment 2 while still ensuring that the spiders could detect the air particle movement, we examined the movement of foreleg trichobothria under a dissecting scope at sound frequencies of 0–150 Hz using the speaker with speaker cone intact (**Figure 1C**, right). The trichobothria were observed to be moving between 70 and 130 Hz. This video shows the clear movement of trichobothria at 100 Hz in the Noise signaling environment.

- Chittka, L., Skorupski, P., and Raine, N. E. (2009). Speed–accuracy tradeoffs in animal decision making. *Trends Ecol. Evol.* 24, 400–407. doi: 10.1016/j.tree.2009.02.010
- Choi, N., Bern, M., Elias, D. O., McGinley, R. H., Rosenthal, M. F., and Hebets, E. A. (2019). A mismatch between signal transmission efficacy and mating success calls into question the function of complex signals. *Anim. Behav.* 158, 77–88. doi: 10.1016/j.anbehav.2019.09.017
- Choi, N., and Hebets, E. A. (2021). The effects of conspecific male density on the reproductive behavior of male *Schizocosa retrorsa* (Banks, 1911) wolf spiders (Araneae: Lycosidae). *J. Arachnol.* 49, 347–357. doi: 10.1636/joA-S-20-079
- Corben, H. C. (1983). Wing-beat frequencies, wing-areas and masses of flying insects and hummingbirds. *J. Theor. Biol.* 102, 611–623. doi: 10.1016/0022-5193(83)90394-6
- de Jong, K., Amorim, M. C. P., Fonseca, P. J., and Heubel, K. U. (2018). Noise affects multimodal communication during courtship in a marine fish. *Front. Ecol. Evol.* 6:113. doi: 10.3389/fevo.2018.00113
- DeVoe, R. D. (1972). Dual sensitivities of cells in wolf spider eyes at ultraviolet and visible wavelengths of light. *J. Gen. Physiol.* 59, 247–269. doi: 10.1085/jgp.59.3.247
- DeVoe, R. D., Small, R. J. W., and Zvargulis, J. E. (1969). Spectral sensitivities of wolf spider eyes. *J. Gen. Physiol.* 54, 1–32. doi: 10.1085/jgp.54.1.1
- Diaz Pauli, B., and Lindström, K. (2021). Trade-off between mate choice speed and decision accuracy under mating competition in female sand gobies. *J. Ethol.* 39, 55–64. doi: 10.1007/s10164-020-00673-z
- Eakin, R. M. (1972). “Structure of invertebrate photoreceptors,” in *Photochemistry of Vision*, Vol. 7, ed. H. J. A. Dartnall (Berlin: Springer), 625–684. doi: 10.1007/978-3-642-65066-6_16
- Elias, D. O., Maddison, W. P., Peckmezian, C., Girard, M. B., and Mason, A. C. (2012). Orchestrating the score: complex multimodal courtship in the *Habronattus coecatus* group of *Habronattus jumping* spiders (Araneae: Salticidae): MULTIMODAL COURTSHIP IN HABRONATTUS. *Biol. J. Linn. Soc.* 105, 522–547. doi: 10.1111/j.1095-8312.2011.01817.x
- Elias, D. O., Mason, A. C., and Hoy, R. R. (2004). The effect of substrate on the efficacy of seismic courtship signal transmission in the jumping spider *Habronattus dosseus* (Araneae: Salticidae). *J. Exp. Biol.* 207, 4105–4110. doi: 10.1242/jeb.01261
- Elias, D. O., Mason, A. C., Maddison, W. P., and Hoy, R. R. (2003). Seismic signals in a courting male jumping spider (Araneae: Salticidae). *J. Exp. Biol.* 206, 4029–4039. doi: 10.1242/jeb.00634
- Flanigan, K. A. S., Wiegmann, D. D., Hebets, E. A., and Bingman, V. P. (2021). Multisensory integration supports configural learning of a home refuge in the whip spider *Phrynos marginemaculatus*. *J. Exp. Biol.* 224:jeb238444. doi: 10.1242/jeb.238444
- Foelix, R. F. (1996). *Biology of Spiders*. Oxford: Oxford University Press.
- Fowler-Finn, K. D., and Hebets, E. A. (2006). An examination of agonistic interactions in the whip spider *Phrynos marginemaculatus* (Arachnida, Amblypygi). *J. Arachnol.* 34, 62–76. doi: 10.1636/S04-104.1
- Friedel, T., and Barth, F. G. (1997). Wind-sensitive interneurons in the spider CNS (*Cupiennius salei*): directional information processing of sensory inputs from trichobothria on the walking legs. *J. Comp. Physiol. A* 180, 223–233. doi: 10.1007/s003590050043
- Gibson, G., and Russell, I. (2006). Flying in tune: sexual recognition in mosquitoes. *Curr. Biol.* 16, 1311–1316. doi: 10.1016/j.cub.2006.05.053
- Gomes, A. C. R., Funghi, C., Soma, M., Sorenson, M. D., and Cardoso, G. C. (2017). Multimodal signalling in estrildid finches: song, dance and colour are associated with different ecological and life-history traits. *J. Evol. Biol.* 30, 1336–1346. doi: 10.1111/jeb.13102
- Görner, P., and Andrews, P. (1969). Trichobothrien, ein Ferntastsinnesorgan bei Webespinnen (Araneen). *Z. Vgl. Physiol.* 64, 301–317. doi: 10.1007/BF00340548
- Grafe, T. U., Preininger, D., Sztatecsny, M., Kasah, R., Dehling, J. M., Proksch, S., et al. (2012). Multimodal communication in a noisy environment: a case study of the Bornean rock frog *Staurois parvus*. *PLoS One* 7:e37965. doi: 10.1371/journal.pone.0037965
- Halfwerk, W., Varkevisser, J., Simon, R., Mendoza, E., Scharff, C., and Riebel, K. (2019). Toward testing for multimodal perception of mating signals. *Front. Ecol. Evol.* 7:124. doi: 10.3389/fevo.2019.00124
- Hall, J. C. (1994). The mating of a fly. *Science* 264, 1702–1714. doi: 10.1126/science.8209251
- Harland, D. P., and Jackson, R. R. (2002). Influence of cues from the anterior medial eyes of virtual prey on *Portia fimbriata*, an araneophagic jumping spider. *J. Exp. Biol.* 205, 1861–1868. doi: 10.1242/jeb.205.13.1861
- Hayek, S. I. (1990). Mathematical modeling of absorbent highway noise barriers. *Appl. Acoust.* 31, 77–100. doi: 10.1016/0003-682X(90)90054-X
- Hebets, E. A. (2005). Attention-altering signal interactions in the multimodal courtship display of the wolf spider *Schizocosa uetzi*. *Behav. Ecol.* 16, 75–82. doi: 10.1093/beheco/arh133
- Hebets, E. A. (2011). Current status and future directions of research in complex signaling. *Curr. Zool.* 57, i–v. doi: 10.1093/czoolo/57.2.i
- Hebets, E. A., Bern, M., McGinley, R. H., Roberts, A., Kershenbaum, A., Starrett, J., et al. (2021). Sister species diverge in modality-specific courtship signal form and function. *Ecol. Evol.* 11, 852–871. doi: 10.1002/ece3.7089
- Hebets, E. A., Elias, D. O., Mason, A. C., Miller, G. L., and Stratton, G. E. (2008). Substrate-dependent signalling success in the wolf spider, *Schizocosa retrorsa*. *Anim. Behav.* 75, 605–615. doi: 10.1016/j.anbehav.2007.06.021
- Hebets, E. A., and McGinley, R. H. (2019). “Multimodal signaling,” in *Encyclopedia of Animal Behavior*, eds J. Moore and M. Breed (Amsterdam: Elsevier), 487–499. doi: 10.1016/B978-0-12-809633-8.90730-1
- Hebets, E. A., and Papaj, D. R. (2005). Complex signal function: developing a framework of testable hypotheses. *Behav. Ecol. Sociobiol.* 57, 197–214. doi: 10.1007/s00265-004-0865-7
- Hebets, E. A., Stafstrom, J. A., Rodriguez, R. L., and Wilgers, D. J. (2011). Enigmatic ornamentation eases male reliance on courtship performance for mating success. *Anim. Behav.* 81, 963–972. doi: 10.1016/j.anbehav.2011.01.023
- Hebets, E. A., Stratton, G. E., and Miller, G. L. (1996). Habitat and courtship behavior of the wolf spider *Schizocosa retrorsa* (Banks) (Araneae, Lycosidae). *J. Arachnol.* 24, 141–147.
- Hebets, E. A., Vink, C. J., Sullivan-Beckers, L., and Rosenthal, M. F. (2013). The dominance of seismic signaling and selection for signal complexity in *Schizocosa* multimodal courtship displays. *Behav. Ecol. Sociobiol.* 67, 1483–1498. doi: 10.1007/s00265-013-1519-4
- Heidelbach, J., and Dambach, M. (1997). Wing-flick signals in the courtship of the African cave cricket, *Phaeophilacris spectrum*. *Ethology* 103, 827–843. doi: 10.1111/j.1439-0310.1997.tb00124.x
- Heidelbach, J., Dambach, M., and Bohm, H. (1991). Processing wing flick-generated air-vortex signals in the African cave cricket *Phaeophilacris spectrum*. *Naturwissenschaften* 786, 277–278.
- Heuschele, J., Mannerla, M., Gienapp, P., and Candolin, U. (2009). Environment-dependent use of mate choice cues in sticklebacks. *Behav. Ecol.* 20, 1223–1227. doi: 10.1093/beheco/arp123
- Higham, J. P., and Hebets, E. A. (2013). An introduction to multimodal communication. *Behav. Ecol. Sociobiol.* 67, 1381–1388. doi: 10.1007/s00265-013-1590-x
- Humphrey, J. A. C., and Barth, F. G. (2007). Medium flow-sensing hairs: biomechanics and models. *Adv. Insect Physiol.* 34, 1–80. doi: 10.1016/S0065-2806(07)34001-0
- Hüttner, T., Fersen, L., Miersch, L., Czech, N. U., and Dehnhardt, G. (2022). Behavioral and anatomical evidence for electroreception in the bottlenose dolphin (*Tursiops truncatus*). *Anat. Rec.* 305, 592–608. doi: 10.1002/ar.24773
- Igelmund, P. (1987). Morphology, sense organs, and regeneration of the forelegs (whips) of the whip spider *Heterophrynos elaphus* (Arachnida, Amblypygi). *J. Morphol.* 193, 75–89. doi: 10.1002/jmor.1051930108
- Jacobsen, F. (2007). “Sound intensity,” in *Springer Handbook of Acoustics*, ed. T. D. Rossing (New York, NY: Springer), 1093–1114. doi: 10.1007/978-1-4939-0755-7_25
- Johnston, C. (1855). Original communications: auditory apparatus of the *Culex* mosquito. *J. Cell Sci.* s1-s3, 97–102. doi: 10.1242/jcs.s1-3.10.97
- Kinsler, L. E. (ed.). (1999). *Fundamentals of Acoustics*, 4th Edn. Hoboken: Wiley.
- Knowlton, E. D., and Gaffin, D. D. (2019). Female wolf spider, *Schizocosa avida*, vibration receptor responses to male courtship. *Southwest. Entomol.* 44, 213–228. doi: 10.3958/059.044.0124
- Kunc, H. P., Lyons, G. N., Sigwart, J. D., McLaughlin, K. E., and Houghton, J. D. R. (2014). *Anthropogenic Noise Affects Behavior Across Sensory Modalities (Version 1, p. 45568 bytes) [Data set]*. Dryad. Available online at: <https://www.journals.uchicago.edu/doi/10.1086/677545>

- Land, M. F. (1969). Structure of the retinae of the principal eyes of jumping spiders (Salticidae: Dendryphantinae) in relation to visual optics. *J. Exp. Biol.* 51, 443–470. doi: 10.1242/jeb.51.2.443
- Lasbleiz, C., Ferveur, J.-F., and Everaerts, C. (2006). Courtship behaviour of *Drosophila melanogaster* revisited. *Anim. Behav.* 72, 1001–1012. doi: 10.1016/j.anbehav.2006.01.027
- Manabe, K., Sadr, E. I., and Dooling, R. J. (1998). Control of vocal intensity in budgerigars (*Melopsittacus undulatus*): differential reinforcement of vocal intensity and the Lombard effect. *J. Acoust. Soc. Am.* 103, 1190–1198. doi: 10.1121/1.421227
- Manshor, Z., and Augustine Gawin, D. F. (2020). Call types of the oriental magpie robin (*Copsychus saularis*) in suburban areas in Kota Samarahan, Sarawak. *Borneo J. Resour. Sci. Technol.* 10, 37–44. doi: 10.33736/bjrst.2264.2020
- Markl, H., and Tautz, J. (1975). The sensitivity of hair receptors in caterpillars of *Barathra brassicae* L. (Lepidoptera, Noctuidae) to particle movement in a sound field. *J. Comp. Physiol. A* 99, 79–87. doi: 10.1007/BF01464713
- Marshall, J., Cronin, T. W., and Kleinlogel, S. (2007). Stomatopod eye structure and function: a review. *Arthropod Struct. Dev.* 36, 420–448. doi: 10.1016/j.asd.2007.01.006
- Marshall, N. J. (1988). A unique colour and polarization vision system in mantis shrimps. *Nature* 333, 557–560. doi: 10.1038/333557a0
- Masters, W. M., Raver, K. A. S., and Kazial, K. A. (1995). Sonar signals of big brown bats, *Eptesicus fuscus*, contain information about individual identity, age and family affiliation. *Anim. Behav.* 50, 1243–1260. doi: 10.1016/0003-3472(95)80041-7
- McMeniman, C. J., Corfas, R. A., Matthews, B. J., Ritchie, S. A., and Voshall, L. B. (2014). Multimodal integration of carbon dioxide and other sensory cues drives mosquito attraction to humans. *Cell* 156, 1060–1071. doi: 10.1016/j.cell.2013.12.044
- Menda, G., Nitzany, E. I., Shamble, P. S., Wells, A., Harrington, L. C., Miles, R. N., et al. (2019). The long and short of hearing in the mosquito *Aedes aegypti*. *Curr. Biol.* 29, 709–714.e4. doi: 10.1016/j.cub.2019.01.026
- Munoz, N. E., and Blumstein, D. T. (2012). Multisensory perception in uncertain environments. *Behav. Ecol.* 23, 457–462. doi: 10.1093/beheco/arr220
- Nakano, R., Takanashi, T., Fujii, T., Skals, N., Surlykke, A., and Ishikawa, Y. (2009). Moths are not silent, but whisper ultrasonic courtship songs. *J. Exp. Biol.* 212, 4072–4078. doi: 10.1242/jeb.032466
- Nolfo, A. P., Casetta, G., and Palagi, E. (2021). Visual communication in social play of a hierarchical carnivore species: the case of wild spotted hyenas. *Curr. Zool.* 2021:zoab076. doi: 10.1093/cz/zoab076
- Partan, S., and Marler, P. (1999). Communication goes multimodal. *Science* 283, 1272–1273. doi: 10.1126/science.283.5406.1272
- Raboin, M., and Elias, D. O. (2019). Anthropogenic noise and the bioacoustics of terrestrial invertebrates. *J. Exp. Biol.* 222:jeb178749. doi: 10.1242/jeb.178749
- Rinberg, D., and Davidowitz, H. (2000). Do cockroaches 'know' about fluid dynamics? *Nature* 405, 756–756. doi: 10.1038/35015677
- Roberts, J. A., and Uetz, G. W. (2005). Information content of female chemical signals in the wolf spider, *Schizocosa ocreata*: male discrimination of reproductive state and receptivity. *Anim. Behav.* 70, 217–223. doi: 10.1016/j.anbehav.2004.09.026
- Roian Egnor, S. E., and Hauser, M. D. (2006). Noise-induced vocal modulation in cotton-top tamarins (*Saguinus oedipus*). *Am. J. Primatol.* 68, 1183–1190. doi: 10.1002/ajp.20317
- Rosenthal, M. F., and Hebets, E. A. (2012). Resource heterogeneity interacts with courtship rate to influence mating success in the wolf spider *Schizocosa floridana*. *Anim. Behav.* 84, 1341–1346. doi: 10.1016/j.anbehav.2012.08.028
- Rowe, C., and Guilford, T. (1996). Hidden colour aversions in domestic chicks triggered by pyrazine odours of insect warning displays. *Nature* 383, 520–522. doi: 10.1038/383520a0
- Rundus, A. S., Biemüller, R., DeLong, K., Fitzgerald, T., and Nyandwi, S. (2015). Age-related plasticity in male mate choice decisions by *Schizocosa retrorsa* wolf spiders. *Anim. Behav.* 107, 233–238. doi: 10.1016/j.anbehav.2015.06.020
- Rundus, A. S., Owings, D. H., Joshi, S. S., Chinn, E., and Giannini, N. (2007). Ground squirrels use an infrared signal to deter rattlesnake predation. *Proc. Natl. Acad. Sci. U.S.A.* 104, 14372–14376. doi: 10.1073/pnas.0702599104
- Rundus, A. S., Santer, R. D., and Hebets, E. A. (2010). Multimodal courtship efficacy of *Schizocosa retrorsa* wolf spiders: implications of an additional signal modality. *Behav. Ecol.* 21, 701–707. doi: 10.1093/beheco/arq042
- Santer, R. D., and Hebets, E. A. (2008). Agonistic signals received by an arthropod filiform hair allude to the prevalence of near-field sound communication. *Proc. R. Soc. B Biol. Sci.* 275, 363–368. doi: 10.1098/rspb.2007.1466
- Santer, R. D., and Hebets, E. A. (2011). Evidence for air movement signals in the agonistic behaviour of a nocturnal arachnid (Order Amblypygi). *PLoS One* 6:e22473. doi: 10.1371/journal.pone.0022473
- Schaub, A., Ostwald, J., and Siemers, B. M. (2008). Foraging bats avoid noise. *J. Exp. Biol.* 211, 3174–3180. doi: 10.1242/jeb.022863
- Scheffer, S. J., Uetz, G. W., and Stratton, G. E. (1996). Sexual selection, male morphology, and the efficacy of courtship signalling in two wolf spiders (Araneae: Lycosidae). *Behav. Ecol. Sociobiol.* 38, 17–23. doi: 10.1007/s002650050212
- Shamble, P. S., Menda, G., Golden, J. R., Nitzany, E. I., Walden, K., Beatus, T., et al. (2016). Airborne acoustic perception by a jumping spider. *Curr. Biol.* 26, 2913–2920. doi: 10.1016/j.cub.2016.08.041
- Shannon, G., McKenna, M. F., Angeloni, L. M., Crooks, K. R., Frstrup, K. M., Brown, E., et al. (2016). A synthesis of two decades of research documenting the effects of noise on wildlife: effects of anthropogenic noise on wildlife. *Biol. Rev.* 91, 982–1005. doi: 10.1111/brv.12207
- Shimozawa, T., and Kanou, M. (1984). Varieties of filiform hairs: range fractionation by sensory afferents and cereal interneurons of a cricket. *J. Comp. Physiol. A* 155, 485–493. doi: 10.1007/BF00611913
- Shimozawa, T., Murakami, J., and Kumagai, T. (2003). "Cricket wind receptors: thermal noise for the highest sensitivity known," in *Sensors and Sensing in Biology and Engineering*, eds F. G. Barth, J. A. C. Humphrey, and T. W. Secomb (Vienna: Springer), 145–157. doi: 10.1007/978-3-7091-6025-1_10
- Siefkes, M. J., Winterstein, S. R., and Li, W. (2005). Evidence that 3-keto petromyzonol sulphate specifically attracts ovulating female sea lamprey, *Petromyzon marinus*. *Anim. Behav.* 70, 1037–1045. doi: 10.1016/j.anbehav.2005.01.024
- Slabbekoorn, H., and Peet, M. (2003). Birds sing at a higher pitch in urban noise. *Nature* 424, 267–267. doi: 10.1038/424267a
- Smith, C. L., Taylor, A., and Evans, C. S. (2011). Tactical multimodal signalling in birds: facultative variation in signal modality reveals sensitivity to social costs. *Anim. Behav.* 82, 521–527. doi: 10.1016/j.anbehav.2011.06.002
- Spieth, H. T. (1974). Courtship behavior in *Drosophila*. *Annu. Rev. Entomol.* 19, 385–405. doi: 10.1146/annurev.en.19.010174.002125
- Stafstrom, J. A., Menda, G., Nitzany, E. I., Hebets, E. A., and Hoy, R. R. (2020). Ogre-faced, net-casting spiders use auditory cues to detect airborne prey. *Curr. Biol.* 30, 5033–5039.e3. doi: 10.1016/j.cub.2020.09.048
- Starnberger, I., Preininger, D., and Hödl, W. (2014). From uni- to multimodality: towards an integrative view on anuran communication. *J. Comp. Physiol. A* 200, 777–787. doi: 10.1007/s00359-014-0923-1
- Starrett, J., McGinley, R. H., Hebets, E. A., and Bond, J. E. (2022). Phylogeny and secondary sexual trait evolution in *Schizocosa* wolf spiders (Araneae, Lycosidae) shows evidence for multiple gains and losses of ornamentation and species delimitation uncertainty. *Mol. Phylogenet. Evol.* 169:107397. doi: 10.1016/j.ympev.2022.107397
- Stratton, G. E. (2005). Evolution of ornamentation and courtship behavior in *Schizocosa*: insights from a phylogeny based on morphology (Araneae, Lycosidae). *J. Arachnol.* 33, 347–376.
- Suter, R. B. (2003). Trichobothrial mediation of an aquatic escape response: directional jumps by the fishing spider, *Dolomedes triton*, foil frog attacks. *J. Insect Sci.* 3:19. doi: 10.1673/031.003.1901
- Talotte, C., Gautier, P.-E., Thompson, D. J., and Hanson, C. (2003). Identification, modelling and reduction potential of railway noise sources: a critical survey. *J. Sound Vib.* 267, 447–468. doi: 10.1016/S0022-460X(03)00707-7
- Tauber, E., and Eberl, D. F. (2003). Acoustic communication in *Drosophila*. *Behav. Processes* 64, 197–210. doi: 10.1016/S0376-6357(03)00135-9
- Taylor, R. C., Willite, K. O., Ludovici, R. J., Mitchell, K. M., Halfwerk, W., Page, R. A., et al. (2021). Complex sensory environments alter mate choice outcomes. *J. Exp. Biol.* 224:jeb.233288. doi: 10.1242/jeb.233288
- Teeter, J. (1980). Pheromone communication in sea lampreys (*Petromyzon marinus*): implications for population management. *Can. J. Fish. Aquat. Sci.* 37, 2123–2132. doi: 10.1139/f80-254
- Thiagarajan, D., and Sachse, S. (2022). Multimodal information processing and associative learning in the insect brain. *Insects* 13:332. doi: 10.3390/insects13040332

- Tsujiuchi, S., Sivan-Loukianova, E., Eberl, D. F., Kitagawa, Y., and Kadowaki, T. (2007). Dynamic range compression in the honey bee auditory system toward waggle dance sounds. *PLoS One* 2:e234. doi: 10.1371/journal.pone.0000234
- Uetz, G. W., Clark, D. L., and Roberts, J. A. (2016). Multimodal communication in wolf spiders (Lycosidae)—an emerging model for study. *Adv. Study Behav.* 48, 117–159. doi: 10.1016/bs.asb.2016.03.003
- Uetz, G. W., and Roberts, J. A. (2002). Multisensory cues and multimodal communication in spiders: insights from video/audio playback studies. *Brain Behav. Evol.* 59, 222–230. doi: 10.1159/000064909
- Vaccaro, R., Uetz, G. W., and Roberts, J. A. (2010). Courtship and mating behavior of the wolf spider *Schizocosa bilineata* (Araneae: Lycosidae). *J. Arachnol.* 38, 452–459. doi: 10.1636/H109-115.1
- Walcott, C. (1969). A spider's vibration receptor: its anatomy and physiology. *Am. Zool.* 9, 133–144.
- Wilder, S. M., DeVito, J., Persons, M. H., and Rypstra, A. L. (2005). The effects of moisture and heat on the efficacy of chemical cues used in predator detection by the wolf spider *Pardosa milvina* (Araneae, Lycosidae). *J. Arachnol.* 33, 857–861. doi: 10.1636/S03-64.1
- Wolf, H. (2017). Scorpions pectines – idiosyncratic chemo- and mechanosensory organs. *Arthropod Struct. Dev.* 46, 753–764. doi: 10.1016/j.asd.2017.10.002
- Zhou, J., Lai, J., Menda, G., Stafstrom, J. A., Miles, C. I., Hoy, R. R., et al. (2022). Outsourced hearing in an orb-weaving spider that uses its web as an auditory sensor. *Proc. Natl. Acad. Sci. U.S.A.* 119:e2122789119. doi: 10.1073/pnas.2122789119

Conflict of Interest: The authors declare that the research was conducted in the absence of any commercial or financial relationships that could be construed as a potential conflict of interest.

Publisher's Note: All claims expressed in this article are solely those of the authors and do not necessarily represent those of their affiliated organizations, or those of the publisher, the editors and the reviewers. Any product that may be evaluated in this article, or claim that may be made by its manufacturer, is not guaranteed or endorsed by the publisher.

Copyright © 2022 Kundu, Choi, Rundus, Santer and Hebets. This is an open-access article distributed under the terms of the Creative Commons Attribution License (CC BY). The use, distribution or reproduction in other forums is permitted, provided the original author(s) and the copyright owner(s) are credited and that the original publication in this journal is cited, in accordance with accepted academic practice. No use, distribution or reproduction is permitted which does not comply with these terms.



Shape of Evasive Prey Can Be an Important Cue That Triggers Learning in Avian Predators

Daniel Linke^{1,2*}, Marianne Elias³, Irena Klečková¹, Johanna Mappes⁴ and Pável Matos-Maraví¹

¹ Biology Centre of the Czech Academy of Sciences (CAS), Institute of Entomology, České Budějovice, Czechia,

² Department of Zoology, Faculty of Science, University of South Bohemia, České Budějovice, Czechia, ³ Institut

de Systématique, Evolution, Biodiversité, Muséum National d'Histoire Naturelle, CNRS, Sorbonne Université, EPHE, Université des Antilles, Paris, France, ⁴ Organismal and Evolutionary Biology Research Program, Faculty of Biological and Environmental Sciences, University of Helsinki, Helsinki, Finland

OPEN ACCESS

Edited by:

Eunice Jingmei Tan,
Yale-NUS College, Singapore

Reviewed by:

Brett Michael Seymoure,
Colorado State University,
United States
Carlos Cordero,
National Autonomous University
of Mexico, Mexico

*Correspondence:

Daniel Linke
daniel.linke@entu.cas.cz

Specialty section:

This article was submitted to
Behavioral and Evolutionary Ecology,
a section of the journal
Frontiers in Ecology and Evolution

Received: 01 April 2022

Accepted: 10 June 2022

Published: 12 July 2022

Citation:

Linke D, Elias M, Klečková I,
Mappes J and Matos-Maraví P (2022)
Shape of Evasive Prey Can Be an
Important Cue That Triggers Learning
in Avian Predators.
Front. Ecol. Evol. 10:910695.
doi: 10.3389/fevo.2022.910695

Advertising escape ability could reduce predatory attacks. However, the effectiveness of certain phenotypic cues (e.g., color, shape, and size) in signaling evasiveness is still unknown. Understanding the role of such signals in driving predator learning is important to infer the evolutionary mechanisms leading to convergent evasiveness signals among prey species (i.e., evasive mimicry). We aim to understand the role of the color pattern (white patches on dark background) and morphology (extended butterfly hindwings) in driving learning and avoidance of escaping prey by surrogate avian predators, the European blue tit. These cues are common in butterflies and have been suspected to advertise escape ability in nature. We use dummy butterflies harboring shape and color patterns commonly found in skippers (family Hesperidae). The prey models displayed the studied phenotypical cues (hindwing tails and white bands) in factorial combinations, and we tested whether those cues were learned as evasive signals and were generalised to different phenotypes. Our results suggest that hindwing tails and white bands can be associated with prey evasiveness. In addition, wild blue tits might learn and avoid attacking prey models bearing the studied phenotypic cues. Although blue tits seem to have an initial preference for the phenotype consisting of white patches and hindwing tails, the probability of attacking it was substantially reduced once the cues were associated with escaping ability. This suggests that the same morphological cues might be interchangeable as preference/avoidance signals. Further investigation of the salience of hindwing tails vs. white bands as cues for escaping ability, revealed that predators can associate both color pattern and shape to the difficulty of capture, and possibly generalize their aversion to other prey harboring those cues. More studies with larger sample sizes are needed to confirm this trend. Altogether, our results highlight the hitherto overlooked role of shape (butterfly hindwing tails) for signaling prey unprofitability.

Keywords: aposematism, attack avoidance, convergence, Hesperidae, prey selection, phenotypic cues

INTRODUCTION

Anti-predatory interactions can lead to astonishing phenotypic diversity shaped by selection and adaptation. A classic example of natural selection is aposematism, when predators learn to associate a prey phenotype (e.g., a vivid color pattern) with an unpleasant experience (Poulton, 1890; Cott, 1940). This results in the selection of signals advertising unprofitability, which predators can recognize and generalize to avoid defended prey (Ruxton et al., 2004). Aposematic cues are warning signals that are present in prey species and indicate the existence of defense mechanisms, such as secondary chemical compounds (Pawlik et al., 1988; Santos et al., 2016) or primary defenses, such as warning coloration (Johansen et al., 2011; Pinheiro et al., 2016) or elusiveness (FitzGibbon and Fanshawe, 1988; van Belleghem et al., 2020).

In advertising unprofitability associated with a primary defense, there is still little empirical evidence on how predators learn and respond to different phenotypes, and whether signaling evasiveness is beneficial for both prey and predators in nature (Gibson, 1974, 1980; Hancox and Allen, 1991; Pinheiro and Freitas, 2014; Llaurens et al., 2021; Páez et al., 2021). Warning colorations associated with secondary defense mechanisms have been studied extensively and we have already a good understanding that bright, contrasting colors are easy to learn and memorize by predators (Dell'aglio et al., 2016; Casas-Cardona et al., 2018). However, other phenotypic cues, like body shape or combination of cues (e.g., coloration and shape) have been studied much less (but see Valkonen et al., 2011; McLean and Herberstein, 2021) and have not been associated with advertising evasiveness. While the effect of shape has been tested for secondary defense mechanisms (Valkonen et al., 2011; unpalatability – Hegedus et al., 2019), the salience of shape in advertising prey evasiveness is yet to be tested conclusively.

Cues that advertise difficulty of pursuit have been studied in a few living organisms [e.g., weevils (Guerra, 2019) and butterfly/grasshoppers (Balgooyen, 1997)] and largely lacked an experimental design to test for stimulus salience among prey colors and body shapes (Young, 1971; Srygley, 1994; Pinheiro, 1996; Golding et al., 2005). In palatable butterflies, certain color patterns, such as white bands on forewings, have been associated with advertising escape ability, but such conclusions were based only on observations in the field of tropical insectivorous birds aiming to attack flying butterflies (Pinheiro and Freitas, 2014; Pinheiro and Cintra, 2017). Further, butterfly wing shapes are also strongly correlated with flight speed and maneuverability (Ortega et al., 2017; Le Roy et al., 2019), which might as well advertise escape ability in the form of flight behavior and be under strong selection pressure (Srygley, 1994). The evidence for cues solely advertising difficulty of pursuit is also equivocal as certain wing shapes, such as hindwing tails, and certain color patterns, such as eye spots, have been related to deflecting attacks (Weeks, 1903; Blest, 1957; Lyytinen et al., 2004), disruptive cryptic coloration (Tan et al., 2020), and camouflage (Cuthill et al., 2005; Fraser et al., 2007). For example, butterfly hindwing tails are fragile and are attacked more often compared to other body parts, suggesting an evolutionary pressure driven by predators for a deflection effect

and the salience of tails (Chotard et al., 2022). Nonetheless, in the few behavioral experiments to date, it has been shown that signaling evasiveness using colored cues might be as effective as signaling distastefulness in educating naïve predators (Gibson, 1974, 1980; Hancox and Allen, 1991; Páez et al., 2021).

Recent molecular phylogenies have suggested large-scale convergent patterns in wing phenotypes of skipper butterflies (family Hesperiidae), i.e., unrelated species having evolved similar shapes with extended hindwings (tails) and white bands on forewings (Li et al., 2019; Zhang et al., 2019). Skippers possess strong evasive power among butterflies and have one of the fastest startle reflexes in the animal kingdom (Sourakov, 2009). Although the evolutionary mechanisms driving such convergences are not yet known, cues such as white bands might be associated with evasive mimicry in Neotropical butterflies (Pinheiro and Freitas, 2014).

Here, we ask whether prey color patterns and/or wing shapes are effective in signaling evasiveness and in triggering predator learning. Moreover, we investigate whether the generalization of such cues to different prey phenotypes is possible. To test our research question, we use an experimental setup that has recently been deployed to test whether European blue tits (*Cyanistes caeruleus*) learn to avoid colored evasive prey (Páez et al., 2021).

MATERIALS AND METHODS

Wild blue tits have been used in behavioral experiments as surrogate predators because of both their cognitive abilities to learn complex feeding tasks and ease of rearing in the laboratory (Church et al., 1998; Grieco, 1999; Hämäläinen et al., 2020). From December 2020 to March 2021 (Year 1) and November 2021 to February 2022 (Year 2), we caught wild blue tits in the campus vicinity of the University of South Bohemia in České Budějovice, Czechia (48.980N, 14.417E, and 48.992N, 14.435E). The habitat of the birds consisted of moist to xerothermic scrubland with poplar, pine, blackthorn, and oak. During collection, we recorded the birds' age, sex, and weight. We kept the birds individually in breeding cages of 45 cm × 45 cm × 90 cm with the walls covered from the outside by bed linen to reduce stress. The roof of the cage was left open for illumination. The breeding cages were in a room with a 12/12-h light cycle. We fed the birds *ad libitum* with water supplemented with vitamins, sunflower seeds, insect pate, mealworms, and mixed grains. We kept the birds in captivity for a maximum of 10 days, and we released them back to their habitat as soon as they completed the behavioral experiments.

All the necessary permits were obtained for this research: license no. 1004 issued by the National Museum in Prague to capture wild birds, license no. 43873/2019-MZE-18134 issued by the Czech Ministry of Agriculture to keep wild birds in captivity, permit no. 22395/2014-MZE-17214 issued by the Ministry of Agriculture of the Czech Republic, and license no. MZP/2020/630/1544 was granted by the Czech Ministry of Environment to conduct behavioral experiments with wild birds. The study was approved by the Ethics Committee of the Faculty of Science, University of South Bohemia, and the experiments were approved by a licensed person (Petr Veselý – license no.

CZ02766 issued by the Ministry of the Agriculture of the Czech Republic). This research adhered to the Association for the Study of Animal Behaviour/Animal Behaviour Society (ASAB/ABS) guidelines for the use of animals in research and complied with the laws of the Czech Republic and the European Union.

Prey Models

We used paper models (distance between both tips of the forewings: 3 cm; distance between the top of the head and end of the hindwing tail: 3.2 and 1.8 cm for models with and without tails, respectively) of skipper butterflies classified in the tribe Eudamina (Hesperiidae, Eudaminae) as prey. We constructed four phenotypes based on a photograph of the species *Autochton neis* (Geyer, 1832) that was further edited in the software Inkscape v1.0. As we were interested in wing color patterns and shapes triggering learning of evasive prey, we constructed the following models: the presence of hindwing tails (phenotype T), white bands (phenotype W), white bands and hindwing tails (phenotype WT), and neither white bands nor tails (phenotype O) (Figure 1). Such models resemble actual skipper butterfly phenotypes found in the Neotropics (Figures 1A–D). We also created two butterfly dummies having different wing color patterns and shapes, a brown dummy used as a control during the learning phase in Year 1 (Figure 1) and a black dummy used during the Pre-training phase to acclimatize the birds to the experimental setup. The models were printed using a Color LaserJet Pro MFP M277dw printer and REY international paper 80 g/sqm.

Behavioral Experiment

We pre-trained the birds to find almond pieces (rewards) on the underside of the dummy forewings. The Pre-training phase started 2 days after catching the birds, so they were already acclimatized to the breeding cages. The birds were pre-trained in a stepwise manner, by displaying the reward in the breeding cages: (1) two almond flakes with no dummy butterfly, (2) almond flakes fully visible on top of two dummies, (3) almond flakes glued to the underside of two dummies, and partially visible from above, and (4) almond flakes glued to the underside of two dummies, and not visible from above. The pre-training was considered successful and the bird was ready for the experiment once it ate all the almond pieces in each consecutive step.

The behavioural experiments consisting of initial preference, learning, and generalization (Figure 1) was carried out in a dark room and using 50 cm × 50 cm × 80 cm experimental boxes made of plywood as described in Páez et al. (2021) (except that we illuminated the cages using LED strips SQ3-300, 4800K, 74 CRI, no UV emission, 30 cm per box). The box was equipped with a wooden perch (25 cm height), a bowl of fresh water, two iron rails on either side for pulling the butterfly's dummies, and the floor was covered with a light brown wrapping paper. The front side of the experimental box was outfitted with polarized Plexiglas to allow observations of birds' behavior with minimal stress for the birds. To evaluate the motivation of the birds before the experiments, we offered two black pre-training dummies with hidden almonds on the underside of the model, and we waited for their consumption.

The initial preference (*Initiation phase*) of blue tits for any of the study phenotypes was tested using a subset of 17 birds during the winter of Year 1 (December–March) and 49 birds during the winter of Year 2 (November–February). The Initiation phase was conducted by simultaneously offering all four butterfly dummies (WT, T, W, and O), all arranged randomly in every trial and recording the attack order and attack time. We waited until all four dummies were attacked or a maximum of 10 min.

During the *Learning phase*, we displayed two different butterfly dummies with hidden almonds: the control and the escape models. Controls were allowed to be consumed. Escape models were not allowed to be consumed. To resemble an evasive behavior by the escaping model, we rapidly pulled the butterfly dummy out of the cage (<1 s) as soon as the bird showed signs of attacking the prey and was closer than 5 cm to it. The learning experiment consisted of a maximum of 80 trials per bird. During the first five trials, we allowed the bird to approach both models to kickstart the learning process (see the video in **Supplementary Material 1**). Afterward, we allowed the bird to make only one choice per trial, leaving the control dummy to be consumed or pulling the escape phenotype out of the cage. After every trial, we swapped the sides where we placed the escaping and control dummies, either to the left or to the right of the experimental cage. We considered the Learning phase successful once the control dummy was consumed in 10 consecutive trials, allowing a maximum of 2 mistakes in between. Two different learning setups were used, hereafter called combined cues (investigation of whether white bands and hindwing tails combined trigger learning of evasive prey) and separate cues (investigation of whether white bands or hindwing tails trigger more effective and memorable learning of evasive prey).

During the *Generalization phase*, we evaluated the salience of the learned traits: shape (hindwing tails) or color pattern (white bands). We gave a minimum of a 30-min break to every bird after completing the Learning phase. If the bird showed signs of fatigue (i.e., falling asleep on the perch or being uninterested in the butterfly models and offered food) after the Learning phase, we continued with the Generalization phase the following day.

Combined-Cues – Learning and Generalization Phases

We studied the salience of the combination of the white band (color) and hindwing tail (shape) when associated with escaping behavior. During the experimental season of Year 1, the escaping model in the Learning phase was the white bands and hindwing-tailed phenotype (WT), and the control was represented by a brown butterfly model with different wing shapes. The Generalization phase was conducted in the same way as the Initiation phase, that is, all four phenotypes (WT, T, W, and O) were simultaneously offered with the position of phenotypes arranged randomly for every bird. We recorded the amount of time it took the bird to attack each phenotype model for a maximum of 10 min. If cues are memorized and generalized, we expected that the birds avoid the WT phenotype after learning its evasive abilities, followed by a model bearing the most salient cue – color (W phenotype) or shape (T phenotype).

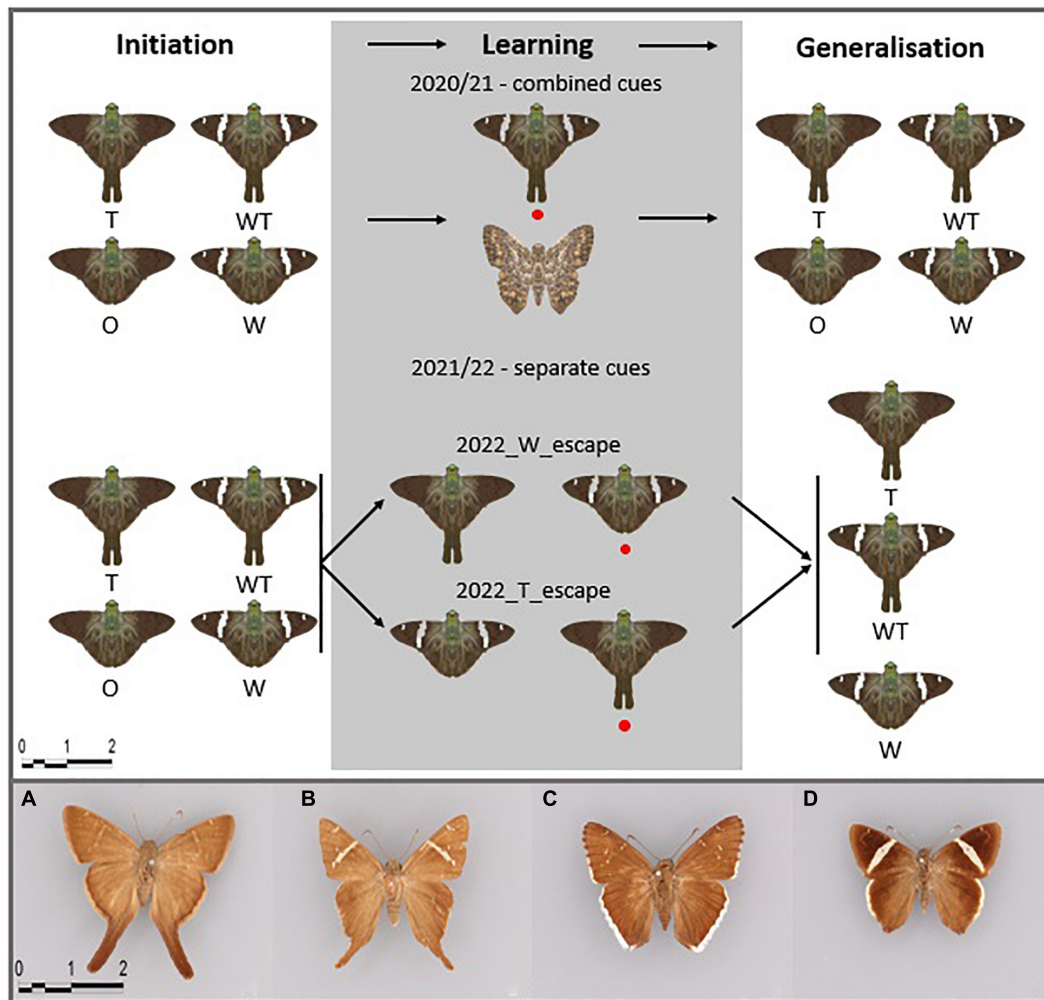


FIGURE 1 | Experimental setup for the three behavioral tests of learning and generalization abilities of pre-trained blue tits and depiction of used butterfly phenotypes: T, hindwing tails; W, white bands; WT, white bands and hindwing tails; O, neither hindwing tails nor white bands. The red circle marks the evasive model during the Learning phase. Initiation was introduced during the winter of Year 1 resulting in a lower sample size. The phenotypes resemble Neotropical butterflies: **(A)** *Spicauda simplicioides* (Stoll, 1790), **(B)** *Cecropterus carmelita* (Herrich-Schäffer, 1868), **(C)** *C. casica* (Herrich-Schäffer, 1868), and **(D)** *C. zarex* (Hübner, 1818) (captured in the Natural History Museum Berlin).

During Year 1 additional birds were processed using an altered generalization setup, while the initiation and learning phases were kept the same. However, due to an insufficient sample size for this subset, the generalization results were not used, but the Learning and Initiation results were merged with the remaining experimental data of Year 1 discussed here (full bird list, see **Supplementary Material 2**).

Separate-Cues – Learning and Generalization Phases

We tested the relative strength of either color (white bands) or shape (tails), in triggering the learning and generalization of evasive prey. Individual birds were used for one of the two Learning phase setups, each differing in the escaping model: with T as the escape model and W as the control (Year 2_T_evasive), and with W as the escape model and T as the control (Year

2_W_evasive) (**Figure 1**). We used either W or T phenotypes as control models during Year 2 because cue efficiency might differ between both stimuli (color and shape) and might depend on which cue is associated with positive (control) or negative experiences (evasive phenotype). The generalization setup was the same for both experiments and consisted of displaying W, T, and WT models (**Figure 1**). We expected that white bands and tails will be similarly important signals for the bird predators, thus, the birds during generalization would avoid the learned evasive phenotype followed by the model-harboring phenotype WT, since it harbors the salient cue (either tail or white band).

Statistical Analyses

We tested differences in attack rates between the escaping and control models, in relation to the number of learning trials. To evaluate the learning curves, we used generalized linear mixed

model (GLMMs) with binomial distribution using the *lme4* package (Bates et al., 2015) in R x64 4.0.2 (R Foundation for Statistical Computing, 2020). For both GLMMs we considered data from all tested birds (including birds that failed the learning criterion or were non-cooperative). The GLMMs, thus, gave a better understanding of the actual learning behavior compared to the average number of trials needed to learn the evasive phenotype. Using model selection, we accounted for all additive, direct interactions between four additional factors (age, sex, year, experiment – i.e., either WT, W, or T as the evasive phenotype), as well as all possible second-order interactions between these factors. Automatic model selection was facilitated using the *MUMIn* package (Burnham and Anderson, 2010). Additionally, the learning difference between both experiments in Year 2, i.e., evasive phenotypes W and T, was compared using a reduced GLMM by omitting data from Year 1 using the same model selection tools as explained previously, and all parameters (experiment, age, and sex) including their second-order interactions.

To compare success rates (in the Pre-training and Learning phases), as well as sex and age ratios, we employed Chi-square tests; we compared the observed rates during Year 2 to the expected rates based on the results from Year 1. We used standard Chi-square tests in the Initiation and Generalization phases to test if birds had any biases to prefer or avoid any of the four prey types. In addition, for the comparison between attack rates during the Initiation and Generalization phases, a Chi-square test was used, where the initial preference's probabilities were considered as the null model. This was possible only for the experiments in Year 1, where Initiation and Generalization designs were similar, and not for experiments in Year 2, where O was deliberately excluded from the Generalization phase to investigate exclusively the effect of T and W. Instead, generalization results for birds that were exposed to the two different types of evasive prey (i.e., T and W) were compared with each other. In all comparisons, only the first attack was used for statistical analysis. As a complementary analysis to our Chi-square tests, we also conducted log-likelihood tests following Pérez et al. (2021); see also (Mérot et al., 2015; Willmott et al., 2017). We compared scenarios with different configurations of attack rates (e.g., identical attack rates on all prey, attack rates all different, and attack rate different for WT) and compared them using AICc values (all scenarios are presented in **Supplementary Material 3**). For Year 1 we were also able to implement a model matching the attack rates observed during the Initiation phase.

Graphics were generated using R x62 4.0.2 (R Foundation for Statistical Computing, 2020) using the *ggplot2* package (Wickham, 2016).

RESULTS

During the experiments in Year 1 (combined cues), the Pre-training phase was completed by 43 out of 46 caught birds (93%), and 36 pre-trained birds (84%) learned to avoid the escaping butterfly (phenotype WT). Of the 36 birds that passed

the Learning phase, 15 (42%) were males and 21 (58%) were females. Three birds (8%) were juvenile hatchlings of 2020 (i.e., younger than 6 months), and 33 birds (92%) were at least 6-month-old. These numbers differ significantly from those of the birds caught during Year 2 (separate cues) (**Table 1**), when 63 blue tits were caught, and only 49 of these completed the Pre-training phase (78%). Further, only 34 pre-trained birds completed the Learning phase successfully (69%). Of the birds that completed the Learning phase, 15 (44%) were females and 19 (56%) were males, while 16 (47%) were juveniles (caught mostly in November and December) and 18 (53%) were adults (see **Table 1**). All 34 birds completed the Generalization phase successfully, but 1 of them was excluded because a wrong combination of phenotypes was offered during Generalization. During Year 2, significantly more birds failed the Pre-training phase ($N = 63$; $df = 1$, $\chi^2 = 25.4$, $p < 0.001$) and the Learning phase ($N = 49$; $df = 1$, $\chi^2 = 7.4$, $p = 0.007$) compared to the experiments in the winter of Year 1. Additionally, during Year 2 the proportion of juveniles was significantly higher compared to Year 1 ($N = 34$; $df = 1$, $\chi^2 = 66.7$, $p < 0.001$). No differences in the sex ratio between years were detected ($N = 34$; $df = 1$, $\chi^2 = 0.08$, $p = 0.77$) (**Table 1**). Further, no direct influence of age, sex, or experiment was detected in the model selection using GLMMs. Summarizing table for all birds is found in **Supplementary Material 2**.

Initiation

Although not statistically significant, results of the Initiation phases suggest some form of prey preference for the phenotype WT across years (**Figure 2**). These results were more obvious during the experimental season in Year 1 when almost half (47%) of the birds attacked the WT model (white bands and hindwing tails), followed by the O model (neither tails nor bands, 29%). While those differences were not statistically significant with the Chi-squared test ($N = 17$; $df = 3$, $\chi^2 = 5.82$, $p = 0.12$), the log-likelihood analysis highlighted three equally likely scenarios (i.e., $\Delta AICc < 2$; **Supplementary Material 4**): (1) all models are attacked at the same rate ($AICc = 35.48$), (2) WT is attacked more frequently than the other prey ($AICc = 35.71$), and (3) WT and O are attacked more frequently than W and T ($AICc = 35.20$).

During Year 2, a similar initial preference pattern was detected, although the differences were less pronounced as 33% of all birds attacked WT first, followed by the O and T phenotypes with 25% each. Again, no significant difference among the attacked prey was detected with the Chi-square test ($N = 36$; $df = 3$, $\chi^2 = 2.02$, $p = 0.57$) (**Figure 2**), but under the log-likelihood framework three models were equally likely: (1) all models are attacked at the same rate ($AICc = 97.82$), (2) WT is attacked more frequently than the other prey ($AICc = 99.14$), and (3) W is attacked less frequently than the other prey ($AICc = 99.30$, **Supplementary Material 4**). Although not fully conclusive, the observations of a possible attack preference for phenotype WT are consistent across years and the only difference is that in Year 2 there appears to be less preference towards W, whereas in Year 1 the models W and T were less preferred.

All Initiation diagrams depicting all four attacks can be found in **Supplementary Material 5**.

TABLE 1 | Comparison between Year 1 and Year 2 regarding number of caught birds, successful birds (Pre-training and Learning phase), sex ratio, and proportion of juveniles.

	Total	Pre-training phase*		Learning phase*		Sex ratio (successful birds)		Age ratio (successful birds)*	
		Passed	Failed	Passed	Failed	Males	Females	Juveniles	Adults
Year 1	46	43	3	36	7	15	21	3	33
Year 2	63	49	14	34	15	15	19	16	18
		df = 1, $\chi^2 = 25.5$, $p < 0.001$		df = 1, $\chi^2 = 7.4$, $p = 0.007$		df = 1, $\chi^2 = 0.08$, $p = 0.77$		df = 1, $\chi^2 = 66.7$, $p < 0.001$	

We compared the values from Year 2 to the expected values based on rates observed during Year 1. The asterisk (*) indicates significant differences between Year 1 and Year 2 (as determined by Chi-square tests) for this category.

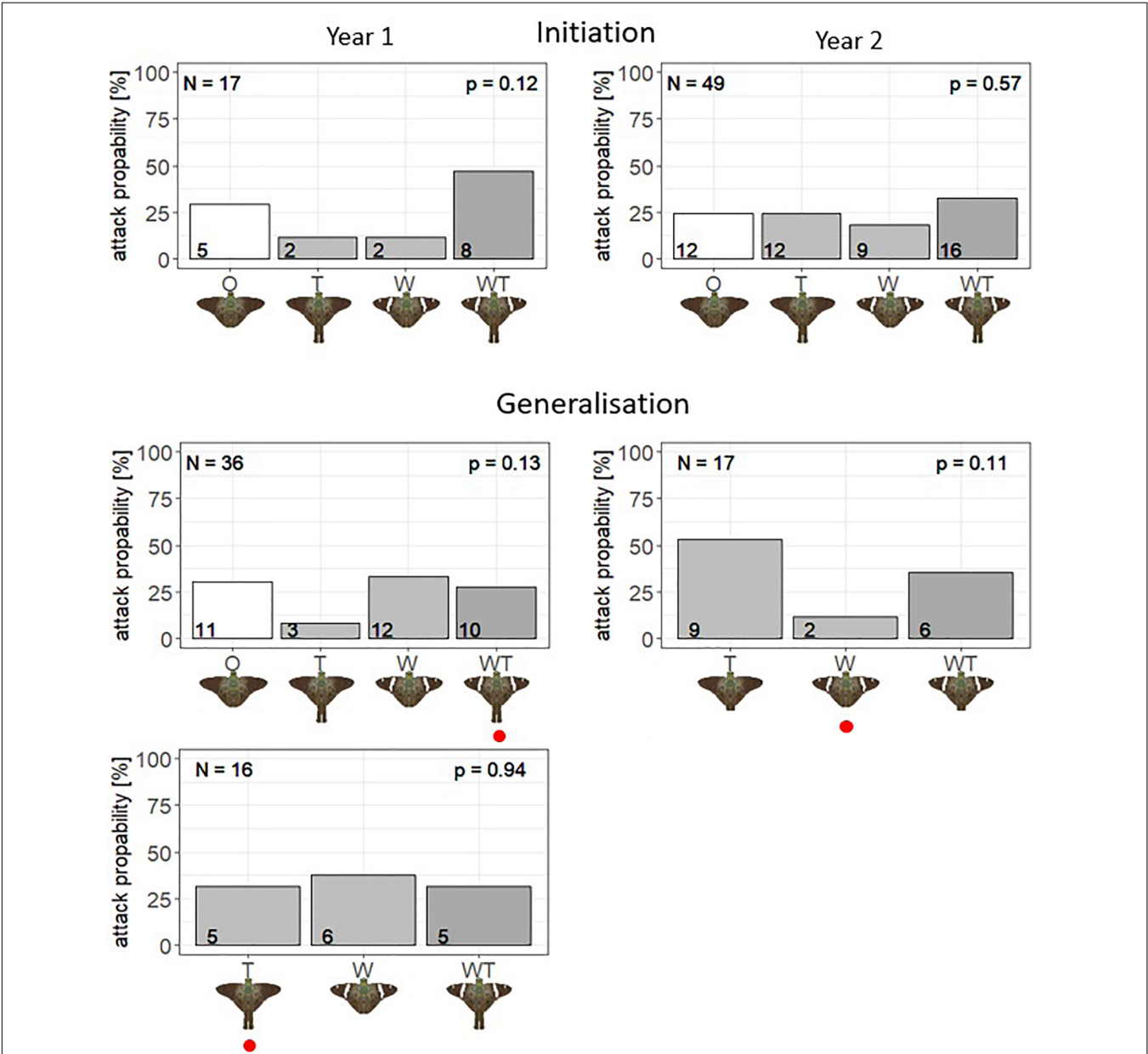


FIGURE 2 | Proportion of blue tits to first attack the different offered butterfly dummies (O, T, W, and WT) during Year 1 (left column), and Year 2 (right column). The first row represents Initiation results, while the second and third rows are representing Generalization results. The number in each bar indicates the absolute number of first attacks on this phenotype and the *p*-value is the result of the Chi-square test comparing any difference in attack rates among prey models within each experiment. The red circle marks the evasive model during the Learning phase.

TABLE 2 | Generalized linear mixed models (GLMMs) to assess the learning capabilities of evasive phenotypes (evasive phenotype in comparison to control model) by European blue tits in dependence sex, experiment, year, and age including all second-order interactions and a delta Akaike information criterion corrected for small sample sizes (dAICc) value of below 2.

Age	Experiment	Sex	Trial	Year	Age: experiment	Age: sex	Age: trial	Age: year	Experiment: sex	Experiment: trial	Sex: trial	Sex: year	Trial: year	df	AICc	Delta
+	+		+	+		+	+					+	+	9	5696.30	0
	+		+	+			+					+	+	7	5696.43	0.13
	+		+	+			+					+	+	10	5697.16	0.86
	+	+	+	+			+			+		+	+	10	5697.16	0.86
		+	+	+							+	+	+	9	5697.26	0.96
			+	+								+	+	8	5697.31	1.01
			+	+						+		+	+	8	5697.31	1.01
		+	+	+		+	+				+	+	+	12	5697.36	1.06
			+	+			+							5	5697.75	1.45
+	+		+	+		+	+					+	+	11	5697.75	1.45
	+		+	+			+				+	+	+	11	5698.07	1.77
			+	+							+	+	+	10	5698.10	1.8
			+	+						+	+	+	+	10	5698.10	1.8
		+	+	+				+				+	+	10	5698.26	1.96
+	+		+	+			+	+					+	10	5698.30	2

Highlighted model is the best model by model selection.

Learning

Although the wild blue tits seem to have an initial preference for the phenotype WT during the winter of Year 1, they successfully learned to avoid such a phenotype when associated with escaping prowess (36 of 43 birds were successful, while 6 adult females and 1 adult male did not successfully pass the learning criteria). Among birds that succeeded in learning, the females took on average 34.5 ± 21.8 ($N = 26$) trials, while the males took 36.5 ± 22.6 ($N = 15$) trials to fulfill our learning criteria (Figure 3).

During Year 2, the blue tits (18 of 23 birds were successful, 2 females and 2 males were unsuccessful, 1 male bird was a juvenile) that learned that phenotype T is evasive (i.e., successful birds) required on average 35.5 ± 22 trials [$N = 18$; males ($N = 11$) = 35 ± 25 , females ($N = 7$) = 36.3 ± 24.5]. Birds (16 of 26 were successful, 9 adult females, and 1 juvenile male failed learning), learning that phenotype W is evasive, took on average 40.5 ± 26.1 trials [$N = 16$, males ($N = 8$) = 43 ± 25.8 , and females ($N = 8$) = 38 ± 25.1].

In the GLMM analysis accounting for the effect of trial, experiment type (i.e., WT, T, or W, as evasive models), year, sex, age, and their interactions, 15 models were within 2 units of AICc from the model with the lowest AICc (Table 2). The effect of trial was present in all best-fit models, while the effect of year was present in all best-fit models but one. Age, sex, and experiment were present in about half (eight models for age and six for sex and Experiment) of the models. The model with the lowest number of parameters (excluding the null model, which was not retained among the best model) had an only trial as a factor. Therefore, the birds' avoidance of learning of the escaping prey was best explained by the number of experiences with the escape model represented by the learning trials, since this factor appeared in all retained models, including the simplest one. In addition to trial, the influence of different combinations of factors cannot be ruled out, as they appear in some of the retained models.

Based on the learning curves (Figure 3), the escaping phenotype WT (shape and color) appeared to trigger the fastest learning behavior, followed by the escaping phenotype T (shape) and the escaping phenotype W (color). Thus, the prey shape seemed to trigger a faster learning behavior compared to the color cue alone (phenotype W). Additionally, males seem to learn faster than females and juveniles faster than adults (Figure 3), although sex and age factors were present in only half of the models (Table 2), meaning their effect cannot be ruled out. The GLMM, encompassing only the data from Year 2 to test for an effect of the experiment (either W or T escaping) without the confounding factor of year or experiment, revealed 17 models within 2 units of the AICc of the best model (Supplementary Material 6). The effect of the experiment was included in 12 of these models, supporting the observation of faster learning of the shape cue (phenotype T) than the color cue (phenotype W).

Generalization

In the experiment during Year 1, the proportion of first attacks of ~50% on WT in the initial preference phase was reduced

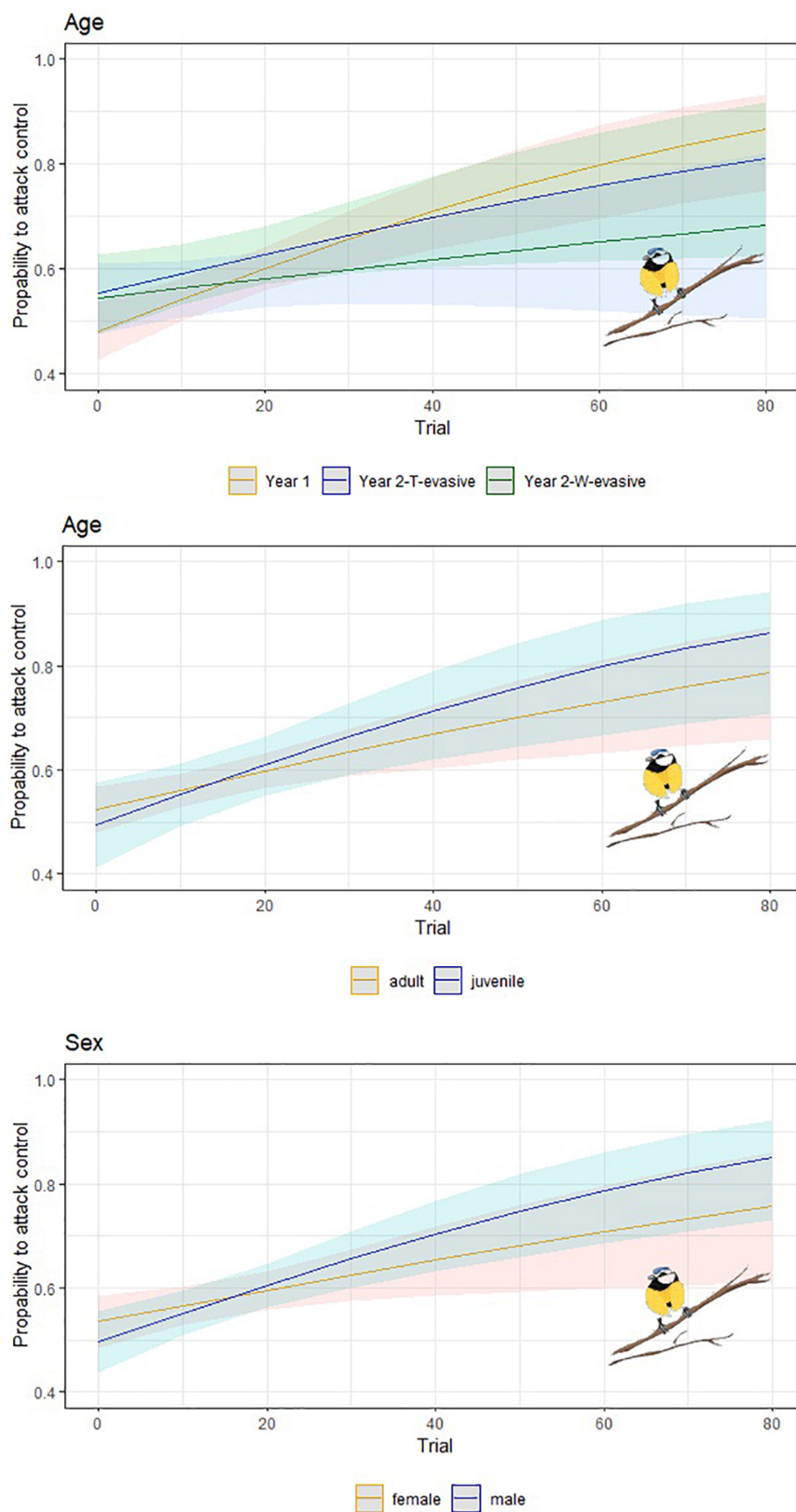


FIGURE 3 | Predicted probability of attacks targeting the escaping model by blue tits in dependence on the number of trials. **Upper-left:** learning behavior separated between different experiments; **upper-right:** difference in learning behavior between adult and juvenile birds; **lower-left:** difference between female and male ones. Including 95% confidence intervals.

to ~30% after learning that WT is an evasive prey (**Figure 2**). By contrast, the attack probability to the phenotype W (white bands) rose roughly threefold, from 12 to 34%. All tailed butterfly models (phenotypes WT and T) were more avoided than the non-tailed models (phenotypes W and O) during the Generalization phase, as about 58% of first attacks toward tailed models during the Initiation phase were reduced to 36% in the Generalization phase. Yet, the attack probabilities among the four model types during Generalization were not significantly different from random expectations based on the Chi-square test ($N = 36$, $df = 3$, $\chi^2 = 5.56$, $p = 0.14$). Nevertheless, a statistical comparison between the first attack probabilities in the Initiation and Generalization phases revealed a significant shift in the observed attack pattern driven by our Learning experiment (Chi-square test using Initiation attack rates as the null model: $N = 36$, $df = 3$, $\chi^2 = 17.46$, $p < 0.005$).

Further exploration using log-likelihood indicated that three scenarios were equally likely (**Supplementary Material 3**): (1) all phenotypes are attacked at the same rate ($AICc = 72.45$), (2) lower attack rate on T and WT (i.e., aversion toward tails, $AICc = 73.07$), and (3) lower attack rate on phenotype T ($AICc = 71.07$). Importantly, the scenario wherein the Generalization attack patterns matched the initiation was not supported ($AICc = 74.24$, **Supplementary Material 4**), again suggesting a shift in attack decisions driven by the Learning phase (specifically, a decrease in attack rate toward WT). Overall, these results suggest that birds might have retained the aversion for WT that was built during the Learning phase in a setting different from that of the Learning phase, despite the initial preference for this phenotype. However, there is no evidence for generalization toward models bearing some of the learned cues: T models suffer a lower attack rate in one of the scenarios, but this was already the case in the Initiation phase, as testified by one of the retained scenarios. Regarding the white band, while W had a lower attack rate during Initiation (testified by one of the best scenarios), during generalization it is the phenotype that suffers the largest number of attacks.

In the experiments during Year 2, when W was the escaping model, 53% of all birds attacked the T model first, followed by WT (35%) and W (12%) (**Figure 2**). The Chi-square test revealed no significant difference between these figures, possibly because of a low sample size ($N = 17$, $df = 2$; $\chi^2 = 4.35$, $p = 0.11$). In the log-likelihood analysis, two scenarios are equally likely (**Supplementary Material 3**): (1) all models are attacked at a similar rate ($AICc = 30.46$), and (2) W is attacked at a lower rate ($AICc = 30.47$, **Supplementary Material 4**). Both these scenarios were already represented during the Initiation but we were unable to compare the two phases directly because the setting was not the same (no O phenotype during Generalization). Nevertheless, there seemed to be a shift in attack rates between Initiation and Generalization, with attacks on T accounting for more than half of all attacks (i.e., on T + W + WT), whereas this proportion was only one third during Initiation. This suggests that the learned avoidance of W might have been retained, triggering the generalization of white bands with evasiveness to the phenotype WT.

When T was the escaping model, there was a slightly higher attack rate on W (T = 31%, WT = 31%, W = 38%), but this was not significant in either the Chi-square test or the log-likelihood analysis (Chi-square test: $N = 16$, $df = 2$; $\chi^2 = 0.13$, $p = 0.93$; log-likelihood: single best model has equal attack rates, $AICc = 28.82$, **Supplementary Material 4**). However, the fact that one of the best scenarios in Initiation, with higher attack rates for T and WT, is not found any more in Generalization suggests that birds might have retained aversion against T and generalized it toward WT.

Finally, a Chi-square test comparing the generalization results of both experiments showed a marginally significant difference driven by attacks on T and W ($N = 17$, $df = 2$; $\chi^2 = 5.65$, $p = 0.06$), suggesting again that the impact of the Learning phase may extend to the Generalization phase.

All Generalization diagrams depicting all four attacks can be found in **Supplementary Material 7**.

Overall, for Year 2, our results pointed toward learning of evasive prey driven by butterfly hindwing tails and white bands. However, our results were inconclusive regarding cue salience, possibly due to the high variability in behavioral studies stipulating large sample sizes to achieve significance, and a potential initial preference bias toward WT (and possibly against W). Nevertheless, our results hint at memorization of the escaping phenotype (i.e., the perfect mimic) in a context different from that of the Learning phase, and, possibly, to the generalization of the learned avoidance of prey that bears cues of the escape model, i.e., imperfect evasive mimics.

DISCUSSION

In this study, we show that coloration (white bands) and butterfly wing shapes (hindwing tails) might be important cues in advertising prey escape prowess. Although blue tits showed some signs of an initial attack preference toward the white-banded and hindwing-tailed model (phenotype WT), the birds associated such cues with escaping prey and avoided attacking them. This suggests that initial preference for color and shape cues can be readily shifted toward aversion. This is in line with the expectations of signal theory, wherein effective signals (both sexual and warning) are those that the receiver pays more attention to and can be rapidly learned (Smallegange et al., 2006; Rodrigues et al., 2010; Finkbeiner et al., 2014). The patterns observed by our study represent the first step toward a deeper understanding of the importance of color and shape in signaling prey evasiveness. Both factors can act as important cues and can be memorized by cognitive predators in different attack contexts, and potentially foster generalization of learned avoidance to other prey bearing similar cues.

Indeed, our results suggest that differences in shape and color, such as the presence of tails or of white bands, can be learned and associated with escape abilities. Although white coloration is not considered a strong aposematic signal (Cibulková et al., 2014), its combination with other cues such as shape might result in stronger predator learning to avoid an unprofitable prey. Our results suggest that learning to avoid evasive prey with expected weaker warning colorations, in this case, white

bands instead of yellow, orange, or red, is possible (**Figure 2**) and relatively fast compared to earlier escape experiments investigating conspicuous color patterns (Páez et al., 2021). In the case of the studied skipper butterfly phenotypes, it is possible that distantly related and co-occurring species in the wild converge to similar signals (white bands, hindwing tails) driven by predatory selection. Our results also suggest that a surrogate avian predator can learn and associate shape and color cues with evasive behavior, either in combination (phenotype WT) or separately (phenotypes W and T). As similar phenotypic patterns occur in sympatric species, the possibility of sexual selection in driving such convergences is limited, making the escape mimicry scenario a more plausible explanation (Pinheiro and Freitas, 2014; Penz et al., 2017).

Memorability and generalization in blue tits seem to depend on the cue combination associated with unprofitability during the Learning phase. When WT was the escaping model (Year 1), there was evidence for memorability, but not for generalization to either W (increased attack rate) or T (low attack rate, but this was already the case during Initiation). By contrast, when the escaping model displayed only one of these cues (W or T, Year 2), our results hint toward the possible generalization of avoidance to WT, although this remains to be confirmed with increased sample size. No conclusive explanation can be given for this pattern. However, it is possible that when several salient cues are combined, the effectiveness in advertising unprofitability might be increased.

We cannot rule out other external drivers of preference and memorability abilities of birds to certain phenotypic cues acting in different years. Birds caught during Year 2 required slightly more learning trials to succeed in our learning criteria compared to birds caught the previous year. In addition, proportionally fewer birds were able to successfully pass our Generalization phase in Year 2 (53.2%) compared to Year 1 (78.5%). One explanation is that the warmer conditions in Year 2, with almost no snow cover nor longer freezing temperatures in the study locality, might have influenced the learning and memorability abilities of the birds. Similar observations were made in Finland (J. Mappes, pers. obs.) and it has been shown that ambient temperature influences foraging behavior in birds (Chatelain et al., 2013). Alternatively, the higher amount of caught juveniles during Year 2 (47%) compared to Year 1 (8%) might have also influenced the observed differences in learning and generalization. Likewise, the apparent initial preference for the phenotype WT detected in Year 1 might be explained by the higher ratio of caught adults with likely more experience with handling prey in the wild, compared to the experiments in Year 2, when the preference for the phenotype WT was less pronounced.

Blue tits seem to prefer attacking prey with specific coloration and shape combinations, such as those found in red firebugs (Propokova et al., 2010). In the case of wild European blue tits, the marginal preference shown for white bands and hindwing tails (phenotype WT) might come from previous experience with butterfly phenotypes, having similar white markings, including the palatable nymphalid butterfly *Araschnia levana* (Linnaeus, 1758) (summer form) and the day flying geometrid *Chiasmia clathrata* (Linnaeus, 1758). However, no European butterfly

species exactly resembles the phenotype WT found in the Neotropics. Another explanation for our findings is an apparent preference for large dummies with tails (body size), but the phenotype T with the same sizes were attacked at a lower rate in our initiation tests in Year 1 when a higher ratio of adult birds was caught. It is still puzzling that the birds did neither prefer hindwing-tailed (shape, phenotype T) nor white-banded butterflies (color, phenotype W), but the combination of both is only present in the escaping model WT (color and shape). However, it is clear that cues associated with escaping ability, either shape or color, are effective signals as the three escaping models W, T, and WT were learned by the blue tits.

Escape mimicry involves a primary prey defense, escape ability, which a predator might learn following unsuccessful attacks, which is before the capture or subjugation of prey (Marden and Chai, 1991; Speed et al., 2010). This is in contrast with mimicry involving secondary defenses in prey, such as unpalatability and toxicity, which require the capture, handling, and potential death of prey to educate naïve predators (McLain, 1984; Mallet and Gilbert, 1995). For both predator and prey, mimicry has benefits: prey species reduce attacks of cognitive predators by advertising unprofitability, while predators generalize signals from aversive experiences to make a cost-effective decision before pursuing a prey (MacDougall and Dawkins, 1998; Ihalaenen et al., 2012). In Müllerian mimicry (Müller, 1878), aposematic signals are shared among two unprofitable species, thereby, sharing the cost to educate and deter predators, whereas, in Batesian mimicry (Bates, 1862), undefended species mimic an unprofitable model species. While theoretical (Ruxton et al., 2004), experimental, and observational evidence (Edmunds, 1974; Gibson, 1974, 1980; Llaurens et al., 2021; Páez et al., 2021) supports the existence of escape mimicry, it is yet unknown how prevalent it is in nature nor what cues in hard-to-catch prey (color, shape) are more memorable for predators. Here, we show that both color and shape are strong cues in advertising evasiveness and that they can be learned effectively by naïve predators. Because of our relatively low sample size and the high variability in individual bird responses, we still lack statistical power to assess the relative effectiveness of each cue (shape and color). Thus, our study only partially supports the hypothesis that the convergence of white bands observed in evasive Neotropical butterflies might be related to escape mimicry driven by avian predators (Pinheiro and Freitas, 2014).

Hindwing tails in Lepidoptera (butterflies and moths) are hypothesized to divert the attacks of predators to non-essential parts of the wing (Weeks, 1903; Blest, 1957; Chotard et al., 2022). Our results suggest that hindwing tails might as well be involved in signaling evasive behavior for visual predators, thereby, further reducing the risk of fatal attacks. When wild evasive butterflies lose the hindwing tails, the coloration of the forewings might still serve as cues signaling unprofitability, hence acting as a two-tiered system in diverting attack and advertising evasiveness. Nevertheless, further behavioral experiments are needed to determine whether the salience of shape remains when combined with stronger aposematic colorations such as yellow, orange, or red. Our results are hinting at a more

complex predator-prey selection dynamic where both shape and coloration together might be of importance during learning of prey evasive capabilities.

DATA AVAILABILITY STATEMENT

The raw data supporting the conclusions of this article are available at doi: 10.5281/zenodo.6790077 and any further enquiries should be directed to the corresponding author.

ETHICS STATEMENT

The animal study was reviewed and approved by license no. MZP/2020/630/1544 granted by the Czech Ministry of Environment to conduct behavioral experiments with wild birds.

AUTHOR CONTRIBUTIONS

DL: investigation, methodology, data curation and analysis, writing – original draft, review, and editing. ME: conceptualization, methodology, data analysis, review, and editing. IK: investigation, methodology, review, and editing. JM: conceptualization, methodology, review, and editing. PM-M: funding acquisition, investigation, methodology, conceptualization, review, and editing. All authors contributed to the article and approved the submitted version.

REFERENCES

- Balگوoyen, T. G. (1997). Evasive mimicry involving a butterfly model and grasshopper mimic. *Am. Midland Natur.* 137:183. doi: 10.2307/2426768
- Bates, D., Mächler, M., Bolker, B., and Walker, S. (2015). Fitting linear mixed-effects models using lme4. *J. Statist. Softw.* 67:i01. doi: 10.18637/jss.v067.i01
- Bates, H. W. (1862). Contributions to an insect fauna of the amazon valley (lepidoptera: heliconidae). *Biol. J. Lin. Soc.* 16, 41–54. doi: 10.1111/j.1095-8312.1981.tb01842.x
- Blest, A. D. (1957). The function of eyespot patterns in the lepidoptera. *Behavior* 11, 209–256.
- Burnham, K. P., and Anderson, D. R. (2010). *Model Selection And Multimodel Inference. A Practical Information-Theoretic Approach*. New York, NY: Springer.
- Casas-Cardona, S., Márquez, R., and Vargas-Salinas, F. (2018). Different color morphs of the poison frog *Andinobates bombetes* (dendrobatidae) are similarly effective visual predator deterrents. *Ethology* 124, 245–255. doi: 10.1111/eth.12729
- Chatelain, M., Halpin, C. G., and Rowe, C. (2013). Ambient temperature influences birds' decisions to eat toxic prey. *Animal Behav.* 86, 733–740. doi: 10.1016/j.anbehav.2013.07.007
- Chotard, A., Ledamoisel, J., Decamps, T., Herrel, A., Chaine, A., Llaurens, V., et al. (2022). Evidence of attack deflection suggests adaptive evolution of wing tails in butterflies. *Proc. R. Soc. B.* 2022:562. doi: 10.1098/rspb.2022.0562
- Church, S. C., Bennett, A. T. D., Cuthill, I. C., and Partridge, J. C. (1998). Ultraviolet cues affect the foraging behavior of blue tits. *Proc. Biol. Sci.* 265, 1509–1514. doi: 10.1098/rspb.1998.0465
- Cibulková, A., Vesely, P., and Fuchs, R. (2014). Importance of conspicuous colors in warning signals: the great tit's (*parus major*) point of view. *Evolu. Ecol.* 28, 427–439. doi: 10.1007/s10682-014-9690-2
- Cott, H. B. (1940). *Adaptive Coloration in Animals*. London: Methuen.
- Cuthill, I. C., Stevens, M., Sheppard, J., Maddocks, T., Párraga, C. A., and Troscianko, T. S. (2005). Disruptive coloration and background pattern matching. *Nature* 434, 72–74. doi: 10.1038/nature03312

FUNDING

This study was provided by the Junior GAČR grant (GJ20-18566Y) and the PPLZ program of the Czech Academy of Sciences (fellowship grant L20096195), as well as GAJU n. 04-048/2019/P and n. 014/2022/P.

ACKNOWLEDGMENTS

We would like to extend our gratitude toward Petr Veselý and Michaela Syrová who helped us to catch and transport wild blue tits to the laboratory, as well as determined their age and sex. Furthermore, we would like to thank Klára Aurová, Stanislav Vrba, Legi Sam, Kateřina Sam, and student assistants Ladislava Krausová, Alena Fischerová, Marika Davidkova, Petra Krejčova, Tereza Hyblova, Barbora Belovska, and Jan Pixa during the experiments. We would also like to thank Leonardo Ré Jorge for his advice in statistical tests, and Théo Léger for the possibility to photograph butterflies in the MFN Berlin.

SUPPLEMENTARY MATERIAL

The Supplementary Material for this article can be found online at: <https://www.frontiersin.org/articles/10.3389/fevo.2022.910695/full#supplementary-material>

- Dell'aglio, D. D., Stevens, M., and Jiggins, C. D. (2016). Avoidance of an aposematically colored butterfly by wild birds in a tropical forest. *Ecol. Entomol.* 41, 627–632. doi: 10.1111/een.12335
- Edmunds, M. (1974). *Defence in Animals. A Survey Of Anti-Predator Defences / M. Edmunds*. Harlow: Longman.
- Finkbeiner, S. D., Briscoe, A. D., and Reed, R. D. (2014). Warning signals are seductive: relative contributions of color and pattern to predator avoidance and mate attraction in *Heliconius* butterflies. *Evolution* 68, 3410–3420. doi: 10.1111/evo.12524
- FitzGibbon, C. D., and Fanshawe, J. H. (1988). Stotting in thomson's gazelles: an honest signal of condition. *Behav. Ecol. Sociobiol.* 23, 69–74. doi: 10.1007/BF00299889
- Fraser, S., Callahan, A., Klassen, D., and Sherratt, T. N. (2007). Empirical tests of the role of disruptive coloration in reducing detectability. *Proc. Biol. Sci.* 274, 1325–1331. doi: 10.1098/rspb.2007.0153
- Geyer, C. (1832). *Zuträge zur Sammlung Exotischer Schmettlinge, Zuträge Sammlung Exotischer Schmetterlinge*. Augsburg: Im Verlag der Hübnerschen Werke bei C. Geyer.
- Gibson, D. O. (1974). Batesian mimicry without distastefulness? *Nature* 250, 77–79. doi: 10.1038/250077a0
- Gibson, D. O. (1980). The role of escape in mimicry and polymorphism: I. the response of captive birds to artificial prey. *Biol. J. Lin. Soc.* 14, 201–214. doi: 10.1111/j.1095-8312.1980.tb00105.x
- Golding, Y. C., Edmunds, M., and Ennos, A. R. (2005). Flight behavior during foraging of the social wasp *vespula vulgaris* (hymenoptera: vespidae) and four mimetic hoverflies (diptera: syrphidae) *Sericomyia silentis*, *Myathropa florea*, *helophilus* sp. and *syrphus* sp. *J. Exp. Biol.* 208(Pt. 23), 4523–4527. doi: 10.1242/jeb.01932
- Grieco, F. (1999). Prey selection in blue tits *Parus caeruleus* as a response to food levels. *Acta Ornithol.* 34, 199–203.
- Guerra, T. J. (2019). Evasive mimicry. too beetle, or not too beetle? *Ecology* 100, 1–3.

- Hämäläinen, L., Mappes, J., Rowland, H. M., Teichmann, M., and Thorogood, R. (2020). Social learning within and across predator species reduces attacks on novel aposematic prey. *J. Animal Ecol.* 89, 1153–1164. doi: 10.1111/1365-2656.13180
- Hancox, A. P., and Allen, J. A. (1991). A simulation of evasive mimicry in the wild. *J. Zool.* 223, 9–13. doi: 10.1111/j.1469-7998.1991.tb04745.x
- Hegedus, M., Devries, P., and Penz, C. M. (2019). The influence of mimicry on wing shape evolution in the butterfly *papilio dardanus* (lepidoptera: papilionidae). *Ann. Entomol. Soc. Am.* 112, 33–43. doi: 10.1093/aesa/say045
- Herrich-Schäffer (1868). *Prodromus systematics lepidopterorum prodr. Syst. Lep.* 3, 1–84.
- Hübner (1818). *Zuträge zur Sammlung exotischer Schmettlinge. Z. Samml. Exot. Schmett.* 1, 4–6, 8–32, l.[1–2], f.1–12; l.[3–25], f.13–146; l.[26–35], f.147–200.
- Ihalainen, E., Rowland, H. M., Speed, M. P., Ruxton, G. D., and Mappes, J. (2012). Prey community structure affects how predators select for *Mullerian mimicry*. *Proc. Biol. Sci.* 279, 2099–2105. doi: 10.1098/rspb.2011.2360
- Johansen, A. I., Tullberg, B. S., and Gambralle-Stille, G. (2011). Motion level in *Graphosoma lineatum* coincides with ontogenetic change in defensive coloration. *Entomol. Exp. Appl.* 141, 163–167. doi: 10.1111/j.1570-7458.2011.01182.x
- Le Roy, C., Debat, V., and Llaurens, V. (2019). Adaptive evolution of butterfly wing shape: from morphology to behavior. *Biol. Rev.* 94, 1261–1281. doi: 10.1111/brv.12500
- Li, W., Cong, Q., Shen, J., Zhang, J., Hallwachs, W., Janzen, D. H., et al. (2019). Genomes of skipper butterflies reveal extensive convergence of wing patterns. *Proc. Natl. Acad. Sci.* 116, 6232–6237. doi: 10.1073/pnas.1821304116
- Linnaeus, C. (1758). *Systema naturae per regna tria naturae, secundum clases, ordines, genera, species, cum characteribus, differentiis, synonymis, Locis.* Tomis I. 10th Edition. *Syst. Nat.* 1, 1–338, 339–824.
- Llaurens, V., Le Poul, Y., Puissant, A., Blandin, P., and Debat, V. (2021). Convergence in sympatry: evolution of blue-banded wing pattern in *Morpho* butterflies. *J. Evol. Biol.* 34, 284–295. doi: 10.1111/jeb.13726
- Lyttinen, A., Brakefield, P. M., Lindström, L., and Mappes, J. (2004). Does predation maintain eyespot plasticity in *Bicyclus anynana*? *Proc. R. Soc. B* 271, 279–283. doi: 10.1098/rspb.2003.2571
- MacDougall, A., and Dawkins, M. S. (1998). Predator discrimination error and the benefits of *Müllerian mimicry*. *Animal Behav.* 55, 1281–1288. doi: 10.1006/anbe.1997.0702
- Mallet, J., and Gilbert, L. E. (1995). Why are there so many mimicry rings? Correlations between habitat, behavior and mimicry in *Heliconius* butterflies. *Biol. J. Linn. Soc.* 55, 159–180. doi: 10.1111/j.1095-8312.1995.tb01057.x
- Marden, J. H., and Chai, P. (1991). Aerial predation and butterfly design: how palatability, mimicry, and the need for evasive flight constrain mass allocation. *Am. Natur.* 138, 15–36. doi: 10.1086/285202
- McLain, D. K. (1984). Coevolution: müllerian mimicry between a plant bug (miridae) and a seed bug (lygaeidae) and the relationship between host plant choice and unpalatability. *Oikos* 43:143. doi: 10.2307/3544761
- McLean, D. J., and Herberstein, M. E. (2021). Mimicry in motion and morphology: do information limitation, trade-offs or compensation relax selection for mimetic accuracy? *Proc. Biol. Sci.* 288:20210815. doi: 10.1098/rspb.2021.0815
- Mérot, C., Frérot, B., Leppik, E., and Joron, M. (2015). Beyond magic traits: multimodal mating cues in *Heliconius* butterflies. *Evolution* 69, 2891–2904. doi: 10.1111/evo.12789
- Müller, F. (1878). Über die Vortheile der mimicry bei Schmetterlingen. *Zool. Anz.* 1, 54–55.
- Ortega, A., Eastwood, R., Vogt, D., Ithier, C., Smith, M., Wood, R., et al. (2017). Aerodynamic evaluation of wing shape and wing orientation in four butterfly species using numerical simulations and a low-speed wind tunnel, and its implications for the design of flying micro-robots. *Int. Focus* 7:20160087. doi: 10.1098/rsfs.2016.0087
- Páez, E., Valkonen, J. K., Willmott, K. R., Matos-Maraví, P., Elias, M., and Mappes, J. (2021). Hard to catch: experimental evidence supports evasive mimicry. *Proc. Biol. Sci.* 288:20203052. doi: 10.1098/rspb.2020.3052
- Pawlik, J. R., Kernan, M. R., Molinski, T. F., Harper, M. K., and Faulkner, D. J. (1988). Defensive chemicals of the spanish dancer nudibranch hexabranchus sanguineus and its egg ribbons: macrolides derived from a sponge diet. *J. Exp. Mari. Biol. Ecol.* 119, 99–109. doi: 10.1016/0022-0981(88)90225-0
- Penz, C. M., Casagrande, M. M., Devries, P., and Simonsen, T. J. (2017). Documenting diversity in the amazonian butterfly genus (lepidoptera, nymphalidae). *Zootaxa* 4258, 201–237. doi: 10.11646/zootaxa.4258.3.1
- Pinheiro, C. E. G. (1996). Palatability and escaping ability in *Neotropical butterflies*: tests with wild kingbirds (*Tyrannus melancholicus*, tyrannidae). *Biol. J. Lin. Soc.* 59, 351–365. doi: 10.1111/j.1095-8312.1996.tb01471.x
- Pinheiro, C. E. G., and Cintra, R. (2017). Butterfly predators in the neotropics: which birds are involved? *J. Lepidopt. Soc.* 71, 109–114. doi: 10.18473/lepi.7112.a5
- Pinheiro, C. E. G., and Freitas, A. V. L. (2014). Some possible cases of escape mimicry in neotropical butterflies. *Neotr. Entomol.* 43, 393–398. doi: 10.1007/s13744-014-0240-y
- Pinheiro, C. E. G., Freitas, A. V. L., Campos, V. C., DeVries, P. J., and Penz, C. M. (2016). Both palatable and unpalatable butterflies use bright colors to signal difficulty of capture to predators. *Neotr. Entomol.* 45, 107–113. doi: 10.1007/s13744-015-0359-5
- Poulton, E. B. (1890). *The Colors of Animals, Their Meaning and Use, Especially Considered in the Case of Insects.* New York, NY: D. Appleton and Company.
- Propokova, M., Vesely, P., Fuchs, R., and Zrzavy, J. A. N. (2010). The role of size and color pattern in protection of developmental stages of the red firebug (*Pyrrhocoris apterus*) against avian predators. *Biol. J. Lin. Soc.* 100, 890–898. doi: 10.1111/j.1095-8312.2010.01463.x
- R Foundation for Statistical Computing (2020). *R: A language and environment for statistical computing.* Vienna, Austria: R Core Team.
- Rodrigues, D., Goodner, B. W., and Weiss, M. R. (2010). Reversal learning and risk-averse foraging behavior in the monarch butterfly, *danaus plexippus* (lepidoptera: nymphalidae). *Ethology* 116, 270–280. doi: 10.1111/j.1439-0310.2009.01737.x
- Ruxton, G. D., Speed, M., and Sherratt, T. N. (2004). Evasive mimicry: when (if ever) could mimicry based on difficulty of capture evolve? *Proc. Biol. Sci.* 271, 2135–2142. doi: 10.1098/rspb.2004.2816
- Santos, J. C., Tarvin, R. D., and O'Connell, L. A. (2016). “A review of chemical defense in poison frogs (dendrobatidae): ecology, pharmacokinetics, and autoresistance,” in *Chemical Signals in Vertebrates 13. Cham, 2016*, eds B. A. Schulte, T. E. Goodwin, and M. H. Ferkin (Cham: Springer), 305–337.
- Smallegange, R., Everaarts, T., and van Loon, J. (2006). Associative learning of visual and gustatory cues in the large cabbage white butterfly, *Pieris brassicae*. *Animal Biol.* 56, 157–172. doi: 10.1163/1570756060777304159
- Sourakov, A. (2009). Extraordinarily quick visual startle reflexes of skipper butterflies (lepidoptera: hesperidae) are among the fastest recorded in the animal kingdom. *Florida Entomol.* 92:653. doi: 10.1653/024.092.0420
- Speed, M. P., Brockhurst, M. A., and Ruxton, G. D. (2010). The dual benefits of aposematism: predator avoidance and enhanced resource collection. *Evolution* 64, 1622–1633. doi: 10.1111/j.1558-5646.2009.00931.x
- Srygley, R. B. (1994). Locomotor mimicry in butterflies? The associations of positions of centres of mass among groups of mimetic, unprofitable prey. *Philos. Trans. R. Soc. London Ser. B Biol. Sci.* 343, 145–155. doi: 10.1098/rstb.1994.0017
- Stoll, C. (1790). *Aanhangsel van het Werk, de Uitlandsche Kapellen Aanhangsel Werk. Uitl. Kapellen* 1–42, 1–8.
- Tan, E. J., Wilts, B. D., Tan, B. T. K., and Monteiro, A. (2020). What's in a band? The function of the color and banding pattern of the banded swallowtail. *Ecol. Evolu.* 10, 2021–2029. doi: 10.1002/ece3.6034
- Valkonen, J. K., Nokelainen, O., and Mappes, J. (2011). Antipredatory function of head shape for vipers and their mimics. *PLoS One* 6, e22272. doi: 10.1371/journal.pone.0022272
- van Belleghem, S. M., Alicea Roman, P. A., Carbia Gutierrez, H., Counterman, B. A., and Papa, R. (2020). Perfect mimicry between *Heliconius* butterflies is constrained by genetics and development. *Proc. Biol. Sci.* 287:20201267. doi: 10.1098/rspb.2020.1267
- Weeks, A. C. (1903). Theory as to evolution of secondaries of moths of the genus *catocala*. *J. N.Y. Entomol. Soc.* 11, 221–226.
- Wickham, H. (2016). *Ggplot2. Elegrat graphics for data analysis / Hadley Wickham; with contributions by Carson Sievert.* Switzerland: Springer.
- Willmott, K. R., Robinson Willmott, J. C., Elias, M., and Jiggins, C. D. (2017). Maintaining mimicry diversity: optimal warning color patterns differ among

- microhabitats in Amazonian clearwing butterflies. *Proc. Biol. Sci.* 284:1855. doi: 10.1098/rspb.2017.0744
- Young, A. M. (1971). Wing coloration and reflectance in *Morpho* butterflies as related to reproductive behavior and escape from avian predators. *Oecologia* 7, 209–222. doi: 10.1007/BF00345212
- Zhang, J., Cong, Q., Shen, J., Brockmann, E., and Grishin, N. V. (2019). Genomes reveal drastic and recurrent phenotypic divergence in firetip skipper butterflies (hesperiidae: pyrrhopyginae). *Proc. Biol. Sci.* 286:20190609. doi: 10.1098/rspb.2019.0609

Conflict of Interest: The authors declare that the research was conducted in the absence of any commercial or financial relationships that could be construed as a potential conflict of interest.

Publisher's Note: All claims expressed in this article are solely those of the authors and do not necessarily represent those of their affiliated organizations, or those of the publisher, the editors and the reviewers. Any product that may be evaluated in this article, or claim that may be made by its manufacturer, is not guaranteed or endorsed by the publisher.

Copyright © 2022 Linke, Elias, Klečková, Mappes and Matos-Maraví. This is an open-access article distributed under the terms of the Creative Commons Attribution License (CC BY). The use, distribution or reproduction in other forums is permitted, provided the original author(s) and the copyright owner(s) are credited and that the original publication in this journal is cited, in accordance with accepted academic practice. No use, distribution or reproduction is permitted which does not comply with these terms.



OPEN ACCESS

EDITED BY

Jennifer M. Gleason,
University of Kansas, United States

REVIEWED BY

Gerhard Johannes Gries,
Simon Fraser University, Canada
Astrid T. Groot,
University of Amsterdam, Netherlands

*CORRESPONDENCE

Mark A. Elgar
m.elgar@unimelb.edu.au
Matthew R. E. Symonds
matthew.symonds@deakin.edu.au

SPECIALTY SECTION

This article was submitted to
Behavioral and Evolutionary Ecology,
a section of the journal
Frontiers in Ecology and Evolution

RECEIVED 13 April 2022

ACCEPTED 03 August 2022

PUBLISHED 26 August 2022

CITATION

Johnson TL, Elgar MA and
Symonds MRE (2022) Movement
and olfactory signals: Sexually
dimorphic antennae and female
flightlessness in moths.
Front. Ecol. Evol. 10:919093.
doi: 10.3389/fevo.2022.919093

COPYRIGHT

© 2022 Johnson, Elgar and Symonds.
This is an open-access article
distributed under the terms of the
[Creative Commons Attribution License](#)
(CC BY). The use, distribution or
reproduction in other forums is
permitted, provided the original
author(s) and the copyright owner(s)
are credited and that the original
publication in this journal is cited, in
accordance with accepted academic
practice. No use, distribution or
reproduction is permitted which does
not comply with these terms.

Movement and olfactory signals: Sexually dimorphic antennae and female flightlessness in moths

Tamara L. Johnson¹, Mark A. Elgar^{1*} and
Matthew R. E. Symonds^{2*}

¹School of Biosciences, The University of Melbourne, Melbourne, VIC, Australia, ²Centre for Integrative Ecology, School of Life and Environmental Sciences, Deakin University, Burwood, VIC, Australia

Darwin argued a role for sexual selection in the evolution of male sensory structures, including insect antennae, the strength of which will depend upon the importance of early arrival at receptive females. There is remarkable variation in the nature and degree of sexual dimorphism in moth antennae, with males of some species having spectacular, feathery antennae. Although it is widely assumed that these elaborate structures provide greater sensitivity to chemical signals (sex pheromones), the factors underlying the interspecific diversity in male antennal structure and size are poorly understood. Because male antennal morphology may be affected by several female life-history traits, including flight ability, we conducted a phylogenetic comparative analysis to test how these traits are linked, using data from 93 species of moths across 11 superfamilies. Our results reveal that elaborate antennae in males have evolved more frequently in species where females are monandrous. Further, female loss of flight ability evolved more frequently in species where males have elaborate antennae. These results suggest that elaborate antennae have evolved in response to more intense male competition, arising from female monandry, and that the evolution of elaborate antennae in males has, in turn, shaped the evolution of female flightlessness.

KEYWORDS

sex pheromone, sexual selection, mating system, antennal morphology, flightless moth, mate location

Introduction

Signalling is a crucial component of reproduction for mobile diocious species, playing a role in both bringing mates together and in facilitating mechanisms of pre-mating sexual selection (e.g., Darwin, 1871; Andersson, 1994; Rosenthal, 2017). The latter is responsible for the evolution of an extraordinary diversity of conspicuous, sexually selected signals, across the range of sensory modalities, and has attracted very extensive research interest. In many moths, females use sex pheromones (olfactory

signals) to advertise their location to mate searching males. Although long-distance location-revealing sex pheromones are typically not regarded as being subject to sexual selection [see [Johansson and Jones \(2007\)](#)], they may cause sexual selection to act on male receptor organs ([Darwin, 1871](#); [Elgar et al., 2019](#)).

[Darwin \(1871\)](#) suggested that sexual selection will favour improvements in “organs of sense” if that improves the likelihood of male mating success in a competitive environment. Darwin did not explicitly mention antennae as “organs of sense,” because pheromones and the odour receptors located on antennal sensilla (e.g., [Hansson, 1995](#)) were not known at that time ([Elgar et al., 2019](#)). Nevertheless, his perspective suggests that selection will favour males with antennal features that improve the speed of detection of sex pheromones if that allows males to locate females more quickly than rival males. The taxonomically widespread sexual dimorphism in insect antennal morphology (e.g., [Schneider, 1964](#); [Elgar et al., 2018](#)), together with several lines of empirical evidence, are consistent with this perspective ([Elgar et al., 2019](#)). Field experiments on a sexually dimorphic moth, the gum-leaf skeletonizer *Uraba lugens*, demonstrated that males with longer antennae were more likely to detect lower amounts of pheromone ([Johnson et al., 2017b](#)), and laboratory experiments with the same species revealed that larvae developing in higher densities (thereby anticipating greater reproductive competition as adults) resulted in males with larger antennae and testes ([Johnson et al., 2017a](#)), and in females releasing more attractive sex pheromone ([Pham et al., 2020](#)).

Sexual dimorphism in some species of moths is remarkably striking, with the elaborate, feathery, pennate antennae of males contrasting with the simple threadlike or filiform antennae of females ([Schneider, 1964](#); [Young, 1997](#)). Phylogenetic comparative analyses indicate that while elaborate antennae are linked with larger body size, suggesting a functional cost to these structures, this pattern is not necessarily consistent with a greater capacity to detect chemical signals, because larger females might be expected to release larger quantities of pheromone ([Symonds et al., 2012](#)). On the other hand, in species where males have elaborate antennae, there is a negative correlation between male abundance and male antennal length. This result suggests that lower population densities with concomitantly lower concentrations of pheromone, may select for larger antennae in males, at least in species where males have elaborate antennae ([Symonds et al., 2012](#)). Regardless, males of most moth species possess relatively simple filiform antennae, whilst females still emit long-distance sex pheromones. This suggests that the strength of selection on male antennal morphology is linked to other factors that determine the importance of quickly locating a female, and thus rapidly detecting her sex pheromone. A previous comparative analysis of male elaborate antennae in geometrid moths ([Javoiš et al., 2019](#)) found that they were more likely to be found in species where females were capital breeders (i.e.,

that eclose with greater body reserves already available for breeding). [Javoiš et al. \(2019\)](#) suggested that such a strategy may be associated with traits that make them more difficult for males to locate quickly, such as reduced mobility.

There is emerging interest in the effects of movement on the production and detection of signals and cues, although research is largely confined to visual and auditory sensory modalities ([Tan and Elgar, 2021](#)). Nevertheless, movement may be consequential for chemical signalling: female moths may adjust the detectability of their sex pheromones by selecting different kinds of locations where they call (emit pheromones). For example, pheromones released in closed habitats may be less easily detected, and females may compensate by moving to a more open location ([Murlis et al., 1992](#)). Clearly this option is not available to less mobile, flightless female moths. Females are flightless in roughly 1% of lepidopteran species, although it is taxonomically widespread, occurring in 25 families ([Sattler, 1991](#)). Female wing loss in these species varies from a complete loss of wings (aptery) to retaining full sized wings but with a loss of function ([Tweedie, 1976](#); [Sattler, 1991](#)). Flightlessness is associated with winter-active adults and spring feeding, as well as high host breadth ([Hunter, 1995](#)). In most flightless species, the females are unable to move far and remain on or near their pupation site throughout their typically short adult life ([Sattler, 1991](#)). [Hackman \(1966\)](#) noted that these locations may not necessarily be optimal for calling and suggested that this selects for greater sensitivity to the pheromone in males. The converse may also be possible: that loss of flight evolved in part due to the speed with which highly sensitive males can locate females.

Here we use a phylogenetic comparative approach to examine several potential selection pressures favouring male antennal complexity in moths, including flightlessness and other life-history traits. Specifically, we ask whether certain female traits that potentially reduce their reproductive window (i.e., monandry, short lifespan, and the stage of egg development) are associated with the evolution of elaborate male antennae. Our hypothetical framework is that rapid location of a female would be favoured under female monandry, or when females eclose with a full complement of eggs (proovigeny): slower males may arrive after a female has mated and is no longer receptive, or after she has commenced ovipositing, and thus their sperm will fertilise fewer eggs ([Jervis et al., 2005](#); [Shuker, 2014](#)). We hypothesise that these female life-history traits would likely increase the level of competition among males and increase the strength of selection favouring elaborate antennae, because such antennae should increase the male's likelihood of locating the female more quickly.

Subsequently, we explore the links between male antennal morphology, female life-history and the evolution of female flightlessness. We specifically test the hypothesis proposed by [Hackman \(1966\)](#) that female flightlessness will be associated with the need for greater male sensitivity to sex pheromone, and hence with male elaborate antennae.

Materials and methods

Data collection

We collected information on female mating strategy, male antenna type, female flight ability, egg development, oviposition behaviour, lifespan, and fecundity for 93 species of moths from 11 superfamilies. The species were selected based on the availability of these data, which were collated from various sources including published literature, field guides and online lepidopterist resources (see [Table 1](#)).

We characterised male antennae as either simple or elaborate: the former is filiform or ciliate, whereas elaborate antennae have one or more side branches (pectinate, bipectinate, quadripectinate). Information on male antennae was obtained from published descriptions or images from various resources (see [Table 1](#) for a full list). Females were designated as capable of flying (macropterous) or flightless: flightless females may still have wings, but do not fly (e.g., *Lymantria dispar*) or may be brachypterous (small remnant wings) or apterous (wingless).

Mating strategies of females were classified as either monandrous or polyandrous, using information on female remating frequencies (mating frequency of males was not taken into account, as less information is available on this). Monandrous species are those with a remating frequency of 30% or less. This is a conservative value compared with rates previously used to categorise monandry [for example, <50% in [Arnqvist et al. \(2000\)](#), and <40% in [Torres-Vila et al. \(2002\)](#)]. Where detailed data on remating frequency were not available, we followed published qualitative descriptions of species as being either monandrous (including mostly monandrous) or polyandrous.

Females were classified as either synovigenic (continuing to form eggs during their adult life) or proovigenic (eclosing as an adult with a full complement of mature eggs). Species where females eclose with some mature eggs but produce more as an adult were classified as synovigenic. We also distinguished between females that oviposit eggs singly, in multiple small clutches of eggs, or in a single clutch. We then made this classification binary by combining the data for species in the latter two categories who did not lay eggs singly, as this was necessary for statistical analysis (see below). The fecundity and lifespan of the females were obtained from published papers, and we included the midpoint if a range was given. Fecundity was the total reported number of eggs laid over the lifespan. Female lifespan was the average number of days as an adult, as observed in natural field populations where possible. Finally, as body size may affect aspects of mating behaviour ([Blanckenhorn, 2000](#)) and male antennal morphology ([Symonds et al., 2012](#)), we also obtained measures of the maximum wingspan to use as a proxy for body size ([Miller, 1977, 1997](#)). We included male wingspan if the wingspan of both sexes were reported, and the midpoint of the range if a range was reported.

Phylogenetic comparative analysis

We used phylogenetic comparative methods to control for common ancestry ([Harvey and Pagel, 1991](#)) in our analysis of evolutionary associations between traits. There is no single phylogeny that incorporates all the species in our sample, and genetic data covering these species is sufficiently poor to make phylogenetic estimation unreliable. Following recommendations by [Beaulieu et al. \(2012\)](#), we compiled a composite phylogeny from the published phylogenies of the families included in our sample. The full tree, along with character mapping for binary traits, is presented in [Figure 1](#).

The main framework for the phylogeny was the superfamilial tree constructed by [Heikkilä et al. \(2015\)](#). The superfamilies Hepialoidea, Sesoidea, and Zygaenoidea each contained two species only, and so further resolution was not necessary. Any species from the same genus were also grouped together. We used the phylogeny from [Regier et al. \(2012b\)](#) to resolve relationships within the Pyraloidea. No further details were available for the Phycitinae family, leaving this group of eight species as a polytomy except for those species from the same genus, which were grouped together. The Tortricioidea were resolved to species level where possible following [Regier et al. \(2012a\)](#). Within the Tortricioidea, *Paralobesia viteana* was absent from all published phylogenies and therefore its position was left unresolved as a basal polytomy within this clade. The Archipini was also lacking detail on species from our analysis leaving those four species unresolved. [Sohn et al. \(2013\)](#) was used to fully resolve the Yponomeutoidea phylogeny, whereas [Löfstedt et al. \(1991\)](#) was used to resolve the three species in the genus *Yponomeuta*. The Bombycoidea phylogeny was taken from [Mutanen et al. \(2010\)](#). [Mutanen et al. \(2010\)](#) also provided further resolution to the Psychidae, although two species were missing rendering this group not fully resolved. [Yamamoto and Sota \(2007\)](#) and [Sihvonen et al. \(2011\)](#) were used to resolve the Geometroidea to subfamily, but no further details were available for all species present in our phylogeny leaving the six species of the Ennominae unresolved as well as the three species in the genus *Operophtera*. The Noctuidae were resolved using [Zahiri et al. \(2013\)](#), and the *Lymantria* phylogeny was taken from [Sutrisno \(2014\)](#). The superfamily Gracillariidae was fully resolved using the phylogeny from [Regier et al. \(2013\)](#). Relationships within the Gelechiidae were taken from [Kaila et al. \(2011\)](#) and [Heikkilä et al. \(2014\)](#).

In the absence of branch length information, all branches were assigned equal length (=1). The exception to this rule was cases where there remained uncertainty over the branching pattern; any polytomies were arbitrarily resolved but the resolved branches were assigned minimal branch lengths of 0.00001, giving them negligible weight in the analyses. This resolution was necessary because the phylogenetic comparative analysis approach requires fully dichotomously resolved phylogenies.

TABLE 1 Classification of species for traits examined.

Species	AS	FA	MS	ED	OB	LS	F	WS	References
<i>Acentria ephemerella</i>	S	F			B	1	180	12	3, 18, 28, 125
<i>Achroia grisella</i>	S	M	M			20		18.5	12, 27, 66, 107, 229
<i>Adoxophyes orana</i>	S	M	P		M		300	19.5	25, 156, 215, 222
<i>Alsophila pomataria</i>	S	F	M	P	B		100	27.5	37, 150, 171, 188
<i>Anarsia lineatella</i>	S	M			M	24	120	13.5	55, 87, 152, 194
<i>Auchmophila kordofensis</i>	E	F			B	21		30	133
<i>Austromusotima camptozonale</i>	S	M	M		M	5.7			24, 241
<i>Autographa gamma</i>	S	M			S	12	210	40	37, 85, 138, 230
<i>Biston betularia</i>	E	M		P	M		670	52.5	37, 106, 171
<i>Bupalus piniaria</i>	E	M			M	10	150	35	16, 44
<i>Cadra cautella</i>	S	M	P	S			200	17	12, 106, 124, 142, 143, 229
<i>Callimorpha (Panaxia) dominula</i>	S	M	M		S	6.25	250	48	50, 51, 71, 230
<i>Chilo suppressalis</i>	S	M	M			10	250	22	54, 108, 159, 160, 206
<i>Chloridea (Heliothis) virescens</i>	S	M	P	S	M		800	32	140, 164, 175, 201, 211, 215, 229
<i>Choristoneura fumiferana</i>	S	M	P	S	M		94	22.5	57, 184, 215, 225, 229
<i>Choristoneura rosaceana</i>	S	M	P	S			750		29, 57, 136
<i>“Cnephasia” jactatana</i>	S	M	P	S			137		109, 110, 111, 161
<i>Corcyra cephalonica</i>	S	M	M	S	S	8.2	160	17	68, 163, 189
<i>Cornutiplusia circumflexa</i>	S	M							129, 138, 185
<i>Cryptoblabes gnidella</i>	S	M	M	S	M	12.7	105	15	9, 100, 151, 238
<i>Cydia pomonella</i>	S	M	P	P	S	17	200	18.5	26, 96, 120, 229
<i>Dahlica lichenella</i>		F	M		B	10	70	15	64
<i>Dasystoma salicella</i>	S	F			M	10	440	18.5	48, 112, 174
<i>Desmia funeralis</i>	S	M			S	9	200	25	19
<i>Diparopsis castanea</i>		M	P	S	S	11.4	152	30	45, 106, 137
<i>Earias insulana</i>	S	M	P	S		7	300	16.5	8, 115, 116, 201, 203, 229
<i>Elcysma westwoodi</i>	E	M	M		M				121, 122
<i>Ephestia elutella</i>	S	M	P		M	21	175	17	10, 124, 189
<i>Ephestia kuehniella</i>	S	M	P	S	S	9	264	2.25	7, 106, 114, 124, 189, 208, 239
<i>Epiphyas postvittana</i>	S	M	P	S	M		400	18.5	25, 72, 73, 82, 110, 126, 215
<i>Epirrita autumnata</i>	S	M	M	P	S	10	150	35	5, 89, 197, 205, 207
<i>Etiella hobsoni</i>	S	M	M				65		63, 157
<i>Etiella zinckenella</i>	S	M	M	S		10	166	25	63, 88, 135, 229
<i>Euproctis chrysorrhoea</i>	E	M			M		200	37.5	37, 74, 80, 118, 139
<i>Euxoa messoria</i>	E	M	M	S	S	14.2	1,303	34	29, 43, 65, 106
<i>Grapholita molesta</i>	S	M	P		S	34	245	12.5	11, 26, 33, 62, 96, 167
<i>Helicoverpa (Heliothis) armigera</i>	S	M	P	S	S	9.75	380	35.5	52, 104, 158, 201, 229, 243
<i>Helicoverpa (Heliothis) punctigera</i>	S	M	P	S	S		1,400		201, 243
<i>Helicoverpa zea</i>	S		P	S	S	15	600	38.5	2, 49, 69, 119, 201, 229
<i>Heterogynis penella</i>	E	F			B				123, 220
<i>Homoeosoma electellum</i>		M	M	S		14	337	19	58, 144, 183
<i>Hyalophora cecropia</i>	E	M	M	P				135	38, 182, 216, 229, 233
<i>Lambdina fiscellaria</i>	E	M	M		S	22.5	200		91, 92, 153, 197, 236
<i>Leucoma salicis</i>	E	M	P		M	9.4	650	45	75, 80, 221, 226, 229
<i>Leucoptera coffeella</i>	S	M	M	S	M	14	75	6.5	83, 132, 147, 148
<i>Lobesia botrana</i>	S	M	M	S	S		100	12	26, 100, 213, 215
<i>Lymantria dispar*</i>	E	F	M	P	B	8	800	50	34, 42, 80, 181, 226, 229

(Continued)

TABLE 1 (Continued)

Species	AS	FA	MS	ED	OB	LS	F	WS	References
<i>Lymantria fumida</i>	E	M							99, 226
<i>Lymantria mathura</i>	E	M			M		375	45	56, 226
<i>Lymantria monacha</i>	E	M	M	P	M		190	45	37, 80, 106, 192, 226
<i>Lymantria obfuscata</i>	E	F	M		M	7.6	285	31.8	60, 84, 209, 226
<i>Lymantria xylina</i>	E	M			B		800		40, 195, 226
<i>Mamestra configurata</i>		M	P	S	M		2,150	40	97, 232
<i>Manduca sexta</i>	S	M		S	S		250	100	61, 117, 169, 229, 240
<i>Metisa plana</i>	E	F	M	P	B	7	155		177, 179
<i>Mnesampela privata</i>	S	M	M	S	M	11.8	300	41	196, 197, 201, 223, 224
<i>Mythimna separata</i>		M	P	S		6.5	850	35	94, 231
<i>Mythimna unipuncta</i>		M	P	S	M	14	1,500	40	32, 199
<i>Oiketicus kirbyi</i>	E	F	M		B		6,400		17, 177, 178
<i>Oncopera fasciculatus</i>	S	M	M		M		1,500		47, 131
<i>Operophtera bruceata</i>	S	F			S			27.5	75, 90, 170
<i>Operophtera brumata</i>	S	F	P	P	M	8.8	100	26.5	30, 90, 106, 218, 219, 229
<i>Operophtera fagata</i>	S	F						31.5	90, 193, 229
<i>Orgyia antiqua</i>	E	F	M	P	B	7	175	25	38, 106, 180, 204, 226
<i>Orgyia leucostigma</i>	E	F		P	B		167	32.5	38, 79, 204, 210
<i>Orgyia pseudotsugata</i>	E	F	M		B		180	34	67, 98, 200, 226
<i>Ostrinia nubilalis</i>	S	M	P	S	M	15	750	30	70, 106, 186, 229
<i>Paleacrita vernata</i>	E	F			M		251		29, 149, 171
<i>Panolis flammea</i>	S	M		S	M	11	100	36	106, 127, 128, 201
<i>Paralobesia viteana</i>	S	M			S	18.5	33	10	39, 100, 113
<i>Phigalia titea</i>	E	F			M		110	35	31, 53, 170, 171
<i>Phthorimaea operculella</i>	S	M	P	S	M	18.3	100	14	46, 134, 155, 229
<i>Platynota stultana</i>	S	M	M		M		307	12.5	22, 78, 81, 233, 234
<i>Plodia interpunctella</i>	S	M	P	S			80	15.5	7, 50, 76, 106, 124, 215, 229
<i>Plutella xylostella</i>	S	M	M	S	S	18.8	100	13	106, 202, 227, 229
<i>Siederia listerella</i>		F	M		B	10	50	15	64
<i>Sitotroga cerealella</i>		M	P		M	11.5	125	11.2	4, 189
<i>Sparganothis sulfureana</i>	S	M			M			20	59, 78, 168,
<i>Spodoptera exigua</i>	S	M	P	P	M	13.9	1,000	27.5	1, 37, 212, 214, 245
<i>Spodoptera littoralis</i>	S	M	P	S	M	16	1,800	38	6, 77, 115, 187, 229
<i>Spodoptera litura</i>	S		P	S	M		1,849	30	106, 141, 190, 245
<i>Sitthenopsis argenteomaculatus</i>	S	M						80	37
<i>Synanthedon pictipes</i>		M	M	S	S	9.2	140	24.5	106, 176, 237
<i>Teia anartoides</i>	E	F	M	P	B		400	25	41, 86, 198, Pers. Obs.
<i>Thyrocopa kikaelekea</i>	S	F							145
<i>Trichoplusia ni</i>	S	M	P	S	S	18	1,500	35.5	191, 228, 229, 242, 244, 245
<i>Utetheisa ornatrix</i>	S	M	P	S	M	17	350	37.5	23, 37, 101, 102, 103, 130
<i>Vitacea polistiformis</i>	E	M	M	P	S	7	350		21, 162, 166, 235
<i>Yponomeuta cagnagella</i>	S	M	P	S	M	50		23	13, 95, 146, 165, 217, 229
<i>Yponomeuta evonymella</i>	S	M			M	13			105, 146, 217
<i>Yponomeuta padella</i>	S	M	P		M	31			13, 93, 165, 173, 217

(Continued)

TABLE 1 (Continued)

Species	AS	FA	MS	ED	OB	LS	F	WS	References
<i>Zeiraphera canadensis</i>		M	M	S	M	28	79	13.5	35, 36, 154, 172
<i>Zeiraphera diniana</i>	S	M	M	S		30	150	19	14, 15, 20, 26

Male antennal structure (AS) = simple (S) or elaborate (E); Female flight ability (FA) = macropterous (M) or flightless (F); Female mating strategy (MS) = monandrous (M) or polyandrous (P); Egg development strategy (ED) = synovigenic (S) or proovigenic (P); Oviposition behaviour (OB) = single (S), multiple batches (M), or one batch (B); Lifespan of adult females (LS) = number of days; Fecundity (F) = number of eggs; Male wingspan (WS) = mm.

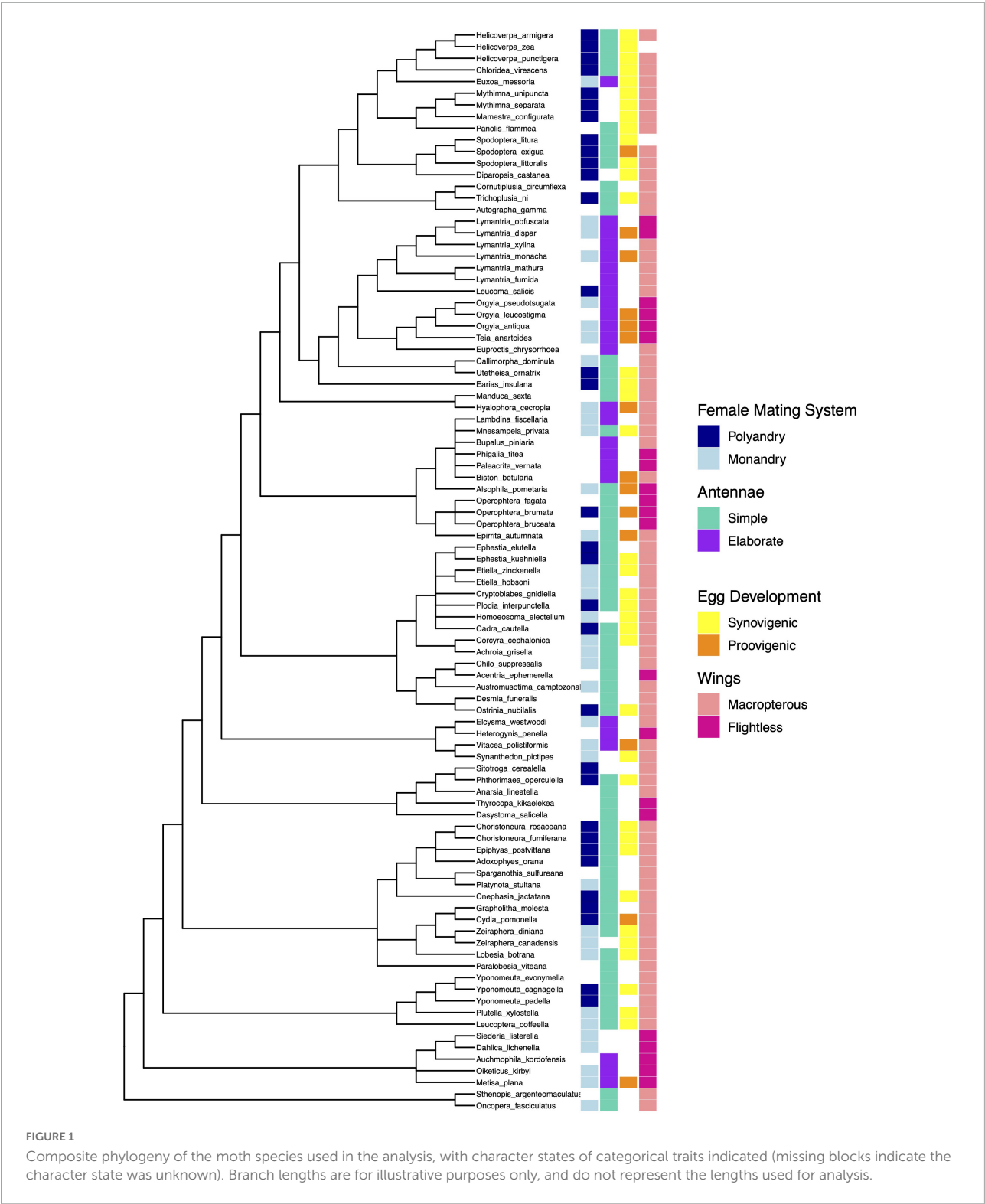
*The subspecies of *Lymantria dispar* used for this study was the European or North American spongy moth, which is flightless in nature and has the most available data.

¹Abdullah et al. (2000); ²Abernathy et al. (1994); ³Kipp et al. (2022); ⁴Akter et al. (2013); ⁵Ammunet et al. (2009); ⁶Anderson et al. (2007); ⁷Anderson and Lofqvist (1996); ⁸Anwar et al. (1973); ⁹Ascher et al. (1983); ¹⁰Ashworth (1993); ¹¹Atanassov and Shearer (2005); ¹²Australian moths online (2018) (moths.csiro.au); ¹³Bakker et al. (2008); ¹⁴Baltensweiler (1993); ¹⁵Baltensweiler and Fischlin (1988); ¹⁶Barbour (1988); ¹⁷Barnes (2002); ¹⁸Batra (1977); ¹⁹Bentley and Coviello (2012); ²⁰Benz (1969); ²¹Bergh (2012); ²²Bettiga (2013); ²³Bezzarides et al. (2008); ²⁴Boughton et al. (2007); ²⁵Bradley et al. (1973); ²⁶Bradley et al. (1979); ²⁷Brandt et al. (2005); ²⁸Buckingham and Ross (1981); ²⁹Bugguide (2017); ³⁰Buse and Good (1996); ³¹Butler (1985); ³²Capinera (2008); ³³Cardé and Baker (1984); ³⁴Cardé and Hagaman (1983); ³⁵Carroll (1994); ³⁶Carroll and Quiring (1993); ³⁷Carter (1984); ³⁸Carter (2004); ³⁹Cha et al. (2008); ⁴⁰Chao et al. (2001); ⁴¹Charles et al. (2006); ⁴²Charlton et al. (1993); ⁴³Cheng (1972); ⁴⁴Cheraghian (2013); ⁴⁵Chijikwa (2012); ⁴⁶Coll et al. (2000); ⁴⁷Common (1990); ⁴⁸Contant (1988); ⁴⁹Cook and Weinzierl (2004); ⁵⁰Cook and Gage (1995); ⁵¹Cook and Wedell (1999); ⁵²Coombs et al. (1993); ⁵³Covell (2005); ⁵⁴Cuong and Cohen (2003); ⁵⁵Damos and Savopoulou-Soulitani (2008); ⁵⁶European and Mediterranean Plant Protection Organization (2005); ⁵⁷Delisle et al. (2000); ⁵⁸DePew (1988); ⁵⁹Deutsch et al. (2015); ⁶⁰Dharmadhikari et al. (1985); ⁶¹Diamond et al. (2010); ⁶²Dustan (1964); ⁶³Edmonds et al. (2000); ⁶⁴Elzinga et al. (2011); ⁶⁵Encyclopedia of Life (2018) (eol.org); ⁶⁶Engqvist et al. (2014); ⁶⁷EPPO (2017); ⁶⁸Etman et al. (1988); ⁶⁹Evenden et al. (2003); ⁷⁰Fadamiro and Baker (1999); ⁷¹Fisher and Ford (1947); ⁷²Foster and Ayers (1996); ⁷³Foster and Howard (1999); ⁷⁴Frago et al. (2009); ⁷⁵Furniss and Carolin (1977); ⁷⁶Gage (1995); ⁷⁷Gerling and Schwartz (1974); ⁷⁸Gilligan and Epstein (2014); ⁷⁹Grant et al. (2014); ⁸⁰Grijpma et al. (1987); ⁸¹Groenen and Baixeras (2013); ⁸²Gu and Dathanarayana (2000); ⁸³Guerreiro Filho (2006); ⁸⁴Gupta and Tara (2013); ⁸⁵Haraki (1975); ⁸⁶Harris (1988); ⁸⁷Hart (2006); ⁸⁸Hattori and Sato (1983); ⁸⁹Haukioja and Neuvonen (1985); ⁹⁰Hausmann and Viidalepp (2012); ⁹¹Hébert and Brodeur (2013); ⁹²Hébert et al. (2003); ⁹³Hendrikse (1986); ⁹⁴Hirai (1984); ⁹⁵Horak and Roessingh (1999); ⁹⁶Horak and Komai (2006); ⁹⁷Howlader and Gerber (1986); ⁹⁸Hunter (1995); ⁹⁹Identification guide of Japanese Moths (2018) (jpmoth.org); ¹⁰⁰Ioriatti et al. (2012); ¹⁰¹Iyengar and Eisner (1999); ¹⁰²Iyengar and Eisner (2002); ¹⁰³Iyengar et al. (2002); ¹⁰⁴Jallow et al. (1999); ¹⁰⁵Javois et al. (2005); ¹⁰⁶Jervis et al. (2005); ¹⁰⁷Jia and Greenfield (1997); ¹⁰⁸Jiao et al. (2006); ¹⁰⁹Jiménez-Pérez and Wang (2004a); ¹¹⁰Jiménez-Pérez and Wang (2004b); ¹¹¹Jiménez-Pérez et al. (2002); ¹¹²Jonko (2004–2022); ¹¹³Jordan, 2014; ¹¹⁴Karalius and Būda (1995); ¹¹⁵Kehat and Gordon (1975); ¹¹⁶Kehat and Gordon (1977); ¹¹⁷Keil (1989); ¹¹⁸Kelly et al. (1988); ¹¹⁹Kingan et al. (1993); ¹²⁰Knight (2007); ¹²¹Koshio (1996); ¹²²Koshio et al. (2007); ¹²³Kristensen (2003); ¹²⁴Landcare Research (2018). Manaaki Whenua (www.landcareresearch.co.nz); ¹²⁵Lau et al. (2007); ¹²⁶Lawrence and Bartell (1972); ¹²⁷Leather (1984); ¹²⁸Leather (1994); ¹²⁹Lepiforum e. V. (2018). (lepiforum.org); ¹³⁰Lim and Greenfield (2008); ¹³¹Madge (1954); ¹³²Magalhaes et al. (2008); ¹³³Mahmoud (2015); ¹³⁴Makee and Saour (2001); ¹³⁵Malinen (2007); ¹³⁶Marcotte et al. (1992); ¹³⁷Marks (1976); ¹³⁸Mazor and Dunkelblum (2005); ¹³⁹Mazzei et al. (1999–2022); ¹⁴⁰Mbatia and Ramaswamy (1990); ¹⁴¹McCormack (2007); ¹⁴²McNamara et al. (2009a); ¹⁴³McNamara et al. (2009b); ¹⁴⁴McNeil and Delisle (1989); ¹⁴⁵Medeiros and Gillespie (2011); ¹⁴⁶Menken et al. (1992); ¹⁴⁷Michereff et al. (2007); ¹⁴⁸Michereff et al. (2004); ¹⁴⁹Millar et al. (1990); ¹⁵⁰Mitter and Klun (1987); ¹⁵¹Molet (2013); ¹⁵²Molinari and Zanrei (2004); ¹⁵³Moths of Canada (2016). Canadian Biodiversity Information Facility (2013–2017); ¹⁵⁴Mutuura and Freeman (1966); ¹⁵⁵Nabi and Harrison (1983); ¹⁵⁶Nagata et al. (1972); ¹⁵⁷Naito et al. (1986); ¹⁵⁸Naseri et al. (2009); ¹⁵⁹Moth Photographers Group (2020); ¹⁶⁰Nozato (1982); ¹⁶¹Ochieng–Odero (1992); ¹⁶²Olien et al. (1993); ¹⁶³Olsen (1995); ¹⁶⁴Park et al. (1998); ¹⁶⁵Parker et al. (2013); ¹⁶⁶Pearson et al. (2004); ¹⁶⁷Phillips and Proctor (1969); ¹⁶⁸Polavarapu et al. (2001); ¹⁶⁹Potter et al. (2011); ¹⁷⁰Powell and Opler (2009); ¹⁷¹Price (1997); ¹⁷²Quiring (1994); ¹⁷³Rajimann and Menken (2000); ¹⁷⁴Raine (1966); ¹⁷⁵Ramaswamy (1990); ¹⁷⁶Reed et al. (1988); ¹⁷⁷Rhainds and Gries (1998); ¹⁷⁸Rhainds et al. (1995); ¹⁷⁹Rhainds et al. (1999); ¹⁸⁰Richards et al. (1999); ¹⁸¹Richerson et al. (1976); ¹⁸²Riddiford and Ashenhurst (1973); ¹⁸³Riemann (1986); ¹⁸⁴Robison et al. (1998); ¹⁸⁵Ronkay and Behounek (2015); ¹⁸⁶Royer and McNeil (1993); ¹⁸⁷Sadek (2001); ¹⁸⁸Schneider (1980); ¹⁸⁹Sedlacek et al. (1995); ¹⁹⁰Seth and Sharma (2002); ¹⁹¹Shorey et al. (1962); ¹⁹²Skuhavy (1987); ¹⁹³Snäll et al. (2007); ¹⁹⁴Sorenson and Gunnell (1955); ¹⁹⁵St. Laurent and McCarthy (2016); ¹⁹⁶Steinbauer (2005); ¹⁹⁷Steinbauer et al. (2001); ¹⁹⁸Suckling et al. (2007); ¹⁹⁹Svard and McNeil (1994); ²⁰⁰Swaby et al. (1987); ²⁰¹Symonds et al. (2012); ²⁰²Talekar and Shelton (1993); ²⁰³Tamhankar (1995); ²⁰⁴Tammaru et al. (2002); ²⁰⁵Tammaru et al. (1996); ²⁰⁶Tang et al. (2014); ²⁰⁷Tanhuanpää et al. (2003); ²⁰⁸Tarlack et al. (2015); ²⁰⁹Thakur et al. (2016); ²¹⁰Thurston and MacGregor (2003); ²¹¹Tingle and Mitchell (1991); ²¹²Tisdale and Sappington (2001); ²¹³Torres-Vila et al. (2002); ²¹⁴Torres-Vila et al. (2001); ²¹⁵Torres-Vila et al. (2004); ²¹⁶Tuskes et al. (1996); ²¹⁷Van der Pers et al. (1980); ²¹⁸Van Dongen et al. (1998); ²¹⁹Van Dongen et al. (1999); ²²⁰Vegliante (2005); ²²¹Wagner and Leonard (1979); ²²²Walker (2005); ²²³Walker and Allen (2010); ²²⁴Walker and Allen (2011); ²²⁵Wallace et al. (2004); ²²⁶Wallner (1989); ²²⁷Wang et al. (2005); ²²⁸Ward and Landolt (1995); ²²⁹Watson et al. (1975); ²³⁰Watson and Dallwitz (2003–2022); ²³¹Watson and Hill (1985); ²³²WCCP (1995); ²³³Webster and Cardé (1984); ²³⁴Webster and Cardé (1982); ²³⁵Weihman (2005); ²³⁶West and Bowers (1994); ²³⁷Wong et al. (1969); ²³⁸Wysoki et al. (1993); ²³⁹Xu et al. (2008); ²⁴⁰Yamamoto and Sota (2007); ²⁴¹Yen et al. (2004); ²⁴²Zacharuk (1985); ²⁴³Zalucki et al. (1986); ²⁴⁴Zhu et al. (1997); ²⁴⁵Ziaee (2012).

Following Ives and Garland (2014), we ran multiple tests to improve the strength of our inferences. These tests included generalised linear mixed models with Bayesian estimation (MCMCglmm) (Hadfield and Nakagawa, 2010) and the concentrated changes test (Maddison, 1990). The MCMCglmm models were conducted using the MCMCglmm package in R (Hadfield, 2010; R Core Team, 2014). To determine which traits are linked to our dependent variables when controlling for phylogenetic relatedness, all independent variables of interest were tested using MCMCglmm in separate models where wingspan was included as the covariate to control for body size. Specifically we performed one set of tests with antennal morphology as the dependent variable, coded as simple (1) and elaborate (2) antennae. In these tests the independent variables were female mating system (monandrous/polyandrous), egg development (proovigenic/synovigenic), and lifespan. In the second set of tests the dependent variable was female wing type coded as macropterous (1) or flightless (2). In these tests the

independent predictors were female mating system, lifespan, antenna type, egg development, oviposition strategy (single eggs laid/multiple eggs clutches), and fecundity.

These models cannot incorporate missing data; therefore, the data sets were reduced to include only those species where all data were available for the variables being tested in each analysis. These tests require a prior to be set, and when the response variable is categorical in nature the prior for the residual variance should be fixed. For our analyses, we set the residual variance to 1 and used a χ^2 distribution with 1 degree of freedom ($v = 1$, $nu = 1000$, $alpha.mu = 0$, $alpha.V = 1$) for the random effects variance, as suggested by Villemereuil et al. (2013). We used the categorical family response, and used the slice function to improve mixing. To obtain adequate mixing with low autocorrelation, 5×10^7 iterations were used with a 10,000 burnin period, followed by sampling every 2,500 iterations (thinning). The R code used in this procedure is provided in the Supplementary material.



The Concentrate Changes Test (CCT) was used to investigate the co-evolution of two binary discrete characters across a phylogeny, using the computer program MacClade 4 (Maddison and Maddison, 2005). CCTs examine changes

from one state to another in a character of interest (the dependent variable) and whether these are more concentrated in lineages that have evolved a particular state of interest in another character (the independent variable) than would be

expected by chance (determined by comparison with 1,000 permutations of the dependent variable on the phylogeny). When characters are mapped onto the phylogeny, the most parsimonious reconstruction of the character is applied for all species, including those with missing data, allowing us to leave all 93 species in each analysis. CCTs require a fully resolved phylogeny and we used MacClade to randomly resolve any polytomies 20 times in our composite phylogeny, performing the analysis on each tree individually, thereby yielding a mean p -value \pm SEM. For each pair of traits, the tests were run in both directions, with the independent and dependent traits switched, to determine the order of evolution. We also applied the test only to changes where the parsimonious resolution of the evolution of the dependent was unequivocal. These tests lack the statistical power of MCMCglmm, and cannot control for body size, but unlike the MCMCglmm, they do provide information about the direction of evolution (i.e., which correlated trait preceded the evolution of the other), and possible patterns of causality.

Results

We found a significant association between antennal type and female mating system (MCMCglmm analysis: [Table 2](#)), with the concentrated changes test indicating weakly ($p = 0.062$) that elaborate male antennae evolve more frequently in species where females are monandrous (CCT analysis: [Table 3](#)). Indeed, most species in our analysis with elaborate male antennae have monandrous females, whereas most species with simple male antennae have polyandrous females ([Figure 2A](#)). Similarly, male antenna type is also associated with egg development pattern, with elaborate male antennae being associated with proovigenic females ([Table 2](#)). Indeed, within our sample of species with elaborate male antennae, only one is synovigenic, producing eggs as an adult ([Figure 2B](#)). However, the CCT analysis suggests (again weakly: $p = 0.081$) that proovigeny has evolved more frequently in species where males have elaborate antennae ([Table 3](#)). The type of male antennae was not associated with female lifespan ([Table 2](#)).

We found a link between female flight ability and male antenna type ([Table 2](#)), with the CCT analysis suggesting that female flightlessness is more likely to have evolved in species where males have elaborate antennae, rather than *vice versa* ([Table 3](#) and [Figure 3C](#)). Female flightlessness is also associated with a shorter female lifespan ([Table 2](#)), and the association between flight ability and oviposition strategy (single eggs vs. batches) approached significance in the MCMCglmm analysis ($p = 0.056$, [Table 2](#) and [Figure 3D](#)). The CCT results suggest that flightlessness has evolved more often in species where females lay eggs in clutches ([Table 3](#)). While all the flightless species in our sample are proovigenic ([Figure 3B](#)), the lack of transitions from synovigenic to proovigenic severely limits the power for the MCMCglmm analysis, and these analyses did

not converge, so we do not include these tests in our analysis. Although most flightless species have monoandrous females ([Figure 3A](#)), the phylogenetic comparative analyses found no significant association between female flight ability and mating system, or between flight ability and fecundity ([Tables 2, 3](#)).

Discussion

Prevailing wisdom states that elaborate antennae in males evolved to increase their ability to detect odours (specifically the sex pheromone of females). However, this hypothesis is contradicted by the considerable number of moth species where males do not possess elaborate antennae, despite most species utilising long-distance female sex pheromones. Our results suggest a more nuanced version of the hypothesis where ability to detect and locate females quickly is advantageous in some species: elaborate male antennae being more common in species where females are monandrous, proovigenic, or flightless. Concentrated changes tests indicate that it is more likely that the evolution of elaborate male antennae is concentrated lineages where females are monoandrous rather than *vice versa* (suggesting that the mating system evolved prior to the antennal morphology). Similarly, that the CCTs suggest that female flightlessness is more likely to have evolved in lineages where elaborate male antennae had already evolved rather than the opposite, which argues against the [Hackman \(1966\)](#) hypothesis that female flightlessness selects for males with more sensitive antennae. These trends provide some insights into the conditions leading to the evolution of both male elaborate antennae and female flightlessness, and more generally highlight how olfactory signal perception can be linked with movement.

[Darwin's \(1871\)](#) conjecture that sexual selection favours male sensory receptor traits that improve the ability to detect and locate females more quickly is supported by the strong association between complex male antennal structure and female monandry. Female monandry places a premium on males being able to rapidly locate virgin females, whose numbers may decline during the male's adult lifespan, and larger or more elaborate male antennae apparently facilitate this process [see also [Johnson et al. \(2017b\)](#)]. This interpretation implicitly assumes that elaborate antennae bestow greater sensory capabilities, and this has been widely assumed in previous analyses of antennal morphology in moths ([Symonds et al., 2012](#); [Javoš et al., 2019](#)). However, while elaborate antennae might facilitate the trapping of air flow and hence chemical compounds ([Loudon and Koehl, 2000](#)), the direct evidence that they have higher sensitivity is surprisingly rare. In this context exceptions to the patterns outlined above can be informative. For example, selection may still favour elaborate male antennae in the polyandrous satin moth *Leucoma salicis* because females initially oviposit a large clutch of eggs, and subsequently lay smaller clutches ([Wagner and Leonard, 1979](#)),

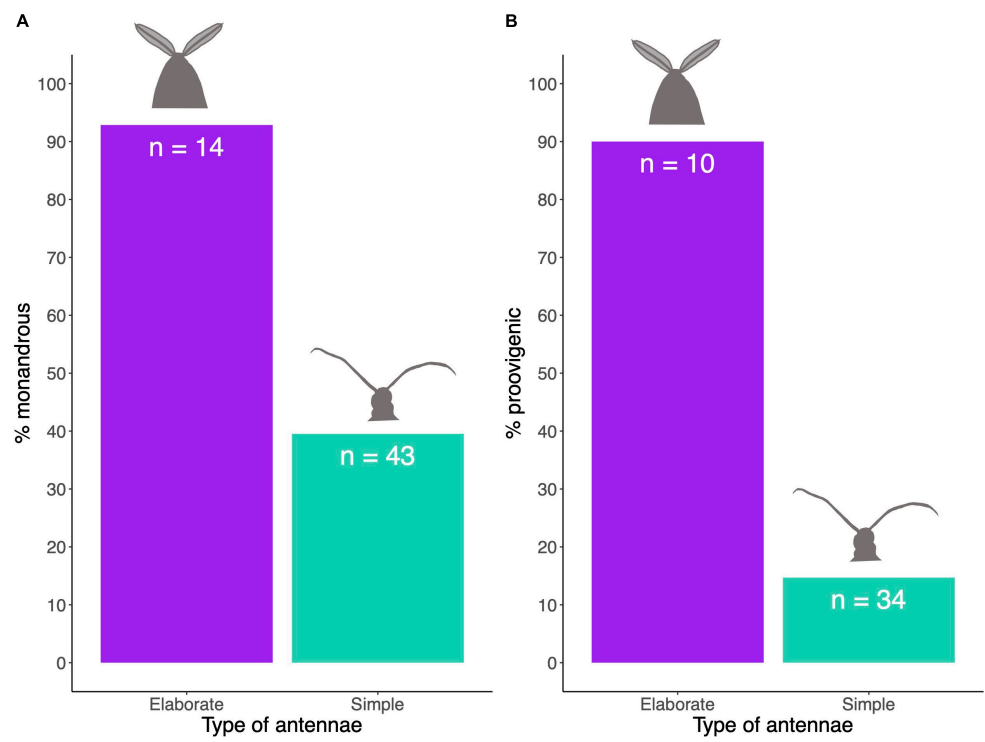


FIGURE 2
(A,B) Percentage of species with particular traits relative to the type of male antennae.

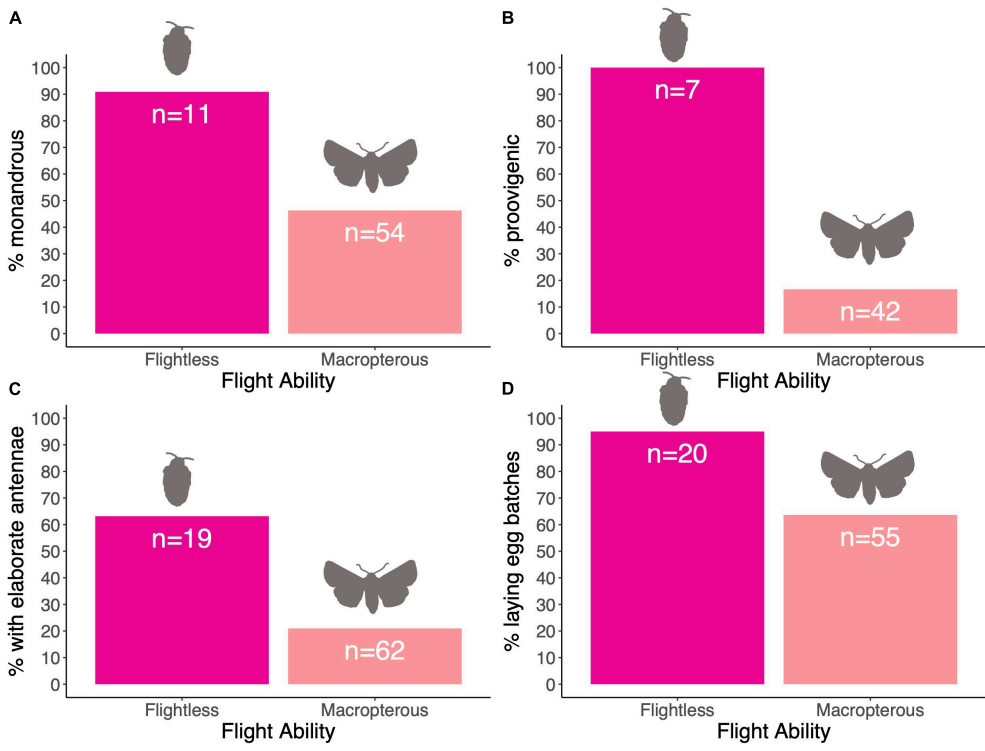


FIGURE 3
(A–D) Percentage of species with particular traits relative to the flight ability of female.

TABLE 2 Results from the MCMCglmm analysis comparing the dependent variable (male antennal type, female wing type) to the independent variable, controlling for body size (male wingspan).

Dependent variable	Independent variable	N		Posterior mean	95% CI	P-value
Male antennae—Simple (1), Elaborate (2)	Female mating system—Monandry (1), Polyandry (2)	45	Mating	−6.17	−13.69, 0.43	0.043
			WSpan	0.22	−0.01, 0.50	0.017
	Egg development—Synovigenic (1), Proovigenic (2)	39	EggDevel	7.59	1.02, 15.57	0.005
			WSpan	0.10	−0.02, 0.24	0.051
Female wing type—Macropterous (1), Flightless (2)	Female lifespan	40	Lifespan	−0.15	−0.53, 0.20	0.410
			WSpan	0.16	−0.05, 0.39	0.112
	Female mating system—Monandry (1), Polyandry (2)	53	Mating	−3.39	−8.78, 1.36	0.155
			WSpan	−0.16	−0.41, 0.04	0.115
	Female lifespan	48	Lifespan	−0.64	−1.29, −0.06	0.005
			WSpan	−0.002	−0.23, 0.23	0.979
	Male antennae—Simple (1), Elaborate (2)	62	Antennae	5.21	0.02, 10.92	0.028
			WSpan	−0.20	−0.43, −0.01	0.014
	Oviposition—Single eggs (1), Egg batches (2)	60	Oviposition	4.47	−0.47, 10.3	0.056
			WSpan	−0.17	−0.40, 0.04	0.08
	Fecundity	64	Fecundity	−0.002	−0.01, 0.01	0.556
			WSpan	−0.16	−0.39, 0.04	0.113

Each categorical variable was given a value (1 or 2) according to the state (e.g., polyandry = 2 and monandry = 1). N values for each model are listed. The model of wing type vs. egg development is not included due to lack of transitions with which to adequately test the relationship. Bold values indicate statistically significant relationships.

TABLE 3 Results from the concentrated changes test investigating evolutionary associations between discrete characters with the state of interest listed.

Character 1	Character 2	p-value ± SE (Character 1 = dependent)	p-value ± SE (Character 2 = dependent)
Male antennae—Elaborate	Female mating system—Monandry	0.062 ± 0.004	0.317 ± 0.008
	Egg development—Proovigenic	0.159 ± 0.011	0.081 ± 0.002
Female wing type—Macropterous	Female mating system—Monandry	0.093 ± 0.004	0.957 ± 0.002
	Male antennae—Elaborate	0.052 ± 0.003	0.676 ± 0.027
	Oviposition—Egg batches	0.076 ± 0.005	0.983 ± 0.001

Results are presented where characters are assigned as dependent or independent, and then *vice versa*. The p-value ± SE corresponds to the mean p-value obtained from the analysis of the 20 randomly resolved trees. N = 93 in all tests.

which places a premium on males locating virgin females. In this context, it is interesting that there is a relationship between egg development strategy and male antennal morphology, with proovigeny (where females eclose with their full complement of eggs) being associated with elaborate male antennae.

Although the large majority (>90%) of species with elaborate male antennae have monandrous females, males have filiform antennae in 17 of the 30 monandrous species in our sample. In these species, perhaps males with filiform antennae utilise other means of improving sensitivity in detecting female pheromones. For example, detectability may be improved by increasing the number and/or density of sensilla, changing the distribution of the sensilla (Keil, 1989; Lee and Strausfeld, 1990), or adjusting the angle of antennal scales (Wang et al., 2018). Additionally, features of the adult population, such as high population density (Symonds et al., 2012) or male flight speed, may relax selection on rapid detection. Finally,

male mating system may also affect the evolution of antennal morphology, although the nature of the relationship between typical male mating frequency and the strength of selection for greater detection capacity seems unlikely to be independent of other factors, including female mating strategy. Consequently it may be that it is overall mating strategy (monogamy vs. polygamy) that is the stronger determinant of selection on male antennal morphology.

Female flightlessness is thought to allow females to invest more resources in egg production, thereby yielding higher fecundity (Tweedie, 1976; Roff, 1990; Sattler, 1991). Our analyses revealed that female flightlessness is associated with a shorter adult lifespan and confining oviposition to a single clutch of eggs, an unsurprising pattern because laying eggs singly or across multiple clutches would require an ability to disperse to different oviposition sites (Sattler, 1991). However, there was no significant correlation between female

flightlessness and fecundity after controlling for phylogeny and body size. Hunter (1995) reported a positive correlation between female flightlessness and fecundity, but this pattern was phylogenetically constrained, and the correlation was no longer significant after taking account of phylogeny. Our analysis supports that finding. Nevertheless, we cannot rule out the possibility that females can improve reproductive success by increasing egg size rather than egg number. Indeed, the flight ability of female tussock moth *Orgyia thyellina* varies seasonally: individuals eclosing in autumn have reduced wings whilst those emerging in summer have fully functional wings (Kimura and Masaki, 1977). The flightless females produce much larger eggs than females that emerge in summer, a strategy that may improve the survival of eggs that diapause over winter. Males of *O. thyellina* have elaborate, bipectinate antennae (Table 1), and it would be interesting to know if there is a similar seasonal pattern in antennal size.

While our data broadly support the idea that the presence of elaborate antennae in males favoured the evolution of female flightlessness, there are seven species within our data set where females are flightless, and yet males have simple, filiform antennae (Figure 3). Interestingly, females in five of these species are still mobile, either by walking or hopping (Contant, 1988; Sattler, 1991; Medeiros and Gillespie, 2011), and females of the other two species have unusual biological features. Females of *Acentria ephemerella* are aquatic and the loss of flight is likely to be an adaptation that supports this lifestyle (Miler, 2008), highlighting that the evolution of female flightlessness is not linked exclusively with issues associated with mate search. The second species indicates that the strength of selection through mate search can override the relationship between elaborate antennae and flightlessness: around 80% of *Alsophila pometaria* females are pseudogamous asexuals (Mitter and Klun, 1987), who produce asexual offspring after mating, resulting in a strongly female-biased population. So, while the loss of flight has likely evolved due to similar pressures affecting other species in our data set, the pseudogamous nature of this species may relax selection favouring elaborate male antennae.

To conclude, our findings suggest that the communication and mating systems of moths are inherently associated, with elaborate male antennae being associated with lineages where females are monandrous, suggesting that necessity to detect females quickly has selected for more sensitive males. In turn male elaborate antennae may have subsequently driven the evolution of female life-history and flightlessness where having sensitive males promoted selection for complete development of eggs at the expense of movement capability. A key aspect of this narrative is that elaborate antennae in males is associated with greater sensitivity, an assumption that still needs to be more thoroughly tested in moths.

Data availability statement

The original contributions presented in this study are included in the article/Supplementary material, further inquiries can be directed to the corresponding authors.

Author contributions

TJ assembled the comparative data set. TJ and MS conducted the comparative statistical analyses. All authors conceived and designed the research, interpreted the data, prepared and edited the manuscript, and approved the submitted version.

Funding

We thank the Australian Research Council (DP0987360) for financial support.

Acknowledgments

We thank Nina Wedell and the late Matthew Gage for their helpful comments on an earlier version of this manuscript.

Conflict of interest

The authors declare that the research was conducted in the absence of any commercial or financial relationships that could be construed as a potential conflict of interest.

Publisher's note

All claims expressed in this article are solely those of the authors and do not necessarily represent those of their affiliated organizations, or those of the publisher, the editors and the reviewers. Any product that may be evaluated in this article, or claim that may be made by its manufacturer, is not guaranteed or endorsed by the publisher.

Supplementary material

The Supplementary Material for this article can be found online at: <https://www.frontiersin.org/articles/10.3389/fevo.2022.919093/full#supplementary-material>

References

- Abdullah, M., Sarnthoy, O., Chaeychomsri, S., and Sarnthoy, O. (2000). Comparative study of artificial diet and soybean leaves on growth, development and fecundity of beet armyworm, *Spodoptera exigua* (Hübner) (Lepidoptera: Noctuidae). *Nat. Sci.* 34, 339–344.
- Abernathy, R. L., Teal, P. E. A., and Tumlinson, J. H. (1994). Age and crowding affects the amount of sex pheromone and the oviposition rates of virgin and mated females of *Helicoverpa zea* (Lepidoptera: Noctuidae). *Ann. Entomol. Soc. Am.* 87, 350–354. doi: 10.1093/aesa/87.3.350
- Akter, T., Jahan, M., and Bhuiyan, M. (2013). Biology of the angoumois grain moth, *Sitotroga cerealella* (Oliver) on stored rice grain in laboratory condition. *J. Asia. Soc. Bangladesh Sci.* 39, 61–67. doi: 10.3329/jasbs.v39i1.16034
- Ammunet, T., Klemola, N., Heisswolf, A., and Klemola, T. (2009). Larval parasitism of the autumnal moth reduces feeding intensity on the mountain birch. *Oecologia* 159, 539–547. doi: 10.1007/s00442-008-1240-6
- Anderson, P., and Lofqvist, J. (1996). Asymmetric oviposition behaviour and the influence of larval competition in the two pyralid moths *Ephesia kuehniella* and *Plodia interpunctella*. *Oikos* 76, 47–56. doi: 10.2307/3545747
- Anderson, P., Hansson, B. S., Nilsson, U., Han, Q., Sjöholm, M., Skals, N., et al. (2007). Increased behavioral and neuronal sensitivity to sex pheromone after brief odor experience in a moth. *Chem. Senses* 32, 483–491. doi: 10.1093/chemse/bjm017
- Andersson, M. (1994). *Sexual Selection*. New Jersey, NJ: Princeton University Press.
- Anwar, M., Ashraf, M., and Arif, M. D. (1973). Mating, oviposition and gamma sterilization of the spotted bollworm of cotton, *Earias insulana*. *Entomol. Exp. Appl.* 16, 478–482. doi: 10.1111/j.1570-7458.1973.tb00299.x
- Arnqvist, G., Edvardsson, M., Friberg, U., and Nilsson, T. (2000). Sexual conflict promotes speciation in insects. *Proc. Nat. Acad. Sci. U S A.* 97, 10460–10464. doi: 10.1073/pnas.97.19.10460
- Ascher, K. R. S., Eliyahu, M., Gurevitz, E., and Renneh, S. (1983). Rearing the honeydew moth, *Cryptoblabes gnidiella*, and the effect of diflubenzuron on its eggs. *Phytoparasitica* 11, 195–198. doi: 10.1007/BF02980691
- Ashworth, J. R. (1993). The biology of *Ephesia elutella*. *J. Stored Prod. Res.* 29, 199–205. doi: 10.1016/0022-474X(93)90001-K
- Atanassov, A., and Shearer, P. W. (2005). Peach extrafloral nectar impacts life span and reproduction of adult *Grapholita molesta* (Busck) (Lepidoptera: Tortricidae). *J. Agri. Urban Entomol.* 22, 41–47.
- Australian moths online (2018). *CSIRO Australia*. Available online at: <https://moths.csiro.au> (accessed September 2018).
- Bakker, A. C., Roessingh, P., and Menken, S. B. J. (2008). Sympatric speciation in Yponomeuta: no evidence for host plant fidelity. *Entomol. Exp. Appl.* 128, 240–247. doi: 10.1111/j.1570-7458.2008.00684.x
- Baltensweiler, W. (1993). A contribution to the explanation of the larch bud moth cycle, the polymorphic fitness hypothesis. *Oecologia* 93, 251–255. doi: 10.1007/BF00317678
- Baltensweiler, W., and Fischlin, A. (1988). “The larch budmoth in the alps,” in *Dynamics of Forest Insect Populations*, ed. A. Berryman, (Berlin: Springer). doi: 10.1007/978-1-4899-0789-9_17
- Barbour, D. A. (1988). The pine looper in Britain and Europe,” in *Dynamics of Forest Insect Populations*, ed. A. Berryman, (Berlin: Springer). doi: 10.1007/978-1-4899-0789-9_15
- Barnes, M. J. C. (2002). *Moths of the Grenadines*. Available online at <http://www.mbarnes.force9.co.uk/grenadinesmoths/grenadineshome.htm>.
- Batra, S. W. T. (1977). Bionomics of the aquatic moth *Acentropus niveus*, a potential biological control agent for Eurasian water milfoil and Hydrilla. *J. N. Y. Entomol. Soc.* 85, 143–152.
- Beaulieu, J. M., Ree, R. H., Cavender-Bares, J., Weiblen, G. D., and Donoghue, M. J. (2012). Synthesizing phylogenetic knowledge for ecological research. *Ecology* 93, S4–S13. doi: 10.1890/11-0638.1
- Bentley, W. J., and Coviello, R. L. (2012). “Leaf-Eating lepidoptera in north american vineyards,” in *Arthropod Management in Vineyards*, ed N. J. Bostanian, C. Vincent, and R. Isaacs, (Berlin: Springer). doi: 10.1007/978-94-007-4032-7_13
- Benz, G. (1969). Influence of mating, insemination, and other factors on oögenesis and oviposition in the moth *Zeiraphera diniana*. *J. Insect Physiol.* 15, 55–71. doi: 10.1016/0022-1910(69)90212-1
- Bergh, J. C. (2012). “Grape root borer,” in *Arthropod Management in Vineyards*, ed N. J. Bostanian, C. Vincent, and R. Isaacs. (Berlin: Springer). doi: 10.1007/978-94-007-4032-7_16
- Bettiga, L. J. (2013). *Grape Pest Management*. Oakland, CA: UCANR Publications.
- Bezerides, A. L., Iyengar, V. K., and Eisner, T. (2008). Female promiscuity does not lead to increased fertility of fecundity in an Arctiid moth (*Utetheisa ornatrix*). *J. Insect Behav.* 21, 213–221. doi: 10.1007/s10905-008-9121-8
- Blanckenhorn, W. U. (2000). The evolution of body size: what keeps organisms small? *Q. Rev. Biol.* 75, 385–407. doi: 10.1086/393620
- Boughton, A. J., Wu, J., and Pemberton, R. W. (2007). Mating biology of *Austromusotima camptozonale* (Lepidoptera: Crambidae), a potential biological control agent of Old World climbing fern, *Lygodium microphyllum* (Schizaeaceae). *Florida Entomol.* 90, 509–517. doi: 10.1653/0015-4040(2007)90[509:MBOACL]2.0.CO;2
- Bradley, J. D., Tremewan, W. G., and Smith, A. (1973). *British Tortricoid Moths – Cochylidae and Tortricidae: Tortricinae*. London: The Ray Society.
- Bradley, J. D., Tremewan, W. G., and Smith, A. (1979). *British tortricid moths, Tortricidae: Olethreutinae*. London: The Ray Society.
- Brandt, L. S. E., Ludwar, B. C., and Greenfield, M. D. (2005). Co-occurrence of preference functions and acceptance thresholds in female choice: mate discrimination in the lesser wax moth. *Ethology* 111, 609–625. doi: 10.1111/j.1439-0310.2005.01085.x
- Buckingham, G. R., and Ross, B. M. (1981). Notes on the biology and host specificity of *Acentria nivea* (= *Acentropus niveus*). *J. Aqua. Plant Manag.* 19, 32–36.
- Bugguide (2017). *Iowa state university*. Available online at: <https://bugguide.Net> (accessed September 2018).
- Buse, A., and Good, J. (1996). Synchronization of larval emergence in winter moth (*Operophtera brumata* L.) and budburst in pedunculate oak (*Quercus robur* L.) under simulated climate change. *Ecol. Entomol.* 21, 335–343. doi: 10.1046/j.1365-2311.1996.t01-1-00001.x
- Butler, L. (1985). Biology of the half-wing geometer, *Phigalia titea* Cramer (Geometridae), as a member of a looper complex in West Virginia. *J. Lep. Soc.* 39, 177–186.
- Capinera, J. L. (2008). “Armyworm, *Pseudaletia unipuncta* (Haworth) (Lepidoptera: Noctuidae),” in *Encyclopedia of Entomology*, ed. J. P. Capinera, (Berlin: Springer). doi: 10.1007/978-1-4020-6359-6
- Cardé, R. T., and Baker, T. C. (1984). “Sexual communication with pheromones,” in *Chemical Ecology of Insects*, eds W. J. Bell, and R. T. Cardé, (London: Chapman and Hall Ltd), 355–383. doi: 10.1007/978-1-4899-3368-3_13
- Cardé, R. T., and Hagaman, T. E. (1983). Influence of ambient and thoracic temperatures upon sexual behaviour of the gypsy moth, *Lymantria dispar*. *Physiol. Entomol.* 8, 7–14. doi: 10.1111/j.1365-3032.1983.tb00327.x
- Carroll, A. L. (1994). Interactions between body size and mating history influence the reproductive success of males of a tortricid moth, *Zeiraphera canadensis*. *Can. J. Zool.* 72, 2124–2132. doi: 10.1139/z94-284
- Carroll, A. L., and Quiring, D. T. (1993). Interactions between size and temperature influence fecundity and longevity of a tortricid moth, *Zeiraphera canadensis*. *Oecologia* 93, 233–241. doi: 10.1007/BF00317676
- Carter, D. J. (1984). *Pest Lepidoptera of Europe: with Special Reference to the British Isles*. Dordrecht: Dr W. Junk Publishers.
- Carter, N. E. (2004). *Status of forest Pests in New Brunswick in 2003*. Fredericton, NB: New Brunswick Department of Natural Resources.
- Cha, D. H., Nojima, S., Hesler, S. P., Zhang, A., Linn, C. E. Jr, Roelofs, W. L., et al. (2008). Identification and field evaluation of grape shoot volatiles attractive to female grape berry moth (*Paralobesia viteana*). *J. Chem.Ecol.* 34, 1180–1189. doi: 10.1007/s10886-008-9517-0
- Chao, J. T., Lu, S. S., Chen, Y. M., Jaung, L. M., Koh, C. N., and Yeh, W. C. (2001). How fecund is *Lymantria xyliana* Swinhoe (Lepidoptera: Lymantriidae) in Taiwan? *Taiwan J. Forest Sci.* 16, 259–266.
- Charles, J. G., Kean, J. M., and Chhagan, A. (2006). Developmental parameters and voltinism of the painted apple moth, *Teia anartoides* (Lepidoptera: Lymantriidae) in New Zealand. *New Zealand Entomol.* 29, 27–36. doi: 10.1080/00779962.2006.9722138

- Charlton, R. E., Kanno, H., Collins, R. D., and Cardé, R. T. (1993). Influence of pheromone concentration and ambient temperature on flight of the gypsy moth, *Lymantria dispar*, in a sustained-flight wind tunnel. *Physiol. Entomol.* 18, 349–362. doi: 10.1111/j.1365-3032.1993.tb00608.x
- Cheng, H. (1972). Oviposition and longevity of the dark-sided cutworm, *Euxoa messoria* (Lepidoptera: Noctuidae), in the laboratory. *Can. Entomol.* 104, 919–925. doi: 10.4039/Ent104919-6
- Cheraghian, A. (2013). “Pine moth *Bupalus piniarius* Linnaeus Lepidoptera: geometridae,” in *A Guide for Diagnosis Detection Of Quarantine Pests*. (Islamic Republic of Iran: Bureau of Plant Pest Surveillance and Pest Risk Analysis).
- Chijikwa, M. (2012). “Effects of intercropping systems on incidence and damage to cotton by *Diaparopsis castanea* Hampson (Lepidoptera: Actiidae),” in *Magoye, Mazabuka District of Zambia*. M.Sc. thesis, University Of Zambia: Zambia.
- Coll, M., Gavish, S., and Dori, I. (2000). Population biology of the potato tuber moth, *Plthorimaea operculella* (Lepidoptera: Gelechiidae), in two potato cropping systems in Israel. *Bull. Entomol. Res.* 90, 309–315. doi: 10.1017/S0007485300000432
- Common, I. F. B. (1990). *Moths of Australia*. Melbourne, Vic: Melbourne University Press.
- Contant, H. (1988). *Modification of Microclimate by the Blueberry Leaf-tier, Cheimophila salicella (Hbn.) (Lepidoptera: Oecophoridae)*. M.Sc. thesis, University of British Columbia: Vancouver, BC.
- Cook, K. A., and Weinzierl, R. (2004). *Corn earworm (Helicoverpa zea). Insect Fact Sheet. Integrated Pest Management*. Champaign, IL: University of Illinois.
- Cook, P. A., and Gage, M. J. (1995). Effects of risks of sperm competition on the numbers of eupyrene and apyrene sperm ejaculated by the moth *Plodia interpunctella* (Lepidoptera: Pyralidae). *Behav. Ecol. Sociobiol.* 36, 261–268. doi: 10.1007/BF00165835
- Cook, P. A., and Wedell, N. (1999). Non-fertile sperm delay female remating. *Nature* 397, 486–486. doi: 10.1038/17257
- Coombs, M., Del Socorro, A., Fitt, G., and Gregg, P. (1993). The reproductive maturity and mating status of *Helicoverpa armigera*, *H. punctigera* and *Mythimna convecta* (Lepidoptera: Noctuidae) collected in tower-mounted light traps in northern New South Wales, Australia. *Bull. Entomol. Res.* 83, 529–534. doi: 10.1017/S000748530003995X
- Covell, C. V. J. (2005). *A Field Guide to Moths of Eastern North America*. Martinsville, VA: Virginian Museum of Natural History.
- Cuong, N., and Cohen, M. (2003). Mating and dispersal behaviour of Scirpophaga incertulas and *Chilo suppressalis* (Lepidoptera: Pyralidae) in relation to resistance management for rice transformed with *Bacillus thuringiensis* toxin genes. *Int. J. Pest Manag.* 49, 275–279. doi: 10.1080/0967087031000101052
- Damos, P., and Savopoulou-Soulani, M. (2008). Temperature-dependent bionomics and modeling of *Anarsia lineatella* (Lepidoptera: Gelechiidae) in the laboratory. *J. Econ. Entomol.* 101, 1557–1567. doi: 10.1093/jeet/101.5.1557
- Darwin, C. (1871). *The Descent of Man and Selection in Relation to Sex*. London: Murray. doi: 10.5962/bhl.title.2092
- Delisle, J., Picimbon, J. -F., and Simard, J. (2000). Regulation of pheromone inhibition in mated females of *Choristoneura fumiferana* and *C. rosaceana*. *J. Insect Physiol.* 46, 913–921. doi: 10.1016/S0022-1910(99)00198-5
- DePew, L. J. (1988). “Insecticides for control of sunflower moth larvae on sunflower,” in *Keeping up with Research 95* (Manhattan, NY: Agricultural Experimental Station, Kansas State University). doi: 10.4148/2378-5977.7304
- Deutsch, A. E., Rodriguez-Saona, C. R., Zalapa, J. E., and Steffan, S. A. (2015). Temperature-mediated development thresholds of *Sparganothis sulfureana* (Lepidoptera: Tortricidae) in cranberries. *Environ. Entomol.* 44, 400–405. doi: 10.1093/ee/nvu062
- Dharmadhikari, P. R., Ramaseshiah, G., and Achan, P. D. (1985). Survey of *Lymantria obfuscata* and its natural enemies in India. *Entomophaga* 30, 399–408. doi: 10.1007/BF02372346
- Diamond, S. E., Hawkins, S. D., Nijhout, H. F., and Kingsolver, J. G. (2010). Evolutionary divergence of field and laboratory populations of *Manduca sexta* in response to host-plant quality. *Ecol. Entomol.* 35, 166–174. doi: 10.1111/j.1365-2311.2009.01166.x
- Dustan, G. (1964). Mating behaviour of the oriental fruit moth, *Grapholitha molesta* (Busck) (Lepidoptera: Olethreutidae). *Can. Entomol.* 96, 1087–1093. doi: 10.4039/Ent961087-8
- Edmonds, R. P., Borden, J. H., Angerilli, N. P. D., and Rauf, A. (2000). A comparison of the developmental and reproductive biology of two soybean pod borers, *Etiella* spp. in Indonesia. *Entomol. Exp. Appl.* 97, 137–147. doi: 10.1046/j.1570-7458.2000.00724.x
- Elgar, M. A., Johnson, T. L., and Symonds, M. R. E. (2019). Sexual selection and organs of sense: Darwin's neglected insight. *Anim. Biol.* 69, 63–82. doi: 10.1163/15707563-00001046
- Elgar, M. A., Zhang, D., Wang, Q., Wittwer, B., Pham, H., Johnson, T. L., Freeland, C. B., Coquilleau, M. (2018). Insect antennal morphology: the evolution of diverse solutions to odorant perception. *Yale J. Biol. Med.* 91, 457–469.
- Elzinga, J. A., Chevasco, V., Grapputo, A., and Mappes, J. (2011). Influence of male mating history on female reproductive success among monandrous Naryciinae (Lepidoptera: Psychidae). *Ecol. Entomol.* 36, 170–180. doi: 10.1111/j.1365-2311.2010.01258.x
- Encyclopedia of Life (2018). Available online at: <http://eol.org> (accessed September 2018).
- Engqvist, L., Cordes, N., Schwenniger, J., Bakhtina, S., and Schmoll, T. (2014). Female remating behavior in a lekking moth. *Ethology* 120, 662–671. doi: 10.1111/eth.12237
- EPPO (2017). *Data Sheets on Quarantine Pests: Orgyia pseudotsugata*. Paris: EPPO.
- Etman, A., El-Sayed, F., Eesa, N., and Moursy, L. (1988). Laboratory studies on the development, survival, mating behaviour and reproductive capacity of the rice moth, *Corcyra cephalonica* (Stainton) (Lep., Galleriidae). *J. Appl. Entomol.* 106, 232–240. doi: 10.1111/j.1439-0418.1988.tb00588.x
- European and Mediterranean Plant Protection Organization (2005). *Lymantria mathura*. *EPPO Bull.* 35, 464–467. doi: 10.1111/j.1365-2338.2005.00875.x
- Evenden, M. L., Delury, L. E., Judd, G. J. R., and Borden, J. H. (2003). Assessing the mating status of male obliquebanded leafrollers *Choristoneura rosaceana* (Lepidoptera: Tortricidae) by dissection of male and female moths. *Ann. Ent. Soc. Am.* 96, 217–224. doi: 10.1603/0013-8746(2003)096[0217:ATMSOM]2.0.CO;2
- Fadamiro, H. Y., and Baker, T. C. (1999). Reproductive performance and longevity of female european corn borer, *Ostrinia nubilalis*: effects of multiple mating, delay in mating, and adult feeding. *J. Insect Physiol.* 45, 385–392. doi: 10.1016/S0022-1910(98)00137-1
- Fisher, R. A., and Ford, E. B. (1947). The spread of a gene in natural conditions in a colony of the moth *Panaxia dominula*. *Heredity* 1, 143–174. doi: 10.1038/hdy.1947.11
- Foster, S. P., and Ayers, R. H. (1996). Multiple mating and its effects in the lightbrown apple moth, *Epiphyas postvittana* (Walker). *J. Insect Physiol.* 42, 657–667. doi: 10.1016/0022-1910(96)00012-1
- Foster, S. P., and Howard, A. J. (1999). The effects of source dosage, flight altitude, wind speed, and ground pattern on the sex pheromone-mediated flight manoeuvres of male lightbrown apple moth, *Epiphyas postvittana* (Walker). *N. Z. J. Zool.* 26, 97–104. doi: 10.1080/03014223.1999.9518181
- Frago, E., Selfa, J., Pujade-Villar, J., Guara, M., and Baucé, É. (2009). Age and size thresholds for pupation and developmental polymorphism in the browntail moth, *Euproctis chrysorrhoea* (Lepidoptera: Lymantriidae), under conditions that either emulate diapause or prevent it. *J. Insect Physiol.* 55, 952–958. doi: 10.1016/j.jinsphys.2009.06.013
- Furness, R. L., and Carolin, V. M. (1977). *Western Forest Insects*. Washington, D.C.: US Department of Agriculture, Forest Service. doi: 10.5962/bhl.title.131875
- Gage, M. J. G. (1995). Continuous variation in reproductive strategy as an adaptive response to population density in the moth *Plodia interpunctella*. *Proc. Roy. Soc. B* 261, 25–30. doi: 10.1098/rspb.1995.0112
- Gerling, D., and Schwartz, A. (1974). Host selection by *Telenomus remus*, a parasite of Spodoptera littoralis eggs. *Entomol. Exp. Appl.* 17, 391–396. doi: 10.1111/j.1570-7458.1974.tb00357.x
- Gilligan, T. M., and Epstein, M. E. (2014). *Platynota stultana* factsheet. *Tortricids Agricultural Importance*. Available online at https://idtools.org/id/leps/tortai/Platynota_stultana.htm (accessed March 2022).
- Grant, G. G., Liu, W., Slessor, K. N., and Abou-Zaid, M. M. (2006). Sustained production of the labile pheromone component, (Z,Z)-6,9-Heneicosadien-11-one, from a stable precursor for monitoring the whitemarked tussock moth. *J. Chem. Ecol.* 32, 1731–1741. doi: 10.1007/s10886-006-9105-0
- Grijpma, P., Belde, J. J. M., and van der Werf, D. C. (1987). Artificial diets and rearing of the nun moth, *Lymantria monacha*. *Entomol. Exp. Appl.* 45, 219–225. doi: 10.1111/j.1570-7458.1987.tb01087.x
- Groenen, F., and Baixeras, J. (2013). The “Omnivorous Leafroller”, *Platynota stultana* Walsingham, 1884 (Tortricidae: Sparganothini), a new moth for Europe. *Nota Lepidop.* 36, 53–55.
- Gu, H. N., and Danthararayana, W. (2000). Variations in life history traits and flight capacity among populations of the light brown apple moth *Epiphyas postvittana* (Walker) (Lepidoptera : Tortricidae). *Austral Ecol.* 25, 571–579. doi: 10.1046/j.1442-9993.2000.01056.x

- Guerreiro Filho, O. (2006). Coffee leaf miner resistance. *Brazilian J. Plant Physiol.* 18, 109–117. doi: 10.1590/S1677-04202006000100009
- Gupta, R., and Tara, J. S. (2013). Biological studies of I Walker (Lepidoptera: Lymantriidae) on apple plantations (*Malus domestica* Borkh.) in Jammu region of J and K, India. *Munis Entomol. Zool.* 8, 749–755.
- Hackman, W. (1966). On wing reduction and loss of wings in *Lepidoptera*. *Notu. Entomol.* 46, 1–16.
- Hadfield, J. D. (2010). MCMC methods for multi-response generalized linear mixed models: the MCMCglmm R package. *J. Stat. Soft.* 33, 1–22. doi: 10.18637/jss.v033.i02
- Hadfield, J. D., and Nakagawa, S. (2010). General quantitative genetic methods for comparative biology: phylogenies, taxonomies and multi-trait models for continuous and categorical characters. *J. Evol. Biol.* 23, 494–508. doi: 10.1111/j.1420-9101.2009.01915.x
- Hansson, B. S. (1995). Olfaction in *Lepidoptera*. *Experientia* 51, 1003–1027. doi: 10.1007/BF01946910
- Harakly, F. A. (1975). Biological studies on the loopers *Autographa gamma* (L.) and *Cornutiplusia circumflexa* (L.) (Lep., Noctuidae) infesting truck crops in Egypt. *J. Appl. Entomol.* 78, 285–290. doi: 10.1111/j.1439-0418.1975.tb04182.x
- Harris, A. (1988). A first record of the painted apple moth *Teia anartoides* (Lepidoptera: Lymantriidae) intercepted in New Zealand. *N. Z. Entomol.* 11, 68–70. doi: 10.1080/00779962.1988.9722540
- Hart, M. (2006). *The Role of Sonic Signals in the Sexual Communication of Peach Twig Borer, Anarsia lineatella, Zeller (Lepidoptera: Gelechiidae)*. M.Sc. thesis, Biological Sciences Department, Simon Fraser University: Burnaby, BC.
- Harvey, P. H., and Pagel, M. D. (1991). *The Comparative Method in Evolutionary Biology*. Oxford: Oxford University Press.
- Hattori, I., and Sato, A. (1983). Mating and oviposition of the limabean pod borer, *Etiella zinckenella* (Lepidoptera: Pyralidae). *Appl. Entomol. Zool.* 18, 511–516. doi: 10.1303/aez.18.511
- Haukioja, E., and Neuvonen, S. (1985). The relationship between size and reproductive potential in male and female *Epirrita autumnata* (Lep., Geometridae). *Ecol. Entomol.* 10, 267–270. doi: 10.1111/j.1365-2311.1985.tb00723.x
- Hausmann, A., and Viidalepp, J. (2012). *Larentinae I*. Denmark: Apollo Books. doi: 10.1163/9789004260979
- Hébert, C., and Brodeur, J. (2013). “*Lambdina fiscellaria* (Guenée), hemlock looper (Lepidoptera: Geometridae),” in *Biological Control Programmes in Canada 2001–2012*, eds P. G. Mason and D. R. Gillespie, (Wallingford: CABI International), 203–207. doi: 10.1079/9781780642574.0203
- Hébert, C., Jobin, L., Auger, M., and Dupont, A. (2003). Oviposition traps to survey eggs of *Lambdina fiscellaria* (Lepidoptera: Geometridae). *J. Econ. Entomol.* 96, 768–776. doi: 10.1093/jee/96.3.768
- Heikkilä, M., Mutanen, M., Kekkonen, M., and Kaila, L. (2014). Morphology reinforces proposed molecular phylogenetic affinities: a revised classification for Gelechioidea (Lepidoptera). *Cladistics* 30, 563–589. doi: 10.1111/cla.12064
- Heikkilä, M., Mutanen, M., Wahlberg, N., Sihvonen, P., and Kaila, L. (2015). Elusive ditrysian phylogeny: an account of combining systematized morphology with molecular data (Lepidoptera). *BMC Evol. Biol.* 15:260. doi: 10.1186/s12862-015-0520-0
- Hendrikse, A. (1986). The courtship behaviour of *Yponomeuta padellus*. *Entomol. Exp. Appl.* 42, 45–55. doi: 10.1111/j.1570-7458.1986.tb02186.x
- Hirai, K. (1984). Migration of *Pseudaletia separata* Walker (Lepidoptera: Noctuidae): considerations of factors affecting time of taking-off and flight period. *Appl. Entomol. Zool.* 19, 422–429. doi: 10.1303/aez.19.422
- Hora, K. H., and Roessingh, P. (1999). Oviposition in *Yponomeuta cagnagellus*: the importance of contact cues for host plant acceptance. *Physiol. Entomol.* 24, 109–120. doi: 10.1046/j.1365-3032.1999.00120.x
- Horak, M., and Komai, F. (2006). *Olethreutine Moths of Australia (Lepidoptera: Tortricidae)*. Melbourne, Vic: CSIRO Publishing. doi: 10.1071/9780643094086
- Howlader, M. A., and Gerber, G. H. (1986). Effects of age, egg development, and mating on calling behaviour of the bertha armyworm, *Mamestra configurata* (Lepidoptera: Noctuidae). *Can. Entomol.* 118, 1221–1230. doi: 10.4039/Ent1181221-12
- Hunter, A. F. (1995). The ecology and evolution of reduced wings in forest macrolepidoptera. *Evol. Ecol.* 9, 275–287. doi: 10.1007/BF01237773
- Identification guide of Japanese Moths (2018). Available online at: <http://www.jpmoth.org>.
- Ioriatti, C., Lucchi, A., and Varela, L. G. (2012). “Grape berry moths in western European vineyards and their recent movement into the New World,” in *Arthropod Management in Vineyards*, eds N. J. Bostanian, C. Vincent, and R. Isaacs, (Berlin: Springer). doi: 10.1007/978-94-007-4032-7_14
- Ives, A. R., and Garland, T. Jr. (2014). “Phylogenetic regression for binary dependent variables,” in *Modern Phylogenetic Comparative Methods and Their Application in Evolutionary Biology*, ed. L. Z. Garamszegi, (Berlin: Springer). doi: 10.1007/978-3-662-43550-2_9
- Iyengar, V. K., and Eisner, T. (1999). Heritability of body mass, a sexually selected trait, in an arctiid moth (*Utetheisa ornatrix*). *Proc. Natl. Acad. Sci. U S A.* 96, 9169–9171. doi: 10.1073/pnas.96.16.9169
- Iyengar, V. K., and Eisner, T. (2002). Parental body mass as a determinant of egg size and egg output in an arctiid moth (*Utetheisa ornatrix*). *J. Insect Behav.* 15, 309–318.
- Iyengar, V. K., Reeve, H. K., and Eisner, T. (2002). Paternal inheritance of a female moth's mating preference. *Nature* 419, 830–832. doi: 10.1038/nature01027
- Jallow, M. F., Zalucki, M. P., and Fitt, G. P. (1999). Role of chemical cues from cotton in mediating host selection and oviposition behaviour in *Helicoverpa armigera* (Hübner) (Lepidoptera: Noctuidae). *Aust. J. Entomol.* 38, 359–366. doi: 10.1046/j.1440-6055.1999.00131.x
- Javoš, J., Davis, R. B., and Tammaru, T. (2019). A comparative morphometric study of sensory capacity in geometrid moths. *J. Evol. Biol.* 32, 380–389. doi: 10.1111/jeb.13422
- Javoš, J., Tammaru, T., and Käär, M. (2005). Oviposition in an eruptive moth species, *Yponomeuta evonymellus*, is insensitive to the population density experienced during the larval period. *Entomol. Exper. Applic.* 115, 379–386. doi: 10.1111/j.1570-7458.2005.00265.x
- Jervis, M. A., Boggs, C. L., and Ferns, P. N. (2005). Egg maturation strategy and its associated trade-offs: a synthesis focusing on Lepidoptera. *Ecol. Entomol.* 30, 359–375. doi: 10.1111/j.0307-6946.2005.00712.x
- Jia, F. Y., and Greenfield, M. D. (1997). When are good genes good? variable outcomes of female choice in wax moths. *Proc. R. Soc. B* 264, 1057–1063. doi: 10.1098/rspb.1997.0146
- Jiao, X., Xuan, W., and Sheng, C. (2006). Effects of delayed mating and male mating history on longevity and reproductive performance of the rice stem borer, *Chilo suppressalis* (Walker) (Lep., Pyralidae). *J. Appl. Entomol.* 130, 108–112. doi: 10.1111/j.1439-0418.2006.01036.x
- Jiménez-Pérez, A., and Wang, Q. (2004a). Effect of body weight on reproductive performance in *Cnephasia jactatana* (Lepidoptera: Tortricidae). *J. Insect Behav.* 17, 511–522. doi: 10.1023/B:JOIR.0000042538.19559.09
- Jiménez-Pérez, A., and Wang, Q. (2004b). Sexual selection in *Cnephasia jactatana* (Lepidoptera: Tortricidae) in relation to age, virginity, and body size. *Ann. Entomol. Soc. 97*, 819–824. doi: 10.1603/0013-8746(2004)097[0819:SSICJL]2.0.CO;2
- Jiménez-Pérez, A., Wang, Q., and Markwick, N. P. (2002). Adult activity patterns of *Cnephasia jactatana* (Lepidoptera: Tortricidae). *N. Z. Plant Protect.* 55, 374–379. doi: 10.30843/nzpp.2002.55.3935
- Johansson, B. G., and Jones, T. M. (2007). The role of chemical communication in mate choice. *Biol. Rev.* 82, 265–289. doi: 10.1111/j.1469-185X.2007.0009.x
- Johnson, T. L., Symonds, M. R. E., and Elgar, M. A. (2017a). Anticipatory flexibility: larval population density in moths determines male investment in antennae, wings and testes. *Proc. R. Soc. B* 284:20172087. doi: 10.1098/rspb.2017.2087
- Johnson, T. L., Symonds, M. R. E., and Elgar, M. A. (2017b). Sexual selection on receptor organ traits: younger females attract males with longer antennae. *Sci. Nat.* 104:44. doi: 10.1007/s00114-017-1466-4
- Jonko, C. (2004–2022). *Lepidoptera mundi*. Available online at: <https://lepidoptera.eu> (accessed March 2022).
- Jordan, T. A. (2014). *Surveillance of Grape Berry Moth, Paralobesia viteana Clemens (Lepidoptera: Tortricidae), in Virginia vineyards*. Ph.D. thesis, Virginia Polytechnic Institute and State University: Blacksburg, VA.
- Kaila, L., Mutanen, M., and Nyman, T. (2011). Phylogeny of the mega-diverse Gelechioidea (Lepidoptera): adaptations and determinants of success. *Mol. Phylo. Evol.* 61, 801–809. doi: 10.1016/j.ympev.2011.08.016
- Karalius, V., and Būda, V. (1995). Mating delay effect on moths' reproduction: correlation between reproduction success and calling activity in female *Ephesia kuehniella*, *Cydia pomonella*, *Yponomeuta cagnagellus* (Lepidoptera: Pyralidae). *Pheromones* 5, 169–190.

- Kehat, M., and Gordon, D. (1975). Mating, longevity, fertility and fecundity of the cotton leaf-worm, *Spodoptera littoralis* (Boisd.) (Lepidoptera: Noctuidae). *Phytoparasitica* 3, 87–102. doi: 10.1007/BF03158291
- Kehat, M., and Gordon, D. (1977). Mating ability, longevity and fecundity of the spiny bollworm, *Earias insulana* (Lepidoptera: Noctuidae). *Entomol. Exp. Appl.* 22, 267–273. doi: 10.1111/j.1570-7458.1977.tb02716.x
- Keil, T. A. (1989). Fine structure of the pheromone-sensitive sensilla on the antenna of the hawkmoth, *Manduca sexta*. *Tissue Cell* 21, 139–151. doi: 10.1016/0040-8166(89)90028-1
- Kelly, P. M., Sterling, P. H., Speight, M. R., and Entwistle, P. F. (1988). Preliminary spray trials of a nuclear polyhedrosis virus as a control agent for the brown-tail moth, *Euproctis chrysorrhoea* (L.) (Lepidoptera: Lymantriidae). *Bull. Entomol. Res.* 78, 227–234. doi: 10.1017/S0007485300012992
- Kimura, T., and Masaki, S. (1977). Brachypterism and seasonal adaptation in *Orgyia thyellina* (Lepidoptera, Lymantriidae). *Kontyû* 45, 97–106.
- Kingan, T. G., Thomas-Laemont, P. A., and Raina, A. K. (1993). Male accessory gland factors elicit change from 'virgin' to 'mated' behaviour in the female corn earworm moth *Helicoverpa zea*. *J. Exp. Biol.* 183, 61–76. doi: 10.1242/jeb.183.1.61
- Kipp, R. M., Larson, J., and Fusaro, A. (2022). *Acentria ephemerella* Olivier, 1791, U.S. Ann Arbor, MI: Geological Survey, Nonindigenous Aquatic Species Database, Gainesville, FL, and NOAA Great Lakes Aquatic Nonindigenous Species Information System.
- Knight, A. L. (2007). Multiple mating of male and female codling moth (Lepidoptera: Tortricidae) in apple orchards treated with sex pheromone. *Environ. Entomol.* 36, 157–164. doi: 10.1603/0046-225X(2007)36[157:MMOMAF]2.0.CO;2
- Koshio, C. (1996). Reproductive behaviour of the white-tailed zygaenid moth, *Elcysma westwoodii* (Lepidoptera, Zygaenidae). 2. Female mating strategy. *J. Ethol.* 14, 21–25. doi: 10.1007/BF02350088
- Koshio, C., Muraji, M., Tatsuta, H., and Kudo, S. (2007). Sexual selection in a moth: effect of symmetry on male mating success in the wild. *Behav. Ecol.* 18, 571–578. doi: 10.1093/beheco/arm017
- Kristensen, N. P. (2003). *Lepidoptera, Moths and Butterflies Morphology, Physiology, and Development*. Berlin: Walter de Gruyter.
- Landcare Research (2018). *Manaaki Whenua*. Lincoln: Landcare Research
- Lau, T. F. S., Gross, E. M., and Meyer-Rochow, V. B. (2007). Sexual dimorphism and light/dark adaptation in the compound eyes of male and female *Acentria ephemerella* (Lepidoptera: Pyraloidea: Crambidae). *Eur. J. Entomol.* 104, 459–470. doi: 10.14411/eje.2007.066
- Lawrence, L. A., and Bartell, R. J. (1972). The effect of age on calling behaviour of virgin females of *Epiphyas postvittana* (Lepidoptera) and on their pheromone content and ovarian development. *Entomol. Exp. Appl.* 15, 455–464. doi: 10.1111/j.1570-7458.1972.tb00233.x
- Leather, S. R. (1984). The effect of adult feeding on the fecundity, weight loss and survival of the pine beauty moth, *Panolis flammea*. *Oecologia* 65, 70–74. doi: 10.1007/BF00384464
- Leather, S. R. (1994). The effect of temperature on oviposition, fecundity and egg hatch in the pine beauty moth, *Panolis flammea* (Lepidoptera: Noctuidae). *Bull. Entomol. Res.* 84, 515–520. doi: 10.1017/S0007485300032752
- Lee, J. -K., and Strausfeld, N. J. (1990). Structure, distribution and number of surface sensilla and their receptor cells on the olfactory appendage of the male moth *Manduca sexta*. *J. Neurocytol.* 19, 519–538. doi: 10.1007/BF01257241
- Lepiforum e. V. (2018). *Bestimmung von Schmetterlingen (Lepidoptera) und ihren Praimaginalstadien*. Available online at: <https://lepiforum.org> (accessed September 2018).
- Lim, H., and Greenfield, M. D. (2008). Female arctiid moths, *Utetheisa ornatrix*, orient towards and join pheromonal choruses. *Anim. Behav.* 75, 673–680. doi: 10.1016/j.anbehav.2007.07.021
- Löfstedt, C., Herrebut, W. M., and Menken, S. B. (1991). Sex pheromones and their potential role in the evolution of reproductive isolation in small ermine moths (Yponomeutidae). *Chemoecology* 2, 20–28. doi: 10.1007/BF01240662
- Loudon, C., and Koehl, M. A. R. (2000). Sniffing by a silkworm moth: wing fanning enhances air penetration through and pheromone interception by antennae. *J. Exp. Biol.* 203, 2977–2990. doi: 10.1242/jeb.203.19.2977
- Maddison, D. R., and Maddison, W. P. (2005). *MacClade 4, Analysis of Phylogeny and Character Evolution. Version 4.08a*.
- Maddison, W. P. (1990). A method for testing the correlated evolution of two binary characters: are gains or losses concentrated on certain branches of a phylogenetic tree? *Evolution* 44, 539–557. doi: 10.1111/j.1558-5646.1990.tb05937.x
- Madge, P. (1954). A field study on the biology of the underground grass caterpillar, *Oncopera fasciculata* (Walker) (Lepidoptera: Hepialidae), in South Australia. *Aust. J. Zool.* 2, 193–204. doi: 10.1071/ZO9540193
- Magalhaes, S. T. V., Guedes, R. N. C., Demuner, A. J., and Lima, E. R. (2008). Effect of coffee alkaloids and phenolics on egg-laying by the coffee leaf miner *Leucoptera coffeella*. *Bull. Entomol. Res.* 98, 483–489. doi: 10.1017/S0007485308005804
- Mahmoud, M. E. E. (2015). *Host Range, Behaviour, Natural Enemies and Control of the Acacia Bagworm (Auchmophila kordofensis Rebele) in North Kordofan (Sudan)*. M.Sc. thesis, University of Khartoum: Khartoum.
- Makee, H., and Saour, G. (2001). Factors influencing mating success, mating frequency, and fecundity in *Phthorimaea operculella* (Lepidoptera: Gelechiidae). *Environ. Entomol.* 30, 31–36. doi: 10.1603/0046-225X-30.1.31
- Malinen, P. (2007). *Etiella zinckenella*. Available online at: <http://www.insects.fi> (accessed September 2018).
- Marcotte, M., Delisle, J., and McNeil, J. N. (2006). Impact of male mating history on the postmating resumption of sexual selection receptivity and lifetime reproductive success in *Choristoneura rosaceana* females. *Physiol. Entomol.* 31, 227–233. doi: 10.1111/j.1365-3032.2006.00510.x
- Marks, R. (1976). Mating behaviour and fecundity of the red bollworm *Diparopsis castanea* Hmps. (Lepidoptera Noctuidae). *Bull. Entomol. Res.* 66, 145–158. doi: 10.1017/S0007485300006568
- Mazor, M., and Dunkelblum, E. (2005). Circadian rhythms of sexual behavior and pheromone titers of two closely related moth species *Autographa gamma* and *Cornutiplusia circumflexa*. *J. Chem. Ecol.* 31, 2153–2168. doi: 10.1007/s10886-005-6082-7
- Mazzei, P., Morel, D., and Panfili, R. (1999–2022). *Moths and Butterflies of Europe and North Africa*. Available online at: <https://www.leps.it> (accessed March 2022).
- Mbata, G. N., and Ramaswamy, S. B. (1990). Rhythmicity of sex pheromone content in female *Heliothis virescens*: impact on mating. *Physiol. Entomol.* 15, 423–432. doi: 10.1111/j.1365-3032.1990.tb00531.x
- McCormack, G. (2007). *Cook Island Biodiversity Database*. Rarotonga: Cook Island Natural Heritage Trust.
- McNamara, K. B., Elgar, M. A., and Jones, T. M. (2009a). Adult responses to larval population size in the Almond moth, *Cadra cautella*. *Ethology* 116, 39–46. doi: 10.1111/j.1439-0310.2009.01714.x
- McNamara, K. B., Elgar, M. A., and Jones, T. M. (2009b). Large spermatophores reduce female receptivity and increase male paternity success in the almond moth, *Cadra cautella*. *Anim. Behav.* 77, 931–936. doi: 10.1016/j.anbehav.2009.01.007
- McNeil, J. N., and Delisle, J. (1989). Host plant pollen influences calling behavior and ovarian development of the sunflower moth, *Homoeosoma electellum*. *Oecologia* 80, 201–205. doi: 10.1007/BF00380151
- Medeiros, M. J., and Gillespie, R. G. (2011). Biogeography and the evolution of flightlessness in a radiation of Hawaiian moths (Xyloryctidae: Thyrocopa). *J. Biogeog.* 38, 101–111. doi: 10.1111/j.1365-2699.2010.02402.x
- Menken, S. B., Herrebut, W., and Wiebes, J. (1992). Small ermine moths (Yponomeuta): their host relations and evolution. *Ann. Rev. Entomol.* 37, 41–66. doi: 10.1146/annurev.en.37.010192.000353
- Michereff, M. F. F., Filho, M. M., and Vilela, E. F. (2007). Mating behavior of the coffee leaf-miner *Leucoptera coffeella* (Lepidoptera: Lyonetiidae). *Neotropical Entomol.* 36, 376–382. doi: 10.1590/S1519-566X2007000300005
- Michereff, M. F. F., Vilela, E. F., Michereff, M., Nery, D. M. S., and Thiebaut, J. T. (2004). Effects of delayed mating and male mating history on the reproductive potential of *Leucoptera coffeella* (Lepidoptera: Lyonetiidae). *Agric. Forest Entomol.* 6, 241–247. doi: 10.1111/j.1461-9555.2004.00227.x
- Miler, O. (2008). *The Aquatic Moth Acentria ephemerella as a Key Species in Submerged Aquatic Vegetation: Direct and Trait-mediated Interactions with Predators and Food Plants*. Ph.D thesis, University of Konstanz: Konstanz.
- Millar, J. G., Giblin, M., Barton, D., Reynard, D. A., Neill, G. B., and Underhill, E. W. (1990). Identification and field testing of female-produced sex pheromone components of the spring cankerworm, *Paleacrita vernata* Peck (Lepidoptera: Geometridae). *J. Chem. Ecol.* 16, 3393–3409. doi: 10.1007/BF00982106
- Miller, W. E. (1977). Wing measure as a size index in Lepidoptera: the family Olethreutidae. *Ann. Entomol. Soc. Amer.* 70, 253–256. doi: 10.1093/aesa/70.2.253
- Miller, W. E. (1997). Body weight as related to wing measure in hawkmoths (Sphingidae). *Lepid. Soc.* 51, 91–92.
- Mitter, C., and Klun, J. (1987). Evidence of pheromonal constancy among sexual and asexual females in a population of fall cankerworm, *Alsophila pometaria* (Lepidoptera: Geometridae). *J. Chem. Ecol.* 13, 1823–1831. doi: 10.1007/BF01013231

- Molet, T. (2013). *CPHST Pest Datasheet for Cryptoblabes gnidiella*. Washington, D.C: USDA-APHIS-PPQ-CPHST.
- Molinari, F., and Zanrei, O. (2004). Studies on some developmental parameters of *Anarsia lineatella* Zell. reared on artificial diet. *IOBC WPRS Bull.* 27, 29–36.
- Moth Photographers Group (2020). Available online at: <http://mothphotographersgroup.msstate.edu> (accessed March 2022).
- Moths of Canada (2016). *Canadian biodiversity information facility*. Available online at: <https://www.cbif.gc.ca> (accessed December 2016).
- Murlis, J., Elkinton, J. S., and Carde, R. T. (1992). Odor plumes and how insects use them. *Ann. Rev. Entomol.* 37, 505–532. doi: 10.1146/annurev.en.37.010192.002445
- Mutanen, M., Wahlberg, N., and Kaila, L. (2010). Comprehensive gene and taxon coverage elucidates radiation patterns in moths and butterflies. *Proc. R. Soc. Lond. B* 277, 2839–2848. doi: 10.1098/rspb.2010.0392
- Mutuura, A., and Freeman, T. N. (1966). The North American species of the genus *Zeiraphera*. *J. Res. Lep.* 5, 153–176. doi: 10.5962/p.266928
- Nabi, M., and Harrison, R. (1983). Activity of sperm and fertility in the potato moth, *Phthorimaea operculella*. *J. Insect Physiol.* 29, 431–435. doi: 10.1016/0022-1910(83)90071-9
- Nagata, K., Tamaki, Y., Noguchi, H., and Yushima, T. (1972). Changes in sex pheromone activity in adult females of the smaller tea tortrix moth *Adoxophyes fasciata*. *J. Insect Physiol.* 18, 339–346. doi: 10.1016/0022-1910(72)90132-1
- Naito, A., Iqbal, A., and Hattori, I. (1986). Notes on the morphology and distribution of *Etiella hobsoni* (Butler), a new soybean podborer in Indonesia, with special reference to comparisons with *Etiella zinckenella* (Treitschke) (Lepidoptera: Pyralidae). *Appl. Entomol. Zool.* 21, 81–88. doi: 10.1303/aez.21.81
- Naseri, B., Fathipour, Y., Moharramipour, S., and Hosseiniaveh, V. (2009). Comparative life history and fecundity of *Helicoverpa armigera* (Hubner) (Lepidoptera: Noctuidae) on different soybean varieties. *Entomol. Sci.* 12, 147–154. doi: 10.1111/j.1479-8298.2009.00310.x
- Nozato, K. (1982). Effect of group size, and silicate fertilizer application on the population density of *Chilo suppressalis* Walker (Lepidoptera: Pyralidae). *Japanese J. Entomol. Zool.* 26, 242–248.
- Ochieng-Odero, J. (1992). The effect of three constant temperatures on larval critical weight, latent feeding period, larval maximal weight and fecundity of *Cnephasia jactatana* (Walker) (Lepidoptera: Tortricidae). *J. Insect Physiol.* 38, 127–130. doi: 10.1016/0022-1910(92)90041-B
- Olien, W. C., Smith, B. J., and Hegwood C. P. Jr (1993). Grape root borer: a review of the life cycle and strategies for integrated control. *HortScience* 28, 1154–1156. doi: 10.21273/HORTSCI.28.12.1154
- Olsen, A. R. (1995). “Moths (Insecta: Lepidoptera),” in *Fundamentals of Microanalytical Entomology: A Practical Guide to Detecting and Identifying Filth in Foods*, ed A. Olsen (Boca Raton, FL: CRC Press).
- Park, Y. I., Ramaswamy, S. B., and Srinivasan, A. (1998). Spermatophore formation and regulation of egg maturation and oviposition in female *Heliothis virescens* by the male. *J. Insect Physiol.* 44, 903–908. doi: 10.1016/S0022-1910(98)00065-1
- Parker, G. A., Lessells, C. M., and Simmons, L. W. (2013). Sperm competition games: a general model for precopulatory male–male competition. *Evolution* 67, 95–109. doi: 10.1111/j.1558-5646.2012.01741.x
- Pearson, G. A., Dillery, S., and Meyer, J. R. (2004). Modelling intra-sexual competition in a sex pheromone system: how much can female movement affect female mating success? *J. Theor. Biol.* 231, 549–555. doi: 10.1016/j.jtbi.2004.07.010
- Pham HT, McNamara KB, Elgar MA. (2020). Socially cued anticipatory adjustment of female signalling effort in a moth. *Biol. Lett.* 16:20200614. doi: 10.1098/rsbl.2020.0614
- Phillips, J. H. H., and Proctor, J. R. (1969). Studies of fecundity and behaviour of the oriental fruit moth, *Grapholitha molesta* (Lepidoptera: Tortricidae), on the *Niagara peninsula* of Ontario. *Can. Entomol.* 101, 1024–1033. doi: 10.4039/Ent1011024-10
- Polavarapu, S., Lonergan, G., Peng, H., and Neilsen, K. (2001). Potential for mating disruption of *Sparganothis sulfureana* (Lepidoptera: Tortricidae) in cranberries. *J. Econ. Entomol.* 94, 658–665. doi: 10.1603/0022-0493-94.3.658
- Potter, K. A., Davidowitz, G., and Woods, H. A. (2011). Cross-stage consequences of egg temperature in the insect *Manduca sexta*. *Funct. Ecol.* 25, 548–556. doi: 10.1111/j.1365-2435.2010.01807.x
- Powell, J. A., and Opler, P. A. (2009). *Moths of western North America*. Berkeley, CA: University of California Press. doi: 10.1525/9780520943773
- Price, P. W. (1997). *Insect Ecology*. New York, NY: John Wiley and Sons.
- Quiring, D. T. (1994). Diel activity pattern of a nocturnal moth, *Zeiraphera canadensis*, in nature. *Entomol. Exp. Appl.* 73, 111–120. doi: 10.1111/j.1570-7458.1994.tb01845.x
- R Core Team (2014). *R: A Language and Environment for Statistical Computing*. Vienna: R Foundation for Statistical Computing.
- Rajimann, L. E., and Menken, S. B. J. (2000). Temporal variation in the genetic structure of host-associated populations of the small ermine moth *Yponomeuta padellus* (Lepidoptera, Yponomeutidae). *Biol. J. Linn. Soc.* 70, 555–570. doi: 10.1111/j.1095-8312.2000.tb00217.x
- Raine, J. (1966). Life history of *Dasystoma salicellum* Hnn. (Lepidoptera: Oecophoridae) a new pest of blueberries in British Columbia. *Can. Entomol.* 98, 331–334. doi: 10.4039/Ent98331-3
- Ramaswamy, S. B. (1990). Periodicity of oviposition, feeding, and calling by mated female *Heliothis virescens* in a field cage. *J. Insect Behav.* 3, 417–427. doi: 10.1007/BF01052118
- Reed, D. K., Mikolajczak, K. L., and Krause, C. R. (1988). Ovipositional behavior of lesser peachtree borer in presence of host–plant volatiles. *J. Chem. Ecol.* 14, 237–252. doi: 10.1007/BF01022544
- Regier, J. C., Brown, J. W., Mitter, C., Baixeras, J., Cho, S., Cummings, M. P., et al. (2012a). A molecular phylogeny for the leaf-roller moths (Lepidoptera: Tortricidae) and its implications for classification and life history evolution. *PLoS One* 7:e35574. doi: 10.1371/journal.pone.0035574
- Regier, J. C., Mitter, C., Solis, M., Hayden, J. E., Landry, B., Nuss, M., et al. (2012b). A molecular phylogeny for the pyraloid moths (Lepidoptera: Pyraloidea) and its implications for higher-level classification. *Syst. Entomol.* 37, 635–656. doi: 10.1111/j.1365-3113.2012.00641.x
- Regier, J. C., Mitter, C., Zwick, A., Bazinet, A. L., Cummings, M. P., Kawahara, A. Y., et al. (2013). A large-scale, higher-level, molecular phylogenetic study of the insect order *Lepidoptera* (moths and butterflies). *PLoS One* 8:e58568. doi: 10.1371/journal.pone.0058568
- Rhainds, M., and Gries, G. (1998). Density and pupation site of apterous female bagworms, *Metisa plana* (Lepidoptera: Psychidae), influence the distribution of emergent larvae. *Can. Entomol.* 130, 603–613. doi: 10.4039/Ent130603-5
- Rhainds, M., Gries, G., and Castrillo, G. (1995). Pupation site affects the mating success of small but not large female bagworms, *Oiketicus kirbyi* (Lepidoptera: Psychidae). *Oikos* 74, 213–217. doi: 10.2307/3545650
- Rhainds, M., Gries, G., and Min, M. M. (1999). Size- and density-dependent reproductive success of bagworms, *Metisa plana*. *Entomol. Exp. Appl.* 91, 375–383. doi: 10.1046/j.1570-7458.1999.00505.x
- Richards, A., Speight, M., and Cory, J. (1999). Characterization of a nucleopolyhedrovirus from the vapourer moth, *Orgyia antiqua* (Lepidoptera: Lymantriidae). *J. Invert. Path.* 74, 137–142. doi: 10.1006/jipa.1999.4870
- Richerson, J. V., Cameron, E. A., and Brown, E. A. (1976). Sexual activity of the gypsy moth. *Am. Midl. Nat.* 95, 299–312. doi: 10.2307/2424395
- Riddiford, L. M., and Ashenhurst, J. B. (1973). The switchover from virgin to mated behaviour in female cecropia moths: the role of the bursa copulatrix. *Biol. Bull.* 144, 162–171. doi: 10.2307/1540153
- Riemann, J. G. (1986). Reproductive potential and other aspects of the biology of the sunflower moth, *Homoeosoma electellum* (Hulst) (Lepidoptera, Pyralidae). *J. Kansas Entomol. Soc.* 59, 32–36.
- Robison, D., Abrahamson, L., Raffa, K., and White, E. (1998). Spruce budworm (Lepidoptera: Tortricidae) field fecundity: new insights into its estimation and use. *Forest Ecol. Manag.* 106, 73–81. doi: 10.1016/S0378-1127(97)00225-9
- Roff, D. A. (1990). The evolution of flightlessness in insects. *Ecol. Monog.* 60, 389–421. doi: 10.2307/1943013
- Ronkay, L., and Behounek, G. (2015). *Nyungwe lepidoptera diversity project*. Available online at: <http://driegrain.be> (accessed November 2015).
- Rosenthal, G. G. (2017). *Mate Choice: The Evolution of Sexual Decision Making from Microbes to Humans*. Princeton, NJ: Princeton University Press.
- Royer, L., and McNeil, J. N. (1993). Male investment in the European corn borer, *Ostrinia nubilalis* (Lepidoptera: Pyralidae): impact on female longevity and reproductive performance. *Funct. Ecol.* 7, 209–215. doi: 10.2307/2389889
- Sadek, M. M. (2001). Polyandry in field-collected Spodoptera littoralis moths and laboratory assessment of the effects of male mating history. *Entomol. Exp. Appl.* 98, 165–172. doi: 10.1046/j.1570-7458.2001.00771.x
- Sattler, K. (1991). A review of wing reduction in Lepidoptera. *Bull. British Mus.* 60, 243–288.
- Schneider, D. (1964). Insect antennae. *Ann. Rev. Entomol.* 9, 103–122. doi: 10.1146/annurev.en.09.010164.000535

- Schneider, J. C. (1980). The role of parthenogenesis and female aptery in microgeographic, ecological adaptation in the fall cankerworm, *Alsophila pometaria* Harris (Lepidoptera: Geometridae). *Ecology* 61, 1082–1090. doi: 10.2307/1936827
- Sedlacek, J. D., Weston, P. A., and Barney, R. J. (1995). *Lepidoptera and Psocoptera*. New York, NY: Marcel Dekker, Inc.
- Seth, R., and Sharma, V. (2002). Growth, development, reproductive competence and adult behaviour of *Spodoptera litura* (Lepidoptera: Noctuidae) reared on different diets. *Eval. Lepidoptera Population Suppression Radiation Induced Sterility* 1283, 15–22.
- Shorey, H., Andres, L., and Hale, R. (1962). The biology of *Trichoplusia ni* (Lepidoptera: Noctuidae). I. life history and behavior. *Ann. Entomol. Soc. Am.* 55, 591–597. doi: 10.1093/aesa/55.5.591
- Shuker, D. M. (2014). “Sexual selection theory,” in *The Evolution of Insect Mating Systems*, eds D. M. Shuker, and L. W. Simmons. (Oxford: Oxford University Press), 20–25. doi: 10.1093/acprof:oso/9780199678020.003.0002
- Sihvonen, P., Mutanen, M., Kaila, L., Brehm, G., Hausmann, A., and Staude, H. S. (2011). Comprehensive molecular sampling yields a robust phylogeny for geometrid moths (Lepidoptera: Geometridae). *PLoS One* 6:e20356. doi: 10.1371/journal.pone.0020356
- Skuhravy, V. (1987). A review of research on the nun moth (*Lymantria monacha* L.) conducted with pheromone traps in Czechoslovakia, (1973–1984). *Anz Schädlingskde Pflanzenschutz Umweltschutz* 60, 96–98. doi: 10.1007/BF01906038
- Snäll, N., Tammaru, T., Wahlberg, N., Viidalepp, J., Ruohomäki, K., Savontaus, M., et al. (2007). Phylogenetic relationships of the tribe *Operophterini* (Lepidoptera, Geometridae): a case study of the evolution of female flightlessness. *Biol. J. Linn. Soc.* 92, 241–252. doi: 10.1111/j.1095-8312.2007.00834.x
- Sohn, J. -C., Regier, J. C., Mitter, C., Davis, D., Landry, J. -F., Zwick, A., et al. (2013). A molecular phylogeny for *Yponomeutoidea* (Insecta, Lepidoptera, Ditrysia) and its implications for classification, biogeography and the evolution of host plant use. *PLoS One* 8:e55066. doi: 10.1371/journal.pone.0055066
- Sorenson, C. J., and Gunnell, F. H. (1955). Biology and control of the peach twig borer (*Anarsia lineatella* Zeller) in Utah. Bulletin No. 379. UAES Bulletins: China
- St. Laurent, R., and McCarthy, R. (2016). *Asian Defoliators. National Plant Diagnostic Network. Training and education*. Available online at: https://www.firstdetector.org/sites/firstdetector.org/files/pdf/AsianDefoliator_lookalikes_show.pdf (accessed March 2022).
- Steinbauer, M. J. (2005). How does host abundance affect oviposition and fecundity of *Mnesampela privata*? *Environ. Entomol.* 34, 281–291. doi: 10.1603/0046-225X-34.2.281
- Steinbauer, M. J., McQuillan, P. B., and Young, C. J. (2001). Life history and behavioural traits of *Mnesampela privata* that exacerbate population responses to eucalypt plantations: comparisons with Australian and outbreak species of forest geometrid from the Northern Hemisphere. *Austral Ecol.* 26, 525–534. doi: 10.1046/j.1442-9993.2001.01130.x
- Suckling, D., Barrington, A., Chhagan, A., Stephens, A., Burnip, G., Charles, J., et al. (2007). “Eradication of the Australian painted apple moth *Teia anartoides* in New Zealand: trapping, inherited sterility, and male competitiveness,” in *Area-wide Control of Insect Pests*, eds M. J. B. Vreysen, A. S. Robinson, and J. Heinrichs. Springer: Berlin.
- Sutrisno, H. (2014). Molecular phylogeny of Indonesian *Lymantria* Tussock moths (Lepidoptera: Erebiidae) based on COI gene sequences. *J. Species Res.* 3, 7–16. doi: 10.12651/JSR.2014.3.1.007
- Svard, L., and McNeil, J. N. (1994). Female benefit, male risk – polyandry in the true armyworm *Pseudaletia unipuncta*. *Behav. Ecol. Sociobiol.* 35, 319–326. doi: 10.1007/BF00184421
- Swaby, J. A., Daterman, G. E., and Sower, L. L. (1987). Mating behavior of douglas-fir tussock moth, *Orygia pseudotsugata* (Lepidoptera: Lymantriidae), with special reference to effects of female age. *Ann. Entomol. Soc. Am.* 80, 47–50. doi: 10.1093/aesa/80.1.47
- Symonds, M. R. E., Johnson, T. L., and Elgar, M. A. (2012). Pheromone production, male abundance, body size, and the evolution of elaborate antennae in moths. *Ecol. Evol.* 2, 227–246. doi: 10.1002/ece3.81
- Talekar, N. S., and Shelton, A. M. (1993). Biology, ecology, and management of the diamondback moth. *Ann. Rev. Entomol.* 38, 275–301. doi: 10.1146/annurev.en.38.010193.001423
- Tamhankar, A. J. (1995). Host influence on mating behavior and spermatophore reception correlated with reproductive output and longevity of female *Earias insulana* (Biosduval) (Lepidoptera: Noctuidae). *J. Insect Behav.* 8, 499–511. doi: 10.1007/BF01995322
- Tammaru, T., Esperk, T., and Castellanos, I. (2002). No evidence for cost of being large in females of *Orygia* spp. (Lepidoptera, Lymantriidae): larger is always better. *Oecologia* 133, 430–438. doi: 10.1007/s00442-002-1057-7
- Tammaru, T., Ruohomäki, K., and Saikkonen, K. (1996). Components of male fitness in relation to body size in *Epirrita autumnata* (Lepidoptera, Geometridae). *Ecol. Entomol.* 21, 185–192. doi: 10.1111/j.1365-2311.1996.tb01186.x
- Tan, E. J., and Elgar, M. A. (2021). Motion: enhancing signals and concealing cues. *Biol. Open* 10:bio058762, doi: 10.1242/bio.058762
- Tang, H., Li, J., Wu, J., Gao, H., and Zhang, S. (2014). Development characteristics and controlling countermeasures of rice stem borer, *Chilo suppressalis* (walker). *Ag. Sci. Technol.* 15, 843–845.
- Tanhuanpää, M., Ruohomäki, K., and Kaitaniemi, P. (2003). Influence of adult and egg predation on reproductive success of *Epirrita autumnata* (Lepidoptera: Geometridae). *Oikos* 102, 263–272. doi: 10.1034/j.1600-0706.2003.12.546.x
- Tarlack, P., Mehrkhou, F., and Mousavi, M. (2015). Life history and fecundity rate of *Ephesia kuehniella* (Lepidoptera: Pyralidae) on different wheat flour varieties. *Arch. Phytopath. Plant Protect.* 48, 95–103. doi: 10.1080/03235408.2014.882135
- Thakur, B., Chakrabarti, S., and Mattu, V. K. (2016). Re-description of the adults of indian gypsy moth *Lymantria obfuscata* Walker (Lepidoptera: Lymantriidae) in Himachal Pradesh, India. *Munis Entomol. Zool.* 11, 105–113.
- Thurston, G. S., and MacGregor, J. D. (2003). Body size–realized fecundity relationship of whitemarked tussock moth. *Can. Entomol.* 135, 583–586. doi: 10.4039/n02-104
- Tingle, F. C., and Mitchell, E. R. (1991). Effect of oviposition deterrents from elderberry on behavioral responses by *Heliothis virescens* to host–plant volatiles in flight tunnel. *J. Chem. Ecol.* 17, 1621–1631. doi: 10.1007/BF00984693
- Tisdale, R. A., and Sappington, T. W. (2001). Realized and potential fecundity, egg fertility, and longevity of laboratory–reared female beet armyworm (Lepidoptera: Noctuidae) under different adult diet regimes. *Ann. Entomol. Soc. Am.* 94, 415–419. doi: 10.1603/0013-8746(2001)094[0415:RAPFEF]2.0.CO;2
- Torres-Vila, L. M., Gragera, J., Rodríguez-Molina, M. C., and Stockel, J. (2002). Heritable variation for female remating in *Lobesia botrana*, a usually monandrous moth. *Anim. Behav.* 64, 899–907. doi: 10.1006/anbe.2003.2000
- Torres-Vila, L. M., Rodríguez-Molina, M. C., and Jennions, M. D. (2004). Polyandry and fecundity in the *Lepidoptera*: can methodological and conceptual approaches bias outcomes? *Behav. Ecol. Sociobiol.* 55, 315–324. doi: 10.1007/s00265-003-0712-2
- Torres-Vila, L. M., Rodríguez-Molina, M. C., Gragera, J., and Bielza-Lino, P. (2001). Polyandry in *Lepidoptera*: a heritable trait in *Spodoptera exigua* Hübner. *Heredity* 86, 177–183. doi: 10.1046/j.1365-2540.2001.00821.x
- Tuskes, P. M., Tuttle, J. P., and Collins, M. M. (1996). *The Wild Silk Moths of North America: A Natural History of the Saturniidae of the United States and Canada*. Ithaca, NY: Cornell University Press., doi: 10.7591/9781501738005
- Tweedie, M. W. F. (1976). A note on moths with flightless females. *Entomol. Gaz.* 27, 2–3.
- Van der Pers, J., Cuperus, P., and Den Otter, C. (1980). Distribution of sense organs on male antennae of small ermine moths, *Yponomeuta* spp. (Lepidoptera: Yponomeutidae). *Int. J. Insect Morph. Embryol.* 9, 15–23. doi: 10.1016/0020-7322(80)90032-X
- Van Dongen, S., Matthysen, E., Sprengers, E., and Dhondt, A. A. (1998). Mate selection by male winter moths *Operophtera brumata* (Lepidoptera, Geometridae): adaptive male choice or female control? *Behaviour* 135, 29–42. doi: 10.1163/156853998793066401
- Van Dongen, S., Sprengers, E., Lofstedt, C., and Matthysen, E. (1999). Fitness components of male and female winter moths (*Operophtera brumata* L.) (Lepidoptera, Geometridae) relative to measures of body size and asymmetry. *Behav. Ecol.* 10, 659–665. doi: 10.1093/beheco/10.6.659
- Vegliante, F. (2005). Larval head anatomy of *Heterogynis penella* (Zygaenoidea, Heterogynidae), and a general discussion of caterpillar head structure (Insecta, Lepidoptera). *Acta Zool.* 86, 167–194. doi: 10.1111/j.1463-6395.2005.00198.x
- Villemereuil, P., Gimenez, O., and Doligez, B. (2013). Comparing parent-offspring regression with frequentist and Bayesian animal models to estimate heritability in wild populations: a simulation study for Gaussian and binary traits. *Meth. Ecol. Evol.* 4, 260–275. doi: 10.1111/2041-210X.12011
- Wagner, T. L., and Leonard, D. E. (1979). Aspects of mating, oviposition, and flight in the satin moth, *Leucoma salicis* (Lepidoptera, Lymantriidae). *Can. Entomol.* 111, 833–840. doi: 10.4039/Ent111833-7
- Walker, K. (2005). *Summer fruit tortrix (Adoxophyes orana)*. Available online at: <https://www.padil.gov.au> (accessed March 2022).
- Walker, P. W., and Allen, G. R. (2010). Mating frequency and reproductive success in an income breeding moth, *Mnesampela privata*. *Entomol. Exp. Appl.* 136, 290–300. doi: 10.1111/j.1570-7458.2010.01028.x

- Walker, P. W., and Allen, G. R. (2011). Delayed mating and reproduction in the autumn gum moth *Mnesampela privata*. *Ag. Forest Entomol.* 13, 341–347. doi: 10.1111/j.1461-9563.2011.00524.x
- Wallace, E., Albert, P., and McNeil, J. (2004). Oviposition behavior of the eastern spruce budworm *Choristoneura fumiferana* (Clemens) (Lepidoptera: Tortricidae). *J. Insect Behav.* 17, 145–154. doi: 10.1023/B:JOIR.0000028565.41613.1a
- Wallner, W. E. (1989). “Overview of pest lymantriidae of North America,” in *Proceedings: Lymantriidae: a Comparison of Features of New and Old World Tussock Moths*, eds W. E. Wallner, and K. A. McManus (New Haven, CT: USDA Forest Service), 65–79.
- Wang, Q., Shang, Y., Hilton, D., Inthavong, K., Zhang, D., and Elgar, M. A. (2018). Antennal scales improve signal detection efficiency for moth communication. *Proc. R. Soc. Lond. B* 285:20172832. doi: 10.1098/rspb.2017.2832
- Wang, X. P., Fang, Y. -L., and Zhang, Z. N. (2005). Effect of male and female multiple mating on the fecundity, fertility, and longevity of diamondback moth, *Plutella xylostella*. *J. Appl. Entomol.* 129, 39–42. doi: 10.1111/j.1439-0418.2005.00931.x
- Ward, K. E., and Landolt, P. J. (1995). Influence of multiple matings on fecundity and longevity of female cabbage looper moths (Lepidoptera: Noctuidae). *Ann. Entomol. Soc. Am.* 88, 768–772. doi: 10.1093/aesa/88.6.768
- Watson, A., Whalley, P. E. S., and Duckworth, W. D. (1975). *The Dictionary of Butterflies and Moths in Color*. New York, NY: McGraw-Hill.
- Watson, L., and Dallwitz, M. J. (2003–2022). *Insects of Britain and Ireland: the genera of Lepidoptera– Noctuidae*. Available online at: <https://www.delta-intkey.com/britin/noc/intro.htm> (accessed March 2022).
- Watson, R., and Hill, M. (1985). Pests of maize in New Zealand. maize - management to market. *Agronomy Soc. New Zealand Special Publ.* 4, 47–58.
- WCCP (1995). “Western committee on crop pests,” in *Proceedings of the Minutes of the 34th Annual Meeting* (Columbia: British Columbia).
- Webster, R., and Cardé, R. (1982). Influence of relative humidity on calling behaviour of the female European corn borer moth (*Ostrinia nubilalis*). *Entomol. Exp. Appl.* 32, 181–185. doi: 10.1111/j.1570-7458.1982.tb03200.x
- Webster, R., and Cardé, R. (1984). The effects of mating, exogenous juvenile hormone and a juvenile hormone analogue on pheromone titre, calling and oviposition in the omnivorous leafroller moth (*Platynota stultana*). *J. Insect Physiol.* 30, 113–118. doi: 10.1016/0022-1910(84)90114-8
- Weihman, S. (2005). *Monitoring and Control Tactics for Grape Root Borer Vitacea polistiformis Harris (Lepidoptera: Sesiidae) in Florida vineyards*. M.Sc. thesis, Gainesville, FL: University of Florida.
- West, R. J., and Bowers, W. W. (1994). Factors affecting calling behavior by *Lambdina fiscellaria* fiscellaria (Lepidoptera: Geometridae), under field conditions. *Environ. Entomol.* 23, 122–129. doi: 10.1093/ee/23.1.122
- Wong, T. T. Y., Clevelan, M. L., and Davis, D. G. (1969). Sex attraction and mating of lesser peach tree borer moths. *J. Econ. Entomol.* 62:789. doi: 10.1093/jee/62.4.789
- Wysoki, M., Yehuda, S. B., and Rosen, D. (1993). Reproductive behavior of the honeydew moth, *Cryptoblabes gnidiella*. *Invert. Reprod. Develop.* 24, 217–223. doi: 10.1080/07924259.1993.9672355
- Xu, J., Wang, Q., and He, X. (2008). Emergence and reproductive rhythms of *Ephesia kuehniella* (Lepidoptera: Pyralidae). *N. Z. Plant Protect.* 61, 277–282. doi: 10.30843/nzpp.2008.61.6806
- Yamamoto, S., and Sota, T. (2007). Phylogeny of the Geometridae and the evolution of winter moths inferred from a simultaneous analysis of mitochondrial and nuclear genes. *Mol. Phyl. Evol.* 44, 711–723. doi: 10.1016/j.ympev.2006.12.027
- Yen, S. -H., Solis, M. A., and Goolsby, J. A. (2004). *Austromusotima*, a new *Musotimina* genus (Lepidoptera: Crambidae) feeding on old world climbing fern, *Lygodium microphyllum* (Schizaceaceae). *Ann. Entomol. Soc. Am.* 97, 397–410. doi: 10.1603/0013-8746(2004)097[0397:AANMGL]2.0.CO;2
- Young, M. (1997). *The Natural History of Moths*. London: T and A D Poyser Ltd.,
- Zacharuk, R. Y. (1985). “Antennae and sensilla,” in *Comprehensive Insect Physiology Biochemistry and Pharmacology*, eds G. A. Kerkut, and L. I. Gilbert (London: Pergamon Press).
- Zahiri, R., Lafontaine, D., Schmidt, C., Holloway, J. D., Kitching, I. J., Mutanen, M., et al. (2013). Relationships among the basal lineages of Noctuidae (Lepidoptera, Noctuoidea) based on eight gene regions. *Zool. Scripta* 42, 488–507. doi: 10.1111/zsc.12022
- Zalucki, M. P., Daglish, G., Firempong, S., and Twine, P. (1986). The biology and ecology of *Heliothis armigera* and *H. punctigera* in Australia: what do we know? *Aust. J. Zool.* 34, 779–814. doi: 10.1071/ZO9860779
- Zhu, J., Chastain, B. B., Spohn, B. G., and Haynes, K. F. (1997). Assortative mating in two pheromone strains of the cabbage looper moth, *Trichoplusia ni*. *J. Insect Behav.* 10, 805–817. doi: 10.1023/B:JOIR.0000010414.28494.9a
- Ziaee, M. (2012). “Oilseed pests,” in *Oilseeds*, eds U. G. Akpan (Croatia: InTech), 117–184.



OPEN ACCESS

EDITED BY
Cristiano Bertolucci,
University of Ferrara, Italy

REVIEWED BY
Thomas Cronin,
University of Maryland, Baltimore
County, United States
Karen Carleton,
University of Maryland, College Park,
United States

*CORRESPONDENCE
Audrey E. Miller
audreyem@princeton.edu

SPECIALTY SECTION
This article was submitted to
Behavioral and Evolutionary Ecology,
a section of the journal
Frontiers in Ecology and Evolution

RECEIVED 30 June 2022
ACCEPTED 25 August 2022
PUBLISHED 30 September 2022

CITATION
Miller AE, Hogan BG and Stoddard MC
(2022) Color in motion: Generating
3-dimensional multispectral models
to study dynamic visual signals
in animals.
Front. Ecol. Evol. 10:983369.
doi: 10.3389/fevo.2022.983369

COPYRIGHT
© 2022 Miller, Hogan and Stoddard.
This is an open-access article
distributed under the terms of the
[Creative Commons Attribution License](https://creativecommons.org/licenses/by/4.0/)
(CC BY). The use, distribution or
reproduction in other forums is
permitted, provided the original
author(s) and the copyright owner(s)
are credited and that the original
publication in this journal is cited, in
accordance with accepted academic
practice. No use, distribution or
reproduction is permitted which does
not comply with these terms.

Color in motion: Generating 3-dimensional multispectral models to study dynamic visual signals in animals

Audrey E. Miller*, Benedict G. Hogan and
Mary Caswell Stoddard

Department of Ecology and Evolutionary Biology, Princeton University, Princeton, NJ, United States

Analyzing color and pattern in the context of motion is a central and ongoing challenge in the quantification of animal coloration. Many animal signals are spatially and temporally variable, but traditional methods fail to capture this dynamism because they use stationary animals in fixed positions. To investigate dynamic visual displays and to understand the evolutionary forces that shape dynamic colorful signals, we require cross-disciplinary methods that combine measurements of color, pattern, 3-dimensional (3D) shape, and motion. Here, we outline a workflow for producing digital 3D models with objective color information from museum specimens with diffuse colors. The workflow combines multispectral imaging with photogrammetry to produce digital 3D models that contain calibrated ultraviolet (UV) and human-visible (VIS) color information and incorporate pattern and 3D shape. These “3D multispectral models” can subsequently be animated to incorporate both signaler and receiver movement and analyzed *in silico* using a variety of receiver-specific visual models. This approach—which can be flexibly integrated with other tools and methods—represents a key first step toward analyzing visual signals in motion. We describe several timely applications of this workflow and next steps for multispectral 3D photogrammetry and animation techniques.

KEYWORDS

3D modeling, photogrammetry, multispectral imaging, animation, dynamic, visual signals, color, motion

Introduction

For sensory ecologists interested in how dynamic visual signals are designed and how they evolve, incorporating aspects of motion and geometry into studies of animal color is a pressing goal (Rosenthal, 2007; Hutton et al., 2015; Echeverri et al., 2021). Over the years, biologists have increasingly appreciated the dynamic nature of animal

colors, which can change over a range of timescales due to a variety of mechanisms (Rosenthal, 2007). Dynamic colors can be the result of physiological changes, such as the selective expansion and contraction of chromatophores that elicit rapid color changes in cephalopods (Mäthger et al., 2009; Zylinski et al., 2009) or the seasonal variation in pigmentation that allows snowshoe hares (*Lepus americanus*) to transition between brown summer coats and white winter coats (Zimova et al., 2018). Color change can also arise from behaviorally mediated dynamics, as in the striking courtship display of the superb bird-of-paradise (*Lophorina superba*) (Echeverri et al., 2021). During his display, the male maneuvers around an onlooking female, changing his position and posture to show off his brilliant plumage (Frith and Frith, 1988). As explained by Echeverri et al. (2021), the perception of colorful signals that involve behaviorally mediated color change is affected greatly by the position, distance, and direction of signalers and receivers in relation to one another as well as to the physical environment—referred to as “signaling geometry” (Echeverri et al., 2021). Today, we recognize that most animal colors are, to some degree, dynamic (Hutton et al., 2015; Cuthill et al., 2017; Echeverri et al., 2021). Despite deep interest in dynamic visual signals, the ways in which we measure color have not kept pace with our conceptual understanding of these signals. When quantifying color and pattern, researchers typically rely on static images of colorful phenotypes—ignoring certain spatial and temporal aspects of their expression. Consequently, the spatio-temporal dimensions of animal visual signals remain understudied. This is particularly true of behaviorally mediated color change, which relies strongly on aspects of motion and signaling geometry that are currently missing from most color quantification methods (Rosenthal, 2007; Hutton et al., 2015; Echeverri et al., 2021).

Advances in digital imaging have made it possible for researchers to capture spectral (color) and spatial (pattern) information in static images (Chiao and Cronin, 2002; Stevens et al., 2007; Pike, 2011; Akkaynak et al., 2014; Troscianko and Stevens, 2015; Burns et al., 2017). One technique that has become a widespread and powerful tool for studying animal color is multispectral imaging. Multispectral imaging generally refers to photography in which images capture multiple channels of color information (Leavesley et al., 2005), typically including wavelengths that extend beyond the human-visible (VIS) range of light (~400–700 nm). Recently, multispectral imaging has been used to quantify the colors and patterns of flora and fauna (Troscianko and Stevens, 2015; van den Berg et al., 2019). To be useful for objective color measurements, 2D multispectral photographs need to be calibrated to account for the wavelength sensitivity and non-linearity in the camera sensor and standardized to control for lighting conditions (Troscianko and Stevens, 2015). These calibrations produce objective, camera-independent color data that can be transformed into visual system-specific color metrics (Troscianko and Stevens, 2015)—what we refer to here as “color-accurate” information. Multispectral imaging not

only allows for the collection of color-accurate information beyond the VIS range but also captures the spatial properties of patterns—providing an advantage over spectrophotometry, which measures reflectance at a small point source (Stevens et al., 2007; Troscianko and Stevens, 2015).

Recently, user-friendly software has been developed for processing and analyzing multispectral images (Troscianko and Stevens, 2015; van den Berg et al., 2019), leading to increased adoption of multispectral imaging in animal coloration research. However, multispectral imaging alone is currently unsuitable for capturing motion—a common attribute of dynamic visual signals. In order to capture the relevant color information for many animal signal receivers, external filters that separately capture VIS color and color outside this range (e.g., ultraviolet or UV) are needed to photograph a scene multiple times (Troscianko and Stevens, 2015). While taking these sequential photographs, the subject must remain still so that the separate images can later be overlaid—combining all of the color information into a single image stack (Troscianko and Stevens, 2015). Consequently, this approach is unsuitable for quantifying color from freely moving animals and for capturing the 3D shape of the focal object. So, while technological advances in digital imaging have increased the spatial scale at which we can collect color information, they alone cannot capture all of the spatio-temporal dynamics of color.

Digital 3D modeling techniques offer a potential method for addressing the gaps in dynamic color analyses. In many dynamic color displays, the perceived color change is due (1) to a physiological change such as changes in blood flow, chromatophore action, pigment deposition, etc. (Negro et al., 2006; Mäthger et al., 2009) or (2) to a change in posture—such as tail-cock gestures in many *Ramphastidae* (toucans, toucanets, and aracaris) displays (Miles and Fuxjager, 2019)—and/or position relative to light or the signal receiver, as in iridescent bird plumage (Stavenga et al., 2011). 3D modeling is best suited to studying the second of these display types, where colors on an animal may appear inherently static but can change in appearance with respect to motion and/or angle. Digital images can be used to generate 3D representations of entire animals using photogrammetry—the science of deriving reliable 3D information from photographs (Bot and Irschick, 2019). Photogrammetric techniques, specifically Structure-from-Motion (SfM), can be used to construct a digital 3D model that is faithful to an object’s original form by combining multiple 2D images of an object taken from different angles (Chiari et al., 2008; Westoby et al., 2012; Bot and Irschick, 2019; Medina et al., 2020). Photogrammetry has been used to create 3D models from live animals (Chiari et al., 2008; Bot and Irschick, 2019; Irschick et al., 2020, 2021; Brown, 2022) as well as museum specimens (Chiari et al., 2008; Nguyen et al., 2014; Medina et al., 2020) to capture realistic 3D shape and color for the purpose of scientific application. Recently, Medina et al. (2020) developed a rapid and cost-effective pipeline for digitizing ornithological museum specimens using 3D photogrammetry. This is of particular

interest to visual ecologists since birds possess some of the most diverse phenotypic variation among vertebrates, much of which can be captured by digital 3D models.

While recent advances in photogrammetric software and other computer graphics tools have made generating these digital 3D models more accessible and affordable, the models produced only contain color information from the human-visible spectrum (Nguyen et al., 2014; Bot and Irschick, 2019; Irschick et al., 2020; Medina et al., 2020; Brown, 2022). This poses a problem for studying animal coloration because many organisms have visual systems sensitive to light outside this range (Delhey et al., 2015). For example, birds are tetrachromats. They possess four spectrally distinct color photoreceptors—also called “cones”—that have ultraviolet (λ_{max} : 355–373 nm) or violet (λ_{max} : 402–426 nm), shortwave (λ_{max} : 427–463 nm), mediumwave (λ_{max} : 499–506 nm), and longwave (λ_{max} : 543–571 nm) sensitivity (Hart and Hunt, 2007). Avian retinas also contain “double cones” (dbl), which presumably function in luminance or brightness processing in birds (Osorio and Vorobyev, 2005). Kim et al. (2012) developed a comprehensive method for producing digital 3D models of avian specimens with complete, full-spectrum information from ~395–1,003 nm, a range spanning the near-ultraviolet to the near-infrared. However, their approach requires highly customized and often expensive equipment (3D scanners and hyperspectral cameras) and is fairly complex and computationally intensive to implement. An alternative approach, which we develop here, involves multispectral imaging in combination with photogrammetry and subsequent animation. The integration of these techniques holds great potential for studying dynamic visual signals. By combining multispectral imaging with 3D photogrammetry, we can quickly, inexpensively, and reliably reconstruct an object’s form and color, including color that is outside the human-visible range. Once a digital 3D model is constructed, it can be animated to include the behavioral components of dynamic visual signals.

Computer animation has been used in playback experiments to study animal behavior since the 1990s and continues to be a method for testing behavioral responses of live animals to complex animal stimuli (Künzler and Bakker, 1998; Chouinard-Thuly et al., 2017; Müller et al., 2017; Witte et al., 2017; Woo et al., 2017). However, in more recent years, modeling and animation have also been used to study aspects of animal form (DeLorenzo et al., 2020), locomotion (Bishop et al., 2021), and biomechanics (Fortuny et al., 2015) *in silico* by extracting measurements directly from digital 3D models and simulations. Recently, researchers have highlighted the promise of performing similar virtual experiments for studying colorful visual signals (Bostwick et al., 2017). Bostwick et al. (2017) illustrated how 3D modeling and animation can be a powerful tool for studying dynamic avian color using the courtship display of the male Lawe’s parotia (*Parotia lawesii*) as a case study. They note how 3D simulations of real-world displays

can be used to address questions that are otherwise impossible to test (Bostwick et al., 2017). Specifically, they consider how virtual experiments allow researchers to manipulate aspects of a signaling interaction that are typically difficult to control in behavioral experiments. This includes various aspects of the signal phenotype, the signaling environment, and physical aspects of the signaler and receiver. For example, studying colorful signals in a virtual space lets researchers choose where to “view” a signal from by adding and adjusting virtual camera views in a simulation. The authors point out how controlling the placement of cameras in this way could improve our understanding of the display’s functional morphology since 3D computer simulations would allow them to view the male Lawe’s parotia from the precise location of visiting females (Bostwick et al., 2017).

Clearly, 3D modeling and animation approaches have great potential to improve studies of dynamic animal color. However, we currently lack step-by-step workflows for producing digital 3D models containing objective color information that can be subsequently animated and analyzed in a virtual space. Here, we combine multispectral imaging with photogrammetry to produce color-accurate 3D models that include UV color information. The resulting digital 3D models produced from our workflow replicate diffuse (non-angle dependent) animal color in a virtual space. Since these digital models contain both VIS color as well as color outside this range, we call them “3D multispectral models.” Like the 2D multispectral images used to generate them, these 3D multispectral models can be analyzed from the perspective of diverse animal viewers using visual models. With the addition of animation, we can simulate the visual appearance of animal color patterns during visual displays. 3D multispectral modeling has great predictive power for investigating behaviorally mediated color change. By either replicating or manipulating postural and positional changes of signalers and receivers or conditions in the lighting environment, researchers can study the effect motion has on animal colors in a flexible virtual space. The development of this workflow will open the door to new possibilities for the study of dynamic animal colors.

Materials and methods

In this workflow, we combine multispectral imaging software—micaToolbox (version v2.2.2, Troscianko and Stevens, 2015) for ImageJ (version 1.53e, Java 1.8.0_172 64-bit, Schneider et al., 2012)—with photogrammetric software—Agisoft Metashape Professional Edition (Agisoft LLC, St. Petersburg, Russia)—to generate multispectral 3D models of four male bird specimens. These included a hooded pitta (*Pitta sordida*, specimen #9951), a pink-necked green pigeon (*Treron vernans*, specimen #17548), a summer tanager (*Piranga rubra*, specimen #118), and a vermilion flycatcher (*Pyrocephalus obscurus*, specimen #12452). All four models can be seen

in VIS color in [Supplementary Video 1](#). Specimens were from Princeton University's natural history collection. We outline four main steps for generating multispectral 3D models: (1) image capture, (2) image processing, (3) mesh reconstruction and refinement, and (4) texture generation and refinement. The result of these steps is a 3D multispectral model. The final model for one of these specimens, the hooded pitta, is displayed in [Figure 1A](#). Information derived from multiple 2D multispectral images ([Figure 1B](#)) produce a 3D model that accurately captures the color (see [Supplementary Video 1](#)) and 3D shape ([Figure 1C](#)) of the museum specimen.

Once the multispectral 3D model is complete, color can be extracted and analyzed using image processing software such as MATLAB (Natick, Massachusetts, USA) or micaToolbox. For some applications, creating the 3D model may be the end goal. For other applications, it may be desirable to animate the 3D model using digital animation software such as Autodesk 3ds Max (Autodesk, Inc., San Rafael, California, USA). In a virtual space, an animated model might show how a colorful signal changes in appearance from different angles, or how it changes over different timescales. To demonstrate how a 3D model produced by our pipeline may be animated, we provide an example with the hooded pitta specimen ([Figure 1D](#) and [Supplementary Video 2](#)). [Figure 2](#) is a graphical summary of the entire workflow. In the sections below, we describe the workflow in more detail. All the custom scripts and plugins described below are available on GitHub.¹

Step 1: UV and VIS image capture

The first step in this workflow is to capture both the 3D structure of the specimens and the relevant UV and VIS color of their plumage using UV/VIS photography. To do this, we imaged each bird specimen from multiple angles with a modified DSLR camera. Photographs were captured in RAW format using a Nikon (Minato, Japan) D7000 camera with a Nikon Nikkor 105 mm fixed lens and consistent aperture and ISO settings. Camera settings for each specimen are available in [Supplementary Figure 1](#). The Nikon D7000 was previously modified (via quartz conversion) to be UV- and infrared-sensitive ([Troschianko and Stevens, 2015](#)). A custom 3D-printed filter slider was used to alternate between two filters—a Baader U-Filter (320–380 nm pass) and a Baader (Mammendorf, Germany) UV/IR-Cut/L filter (420–680 nm pass)—to capture both UV and VIS color images of the specimens, respectively. Specimens were photographed under a D65 IWASAKI EYE Color Arc light (Tokyo, Japan) that had its outer coating removed to emit UV light. Most images contained a Labsphere (North Sutton, NH) 40% Spectralon reflectance standard; all other images were calibrated using standards in photographs

captured under the same lighting conditions as in previous images. To capture different viewing angles of the specimen, we used a custom-built motorized turntable. This turntable was controlled by an Arduino microcontroller, which was in turn controlled using custom MATLAB scripts. The turntable was programmed to rotate 360 degrees in increments of 30 degrees, pausing at each position until both the UV and VIS images were collected. MATLAB was also used to control the camera settings and shutter button (via DigiCamControl 2 software).² Thus, the only manual tasks during image capture were alternating between the UV and VIS filters and adjusting the camera height. The camera height was adjusted after each full rotation to capture the specimen at different vertical angles. Seven different vertical positions were used, resulting in 84 unique viewing angles and 168 images of the specimen (2 images—UV and VIS—at each angle).

Step 2: Multispectral image generation and processing

After photographing the specimen, the next step of the workflow is to generate 2D multispectral images that contain color-accurate information. The UV and VIS images were used to generate multispectral images—one for each of the 84 viewing angles—using micaToolbox ([Troschianko and Stevens, 2015](#)) for ImageJ. This process linearizes and normalizes the UV and VIS images and separates them into their composite channels: ultraviolet red (UVR) and ultraviolet blue (UVB) for the UV image and red (R), green (G), and blue (B) for the visible image. Thus, each of the 84 multispectral images comprises a stack of 5 calibrated grayscale images, one for each color channel in the multispectral image. For each 2D multispectral image, the color channel images ($n = 5$) were exported as separate 16-bit TIFF images using a custom ImageJ plugin. These color channel images were used in Step 4 to generate 3D multispectral model textures. In addition, composite RGB images—comprising the RGB channels only—were created from the multispectral image stack; these are images that simulate human vision and are suitable for presentations and figures ([Troschianko and Stevens, 2015](#)). These RGB “presentation images” were used to reconstruct meshes in Step 3.

Step 3: Mesh reconstruction and refinement

The third step of the workflow is to produce a mesh, which is essential for capturing the 3D structure of a specimen. A mesh is the collection of vertices, edges, and faces that make up the base of a 3D model ([Chouinard-Thuly et al., 2017](#)). To reconstruct

¹ <https://github.com/audreyem/ColorInMotion>

² <http://digidigamcontrol.com/>

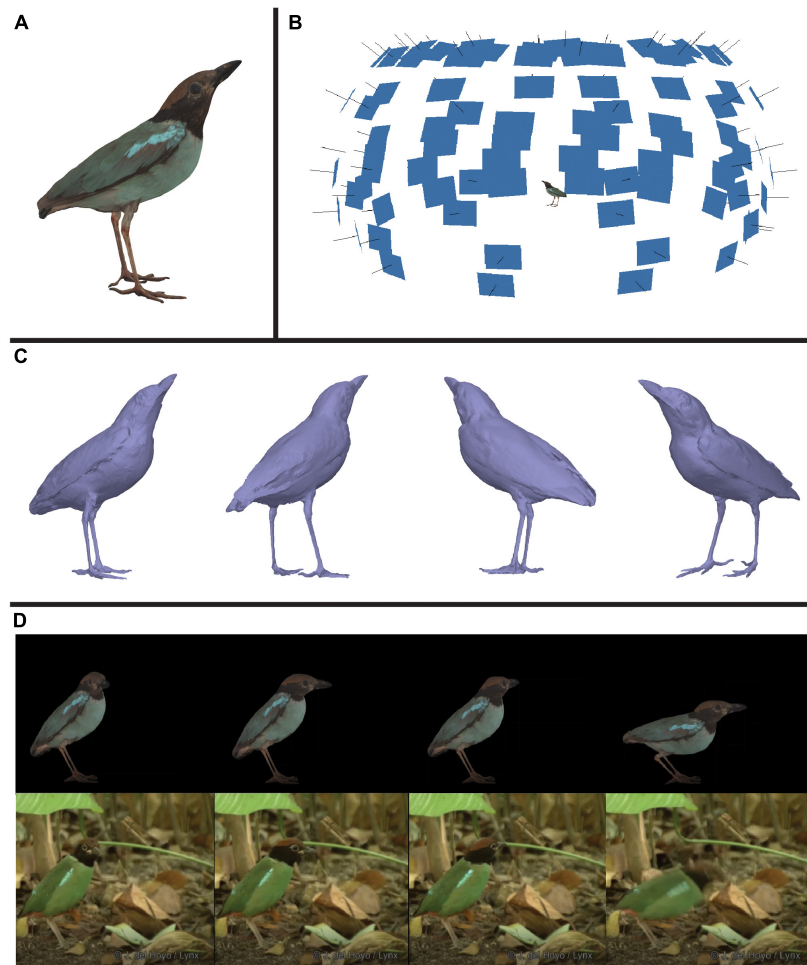


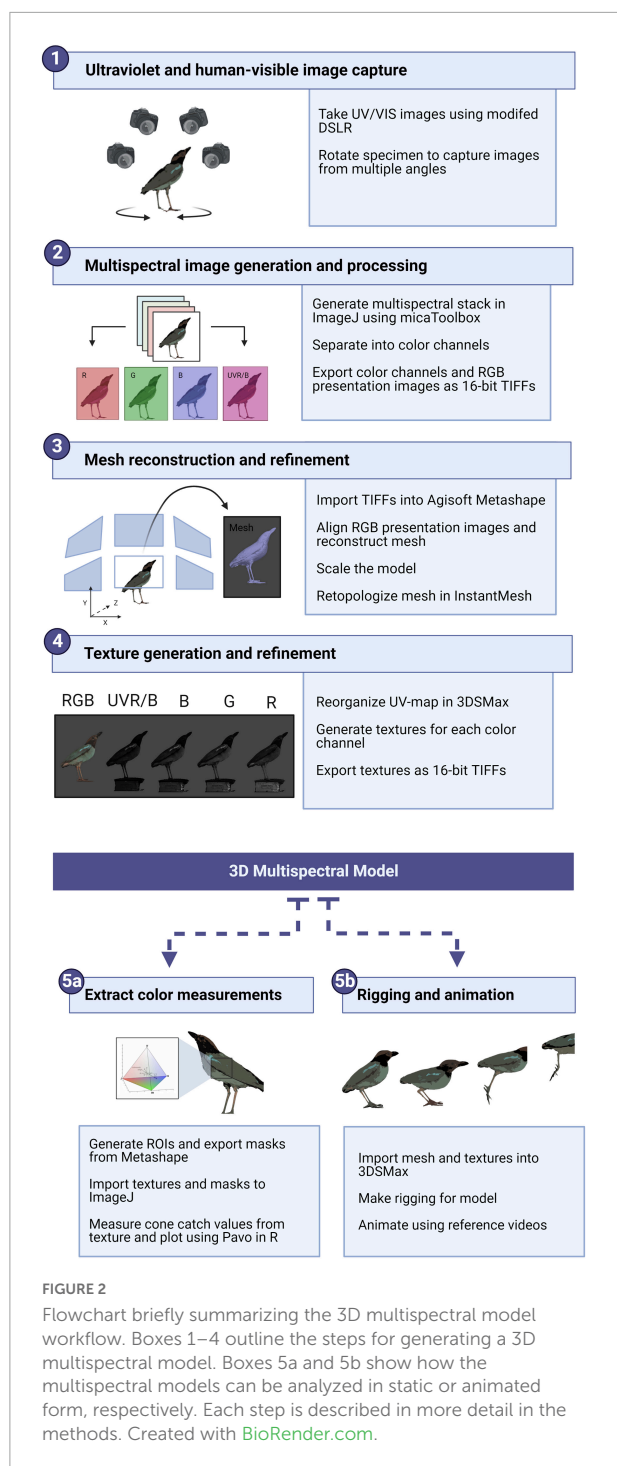
FIGURE 1

An illustration of one product of this workflow: a color-accurate 3D model of a hooded pitta (*Pitta sordida*). (A) An image of the textured model of the hooded pitta. See [Supplementary Video 1](#) to view this model with the calibrated UV/VIS color channel textures and RGB composite texture generated in this workflow. The other three specimen models generated in this paper are also shown with RGB composite textures. (B) The hooded pitta model (center) in a hemisphere of image thumbnails used to generate the model. Each blue rectangle indicates the estimated position of the camera for each captured multispectral image. (C) The untextured hooded pitta model shown from four different angles. (D) Using rotoscoping, we animated the model of the hooded pitta. Shown above are four frames of the animated hooded pitta model matched to four frames of a video of a live hooded pitta (ML201372881) in the wild (below). This video was provided to us by the Macaulay Library at the Cornell Lab of Ornithology. See [Supplementary Video 2](#) to view the animation and video side-by-side.

meshes in this workflow, we used the photogrammetric software Agisoft Metashape. This software requires the purchase of a license. The presentation images made using micaToolbox were imported to Metashape to reconstruct the meshes for the specimen models. Utilizing SfM, Metashape aligns images by estimating the camera positions in space relative to the focal object, based on shared features across images (Westoby et al., 2012). We inspected the alignment at this stage and removed any images that could not be aligned properly. Using this refined alignment, Metashape constructed a dense point cloud, which is a set of 3D points that represent samples of the estimated surface of the focal object. We removed any spurious points from the dense point cloud; these points represented the background or objects in the images we were not interested in

reconstructing. We used the manually edited dense point cloud to reconstruct the 3D polygonal mesh. For more information on mesh reconstruction in Metashape, see the Agisoft Metashape User Manual (Professional Edition, Version 1.8). Since SfM produced 3D objects in a relative “image-based” coordinate space (Westoby et al., 2012), we also needed to scale the meshes to “real-world” dimensions. We scaled each model to the true dimensions of the specimens by using scale bars in the images or by using known measurements of structures on the specimen.

Meshes from Metashape are high-resolution polygonal models made up of randomized triangular polygons, also called “faces.” These meshes have a very high density of faces (a high polygon count) which is good for recreating accurate and detailed geometry. However, these “high-poly” models



can be hard to animate (Bot and Irschick, 2019). When the model structure is deformed during the animation process, any artifacts in the randomly triangulated high-poly mesh will produce unwanted wrinkles (Bot and Irschick, 2019). Following Bot and Irschick (2019), we used InstantMesh (Jakob et al., 2015) to retopologize the models and create a simpler shape with more organized faces. Retopologizing is the process by which the faces on the mesh are changed by reducing the face count, swapping the polygon type (e.g., from triangular

polygons to quad polygons), and adjusting the edge flow, which smooths and aligns faces with the natural curvature of the specimen (Bot and Irschick, 2019). This process results in better-looking deformations during animation (Bot and Irschick, 2019). However, care should be taken when decimating and smoothing the model so that important features and measurements are not lost or changed during the process (see Veneziano et al., 2018).

Step 4: Multispectral texture generation and refinement

Having produced a mesh, the next step is to generate 3D multispectral model textures that contain the color-accurate information captured by the 2D multispectral images. A texture is a 2D projection of the color information associated with a 3D model. Pixel values from multiple images are either selected or averaged together to generate the final pixel values in the model texture. How these pixels are combined depends on the blending model selected. We used mosaic blending to generate the textures in this workflow. Mosaic blending uses a weighted average based on the position of the pixel relative to the orientation of the camera (see Agisoft Metashape User Manual, 2022). A potential benefit to the mosaic blending model is that it may reduce the effect of highlights and shadows present in the UV/VIS images (Brown, 2022). Mosaic blending highly weights pixels that are orientated straight toward the camera—which are typically well-lit areas of the images—and down-weights pixels at extreme angles—typically where shadows occur in the images. This should mean that color in the model texture will be more representative of specimen color under well-lit conditions.

Bot and Irschick (2019) compare textures to sewing patterns, which are 2D templates for garments that are sewn together to fit a 3D surface. As in the sewing pattern analogy, we can define how the projection is laid out and where we “cut” the 3D object, so that it lies flat on one plane with minimal stretching (Bot and Irschick, 2019). When the texture is wrapped back onto a 3D surface, the places where the cuts meet are called the “seams.” This projection is stored as a “UV-Map.” U and V are the height and width coordinate dimensions that inform the program where color should be placed on the model (Chouinard-Thuly et al., 2017; Bot and Irschick, 2019), not to be confused with UV (ultraviolet). In this workflow, textures are stored as 16-bit TIFF image files to retain the uncompressed color information from the 2D multispectral image stacks. UV-Maps generated in Metashape use projections with automatically generated seams that break textures into many small fragments that can be difficult to identify as specific areas on the model. We re-made the UV-Maps (initially generated from Metashape) in Autodesk 3ds Max to generate mappings with larger fragments corresponding to easily recognizable features on the specimens (e.g., parts of the wing or tail).

After both the mesh (Step 3) and texture (Step 4) were refined, we imported the new mesh and texture UV-Maps back into Metashape. We used these as a template to create the final, color-accurate 3D multispectral model textures for each specimen model. To do this, we generated a custom-Python script that swapped the presentation images in Metashape used to reconstruct the mesh (Step 3) for the color channel TIFF images (Step 2). This generated five textures—UVR, UVB, R, G, B—using the new UV-Maps, resulting in calibrated textures for all channels of UV/VIS color information. At this point in the workflow, the multispectral model has been generated and can now be used for subsequent color analyses. Color values may be extracted from the multispectral model directly (Step 5a) or the model may be animated first to add behavioral data (Step 5b) before measuring color.

Step 5a: Extracting color data directly from model textures

The output of Steps 1–4 is a 3D multispectral model. Color can be directly extracted from the textures of the 3D multispectral model using multispectral imaging software such as micaToolbox (Troscianko and Stevens, 2015). 3D multispectral model textures can be converted into images that have visual system-specific color values using cone catch models in micaToolbox (Troscianko and Stevens, 2015). These cone catch models estimate cone stimulation values for a given visual system and lighting environment. The textures may be transformed using cone mapping models that correspond to di-, tri-, and tetrachromatic animal color vision systems (Renoult et al., 2017) or using a human-centric color space like CIE XYZ (Smith and Guild, 1931). We generated a custom plugin for micaToolbox (Troscianko and Stevens, 2015) to convert the separate channel textures to a “texture” image stack that is compatible with other micaToolbox plugins. By directly extracting color measurements from 3D multispectral models, as described here in Step 5a, we tested the color accuracy of the 3D multispectral models for each bird specimen (see section “Verifying the accuracy of color information from the multispectral models”).

Step 5b: Rigging and animation

3D multispectral models generated in Steps 1–4 can also be animated (Step 5b) before color information is extracted from the model textures (Step 5a). Such animations require a mesh, a texture, and a rig (Chouinard-Thuly et al., 2017). As explained above, the mesh is the underlying 3D structure of the 3D model. The mesh holds the texture—the color and pattern information associated with the 3D model. A rig is a

skeletal structure that can be manipulated to deform and move the model (Bot and Irschick, 2019). We rendered one of our 3D multispectral models—the hooded pitta—to demonstrate how to combine dynamic behavioral data with color-accurate data embedded in the 3D multispectral models using animation. Rendering is the process of generating either a still image or an animation from a raw model (Chouinard-Thuly et al., 2017). The rendering process can involve adding virtual cameras to a scene to alter views of the model as well as adding special effects to create aspects of lighting and motion. In 3ds Max, we created a basic rig based on a simplified generic bird skeletal structure to manipulate the model during animation. We used a video of a naturally behaving bird as our reference video for the animation. Specifically, we obtained a video of a hooded pitta (ML201372881) from the Macaulay Library at Cornell University. The video shows a male bird jumping out of frame. We animated the hooded pitta using a method called rotoscoping—an animation technique where a reference video is used to guide the animation of a model (Gatesy et al., 2010). This involves deforming the 3D model to match the pose of a target object in the reference video in select frames, called “key frames.” To generate the final animation, we matched frames from the Macaulay Library video at a few key frames marking the beginning and end of major pose changes throughout the video and had 3ds Max interpolate the rest of the 3D model’s movement between these key frames. Once the 3D multispectral model is animated, color information can then be extracted from stacked frames of the rendered animation similar to the way in which color is extracted from static 2D multispectral image stacks or static 3D multispectral model texture stacks (Step 5a). However, now motion is incorporated in the images used for color quantification. We are still refining this stage in the workflow, but the animation presented here (Figure 1D and Supplementary Video 2) demonstrates how we are moving toward completing this step.

Verifying the accuracy of color information from the multispectral models

In order to verify that color information has been accurately captured and retained through each of the steps from imaging (Step 1) to final texture generation (Step 4), we estimated color from several plumage patches on each 3D multispectral model (Step 5a). We first confirmed that the colors were similar to those of the same patches generated from the original 2D multispectral images (Step 2), then independently compared them to values estimated using spectrophotometry. The rationale for confirming color values using estimates from 2D multispectral images was to ensure that color from the original images was retained during the 3D multispectral model

generation process. We expect the cone catch values estimated from the 3D multispectral model textures to be similar, if not identical, to values estimated from the 2D multispectral images since any view from the 3D multispectral model in effect acts as a 2D multispectral image. However, the blending process during texture generation in Step 4 could alter the color captured from the original 2D multispectral images. By verifying that the cone catch estimates from the 3D multispectral texture were similar to estimates from the original 2D multispectral images (Steps 1 and 2), we could confirm that color information was not being lost or considerably changed during the workflow. The rationale for comparing model cone catches to estimates from spectrophotometry data was to verify that the 3D multispectral models were a reasonably accurate representation of color on the original specimens. Unlike values estimated from the 2D multispectral images, cone catches estimated from the spectrophotometry data acted as an independent estimate of color that we could use to test the color accuracy of the 3D multispectral models.

To validate color measurements in the 3D multispectral models, we used the UV-sensitive visual system of the Eurasian blue tit—*Cyanistes caeruleus* (Hart et al., 2000). Avian visual systems are thought to be generally similar to one another outside variation in the SWS1 cone type, which can be either violet- or UV-sensitive (Hart and Hunt, 2007). Therefore, the blue tit visual system is likely comparable to other UV-sensitive avian visual systems. We generated cone catch values for 1–2 plumage patches on each specimen using three methods: 3D multispectral modeling, 2D multispectral imaging, and spectrophotometry. Samples were taken from the breast and shoulder patch on the hooded pitta, the breast and shoulder patch of the pink-necked green pigeon, the breast of the summer tanager, and the breast of the vermilion flycatcher. Icons in Figures 3, 4 show the general location of color measurements for each plumage patch. For the blue tit visual system, cone catch values represent stimulation of the ultraviolet (uv), shortwave (sw), mediumwave (mw), longwave (lw), and double (dbl)-sensitive cone types. For each 3D multispectral model, we selected small regions of interest (ROIs) using Metashape. The ROIs consisted of one small area within a plumage patch. Color can be quite variable within a plumage patch. For example, both the shoulder and breast patch on the hooded pitta contained some intra-patch variation, producing slightly different cone catch estimates when color was sampled from multiple locations within each patch (Supplementary Figure 1). To attempt to limit the effect of color variation within plumage patches, we sampled only small ROIs on the 3D multispectral texture and 2D multispectral image so that we could make relatively direct comparisons with the point source measurements collected using a spectrophotometer. For each ROI, we generated binary (black and white) masks for both the 3D model texture and all initial 2D multispectral images.

Using micaToolbox (Troschianko and Stevens, 2015), we estimated the average cone catch values for all ROIs from both the model texture and one of the 84 multispectral images where the sampled patch was visible and facing directly toward the camera (i.e., similar to the image taken if only 2D multispectral images of the specimen were obtained). We also obtained reflectance spectra corresponding to the sampled plumage patches. We used a USB4000 UV-VIS spectrophotometer connected to a PX-2 pulsed xenon lamp with a 1/4 inch bifurcated reflectance probe from Ocean Optics (now Ocean Insight) and the OceanView software (Ocean Insight, Dunedin, FL, USA). Three replicate reflectance measurements were collected at a 90°/90° incident light/viewing angle orientation, which were averaged to generate a single reflectance spectrum for the ROI for each patch. Color sampled using the multispectral models, multispectral images, and reflectance spectra were all converted to avian color space using the blue tit receptor sensitivities under D65 light either in micaToolbox (Troschianko and Stevens, 2015)—for the multispectral models and multispectral images—or in R (version 4.0.2, R Core Team, 2017) using the R package pavo (version 2.7.0, Maia et al., 2019)—for the reflectance spectra. To aid comparison, the D65 illuminant spectrum from micaToolbox was used for both analyses. All cone catch values estimated from the 3D multispectral textures, 2D multispectral images, and reflectance spectra were plotted in avian color space (Endler and Mielke, 2005; Stoddard and Prum, 2008) using pavo (Maia et al., 2019). This allowed us to evaluate the degree to which colors estimated using the three methods were similar (Figure 3).

We calculated noise-weighted Euclidean distances—chromatic and achromatic contrast values—to quantify the differences between color values estimated from the 3D multispectral texture, the 2D multispectral images, and the spectra. Pavo (Maia et al., 2019) generates chromatic contrast values using Vorobyev and Osorio (1998) receptor noise limited model (RNL) of vision, which correspond to an estimate of the distance between colors in terms in hue and saturation with noise based on relative photoreceptor densities (see CRAN documentation: White et al., 2021). These values are similar to the just-noticeable difference (JND), which is a contrast threshold that also uses the RNL model to estimate discriminability between two colors based on their distance in color space (White et al., 2021). Two colors that are one (or more) JNDs apart are considered to be discriminable given the assumptions of the model (Maia and White, 2018). Because of uncertainty introduced into the application of the RNL model by unknown (and assumed) variables, it is common to use a more conservative assumption that colors that are 3 or more JNDs apart are discriminable (Gómez et al., 2018; Maia and White, 2018). Noise-weighted Euclidean distances correlate with the threshold of discrimination for JNDs, so we use the JND discrimination threshold here and assume that chromatic contrast values of 3 or below are similar (White et al., 2021).

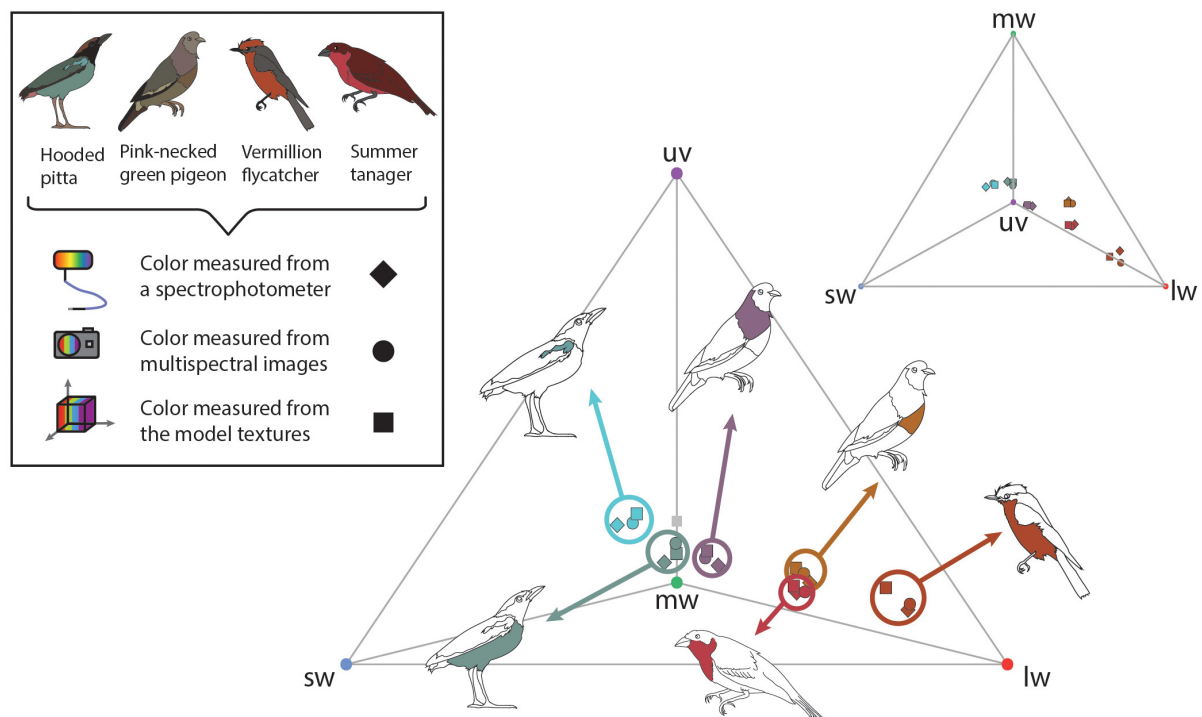


FIGURE 3

To validate the color information on the 3D multispectral models, we compared cone catch values extracted from 3D multispectral model textures, 2D multispectral images, and reflectance spectra. Here these cone catch values are plotted in an avian tetrahedral color space (Endler and Mielke, 2005; Stoddard and Prum, 2008). All avian visible colors can be plotted in the tetrahedral color space according to their relative stimulation of each color cone type in avian retinas, where more saturated colors fall closer to the vertices of the tetrahedron. Vertices of the tetrahedron are colored according to the cone type represented: *uv* (purple), *sw* (blue), *mw* (green), and *lw* (red). Scattered points show the color of patches estimated from the 3D multispectral model texture (squares), 2D multispectral imaging (circles), and spectrophotometry (diamonds). Bird illustrations indicate the plumage patch from which each set of color measurements was collected.

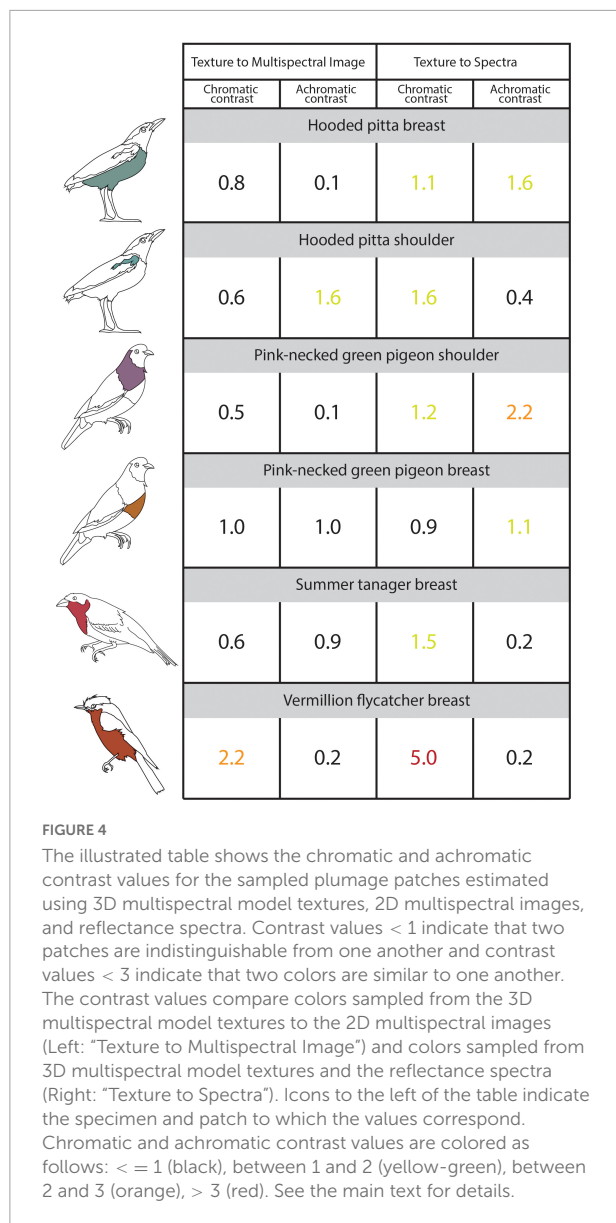
Achromatic contrast values are simple (Weber) contrast values based on a Weber fraction for brightness discrimination (White et al., 2021) and similar to chromatic contrast two colors can be considered similar if the chromatic contrast between them lies between $JND = 0$ and $JND = 3$ (Siddiqi et al., 2004). To calculate chromatic and achromatic contrast, we used a cone ratio of 1 : 2 : 2 : 4 (Maia et al., 2019), a Weber fraction of 0.1 for chromatic contrast (Silvasti et al., 2021) and a Weber fraction of 0.18 for achromatic contrast (Olsson et al., 2018).

Additionally, we performed a supplementary analysis following Troscianko and Stevens (2015) to test color reproduction in our workflow. We compared cone catch values for 36 artist pastels using both our 3D multispectral modeling workflow and spectrophotometry (Supplementary Figure 2). As above, cone catches were estimated using the blue tit visual system under D65 light. Values corresponding to each cone in the blue tit visual system were correlated to assess the fit between the values estimated using our novel workflow (3D multispectral modeling) and values estimated using spectrophotometry. This allowed us to test the performance of our workflow on highly diffuse, saturated, and uniform

colors without the added complexities of natural colors, such as the gloss, iridescence, and intra-patch variation that are often present in avian plumage. The results of this analysis are summarized in Supplementary Figure 2.

Results

We generated 3D multispectral models of four museum specimens that contain UV and VIS color information (Figure 1A). Cone stimulation values—*uv*, *sw*, *mw*, *lw*, and *dbl* cone values—were extracted from the plumage patches on each multispectral model texture. Cone stimulation values were also estimated using two standard methods for quantifying color: 2D multispectral imaging and spectrophotometry. Figure 3 shows the cone stimulation values from each method plotted in tetrahedral color space from two perspectives—one viewing the color space through the *uv*, *sw*, and *lw* face to show variation along these axes (center) and one looking down through the *uv* axis to show variation along the *sw*, *mw*, and *lw* axes (top right). Chromatic and achromatic contrast values that compare (1) the multispectral model textures to the multispectral images



and (2) the multispectral model textures and reflectance spectra are shown in **Figure 4**. The results of this analysis were repeated with a more conservative Weber fraction of 0.05 and are available in **Supplementary Table 2**. This value is generally used for color discrimination on an achromatic background but might produce overly high color discrimination thresholds for more natural conditions (Silvasti et al., 2021). The results of this supplemental analysis are similar to the results of the main paper, which are discussed in more detail below.

Chromatic agreement

Cone catch values estimated using each method—3D multispectral models, 2D multispectral imaging, and

spectrophotometry—for each ROI appeared to closely cluster in the tetrahedral color space (**Figure 3**). In most cases, points representing multispectral textures and multispectral images clustered more closely to each other than to the points representing the reflectance spectra. This was supported by the chromatic contrast values reported in **Figure 4**. Chromatic contrast values between plumage colors estimated from the multispectral model textures and the multispectral images were generally less than or equal to 1.0 (**Figure 4**). The breast patch of the vermilion flycatcher had the highest chromatic contrast value of 2.2, indicating that the 3D multispectral model textures and 2D multispectral images generated slightly different cone catch values. The chromatic contrast values for plumage colors estimated from the 3D multispectral model textures and reflectance spectra were also less than 2, with the exception of the contrast value for the breast patch of the vermilion flycatcher. The vermilion flycatcher had a value of 5.0 (**Figure 4**), indicating that the 3D multispectral model textures and reflectance spectra generated discriminably different cone catch values ($JND > 3$) for this specimen's red breast patch. In general, 3D multispectral models, 2D multispectral images, and reflectance spectra produced similar cone catch estimates for specimen plumage color.

Achromatic agreement

Achromatic contrast values between the plumage colors estimated from the 3D multispectral textures and the 2D multispectral images were all less than 2 (**Figure 4**). The shoulder patch of the hooded pitta had the highest achromatic contrast value of 1.6 (**Figure 4**), while all other patches had values less than or equal to 1.0. This indicates that the 3D multispectral model textures and the 2D multispectral images generate very similar double cone estimates for most plumage patches, except for the hooded pitta shoulder patch. The achromatic contrast values for plumage colors estimated from the model textures and the reflectance spectra were also all less than 2, with the exception of the contrast value for the breast patch of the pink-necked green pigeon. This had a value of 2.2, indicating that 3D multispectral model textures and reflectance spectra generated slightly different double cone estimates, but none that were discriminably ($JND > 3$) different (**Figure 4**). Thus, in general, 3D multispectral models, 2D multispectral images, and reflectance spectra produced similar double cone estimates for specimen plumage color.

Discussion

Using multispectral imaging and photogrammetry, we developed and applied a new workflow to generate 3D models of bird specimens with objective color information that extends

beyond the VIS range. To our knowledge, this is the first workflow to combine multispectral imaging techniques with photogrammetry to produce 3D models that contain UV and VIS color information. This—along with other tools and pipelines being developed in parallel—marks an important step in designing new methods for studying dynamic colorful signals. These 3D models are data-rich representations of color that can be used—even in their static form—to expand the possibilities of color analyses. As expressed by Medina et al. (2020), workflows that utilize 3D photogrammetry have an immediate and promising future in color analysis because they allow for the integration of techniques that have been optimized for color capture—in this case, multispectral imaging. Specifically, this workflow can be used to simulate changes of diffuse animal color as result of motion. With further development, this workflow has great potential to expand to applications that address many other forms of dynamic color. Below, we discuss important considerations and limitations when generating 3D models, and we expand on the applications of multispectral 3D models in both static and dynamic forms.

Workflow validation

Our results support that the 3D multispectral models generated from our workflow are a promising new mode of accurate, objective color measures. Our results show that colors estimated from 3D multispectral models are similar (in terms of cone catch values) to those estimated from 2D multispectral imaging and spectrophotometry for diffuse avian color. Specifically, the chromatic and achromatic contrast values estimated from 3D multispectral model textures and 2D multispectral images all had values under the discrimination threshold of $JND = 3.0$ in a receiver-specific (blue tit) color space (Figure 4). In fact, most color differences fell below the more conservative discrimination value of $JND = 1$ (Figure 4), suggesting that the cone catch estimates generated from 3D multispectral models and 2D multispectral images are very similar. This is unsurprising, since the 2D multispectral images are used to generate the 3D multispectral model textures. These results suggest that color from the 2D multispectral images is being conserved in the 3D multispectral model despite the pixel averaging that occurs during the 3D multispectral texture generation process (Step 4).

When compared to colors estimated from reflectance spectra, those estimated from 3D multispectral models generally resulted in higher contrasts (more difference). However, chromatic and achromatic contrasts were typically below the discrimination threshold of $JND = 3.0$, suggesting that the color values estimated from the 3D multispectral model textures were similar to those estimated using spectrophotometry. These two approaches (3D multispectral models vs. reflectance spectra) are unlikely to generate identical color cone estimates due to

human error when trying to match the area sampled by the ROIs (using a 3D multispectral model) to an area on the physical specimen (using spectrophotometry). For example, the largest color difference between several spectra taken *within* the shoulder patch of the hooded pitta (chromatic contrast = 1.3, Supplementary Figure 1) was larger than the color difference between 3D multispectral models and the reflectance spectra estimates (chromatic contrast = 1.1, Figure 4). This indicates that the color difference between 3D multispectral models and the reflectance spectra falls inside the natural color variation within the hooded pitta shoulder patch. Thus, some of the natural color variation within a plumage patch could be contributing to the color difference found between methods. Color differences between the 3D multispectral models and reflectance spectra may have also arisen during the UV/VIS image capture step of the workflow (Step 1). For example, while the color estimated from the 3D multispectral texture and 2D multispectral images for the shoulder patch of the pink-necked green pigeon was very similar (chromatic contrast = 0.5, achromatic contrast = 0.1; Figure 4), the color estimated from the 3D multispectral texture and the reflectance spectra was slightly different (chromatic contrast = 1.2, achromatic contrast = 2.2; Figure 4). This suggests that color from the 3D multispectral model and the 2D multispectral image is well matched. Rather, color captured in the UV/VIS images from Step 1 likely deviates from the spectral data. Color estimated from the 3D multispectral model, 2D multispectral images, and reflectance spectra was the least similar for the vermillion flycatcher breast patch (chromatic contrast = 2.2 and 5.0; Figure 4). These values may highlight an important limitation of the current workflow—capturing glossy plumage—which we discuss further in the next section.

With this workflow, we aim to introduce 3D multispectral modeling as a potential new avenue for color quantification. We plan to further validate the color accuracy of the models by increasing the number of points sampled from each specimen and by increasing the number and diversity of multispectral models. Generally, our results suggest that to produce color-accurate 3D multispectral models, it is essential to capture high quality UV/VIS images in Step 1 since the 2D multispectral images generated from these photographs (Step 2) are the source of color information for the 3D multispectral models. While our results support that 3D multispectral model textures appropriately retain diffuse plumage color information from 2D multispectral images, researchers will still need to be sensitive to how specimens are prepared, lighting conditions, and complex phenotypes. Specifically, the current workflow is limited to capturing relatively diffuse colors of the specific phenotypic traits that are well preserved by museum specimens. This is highlighted by our supplementary analysis of color reproduction using artist pastels. Cone catches of the highly diffuse pastels estimated using our 3D multispectral modeling workflow are highly correlated with cone catches estimated

using spectrophotometry, suggesting our workflow does very well in reproducing the color of objects that are highly diffuse (**Supplementary Figure 2**). Natural colors with similar properties are likely to be captured better than natural colors that have more specular reflectance, such as glossy or iridescent bird plumage. Therefore, while the current workflow can address behaviorally mediated color changes of diffuse color through postural changes and motion, other physiologically mediated dynamic colors such as iridescence (which is highly angle dependent) and color changes in bare skin patches (which are not captured by museum specimens) will have to be addressed by future extensions of this workflow. We discuss some important considerations and limitations related to specimen type, lighting, and color production mechanism in the next section.

Considerations and limitations

Museum specimens, particularly those in ornithological collections, can be prepared in multiple ways. Skins—also called study skins—represent the largest proportion of avian specimens in most museum collections (**Webster, 2017**). These specimens are prepared to exhibit the bird's outward appearance (**Webster, 2017**) and are commonly configured with the wings, feet, and tail folded and tucked against the body. Some study skins are prepared to display an open wing and/or tail. These are called spread wing/tail preparations and appear less frequently in collections (**Webster, 2017**). Mounted specimens resemble conventional taxidermy preparations, displaying birds in more natural postures. Different specimen preparations may present specific advantages and challenges for 3D modeling and animation. For example, the arrangement of mounted specimens is better suited for rigging and animation because the posture of a naturally posed bird can be better deformed during animation. However, mounted specimens typically have complex 3D form which might require more effort during image capture. In this study, all four specimens we imaged were mounted specimens. Each specimen required seven vertical camera angles to collect enough 3D shape information to produce a sufficient model structure (particularly at the top of the head and underside of the belly/tail), while the study skins imaged by **Medina et al. (2020)** only required three. Many specimens also have areas that are inaccessible for imaging entirely; this is especially true for the underside of wings and tails in many mounted specimens and study skins. Spread wing and tail preparations may provide important phenotypic information, including color and pattern data, that other specimens lack. This would be particularly useful when recreating visual displays that involve revealing concealed patches, such as the tail spread displays many species of insectivorous birds perform to flush prey as they forage. These displays typically reveal highly contrasting

black and white patterns on the bird's tail feathers that are designed to exploit insect escape behavior and startle their prey (**Mumme, 2014**). Future workflows should investigate methods to combine 3D models of multiple specimen types together—leveraging mounts, spread wing/tail preparations, and traditional study skins—to create a model structure that contains the most phenotypic data possible and can be fully rigged and animated.

Lighting is another important consideration, particularly during image capture (Step 1). The lighting of a scene will interact with a specimen's 3D shape and can produce a number of lighting artifacts that may be disadvantageous for color sampling. Directional light can produce shiny highlights if the surface reflectance of the specimen is not Lambertian (i.e., perfectly diffuse) or shadows when the structure of the specimen becomes increasingly complex. Many specimens will have complex 3D structure, particularly mounted specimens which are often posed in natural positions. Therefore, most museum specimens will benefit greatly from being imaged under diffuse lighting. Generating a diffuse broadband (UV+VIS) light environment during imaging is difficult, but lighting artifacts can be minimized by using polytetrafluoroethylene (PTFE) sheets as diffusers to soften directional light and/or by using several identical light sources to illuminate the object from multiple angles. Polarizing filters may also reduce harsh highlights and specular reflections (**Medina et al., 2020**), but these filters should be used with caution when quantifying animal color. Polarizing filters can interact with animal colors in complex ways. Birds, for example, produce colors using pigments, nano- and micro-scale structures in their feather barbs and barbules, or a combination of pigmentary and structural mechanisms (reviewed in **Price-Waldman and Stoddard, 2021**). When photographed with a polarizing filter, there may be little effect on most pigmented plumage, but some structural colors may exhibit shifts in hue. This occurs because polarizing filters block the colored specular reflectance of some plumage, which contributes to the overall perceived color of the plumage patch (K. Nordén, pers. comm.) Here, we only had one light source, so we relied on the mosaic blending model (described in Step 4) and masking of larger shadows to reduce the effects of our directional lighting. In the future, we suggest that researchers modify the lighting set-up to create brighter, more diffuse illumination during the imaging step of this workflow (Step 1). We expect that this will reduce shadows and highlights in the multispectral images and further improve the brightness, hue, and saturation accuracy of the multispectral textures overall.

Highly dynamic colors—such as iridescent and glossy plumage—pose an additional problem for imaging and 3D modeling. These colors, often produced by structural mechanisms, can change considerably in hue, saturation, and brightness across viewing angles. Because textures are generated through the process of blending, any color that exhibits large

changes with viewing angle cannot be captured accurately with our current workflow. While pixel averaging by blending models can help reduce effects of harsh highlights and shadows on diffuse plumage (Brown, 2022), averaging of glossy or iridescent plumage across images will produce pixel values in the final texture that may not correspond to real colors on the physical specimen. This is clearly illustrated by the vermillion flycatcher breast patch, which differed the most in color when estimates from 3D multispectral models were compared to both 2D multispectral images (chromatic contrast = 2.2; Figure 4) and reflectance spectra (chromatic contrast = 5; Figure 4). Glossy red plumage—including that of the vermillion flycatcher—is produced through a combination of pigmentation and feather microstructure modifications (Iskandar et al., 2016). The vermillion flycatcher has thick, flat, smooth feather barbs that make its red plumage—particularly on the crown—appear shinier than reds produced by other birds without this same microstructure modification (Iskandar et al., 2016). The modified, expanded barbs that produce highly saturated reds are good specular reflectors and can produce strong flashes of white reflection with rotation (McCoy et al., 2021; see Supplementary Figure 3). This explains why our methods produced larger color differences for the glossy red breast patch of the vermillion flycatcher (chromatic contrast = 2.2 and 5.0) compared to the color differences for the summer tanager's matte red breast patch (chromatic contrast = 0.6 and 1.5, Figure 4). Some white reflectance from the gloss (see Supplementary Figure 3) was likely averaged with the saturated red of the flycatcher breast patch, producing a less saturated color in the final texture. In contrast, the diffuse plumage of the summer tanager likely remained relatively constant in color across imaged angles so was better represented (lower chromatic contrast; more similar color) in the 3D multispectral model texture. The effects of gloss can also be seen in the shoulder patch of the hooded pitta. However, the gloss of this plumage patch, likely the result of thin-film reflectance from the keratin layer of the feather (Iskandar et al., 2016), resulted in larger differences in brightness values between 3D multispectral models and 2D multispectral images (achromatic contrast = 1.6; Figure 4) than in color (chromatic contrast = 0.6; Figure 4). The color differences seen in both the vermillion flycatcher and the hooded pitta indicate that the blending process can noticeably change the hue, saturation, and brightness of glossy plumage when generating 3D multispectral models.

One benefit of our workflow is that we can readily identify specimens or patches with optical properties such as iridescence and gloss, even if the effects are not obvious to the naked eye. For example, when we inspect the vermillion flycatcher's breast patch across all 2D multispectral images (in which the breast patch is visible), we can see that both the absolute and relative pixel values change with viewing angle. This variation indicates that the glossiness of the feathers is modulating both the overall brightness and the hue and/or saturation of the

color of the plumage patch at different angles of observation. This contrasts with the same measures of the more diffuse plumage on the pink-necked green pigeon shoulder, which show relatively consistent absolute and relative pixel values across 2D multispectral images (Supplementary Figures 4–6). This also differs from the glossy plumage patch on the hooded pitta, which largely differs in absolute pixel value across images, suggesting this type of gloss modulates the brightness of the plumage patch but not the hue or saturation, which are more consistent (Supplementary Figure 6). So, while many avian reds are produced by pigments—making them seemingly good candidates for the current workflow—feather microstructure can produce additional optical effects, such as gloss. This will make capturing color more difficult.

To represent the properties of dynamic colors accurately, it will likely be necessary to generate special shaders to produce the final color on a multispectral model. A shader is a user-defined program that controls the appearance of a digital object at different angles and/or under different lighting conditions. Generic shaders available in rendering software may not be sufficient to accurately produce realistic animal colors (Sun, 2006). Instead, custom iridescent shaders will be necessary for some specimens (see Sun, 2006 for an example of an RGB iridescent shader). These custom shaders should utilize reflectance measurements, like bidirectional reflectance distribution functions (BDRFs), that characterize the directional reflectance of objects (Harvey et al., 2013; Bostwick et al., 2017) and/or optical modeling that accounts for interactions with feather micro- and nano-structure. Overall, developing iridescent/glossy shaders that simulate real color change across the UV/VIS spectrum is an important next step for building more realistic 3D multispectral models.

Finally, this workflow could be improved by automating some of the more time-consuming manual steps in the 3D modeling process, particularly mesh and texture generation/refinement process. This could help reduce the amount of time and expertise needed to generate large numbers of 3D models. Specifically, this workflow could draw from other published procedures (see Bot and Irschick, 2019; Irschick et al., 2020; Medina et al., 2020) that outline rapid and cost-effective photogrammetry pipelines. Certain software used in our current workflow could be substituted for programs used by other studies to reduce the amount of manual effort. For example, while we manually reorganized UV-Maps in this workflow, this step can be automated for faster model generation using SideFX Houdini (SideFX, Software, Toronto, Canada) which—according to Medina et al. (2020)—has more efficient automatic seam generation than Metashape. This software can also be used as an alternative to Instant Meshes for retopologizing, condensing the work of reorganizing UV-Maps and retopologizing to one program. Similarly, automating the animation step of this workflow would greatly reduce the time needed for generating large datasets. Rotoscoping,

while an effective technique, is time-consuming for long, complex animations. While some methods exist for scientific rotoscoping (Gatesy et al., 2010), using machine learning to automate rigging and animation is also a promising area of development for reducing the manual work required during animation (Nath et al., 2019).

Applications of static 3-dimensional multispectral models

By using our workflow to produce a static (unanimated) 3D multispectral model (Steps 1–4), researchers can measure colors (*in silico*, by estimating cone catch values) in a way that is relevant to the visual system of a signal receiver (Step 5a)—in our case, birds. Static 3D multispectral models combine two sets of important phenotypic data often collected from museum specimens—color information and morphometric information. This allows for the sampling of color from across the entire specimen while also accounting for 3D shape and size of the specimen. The ability to sample color and pattern in this way provides unique opportunities for cataloging and analyzing animal colors. Below we describe how producing static 3D multispectral models could (1) improve the digitization of museum specimens; and (2) open new doors for quantifying color with respect to 3D form and lighting.

Static 3D multispectral models, like those generated using our workflow, could become the new “gold standard” for digitizing museum specimens in a way that captures full 3D shape/morphology, color, and patterning. Digitization, in general, increases accessibility of collections by providing easily shareable digital depictions of specimens in the form of images. 3D digitization has the added benefit of increasing the amount of available phenotypic data, because 3D models capture most external features of specimens in three dimensions. Medina et al. (2020) made great strides in developing a 3D digitization pipeline for ornithological collections that is fast, easy, and cost-effective. The avian models generated from their pipeline yield similar bill measurements when compared to the same measurements taken from a specimen by hand, suggesting the 3D models are accurate representations of the specimen’s morphology. However, the models generated by their 3D digitization pipeline do not capture one important phenotypic trait—bird-relevant color information. Our workflow builds on the advantages of 3D photogrammetry pipelines, including the one developed by Medina et al. (2020), by combining the morphometric information of 3D models with the detailed color information of 2D multispectral images. Compared to standard 2D multispectral images, 3D models provide greatly enhanced sampling flexibility, since all angles of the specimen are represented in a single model.

Recently, multispectral images were captured for nearly 6,000 bird species (Cooney et al., 2022) in a study that revealed that tropical passerines are more colorful (have a higher degree

of intra-individual color) than temperate species. In this study, Cooney et al. (2022) collected three multispectral images of each study skin—a dorsal image, a lateral image, and a ventral image—resulting in an expansive dataset of multispectral images for 24,345 specimens. In the future, perhaps such studies will be based on 3D multispectral models, which would provide information (e.g., the surface area and shape of distinct color patches) not necessarily obvious from just three (dorsal, lateral, ventral) images. While the process of generating a 3D model for each specimen is more time-intensive than taking multispectral images from a few standardized angles, the end result is a more flexible, information-rich representation of the specimen.

Finally, static 3D multispectral models can be visualized using 3D computer graphics programs that allow researchers to adjust light and shadows. Specular reflections and shadows are often intentionally reduced during multispectral imaging to help capture accurate measures of surface reflection. However, these lighting elements are important for certain colorful phenotypes, especially those that rely heavily on the interaction between 3D shape and lighting. An example of this is countershading, when dark pigmentation on the dorsal surface of an animal transitions into lighter pigmentation on the underside of the animal (Rowland, 2009). Shadows on the underside of an animal—created by natural overhead illumination—are obliterated by the countershading phenotype, making the animal appear optically flat and therefore harder to detect (Allen et al., 2012). Since countershading relies on the 3D shape of an animal as well as specific lighting conditions, the ability to reproduce specimens with countershaded colors could lead to new insights about camouflage in extant and extinct animals, as in Allen et al. (2012) and Vinther et al. (2016). Using 3D multispectral models, researchers could build on previous studies by systematically illuminating models and manipulating them in a virtual space—adding back realistic shadows and adjusting 3D model dimensions—to better understand how 3D shape interacts with color and pattern in the context of camouflage.

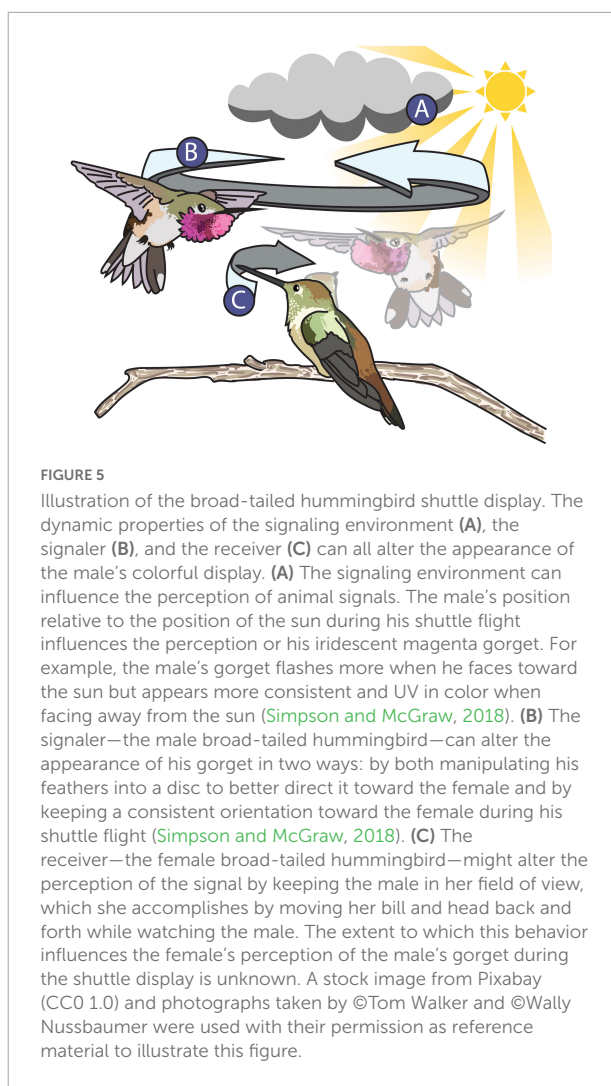
Applications of dynamic 3-dimensional multispectral models

Beyond producing a static 3D multispectral model (Steps 1–4), researchers can measure color (*in silico*, by estimating cone catch values) from an animated 3D multispectral model (Step 5b). The animated model contains color information relevant to a signal receiver (e.g., birds)—along with details about the 3D shape, behavior, and environment of the animal subject. Using the hooded pitta, we demonstrated how the 3D multispectral models produced from this workflow can be animated to include dynamic animal behavior. These animated 3D multispectral models can be used to explore the effects of motion on the design and evolution of dynamic visual signals in a virtual space. Dynamism can be introduced into a signaling interaction through three main pathways: dynamics

introduced by (1) the signaler, (2) the receiver, and (3) the environment. Incorporating motion of signalers, receivers, and the environment into studies of animal color with the use of animated 3D multispectral models could improve our understanding of dynamic animal visual signals.

For example, let us consider the dynamic shuttle courtship display of the male broad-tailed hummingbird (*Selasphorus platycercus*, **Figure 5**). In **Figure 5**, the male broad-tailed hummingbird presents his iridescent throat patch—called the gorget—to an onlooking female by manipulating his feathers into a disc shape to better direct his signal toward the female while maneuvering around her in his repetitive shuttle display. **Simpson and McGraw (2018)** found that males who maintain a more consistent orientation toward the female during the shuttle exhibit greater changes in color and brightness than males who do not. In this way, the male broad-tailed hummingbird (the signaler) is facilitating color changes through behavior, altering the perceived characteristics of his colorful signal. With techniques that utilize animated 3D multispectral models, we can measure color and behavior simultaneously with continuous measures through time and space—a recognized best practice for studying dynamic color (**Hutton et al., 2015**). To successfully animate the model, we can first obtain videos of the display in the field. Many tools for 3D animal tracking (ThruTracker: **Dell et al., 2014**; **Jackson et al., 2016**; Argus: **Corcoran et al., 2021**) and pose estimation (3D Menagerie: **Zuffi et al., 2017**; DeepPoseKit: **Graving et al., 2019**; DeepLabCut: **Nath et al., 2019**; ZooBuilder: **Fangbemi et al., 2020**) are being developed and will make capturing and recreating realistic animal movement for animations achievable. 3D tracking and pose estimation approaches will allow researchers to replicate the movement of objects from the real world, much like film animators use “motion capture,” a technique that allows animators to capture the movements of live actors and map them onto 3D models.

Equally, it is important to consider the position, distance, and direction of the receiver when studying dynamic visual signals. Receivers are usually active participants in signaling interactions and their movement can also influence the way colors are perceived. It is often difficult or impossible to position a camera in the location that best replicates a receiver's view (**Simpson and McGraw, 2018**), but these specific geometric factors will influence an observer's experience of a signal (**Echeverri et al., 2021**). An important advantage of 3D multispectral modeling techniques is the ability to intentionally position and animate cameras around a model during the rendering process. The introduction of unrestricted, user-defined camera views opens a variety of doors for animal coloration research by allowing for more accurate simulations of a receiver's perspective (**Bostwick et al., 2017**). In **Figure 5**, the female broad-tailed hummingbird follows the male with her gaze during his shuttle courtship display. How well the female tracks the male during his display and how that impacts



her perception of the shuttle is still unknown, but animated renders of multispectral models can help shed some light on how receiver motion might impact the appearance of colorful signals. With animated multispectral models, we can recreate the male's movement in relation to the female and also animate virtual cameras to recreate the female's viewing behavior in order to include the influence of receiver movement in a frame-by-frame analysis of male color. Such simulations would help address potential functional hypotheses for this conspicuous female behavior during the broad-tailed courtship display. For example, one hypothesis is that the female keeps the male in a certain area of her visual field to better view his display. Combined with existing tools that could be used to account for important visual properties like spatial resolution and acuity (AcuityView: **Caves and Johnsen, 2018**; QCPA: **van den Berg et al., 2019**), users can further tailor renders to match the receiver's view.

Using animation, we can also simulate dynamism induced by the lighting environment and visual background. Generally, color is measured under consistent lighting conditions

(Hutton et al., 2015) and in the absence of visual background, but signaling environments are often inherently heterogeneous and likely to influence the efficacy of visual signals (Hutton et al., 2015). In order to be conspicuous, signalers need to separate themselves from the physical environment during a signaling interaction. In the case of the broad-tailed hummingbird (Figure 5), the lighting environment can impact the appearance of his gorget during the shuttle display (Simpson and McGraw, 2018). The male's gorget color increases in brightness, chroma, and red hue if the male is oriented toward the sun in his shuttle display. If the male is oriented away from the sun, his gorget appears more consistent in color and is more UV-shifted (Simpson and McGraw, 2018). With animated 3D multispectral modeling, we could simulate the visual background as well as the lighting environment during a male shuttle display and investigate if either strategy—(1) being flashier or (2) being more chromatically consistent—increases the visual saliency of the male against the natural background. Simulating dynamic signals in a virtual environment will be a valuable tool for understanding how animals signal effectively in a dynamic world.

While the current applications of this workflow involve virtual experiments completely *in silico*, a future application for animated 3D multispectral models could be in behavioral playback experiments. For example, it is not yet known what aspects of the male broad-tailed hummingbird shuttle display capture and hold female attention (Figure 5). These alerting components of the male's signal are vital for effective communication of information during courtship (Endler, 1993; Endler and Mappes, 2017). 3D multispectral models could be used to investigate attentional mechanisms in dynamic colorful displays by creating virtual stimuli to present to live animal viewers, like female hummingbirds. Researchers could selectively modify different aspects of the male's shuttle and measure the female's response to determine which component (e.g., speed, gorget color/size/flashiness, sound, etc.), or combination of components, elicit the conspicuous viewing behavior performed by females during naturally occurring displays. One obstacle to this application is that current high-resolution LCD and LED screens do not emit UV light since most display screens are designed for human viewers—a problem that has been recognized for decades and remains unresolved (Cuthill et al., 2000). This is a real limitation for animals—like birds—with a wider range of wavelength sensitivity. However, technology is improving for creating bird-visible colors with LEDs and perhaps more sophisticated screens will be available in the future (Stoddard et al., 2020; Powell et al., 2021).

Conclusion

Recent developments in color quantification, 3D modeling, and animation mean that we are now better equipped

to measure the colorful and often dynamic features of animal phenotypes. Here, we established a workflow for creating color-accurate UV/VIS 3D multispectral models of bird specimens with diffuse coloration—an important first step in generating new methods to quantify dynamic color. Our results suggest that the 3D multispectral models produced by this workflow contain color values comparable to those estimated using 2D multispectral imaging and spectrophotometry. We hope that this initial demonstration of our workflow will promote more work in developing 3D multispectral modeling pipelines. Generating color-accurate 3D multispectral models is an easy and effective way of producing data-rich digital renderings of animal specimens. Such models could transform the study and digitization of natural history museum specimens and inspire novel investigations of animal signaling in virtual worlds.

Data availability statement

The raw data supporting the conclusions of this article will be made available by the authors, without undue reservation.

Author contributions

AEM, BH, and MCS conceptualized the workflow, planned the study, revised, and approved the final manuscript. AEM and BH developed the workflow, collected, and analyzed the data. AEM produced figures and tables and wrote the first draft of the manuscript. All authors contributed to the article and approved the submitted version.

Funding

Funding to AEM was provided by the Princeton University. Funding to MCS was provided by Princeton University, a Packard Fellowship for Science and Engineering, and the National Science Foundation (Award #2029538).

Acknowledgments

We thank the Stoddard Lab for providing valuable feedback on the figures for this manuscript. We appreciate the valuable comments made by Jarome Ali, Klara Nordén, Monica Carlson, Sumudu Fernando, and Sarah Solie on drafts of the manuscript. We are grateful to the Macaulay Library at the Cornell Lab of Ornithology for sharing the video of the hooded pitta (ML201372881).

Conflict of interest

The authors declare that the research was conducted in the absence of any commercial or financial relationships that could be construed as a potential conflict of interest.

Publisher's note

All claims expressed in this article are solely those of the authors and do not necessarily represent those of their affiliated

organizations, or those of the publisher, the editors and the reviewers. Any product that may be evaluated in this article, or claim that may be made by its manufacturer, is not guaranteed or endorsed by the publisher.

Supplementary material

The Supplementary Material for this article can be found online at: <https://www.frontiersin.org/articles/10.3389/fevo.2022.983369/full#supplementary-material>

References

- Agisoft Metashape User Manual, (2022) *Agisoft Metashape User Manual - Professional Edition, Version 1.8*.
- Akkaynak, D., Treibitz, T., Xiao, B., Gürkan, U. A., Allen, J. J., Demirci, U., et al. (2014). Use of commercial off-the-shelf digital cameras for scientific data acquisition and scene-specific color calibration. *J. Opt. Soc. Am. A* 31:312. doi: 10.1364/JOSAA.31.000312
- Allen, W. L., Baddeley, R., Cuthill, I. C., and Scott-Samuel, N. E. (2012). A Quantitative test of the predicted relationship between countershading and lighting environment. *Am. Nat.* 180, 762–776. doi: 10.1086/668011
- Bishop, P. J., Cuff, A. R., and Hutchinson, J. R. (2021). How to build a dinosaur: Musculoskeletal modeling and simulation of locomotor biomechanics in extinct animals. *Paleobiology* 47, 1–38. doi: 10.1017/pab.2020.46
- Bestwick, K. S., Harvey, T. A., and Scholes, E. I. I. (2017). “Leveraging diverse specimen types to integrate behavior and morphophology,” in *The extended specimen: Emerging frontiers in collection-based ornithological research*, ed. M. S. Webster (Boca Raton, FL: CRC Press).
- Bot, J. A., and Irschick, D. J. (2019). “Using 3D photogrammetry to create openness models of live animal: 2D and 3D software solutions,” in *3D/VR in the academic library: Emerging practices and trends*, eds J. Grayburn, Z. L. Katz, K. G. Davis, and V. I. Orlati (Alexandria, VA: Council on Library and Information Resources).
- Brown, D. (2022). A workflow and tips for creating 3D models of amphibians and reptiles using photogrammetry. *Herpetol. Rev.* 53, 34–38.
- Burns, K. J., McGraw, K. J., Shultz, A. J., Stoddard, M. C., and Thomas, D. B. (2017). “Advanced methods for studying pigments and coloration using avian specimens 1, 2,” in *The extended specimen: Emerging frontiers in collections-based ornithological research*, ed. M. S. Webster (Boca Raton, FL: CRC Press).
- Caves, E. M., and Johnsen, S. (2018). AcuityView: An R package for portraying the effects of visual acuity on scenes observed by an animal. *Methods Ecol. Evol.* 9, 793–797. doi: 10.1111/2041-210X.12911
- Chiao, C.-C., and Cronin, T. W. (2002). Hyperspectral imaging for color vision research. *Recent Res. Dev. Optics* 2, 465–482.
- Chiari, Y., Wang, B., Rushmeier, H., and Caccione, A. (2008). Using digital images to reconstruct three-dimensional biological forms: a new tool for morphological studies. *Biol. J. Linnean Soc.* 95, 425–436. doi: 10.1111/j.1095-8312.2008.01055.x
- Chouinard-Thuly, L., Gierszewski, S., Rosenthal, G. G., Reader, S. M., Rieucieu, G., Woo, K. L., et al. (2017). Technical and conceptual considerations for using animated stimuli in studies of animal behavior. *Curr. Zool.* 63, 5–19. doi: 10.1093/cz/zow104
- Cooney, C. R., He, Y., Varley, Z. K., Nouri, L. O., Moody, C. J. A., Jardine, M. D., et al. (2022). Latitudinal gradients in avian colourfulness. *Nat. Ecol. Evol.* 6, 622–629. doi: 10.1038/s41559-022-01714-1
- Corcoran, A. J., Schirmacher, M. R., Black, E., and Hedrick, T. L. (2021). ThruTracker: Open-source software for 2-d and 3-d animal video tracking. *bioRxiv* [Preprint] doi: 10.1101/2021.05.12.443854
- Cuthill, I. C., Allen, W. L., Arbuckle, K., Caspers, B., Chaplin, G., Hauber, M. E., et al. (2017). The biology of color. *Science* 357:eaan0221. doi: 10.1126/science.aan0221
- Cuthill, I. C., Hart, N. S., Partridge, J. C., Bennett, A. T. D., Hunt, S., and Church, S. C. (2000). Avian colour vision and avian video playback experiments. *Acta Ethol.* 3, 29–37. doi: 10.1007/s102110000027
- Delhey, K., Delhey, V., Kempnaers, B., and Peters, A. (2015). A practical framework to analyze variation in animal colors using visual models. *Behav. Ecol.* 26, 367–375. doi: 10.1093/beheco/aru198
- Dell, A. I., Bender, J. A., Branson, K., Couzin, I. D., de Polavieja, G. G., Noldus, L. P. J. J., et al. (2014). Automated image-based tracking and its application in ecology. *Trends Ecol. Evol.* 29, 417–428. doi: 10.1016/j.tree.2014.05.004
- DeLorenzo, L., Linden, A. V., Bergmann, P. J., Wagner, G. P., Siler, C. D., and Irschick, D. J. (2020). Using 3D-digital photogrammetry to examine scaling of the body axis in burrowing skinks. *J. Morphol.* 281, 1382–1390. doi: 10.1002/jmor.21253
- Echeverri, S. A., Miller, A. E., Chen, J., McQueen, E. W., Plakke, M., Spicer, M., et al. (2021). How signaling geometry shapes the efficacy and evolution of animal communication systems. *Int. Comp. Biol.* 61, 787–813. doi: 10.1093/icb/icab090
- Endler, J. A. (1993). Some general comments on the evolution and design of animal communication systems. *Philos. Trans. Biol. Sci.* 340, 215–225. doi: 10.1098/rstb.1993.0060
- Endler, J. A., and Mappes, J. (2017). The current and future state of animal coloration research. *Phil. Trans. R. Soc. B* 372:20160352. doi: 10.1098/rstb.2016.0352
- Endler, J. A., and Mielke, P. W. (2005). Comparing entire colour patterns as birds see them. *Biol. J. Linnean Soc.* 86, 405–431. doi: 10.1111/j.1095-8312.2005.00540.x
- Fangbemi, A. S., Lu, Y. F., Xu, M. Y., Luo, X. W., Rolland, A., and Raissi, C. (2020). ZooBuilder: 2D and 3D pose estimation for quadrupeds using synthetic data. *arXiv* [Preprint]. arXiv: 2009.05389.
- Fortuny, J., Marcé-Nogué, J., Heiss, E., Sanchez, M., Gil, L., and Galobart, À (2015). 3D bite modeling and feeding mechanics of the largest living amphibian, the chinese giant salamander *Andrias davidianus* (Amphibia: Urodela). *PLoS One* 10:e0121885. doi: 10.1371/journal.pone.0121885
- Frith, D. W., and Frith, C. B. (1988). Courtship display and mating of the superb bird of paradise lophorina superb. *EMU - Austral Ornithol.* 88, 183–188. doi: 10.1071/MU9880183
- Gatesy, S. M., Baier, D. B., Jenkins, F. A., and Dial, K. P. (2010). Scientific rotoscoping: a morphology-based method of 3-D motion analysis and visualization. *J. Exp. Zool. Part A: Ecol. Genetics Physiol.* 313A, 244–261. doi: 10.1002/jez.588
- Gómez, J., Ramo, C., Troscianko, J., Stevens, M., Castro, M., Pérez-Hurtado, A., et al. (2018). Individual egg camouflage is influenced by microhabitat selection and use of nest materials in ground-nesting birds. *Behav. Ecol. Sociobiol.* 72:142. doi: 10.1007/s00265-018-2558-7
- Graving, J. M., Chae, D., Naik, H., Li, L., Koger, B., Costelloe, B. R., et al. (2019). DeepPoseKit, a software toolkit for fast and robust animal pose estimation using deep learning. *eLife* 8:e47994. doi: 10.7554/eLife.47994
- Hart, N. S., and Hunt, D. M. (2007). Avian visual pigments: characteristics, spectral tuning, and evolution. *Am. Nat.* 169, S7–S26. doi: 10.1086/510141

- Hart, N. S., Partridge, J. C., Cuthill, I. C., and Bennett, A. T. D. (2000). Visual pigments, oil droplets, ocular media and cone photoreceptor distribution in two species of passerine bird: the blue tit (*Parus caeruleus* L.) and the blackbird (*Turdus merula* L.). *J. Comp. Physiol. Sensory Neural Behav. Physiol.* 186, 375–387. doi: 10.1007/s003590050437
- Harvey, T. A., Bostwick, K. S., and Marschner, S. (2013). Measuring spatially- and directionally-varying light scattering from biological material. *JoVE (J. Vis. Exp.)* 75:e50254. doi: 10.3791/50254
- Hutton, P., Seymoure, B. M., McGraw, K. J., Ligon, R. A., and Simpson, R. K. (2015). Dynamic color communication. *Curr. Opin. Behav. Sci.* 6, 41–49. doi: 10.1016/j.cobeha.2015.08.007
- Irschick, D. J., Corriveau, Z., Mayhan, T., Siler, C., Mandica, M., Gamble, T., et al. (2020). Devices and methods for rapid 3D photo-capture and photogrammetry of small reptiles and amphibians in the laboratory and the field. *Herpetol. Rev.* 51, 716–725.
- Irschick, D. J., Martin, J., Siebert, U., Kristensen, J. H., Madsen, P. T., and Christiansen, F. (2021). Creation of accurate 3D models of harbor porpoises (*Phocoena phocoena*) using 3D photogrammetry. *Mar. Mammal Sci.* 37, 482–491. doi: 10.1111/mms.12759
- Iskandar, J.-P., Eliason, C. M., Astrop, T., Igic, B., Maia, R., and Shawkey, M. D. (2016). Morphological basis of glossy red plumage colours. *Biol. J. Linnean Soc.* 119, 477–487. doi: 10.1111/bij.12810
- Jackson, B. E., Evangelista, D. J., Ray, D. D., and Hedrick, T. L. (2016). 3D for the people: Multi-camera motion capture in the field with consumer-grade cameras and open source software. *Biol. Open* 5, 1334–1342. doi: 10.1242/bio.018713
- Jakob, W., Tarini, M., Panozzo, D., and Sorkine-Hornung, O. (2015). Instant field-aligned meshes. *ACM Trans. Graph.* 34, 1–15. doi: 10.1145/2816795.2818078
- Kim, M. H., Harvey, T. A., Kittle, D. S., Rushmeier, H., Dorsey, J., Prum, R. O., et al. (2012). “3D imaging spectroscopy for measuring hyperspectral patterns on solid objects,” in *Proceedings of the ACM Transactions on Graphics*, (New York, NY). doi: 10.1145/2185520.2185534
- Künzler, R., and Bakker, T. C. M. (1998). Computer animations as a tool in the study of mating preferences. *Behaviour* 135, 1137–1159.
- Leavesley, S., Ahmed, W., Bayraktar, B., Rajwa, B., Strugis, J., and Robinson, J. P. (2005). Multispectral imaging analysis: spectral deconvolution and applications in biology. *Proc. SPIE* 5699:121. doi: 10.1117/12.598065
- Maia, R., Gruson, H., Endler, J. A., and White, T. E. (2019). pavo 2: new tools for the spectral and spatial analysis of colour in R. *Methods Ecol. Evol.* 10, 1097–1107. doi: 10.1111/2041-210X.13174
- Maia, R., and White, T. E. (2018). Comparing colors using visual models. *Behav. Ecol.* 29, 649–659. doi: 10.1093/beheco/ary017
- Mäthger, L. M., Denton, E. J., Marshall, N. J., and Hanlon, R. T. (2009). Mechanisms and behavioural analysis of structural coloration in cephalopods. *J. R. Soc. Interface* 6, S149–S163. doi: 10.1098/rsif.2008.0366.focus
- McCoy, D. E., Shultz, A. J., Vidoudez, C., van der Heide, E., Dall, J. E., Trauger, S. A., et al. (2021). Microstructures amplify carotenoid plumage signals in tanagers. *Sci. Rep.* 11:8582. doi: 10.1038/s41598-021-88106-w
- Medina, J. J., Maley, J. M., Sannapareddy, S., Medina, N. N., Gilman, C. M., and McCormack, J. E. (2020). A rapid and cost-effective pipeline for digitization of museum specimens with 3D photogrammetry. *PLoS One* 15:e0236417. doi: 10.1371/journal.pone.0236417
- Miles, M. C., and Fuxjager, M. J. (2019). Phenotypic diversity arises from secondary signal loss in the elaborate visual displays of toucans and barbets. *Am. Nat.* 194, 152–167. doi: 10.1086/704088
- Müller, K., Smielik, I., Hütwohl, J.-M., Gierszewski, S., Witte, K., and Kuhnert, K.-D. (2017). The virtual lover: Variable and easily guided 3D fish animations as an innovative tool in mate-choice experiments with sailfin mollies-I. Design and implementation. *Curr. Zool.* 63, 55–64. doi: 10.1093/cz/zow106
- Mumme, R. L. (2014). White tail spots and tail-flicking behavior enhance foraging performance in the Hooded Warbler. *Auk* 131, 141–149. doi: 10.1642/AUK-13-199.1
- Nath, T., Mathis, A., Chen, A. C., Patel, A., Bethge, M., and Mathis, M. W. (2019). Using DeepLabCut for 3D markerless pose estimation across species and behaviors. *Nat. Protoc.* 14, 2152–2176. doi: 10.1038/s41596-019-0176-0
- Negro, J. J., Sarasola, J. H., Fariñas, F., and Zorrilla, I. (2006). Function and occurrence of facial flushing in birds. *Comp. Biochem. Physiol. Part A: Mol. Int. Physiol.* 143, 78–84. doi: 10.1016/j.cbpa.2005.10.028
- Nguyen, C. V., Lovell, D. R., Adcock, M., and Salle, J. L. (2014). Capturing natural-colour 3D models of insects for species discovery and diagnostics. *PLoS One* 9:e94346. doi: 10.1371/journal.pone.0094346
- Olsson, P., Lind, O., and Kelber, A. (2018). Chromatic and achromatic vision: parameter choice and limitations for reliable model predictions. *Behav. Ecol.* 29, 273–282. doi: 10.1093/beheco/arx133
- Osorio, D., and Vorobyev, M. (2005). Photoreceptor spectral sensitivities in terrestrial animals: adaptations for luminance and colour vision. *Proc. R. Soc. B.* 272, 1745–1752. doi: 10.1098/rspb.2005.3156
- Pike, T. W. (2011). Using digital cameras to investigate animal colouration: estimating sensor sensitivity functions. *Behav. Ecol. Sociobiol.* 65, 849–858. doi: 10.1007/s00265-010-1097-7
- Powell, S. B., Mitchell, L. J., Phelan, A. M., Cortesi, F., Marshall, J., and Cheney, K. L. (2021). A five-channel LED display to investigate UV perception. *Methods Ecol. Evol.* 12, 602–607. doi: 10.1111/2041-210X.13555
- Price-Waldman, R., and Stoddard, M. C. (2021). Avian coloration genetics: recent advances and emerging questions. *J. Heredity* 112, 395–416. doi: 10.1093/jhered/esab015
- R Core Team (2017). *R: A Language and Environment for Statistical Computing*. Vienna: R Foundation for Statistical Computing.
- Renoult, J. P., Kelber, A., and Schaefer, H. M. (2017). Colour spaces in ecology and evolutionary biology. *Biol. Rev.* 92, 292–315. doi: 10.1111/brv.12230
- Rosenthal, G. G. (2007). Spatiotemporal dimensions of visual signals in animal communication. *Annu. Rev. Ecol. Evol. Syst.* 38, 155–178. doi: 10.1146/annurev.ecolsys.38.091206.095745
- Rowland, H. M. (2009). From Abbott Thayer to the present day: What have we learned about the function of countershading? *Philos. Trans. R. Soc. B* 364, 519–527. doi: 10.1098/rstb.2008.0261
- Schneider, C. A., Rasband, W. S., and Eliceiri, K. W. (2012). NIH Image to ImageJ: 25 years of image analysis. *Nat. Methods* 9, 671–675. doi: 10.1038/nmeth.2089
- Siddiqi, A., Cronin, T. W., Loew, E. R., Vorobyev, M., and Summers, K. (2004). Interspecific and intraspecific views of color signals in the strawberry poison frog *Dendrobates pumilio*. *J. Exp. Biol.* 207, 2471–2485. doi: 10.1242/jeb.01047
- Silvasti, S. A., Valkonen, J. K., and Nokelainen, O. (2021). Behavioural thresholds of blue tit colour vision and the effect of background chromatic complexity. *Vis. Res.* 182, 46–57. doi: 10.1016/j.visres.2020.11.013
- Simpson, R. K., and McGraw, K. J. (2018). Two ways to display: male hummingbirds show different color-display tactics based on sun orientation. *Behav. Ecol.* 29, 637–648. doi: 10.1093/beheco/ary016
- Smith, T., and Guild, J. (1931). The C.I.E. colorimetric standards and their use. *Trans. Opt. Soc.* 33, 73–134. doi: 10.1088/1475-4878/33/3/301
- Stavenga, D. G., Leertouwer, H. L., Marshall, N. J., and Osorio, D. (2011). Dramatic colour changes in a bird of paradise caused by uniquely structured breast feather barbules. *Proc. R. Soc. B: Biol. Sci.* 278, 2098–2104. doi: 10.1098/rspb.2010.2293
- Stevens, M., Párraga, C. A., Cuthill, I. C., Partridge, J. C., and Troscianko, T. S. (2007). Using digital photography to study animal coloration. *Biol. J. Linnean Soc.* 90, 211–237. doi: 10.1111/j.1095-8312.2007.00725.x
- Stoddard, M. C., and Prum, R. O. (2008). Evolution of avian plumage color in a tetrahedral color space: a phylogenetic analysis of new world buntings. *Am. Nat.* 171, 755–776. doi: 10.1086/587526
- Stoddard, M. C., Eyster, H. N., Hogan, B. G., Morris, D. H., Soucy, E. R., and Inouye, D. W. (2020). Wild hummingbirds discriminate nonspectral colors. *Proc. Natl. Acad. Sci. U.S.A.* 117, 15112–15122. doi: 10.1073/pnas.1919377117
- Sun, Y. (2006). Rendering biological iridescences with RGB-based renderers. *ACM Trans. Graphics* 25, 100–129.
- Troscianko, J., and Stevens, M. (2015). Image calibration and analysis toolbox - a free software suite for objectively measuring reflectance, colour and pattern. *Methods Ecol. Evol.* 6, 1320–1331. doi: 10.1111/2041-210X.12439
- van den Berg, C. P., Troscianko, J., Endler, J. A., Marshall, N. J., and Cheney, K. L. (2019). Quantitative Colour Pattern Analysis (QCPA): a comprehensive framework for the analysis of colour patterns in nature. *Methods Ecol. Evol.* 11, 316–332.
- Veneziano, A., Landi, F., and Profico, A. (2018). Surface smoothing, decimation, and their effects on 3D biological specimens. *Am. J. Phys. Anthropol.* 166, 473–480. doi: 10.1002/ajpa.23431
- Vinther, J., Nicholls, R., Lautenschlager, S., Pittman, M., Kaye, T. G., Rayfield, E., et al. (2016). 3D camouflage in an ornithomimid dinosaur. *Curr. Biol.* 26, 2456–2462. doi: 10.1016/j.cub.2016.06.065
- Vorobyev, M., and Osorio, D. (1998). Receptor noise as a determinant of colour thresholds. *Proc. R. Soc. Lond. B* 265, 351–358. doi: 10.1098/rspb.1998.0302

- Webster, M. S. (2017). "The extended specimen," in *The extended specimen: Emerging frontiers in collections-based ornithological research*, ed. M. S. Webster (Boca Raton, FL: CRC Press).
- Westoby, M., Brasington, J., Glasser, N., Hambrey, M., and Reynolds, J. (2012). Structure-from-Motion photogrammetry: a novel, low-cost tool for geomorphological applications. *Geomorphology* 179, 300–314.
- White, T., Maia, R., Endler, J., Eliason, C., and Bitton, P.-P. (2021). *pavo: Perceptual Analysis, Visualization and Organization of Spectral Colour Data. Version 2.7.1*. CRAN.
- Witte, K., Gierszewski, S., Chouinard-Thuly, L., and Guest Editors. (2017). Virtual is the new reality. *Curr. Zool.* 63, 1–4. doi: 10.1093/cz/zow119
- Woo, K. L., Rieucou, G., and Burke, D. (2017). Computer-animated stimuli to measure motion sensitivity: Constraints on signal design in the Jacky dragon. *Curr. Zool.* 63, 75–84. doi: 10.1093/cz/zow074
- Zimova, M., Hackländer, K., Good, J. M., Melo-Ferreira, J., Alves, P. C., and Mills, L. S. (2018). Function and underlying mechanisms of seasonal colour moulting in mammals and birds: what keeps them changing in a warming world? *Biol. Rev.* 93, 1478–1498. doi: 10.1111/brv.12405
- Zuffi, S., Kanazawa, A., Jacobs, D. W., and Black, M. J. (2017). "3D menagerie: Modeling the 3d shape and pose of animals," in *Proceedings of the 2017 IEEE conference on computer vision and pattern recognition (CVPR)*, Honolulu, HI, 5524–5532. doi: 10.1109/CVPR.2017.586
- Zylinski, S., Osorio, D., and Shohet, A. J. (2009). Cuttlefish camouflage: context-dependent body pattern use during motion. *Proc. R. Soc. B: Biol. Sci.* 276, 3963–3969. doi: 10.1098/rspb.2009.1083



OPEN ACCESS

EDITED BY
Nicola Marples,
Trinity College Dublin,
Ireland

REVIEWED BY
Rodrigo Willemart,
University of São Paulo,
Brazil
Nathalia Ximenes,
University of São Paulo,
Brazil, in collaboration with reviewer RW

*CORRESPONDENCE
Eunice J. Tan
✉ yncje@nus.edu.sg

SPECIALTY SECTION
This article was submitted to
Behavioral and Evolutionary Ecology,
a section of the journal
Frontiers in Ecology and Evolution

RECEIVED 10 October 2022
ACCEPTED 23 January 2023
PUBLISHED 09 February 2023

CITATION
Tan EJ, Elgar MA, Bian X and Peters RA (2023)
Interpreting animal behaviors – A cautionary
note about swaying in phasmids.
Front. Ecol. Evol. 11:1065789.
doi: 10.3389/fevo.2023.1065789

COPYRIGHT
© 2023 Tan, Elgar, Bian and Peters. This is an
open-access article distributed under the terms
of the [Creative Commons Attribution License](#)
(CC BY). The use, distribution or reproduction
in other forums is permitted, provided the
original author(s) and the copyright owner(s)
are credited and that the original publication in
this journal is cited, in accordance with
accepted academic practice. No use,
distribution or reproduction is permitted which
does not comply with these terms.

Interpreting animal behaviors – A cautionary note about swaying in phasmids

Eunice J. Tan^{1,2*}, Mark A. Elgar³, Xue Bian^{4,5} and Richard A. Peters⁴

¹Division of Science, Yale-NUS College, Singapore, Singapore, ²Department of Biological Sciences, National University of Singapore, Singapore, Singapore, ³School of BioSciences, University of Melbourne, Melbourne, VIC, Australia, ⁴Animal Behaviour Group, Department of Environment and Genetics, La Trobe University, Melbourne, VIC, Australia, ⁵Gansu Key Laboratory of Biomonitoring and Bioremediation for Environmental Pollution, School of Life Sciences, Lanzhou University, Lanzhou, China

Diverse animals including snakes, spiders and phasmids sway in response to abiotic and biotic factors. Recent research on swaying in phasmids suggest they may adopt distinctive swaying to reduce detection from predators. This view was recently challenged, by interpreting swaying behavior as serving a balancing function related to postural sway and not a form of anti-predator behavior. We dispute this interpretation as the reanalysis of data for balance was based on an erroneous perception of the upright posture of the insects, contrary to the initial study and natural history observations. We present observations collected from four species of more than 300 phasmids over a three-day period and show that the insects seldom adopt an upright posture (4% of observations). While we appreciate that attempts to reinterpret data form a central role of the scientific method, we urge caution when inferring biological function without an accurate knowledge of the species' natural history. Investigations of signals in motion require great care to ensure they are interpreted in a natural environment and context.

KEYWORDS

swaying, phasmids, adaptive function, anti-predator, natural history

Introduction

Animals move for various purposes, such as to forage, find mates, deter rivals and predators and to seek shelter. This movement may draw unwanted attention from natural enemies. It is thus particularly surprising that many species sway, a non-perambulatory movement which involves the lateral rocking of the body, while the legs remain stationary and in contact with the substrate (Bian et al., 2016). This behavior is particularly prevalent in phasmids, but also occurs in diverse taxa, including spiders, mantids and snakes (Fleishman, 1985; Jackson, 1985; Watanabe and Yano, 2009; Tan and Elgar, 2021). Several lines of thought suggest that swaying behavior has a signaling function, providing offensive or defensive mechanisms to improve foraging success or the likelihood of attack from predators. For example, *Portia* spiders sway their palps, legs and bodies to evade detection when they approach their arachnid prey, as the movements give *Portia* the appearance unlike that of a spider or an animal that imposes a threat (Jackson, 1985). Vine snakes *Oxybelis aeneus* oscillate forward and backward, presumably to mimic vegetation movement (Fleishman, 1985). In mantids, swaying can reduce detection by predators, cannibalistic conspecifics and prey (Watanabe and Yano, 2009, 2012, 2013). Several species of phasmids are reported to sway (Rupperecht, 1971; Bian et al., 2016; Pohl et al., 2022), with recent research on phasmids consistent with the view that phasmids adopt swaying to reduce detection (Bian et al., 2016; Pohl et al., 2022). Thus, swaying provides phasmids with a form of concealment between revealing behaviors through motion masquerade, which is the matching of an animal's motion to environmental motion, such that the animal

resembles an inanimate object and prevents detection by an observer (Fleishman, 1985). Through the interpretation of swaying behavior in phasmids, this article emphasizes the importance of inferring biological function with an accurate knowledge of the species' natural history.

Swaying, hanging and perching

Recently, swaying behavior has been interpreted as serving a balancing function (Kelty-Stephen, 2018; Cuthill et al., 2019), based on reanalysis by Kelty-Stephen (2018) using the data presented in Bian et al. (2016). Bian et al. (2016) examined the movement of the phasmid *Extatosoma tiaratum* in response to wind cues. While the insects would sway in response to wind stimulus, the frequency of swaying declined over time. The number of sways was higher in variable wind conditions compared with constant wind conditions, suggesting that the insects react to environmental cues such as wind stimulus and modify their swaying behavior in response. In the presence of plants in the background, insect swaying was consistent with the movement of the wind-blown plants. Reanalyzing part of the same dataset, Kelty-Stephen (2018) proposed that the swaying behavior allows the insects to achieve stability in response to wind-like stimulation. Kelty-Stephen (2018) further proposes that these data provide evidence for multifractal complexity in postural stabilization under wind-like stimulation and point to similarities between phasmid and human postural sway. Kelty-Stephen (2018) proposed that the reduction in sway exhibited by phasmids can be explained by non-linear interactions across time consistent with tensegrity principles and dismissed Bian et al.'s (2016) suggestion of anti-predator behavior on the part of the insects. Such a balancing function could be more relevant to perching than hanging insects, with the latter relying on gravity to remain stable.

We do not seek to question Kelty-Stephen's (2018) analysis. However, we must point out that the author has foremost, incorrectly characterized the phasmids described in Bian et al. (2016) to 'perch upon a branch' (Kelty-Stephen, 2018, p. 8), when they were, in fact, hanging from a branch (Figures 1A,B). It is unclear why Kelty-Stephen (2018) took this

perspective on phasmid swaying behavior and whether this inaccuracy influenced the author's interpretations. While phasmids can walk when perching, it is uncommon. *E. tiaratum* (Phasmatidae) typically hangs from perches, rarely spending time 'upright'. We found a similar pattern for four species of phasmids that we had collected from the field, maintained in the laboratory and observed over a three-day period (Figures 1C–F; Table 1). Hanging from the top or side of the enclosure, host plant or even another phasmid was the overwhelming position observed, while perching was relatively rare (60 out of 1,343 observations, 4%). Swaying behavior was not ubiquitous across these four species: swaying was common in *Lonchodes brevipes* (Diapheromeridae), occasionally observed in *Calvisia flavopennis* (Lonchodidae) and *Marmessoidea rosea* (Lonchodidae), and rarely observed in *Haaniella echinata* (Heteropterygidae). Indeed, our study (Pohl et al., 2022) indicate that even for the same species (*L. brevipes*), individuals at different life stages appear to sway to different extents. More nuanced studies in the future are crucial to understand the factors affecting swaying behavior, but the appropriate biological context to consider stabilizing mechanisms in such systems is of a hanging organism.

Interpreting behavior

We find it surprising that the author misrepresented the work in this way, particularly as the hanging phasmids considered in Bian et al. (2016) contrasts with upright focal organisms in references on postural sway (e.g., Straube et al., 1987; Clayton et al., 2003; Hutchinson et al., 2007; Munafo et al., 2016; Dewolf et al., 2021). Demonstrating tensegrity principles in a hanging organism seems novel and worthy of further attention; but evaluation of the significance and broader implications of these findings are relevant only when the behavior is placed in the correct context. Kelty-Stephen (2018) was, perhaps, too quick to dismiss the potential for sway to represent an adaptive behavior to avoid predators. We do not claim here that the data provides definitive evidence that it does, nor did Bian et al. (2016). However, we argue that Kelty-Stephen (2018) dismisses the possibility based on a limited consideration of the broader investigation, and we do not wish for this premature and inaccurate characterization to propagate (e.g., Cuthill et al., 2019).

In characterizing Bian et al.'s (2016) study, Kelty-Stephen (2018) correctly describes how phasmids decreased swaying over time and that these data were from trials in which no plants were present. It is from this account alone that Kelty-Stephen (2018) rejects the adaptation explanation, suggesting that decreasing sway could be regarded as "a morbid wish to stand out to predators" (p. 16). This is a flawed proposition because there were no plants present in the trial so continuing to sway would also offer no camouflage benefit. What Kelty-Stephen (2018) did not mention is that the aim of the initial experiment by Bian et al. (2016) was to determine whether wind initiates swaying in hanging insects; which was clearly demonstrated. A second experiment subsequently showed that insects swayed more under variable wind, which is a more natural wind stimulus, compared with constant wind as used in the first experiment. Together, these two experiments by Bian et al. (2016) showed that wind initiates swaying and that insects can control swaying. The presence of both wind and insect control of swaying are necessary for a putative motion camouflage explanation; however, neither were undertaken in the presence of plants and make no attempt to relate swaying behavior with plant movement.

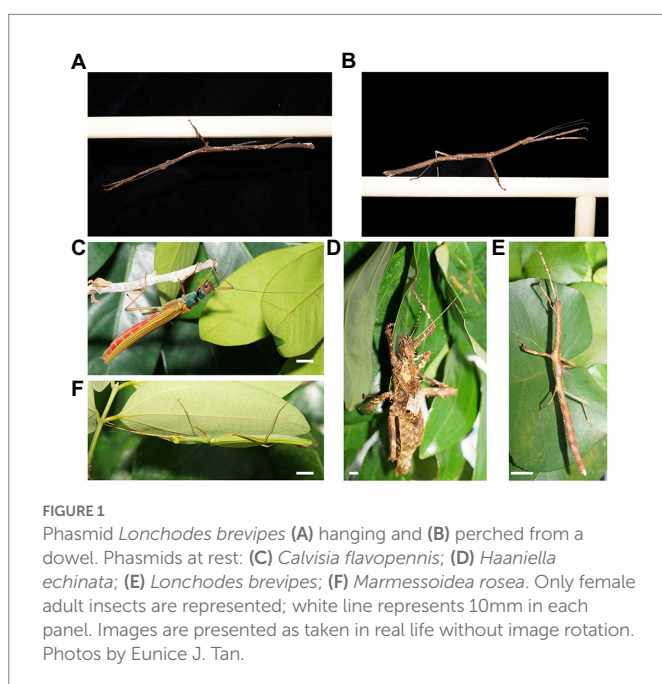


TABLE 1 Observations of phasmids during daylight hours in captive, laboratory conditions.

Species	Age	Hang stationary	Hang and walk	Perch stationary	Perch and walk	Other behaviors	Total	Swaying observed?
<i>Calvisia flavopennis</i>	Nymphs	209	1	10	0	5	346	Sometimes
	Adults	105	4	7	0	5		Sometimes
<i>Haaniella echinata</i>	Nymphs	75	1	19	0	4	104	Rare
	Adults	3	0	2	0	0		Rare
<i>Lonchodes brevipes</i>	Nymphs	273	20	10	1	8	466	Common
	Adults	145	3	5	0	1		Common
<i>Marmessoidea rosea</i>	Nymphs	362	8	1	0	7	427	Sometimes
	Adults	43	0	5	0	1		Rare

Phasmids were observed over a three-day period in October 2020. Each individual was observed only once each day between the daylight hours of 1530 h–1800 h. Only the behaviors of animals with intact limbs and wings were recorded to ensure that the recorded behaviors were not influenced by morphological abnormalities. *Other behaviors* referred to relatively uncommon behaviors such as drinking, feeding and thanatosis. Instances of swaying in the absence of stimuli (e.g., during our observation of the captive insects in the laboratory) are rare. Swaying behaviour was recorded based on our observations of the species over the months of captivity.

Similarities between phasmid and plant movement was investigated in a third experiment. Here insects and plants were filmed in natural conditions and in many circumstance the movement of both matched in the frequency domain. There were some exceptions that serve to highlight the potential for non-moving objects to stand out from moving ones, but also to prompt consideration of the circumstance that do and do not lead to swaying in natural environments. These are outlined in [Bian et al. \(2016\)](#) and highlight the complex factors that contribute to animal behavior, a point which seems to have alluded [Kelty-Stephen \(2018\)](#). Thus, contrary to [Kelty-Stephen's \(2018\)](#) assertion that [Bian et al. \(2016\)](#) “failed to find evidence that phasmids exploited the wind in the way they predicted” (p. 16), the complete dataset in [Bian et al. \(2016\)](#) showed that there most certainly is the potential for insects to benefit from swaying in wind and enough evidence was provided to take the next step, which is to confirm such behavior confers a survival advantage for the insects. Such investigations necessarily require an understanding of predator motion vision systems and behavior.

Conclusion

The range of taxa from phasmids to spiders and snakes that adopt swaying behavior suggests that this behavior may have an adaptive function. To uncover the adaptive function of swaying, further investigations are necessary to examine the circumstances in which individuals within species do and do not sway. We presented several offensive and defensive functions of swaying, which need not be mutually exclusive ([Jackson, 1985](#); [Watanabe and Yano, 2009, 2012, 2013](#); [Bian et al., 2016](#); [Tan and Elgar, 2021](#)). We dispute [Kelty-Stephen's \(2018\)](#) conclusion following reanalysis of the data presented in [Bian et al. \(2016\)](#) and the following assertions, as the reanalysis was based on flawed assumptions – contrary to both the diagrams presented in [Bian et al. \(2016\)](#), and natural history observations, the species hangs rather than perches on the vegetation. A key challenge for studies of animal behavior is to understand the function of animal behaviors. We urge caution when inferring function without sufficient/accurate natural history knowledge, often best achieved by collaboration. Particularly for the investigation of signals in motion such as swaying, great care must be taken to interpret the signals in the natural environment and context.

Data availability statement

The original contributions presented in the study are included in the article/supplementary material, further inquiries can be directed to the corresponding author.

Author contributions

ET and ME conceptualized the project. ET collected the data. ET, ME, and RP wrote the draft. All authors contributed to the manuscript revision, read, and approved the final manuscript.

Funding

This work was supported by Ministry of Education, Singapore, and Yale-NUS College Start-up Grant to ET.

Acknowledgments

We thank Jay Wong for helping with the observations on the phasmids.

Conflict of interest

The authors declare that the research was conducted in the absence of any commercial or financial relationships that could be construed as a potential conflict of interest.

Publisher's note

All claims expressed in this article are solely those of the authors and do not necessarily represent those of their affiliated organizations, or those of the publisher, the editors and the reviewers. Any product that may be evaluated in this article, or claim that may be made by its manufacturer, is not guaranteed or endorsed by the publisher.

References

- Bian, X., Elgar, M. A., and Peters, R. A. (2016). The swaying behavior of *Extatosoma tiaratum*: motion camouflage in a stick insect? *Behav. Ecol.* 27, 83–92. doi: 10.1093/beheco/arv125
- Clayton, H. M., Bialski, D. E., Lanovaz, J. L., and Mullineaux, D. R. (2003). Assessment of the reliability of a technique to measure postural sway in horses. *Am. J. Vet. Res.* 64, 1354–1359. doi: 10.2460/ajvr.2003.64.1354
- Cuthill, I. C., Matchette, S. R., and Scott-Samuel, N. E. (2019). Camouflage in a dynamic world. *Curr. Opin. Behav. Sci.* 30, 109–115. doi: 10.1016/j.cobeha.2019.07.007
- Dewolf, A. H., Ivanenko, Y. P., Mesquita, R. M., and Willems, P. A. (2021). Postural control in the elephant. *J. Exp. Biol.* 224:jeb243648. doi: 10.1242/jeb.243648
- Fleishman, L. J. (1985). Cryptic movement in the vine Snake *Oxybelis aeneus*. *Copeia* 1985, 242–245. doi: 10.2307/1444822
- Hutchinson, D., Ho, V., Dodd, M., Dawson, H. N., Zumwalt, A. C., Schmitt, D., et al. (2007). Quantitative measurement of postural sway in mouse models of human neurodegenerative disease. *Neuroscience* 148, 825–832. doi: 10.1016/j.neuroscience.2007.07.025
- Jackson, R. R. (1985). A web-building jumping spider. *Sci. Am.* 253, 102–115. doi: 10.1038/scientificamerican0985-102
- Kelty-Stephen, D. G. (2018). Multifractal evidence of nonlinear interactions stabilizing posture for phasmids in windy conditions: a reanalysis of insect postural-sway data. *PLoS One* 13:e0202367. doi: 10.1371/journal.pone.0202367
- Munafò, J., Curry, C., Wade, M. G., and Stoffregen, T. A. (2016). The distance of visual targets affects the spatial magnitude and multifractal scaling of standing body sway in younger and older adults. *Exp. Brain Res.* 234, 2721–2730. doi: 10.1007/s00221-016-4676-7
- Pohl, S., Bungum, H. Z., Lee, K., Bin Sani, M., Poh, Y., Wahab, R., et al. (2022). Age and appearance shape behavioural responses of phasmids in a dynamic environment. *Front. Ecol. Evol.* 9:767940. doi: 10.3389/fevo.2021.767940
- Rupprecht, R. (1971). Bewegungsmimikry bei *Carausius morosus* Br. (Phasmida). *Experientia* 27, 1437–1438. doi: 10.1007/BF02154275
- Straube, A., Brandt, T., and Probst, T. (1987). Importance of the visual cortex for postural stabilization: inferences from pigeon and frog data. *Hum. Neurobiol.* 6, 39–43. PMID: 3495526
- Tan, E. J., and Elgar, M. A. (2021). Motion: enhancing signals and concealing cues. *Biol. Open* 10:bio058762. doi: 10.1242/bio.058762
- Watanabe, H., and Yano, E. (2009). Behavioral response of Mantid *Hierodula patellifera* to wind as an Antipredator strategy. *Ann. Entomol. Soc. Am.* 102, 517–522. doi: 10.1603/008.102.0323
- Watanabe, H., and Yano, E. (2012). Behavioral response of male mantid *Tenodera aridifolia* (Mantodea: Mantidae) to windy conditions as a female approach strategy. *Entomol. Sci.* 15, 384–391. doi: 10.1111/j.1479-8298.2012.00535.x
- Watanabe, H., and Yano, E. (2013). Behavioral response of mantid *Tenodera aridifolia* (Mantodea: Mantidae) to windy conditions as a cryptic approach strategy for approaching prey. *Entomol. Sci.* 16, 40–46. doi: 10.1111/j.1479-8298.2012.00536.x

Frontiers in Ecology and Evolution

Ecological and evolutionary research into our natural and anthropogenic world

This multidisciplinary journal covers the spectrum of ecological and evolutionary inquiry. It provides insights into our natural and anthropogenic world, and how it can best be managed.

Discover the latest Research Topics

[See more →](#)

Frontiers

Avenue du Tribunal-Fédéral 34
1005 Lausanne, Switzerland
frontiersin.org

Contact us

+41 (0)21 510 17 00
frontiersin.org/about/contact



Frontiers in Ecology and Evolution

